UNIVERSIDADE DA BEIRA INTERIOR
Engenharia

Planning and Dynamic Spectrum Management in Heterogeneous Mobile Networks with QoE Optimization

Daniel Luís Silveira Robalo

Tese para obtenção do Grau de Doutor em
Engenharia Eletrotécnica e de Computadores
(3º ciclo de estudos)

Orientador: Prof. Doutor Fernando José da Silva Velez
Departamento de Engenharia Electromecânica
Universidade da Beira Interior
Covilhã, Portugal

Covilhã, agosto de 2014

To my beloved family and Sandra Morais

Acknowledgements

This work was only possible thanks to the contribution of many people. Foremost among these is Prof. Fernando J. Velez, my Ph.D. advisor, whose guidance and technical excellence were the keystone to achieve the goals of all research stages.

This work was performed and financially supported within the scope of several projects: Ubiquimesh, Planopti, Opportunistic-CR and CREaTION. The frameworks from these projects were the cornerstone for this thesis. I am grateful to all projects members, coordinators and researchers for their guidance and contributions throughout the years. I would also like to acknowledge the European Cooperation in Science and Technology (COST), namely COST2100, COST IC1004 and COST IC0905 "TERRA".

To Instituto de Telecomunicações (IT) and Universidade da Beira Interior (UBI), I would like to acknowledge the excellent lodging and outstanding working conditions. IT and UBI supported my attendance to research meetings and conferences, essential for my research and to divulge this work.

I would also like to acknowledge Robert Kooij, from TNO ICT, who provided MOS experimental results of gaming applications, Giuseppe Piro, from Politecnico de Bari, for is precious guidance in the implementation of Carrier Aggregation functionalities into LTE-Sim. I am thankful to Maria Camino Noguera and M. Kashif Nazir, former students from UBI and King's College of London, respectively, for their contributions in the formulation of the system capacity and Optimization of the cost/revenue trade-off of fixed WiMAX with and without relays. I am very grateful to Paulo Soeiro and Rui Sancho, from Viatel, who provided information on current LTE equipment prices and installation cost. Additionally, Finally, I would also like to thanks Jessica Acevedo, from IT-UBI, for her suggestions given in the context of the average SINR formulation in the context of LTE-A carrier aggregation.

To my colleagues from WE-Move@Covilhã, João Ferro, Luís Borges, Orlando Cabral, Rui Paulo, João Oliveira, and Jorge Tavares, I would like to thank all for their support and friendship.

I am very grateful to my beloved Sandra Morais for her never ending love, affection, friendship, and relentless praise. To kali, whose playfulness, livelihood and wiggling tail brightens my every day. At last, but never least, I am thankful to my family, especially my parents, and brother for their unconditional love, care and support.

Resumo

O planeamento rádio e otimização de redes são processos que não terminam após o lançamento de uma rede sem fios. De forma a alcançar o melhor equilíbrio entre qualidade e custos, as operadoras recorrem a diversos métodos de forma a melhorar a cobertura bem como a capacidade das suas redes. Por conseguinte, a investigação realizada nesta tese propõe os seguintes métodos: a implementação de *cell zooming* e estações repetidoras (RSs), com modos dinâmicos para a redução de consumo energético, e a agregação de portadoras (CA), a fim de melhorar a cobertura e a capacidade celular.

Inicialmente, apresenta-se um *survey* sobre cenários de implementação de redes em malha ubíquas, e propõe-se uma caracterização atualizada dos requisitos de serviços e aplicações. Definiram-se, ainda, as métricas de desempenho para os parâmetros chave: o atraso, a variação do atraso, perdas de informação e débito, para vários serviços. Dada a atual concorrência existente no mercado das comunicações móveis, o sucesso de uma operadora não depende apenas da qualidade que oferece o seu serviço (QoS), mas, também, se essa responde à expetativa dos clientes, isto é, a qualidade de experiência (QoE). Neste contexto, propõe-se um modelo que mapeia parâmetros de QoS em QoE para tráfego multimédia.

No que concerne ao planeamento e otimização de redes *Worldwide Interoperability for Microwave Access* (WiMAX) fixas com RSs e *cell zooming*, considerou-se o cenário exigente da região montanhosa da Covilhã. Além disso, uma função de custo/proveito foi desenvolvida considerando-se o custo da construção e da manutenção da infraestrutura com RSs. Nesta parte da investigação, analisou-se, também, a eficiência energética e as implicações económicas da utilização dos modos de poupança energética das RSs. Assim, assumindo que as RSs possam ser desligadas nos períodos em que a troca de tráfego é reduzida, tal como noites e fins-de-semana, demonstrou-se que esse consumo pode ser reduzido enquanto a cobertura celular, a capacidade e o desempenho económico podem ser otimização.

Finalmente, propôs-se uma entidade de gestão de recursos rádio integrada (iCRRM) que implementa CA num sistema Long Term Evolution – Advanced (LTE-A) ao agendar recursos entre bandas de 800 MHz e 2.6 GHz disponíveis em Portugal. Posto isto, tendo em conta o tráfego de vídeo, após simulações extensas verificou-se que com os escalonadores de multi banda propostos supera-se a capacidade de sistemas LTE sem CA. Os resultados obtidos demonstram que recorrendo à CA existe uma clara melhoria dos parâmetros de QoS, da QoE e aspetos económicos.

Palavras-chave

Planeamento celular e otimização, cenários de implementação, caracterização de serviços e aplicações, QoS, QoE, WiMAX, SINR, repetidores, *cell zooming*, otimização de custos/proveitos, LTE-A, agregação de portadoras, escalonamento multi banda

Abstract

The radio and network planning and optimisation are continuous processes that do not end after the network has been launched. To achieve the best trade-offs, especially between quality and costs, operators make use of several coverage and capacity enhancement methods. The research from this thesis proposes methods such as the implementation of cell zooming and Relay Stations (RSs) with dynamic sleep modes and Carrier Aggregation (CA) for coverage and capacity enhancements.

Initially, a survey is presented on ubiquitous mesh networks implementation scenarios and an updated characterization of requirements for services and applications is proposed. The performance targets for the key parameters, delay, delay variation, information loss and throughput have been addressed for all types of services. Furthermore, with the increased competition, mobile operator's success does not only depend on how good the offered Quality of Service (QoS) is, but also if it meets the end user's expectations, i.e., Quality of Experience (QoE). In this context, a model for the mapping between QoS parameters and QoE has been proposed for multimedia traffic.

The planning and optimization of fixed Worldwide Interoperability for Microwave Access (WiMAX) networks with RSs in conjunction with cell zooming has been addressed. The challenging case of a propagation measurement-based scenario in the hilly region of Covilhã has been considered. A cost/revenue function has been developed by taking into account the cost of building and maintaining the infrastructure with the use of RSs. This part of the work also investigates the energy efficiency and economic implications of the use of power saving modes for RSs in conjunction with cell zooming. Assuming that the RSs can be switched-off or zoomed out to zero in periods when the traffic exchange is low, such as nights and weekends, it has been shown that energy consumption may be reduced whereas cellular coverage and capacity, as well as economic performance may be improved.

An integrated Common Radio Resource Management (iCRRM) entity is proposed that implements inter-band CA by performing scheduling between two Long Term Evolution – Advanced (LTE-A) Component Carriers (CCs). Considering the bandwidths available in Portugal, the 800 MHz and 2.6 GHz CCs have been considered whilst mobile video traffic is addressed. Through extensive simulations it has been found that the proposed multi-band schedulers overcome the capacity of LTE systems without CA. Result shown a clear improvement of the QoS, QoE and economic trade-off with CA.

Keywords

Cellular planning and optimization, deployment scenarios, services and applications characterization, QoS, QoE, WiMAX, SINR, relays, cell zooming, cost/revenue optimization, LTE-A, carrier aggregation, multi-band scheduling

Table of Contents

List of Figures

List of Tables

List of Acronyms

2D	Bi-dimensional space
3G	Third Generation of Mobile Telecommunications Technology
3GPP	3rd Generation Partnership Project
ACIP	Audio Contribution over IP
AMR	Adaptive Multi-Rate
ATBC	Aggregated Transmission Bandwidth Configuration
ATIS	Alliance for Telecommunications Industry Solutions
AWG	Application Working Group
BER	Bit Error Rate
BPSK	Binary Phase Shift Keying
BS	Base Station
BW	Bandwidth
C/I	Carrier-to-Interference
CA	Carrier Aggregation
CC	Component Carrier
CD	Compact Disc
CNIR	Carrier-to-Noise-Plus-Interference Ratio
COST	European Cooperation in Science and Technology
CP	Cyclic Prefix
CRRM	Common Radio Resource Management
DL	Downlink
DP	Dominant Path
DVD	Digital Versatile Disc
E-mail	Electronic mail
EMBS	Enhanced Multi-Band Scheduling
eNB	Evolved Node B
EU-MESH	Enhanced, Ubiquitous, and Dependable Broadband Access using MESH Networks
E-UTRA	Evolved Universal Terrestrial Radio Access
Fax	Facsimile
FCC	Federal Communications Commission
FDD	Frequency Division Duplexing
FER	Frame Erasure Rate
FFA	Free-For-All
FP7 WG	Seventh Framework Package Working Group
fps	Frames per second
FPS	First Person Shooter
GAP	General Assignment Problem
GMBS	General Multi-Band Scheduling
GPS	Global Positioning System
GSM	Global System for Mobile/Groupe Spécial Mobile
HD	High Definition

HOL	head of line
HSF	Health Science Faculty
HTML	HyperText Markup Language
iCRRM	integrated Common Radio Resource Management
IEEE	Institute of Electrical and Electronics Engineers
IETF	Internet Engineering Task Force
IGeoE	Instituto Geográfico do Exército
iLBC	Internet Low Bitrate Codec
IP	Internet Protocol
IQ	IneoQuest
ISO	International Organization for Standardization
I_{TBS}	Transport Block Size index
ITU	International Telecommunication Union
ITU-T	ITU Telecommunication Standardization Sector
K	Reuse pattern
LTE	Long Term Evolution
MCS	Modulation and Coding Scheme
MH	Mobile Hashing
M-LWDF	Modified Largest Weighted Delay First
MOS	Mean Opinion Score
MP3	MPEG-2 Audio Layer III
MPEG	Moving Picture Experts Group
MSE	Mean Square Error
ODFM	Orthogonal Frequency Division Multiplexing
ODU	Outdoor Data Unit
Ofcom	Office of Communications
P2P	Peer-to-Peer
PC	Personal Computer
PDA	Personal digital assistant
PESQ	Perceptual Evaluation of Speech Quality
PF	Profit Function
PHY	Physical
PL	path loss
PLR	Packet Loss Ratio
PRB	Physical Resource Block
QAM	Quadrature amplitude modulation
QCIF	Quarter Common Intermediate Format
QoE	Quality of Experience
QoS	Quality of Service
QPSK	Quadrature Phase Shift Keying
R	Correlation coefficient
R^2	Determination coefficient
RA	Resource Allocation
RAN	Radio Access Network
RB	Resource Block

RF	Radio Frequency
RNC	Radio Network Controllers
RR	Round Robin
RRHs	Remote Radio Heads
RRM	Radio Resource Management
RS	Relay Station
RT	Ray Tracing
RTT	Round-Trip Time Measurement
SD	Small Definition
SINR	Signal to Interference plus Noise Ratio
SIP	Session Initiation Protocol
SMS	Short Message Service
SS	Subscriber Station
STB	Set-Top-Box
TBS	Transport Block Size
TCP	Transmission Control Protocol
TDD	Time Division Duplexing
TTI	Transmission Time Interval
UE	User Equipment
UL	Uplink
UMTS	Universal Mobile Telecommunication System
VoIP	Voice over Internet Protocol
VPN	Virtual Private Network
WCDMA	Wideband Code Division Multiple Access
WiFi	Wireless Fidelity
WiMAX	Worldwide Interoperability for Microwave Access
WMA	Windows Media Audio
μBS	micro Base Station

List of Symbols

$(R_v)_{cov\_zone}$	revenue in a hexagonal-shaped coverage zone per year
A_{cell}	total affected cell area
A_{ow}	total integration area
$BER\ (CQI_{b,u})$	DL average BER s for user *u* on band *b*
b_{rate}	video bitrate
b_{rf}	bandwidth
C	Carrier
C_{ost}	cost per unit area
C_b	cost per BS
C_{bh}	cost for the normal backhaul
C_{BS}	cost of the BS
C_{fi}	fixed term of the costs
C_{Inst}	cost of the installation of the
$C_{M\&O}$	cost of operation and maintenance
CQI	channel quality indicator
C_{RS}	cost of the RS
d	distance between SS and BS
D	reuse distance
D_{hb}	BS antenna height
D_{HOL}	head of line (HOL) packet delay
f	frequency
f_p	integrand function
Fr	Fraunhofer distance
G_{BS}	BS antenna gain for BS-to-SS and BS-to-RS communications
G_r	receiver antenna gain
G_{RS}	RS antenna gain for RS-to-SS communications
G_{SS}	SS antenna gain for SS-to-BS communications
G_t	transmitter antenna gain
I	interference
I_d	delay impairments
I_{dd}	one-way mouth-to-ear delay impairments
I_{dle}	listener echo impairments
I_{dte}	talker echo impairments
I_e	low bitrate codecs impairments
I_s	voice signal impairments
j	jitter
K	reuse pattern
L_b^{max}	maximum normalised load that can be handled in band *b*
M	interference-to-noise ratio
N	noise

N_f	noise figure
N_{hex}	number of hexagonal coverage zones per unit area
N_{RB_agg}	number of aggregated Resource Blocks
N_{sec}	number of sectors
N_{year}	project lifetime
p	ping
P	profit
P_{BS}	BS power consumption
P_{nh}	total interfering power coming from the neighbour cells
P_{noise}	thermal noise power
P_{ow}	power received from the own cell
P_{RS}	RS power consumption
P_t	transmitter power
R	radius
$R(CQI_{b,u})$	DL throughput for user u on band b
$R_{asymptote}$	vertical asymptote
R_b	physical throughput
$R_{b\text{-}central}$	throughput in the central zone
$R_{b\text{-}ch}$	bit rate of the basic “channel”
$R_{b\text{-}RS\text{-}zone}$	throughput in the RS zone
$R_{b\text{-}sup}$	supported physical throughput
$R_{b\text{-}sup[kb/s]}$	supported throughput per BS or sector
$R_{b\text{-}tot}$	the total throughput in the multihop cell
r_{cc}	co-channel reuse factor
R_f	rating factor
R_i	i-th flow transmission rate
$R_i(k)$	throughput achieved by the i-th flow during the k-th TTI
$r_{i,j}$	instantaneous available throughput (of the i-th flow in the j-th sub-channel)
R_o	basic signal-to-noise ratio
R_{Rb}	revenue of a channel with a throughput $R_{b[kbps]}$
R_v	revenue per unit area per year
R_{z-out}	zoomed out cell radius
S_{rate}	service bit rate
T	talker echo delay
T_a	one-way mouth-to-ear delay
T_{bh}	equivalent duration of busy hours per day
T_r	listener echo delay
$W_{b,u}$	normalised metric for UE u is on band b
$w_{i,j}$	scheduler metric
$w_{i,j,b}$	multi-band scheduler metric
$x_{b,u}$	allocation variable for UE u is on band b

a	orthogonality factor
β	adjustment coefficient for worst case SS position in the cell with relays
γ	propagation exponent
δ_i	maximum probability that $D_{HOL,i}$ exceeds the delay threshold of the i-th flow
μ	expectation
ρ	percentage of loss
σ	standard deviation
τ	delay
τ_i	i-th flow packet delay threshold
φ_1	take-off angle
φ_2	angle of arrival

Chapter 1

Motivation and approach

1.1 Motivation and approach

In nowadays wireless cellular networks, not only mobile services and applications are more and more used by consumers each year, leading to an expansion of mobile data traffic, but the pace at which it is growing is accelerating. According to [1], in 2013 mobile data traffic was nearly 18 times the size of the entire global Internet in 2000. One Exabyte of traffic traversed the global Internet in 2000, and in 2013 mobile networks carried nearly 18 Exabyte's of traffic. In 2013 alone, 526 million mobile devices and connections were added, the global mobile data traffic grew 81 % and mobile video represented 53 % of all mobile traffic and by 2018 it will reach 69 %. Moreover, it is expected that mobile-connected devices will exceed the world's population by 2014. Monthly mobile data traffic will reach 15.9 Exabyte's by 2018 and between 2013 and 2018 the annual growth rate will be 61 %, i.e., mobile data traffic will increase nearly 11-fold between 2013 and 2018. These statistics show beyond the shadow of a doubt that wireless and cellular networks technologies need to be enhanced to support such demands. As so, the research performed in this Ph.D. thesis aims at contributing for the optimization and planning of cellular networks in a context of heterogeneous mobile networks and spectrum management.

The goal of cellular coverage is to provide access to mobile users in a given region, called cell while guaranteeing the quality of the received signal in both directions, uplink (UL) and downlink (DL), even for the users at the longest distance from the cell centre, i.e., at the cell edge. As resources, e.g., radio frequency channels, need to be reused in different geographical zones (but not in the closest proximity), the impact of interference among co-channel cells needs to be evaluated in both DL e UL directions. Furthermore, due to heavy interference in frequency reuse deployment, users at cell edge may suffer low connection quality.

Therefore, in the context of Interoperability for Microwave Access (WiMAX) and Long Term Evolution (LTE) cellular planning, research on the variation of the Carrier-to-Noise-plus-Interference Ratio (CNIR) with different system parameters is critical. As there are limitations in both links, UL and DL, techniques such as sub-channelization need to be applied to reduce the impact of the noise on the link performance. In the context of WiMAX, however, only mobile WiMAX will allow for sub-channelization in the DL while fixed WiMAX only allows for it in the UL and may cause a degradation of performance (mainly owing to the extra noise caused by the largest bandwidth).

In the optimization of cellular planning for next generation wireless networks, the use of Relay Stations (RSs) makes unnecessary a wire-line backhaul, improving the coverage and system capacity significantly. Moreover, the use of RSs with much lower hardware complexity provides the opportunity for cost and energy-efficient aware mobile radio networks. RSs can be switch-off during either the night period or the weekends, when the traffic load is low, providing energy saving, the coverage will then be sustained by the Base Station (BS) associated to the switch-off RSs. Mesh and RS networks may consider cell zooming as a cost-efficient way to achieve green cellular networks. While the BS coverage is zoomed out, RSs are able to work in sleep mode. This way, the air-conditioner and other energy consuming equipments can be switched off within the RS shelter. At these times of low traffic load, users may only be supported by the central zone cell by increasing the BS transmitter power and zooming out. Furthermore, antenna height and antenna tilt of BSs can also be adjusted for cells to zoom in or zoom out.

The presence of neighbouring cells, Subscriber Stations (SS), RSs and other networks increases the interference and noise levels. There are certain CNIR thresholds at the receiver and BS below which the service cannot be granted. Thus all the above aspects must be considered for an adequate radio and network planning, especially for the considered heterogeneous and cooperative mobile wireless networks. The main objective is to achieve the highest values for the carrier-to-Interference ratio, C/I, and, in turn, the maximum supported throughput, by using RSs for a given frequency reuse pattern, e.g., $K = 3$.

To optimize service usage and the management of radio resources, the characterization of the deployment of scenarios, as well as, services and applications requirements must also be addressed. The characterization in terms of quality of service and experience is performed to provide the key features of wireless ubiquitous network applications. As such, the main recommendations from such entities as the International Telecommunication Union Telecommunication Standardization Sector (ITU-T), 3rd Generation Partnership Project (3GPP) and key elements proposed by a major European project, i.e. EU-MESH, are considered. Moreover, detailed video and voice encoding application requirements presented by the WiMAX Forum are also assumed. Besides, rather than developing new and distinct sets of deployment scenarios it is expected that, for a better iteration and perhaps cooperation with the remaining international scientific community, one should rather assume EU-MESH's scenario characterization. In addition, the main key parameters impacting user's quality should be identified and their performance targets for audio, video and data applications must also be considered. This works involves updating the current state of application requirements. For this purpose, one addresses the recommendations from the ITU-T, 3GPP, WiMAX Forum and EU-MESH. This task is required for a deeper understanding, evaluation and optimization of wireless networks system performance.

Furthermore, with the increased competition between network and service providers, improving the quality of the offered services as perceived by users, commonly referred to as Quality of Experience (QoE), becomes very important as well. This constitutes a significant

challenge to service providers who aim to minimize the customer churn while maintaining their competitive edge [2]. Thus, it is very important for operators to accurately measure and improve the users Quality of Service (QoS) and experience. QoS parameters are the most accessible and measurable metrics to assess the overall performance of the network in real time. Nonetheless, QoS measurements are generally defined in terms of network delivery capacity and resource availability but not in terms of the satisfaction to the end-user. In this context, a unified model for the mapping between QoS and QoE will be proposed for different types of services and applications. Hence, values for QoS metrics gathered from various parts of the network must be mapped onto QoE targets. Mean Opinion Score (MOS) experimental results have been widely used and considered one of the most accurate approaches to attain the user's subjective quality assessment. Therefore, the mapping is obtained by means of fitting MOS measurements, which are in turn validated by using the Mean Square Error (MSE) and the coefficients of correlation and determination, R and R^2. The novelty of this approach is to introduce a unified model that provides network and service providers a framework to evaluate user's satisfaction for multimedia applications, i.e., gaming, video, web-browsing and audio.

In nowadays heterogeneous wireless networks topologies the scarce wireless spectrum can be much better utilized [3]. Besides, in the near future, communication systems are anticipated to become pervasive with demands for higher data rates. To accommodate the increased demand for communication bandwidth, the concept of Carrier Aggregation (CA) is introduced by 3GPP in LTE-Advanced (LTE-A). The easiest way to implement CA would be to use contiguous component carriers within the same operating frequency band. However, large portions of continuous spectrum are not often available. Therefore, aggregating smaller bandwidths is another interesting solution to increase data rate. Hence, while considering the available bandwidths and frequency bands in Portugal CA will be addressed in this thesis. On the one hand, CA will enable superior data rates. On the other, it will also provide interference reduction, efficient spectrum use and quantitative quality of service improvement. Moreover, in the context of CA, Radio Resource Management (RRM) plays a key role in wireless system design and involves procedures as power control, cell search, cell reselection, handover, radio link or connection monitoring, connection establishment and re-establishment. Another fundamental element in resource management is scheduling, which prioritizes packets that are ready for transmission. Based on the scheduling algorithm, as well as the traffic characteristics of the multiplexed flows, certain QoS levels can be achieved. Common Radio Resource Management (CRRM) is a class of radio resource management functionality that refer to the set of functions that are devoted to ensure an efficient and coordinated use of the available radio resources in heterogeneous networks scenarios. More specifically, CRRM strategies should ensure that the operator's goals in coverage, resource reuse and QoS are met while providing as high as possible overall capacity (i.e. the sum of the capacities achieved in every single Radio Access Network, RAN). It is also worthwhile to note that, within CRRM, load balancing has become a relevant concern in design.

1.2 Main objectives

The research activities addressed in this thesis aim at contributing to the evolution and optimization of wireless radio and network planning, in a context of multiple heterogeneous and cooperative wireless networks, within a combination of architectures, i.e., cellular topologies in the presence or absence of RSs. The mobile multi-hop relay technology extends the service area of mobile networks and also improves the transmission quality. Such proliferation of architectures should allow for an enhancement of coverage and system capacity. This thesis addresses the planning and radio resource management optimization of fixed WiMAX with RSs in real environments and the challenge of modelling the propagation for hilly rural areas at 3.5 GHz.

The emerging trend towards energy-efficient network operation shifts the focus from system optimization to the energy consumption of the wireless access network infrastructure, which has triggered activities in standardization and regulatory bodies, such as 3GPP, ITU and ATIS [4]. One technology enabling cost-efficient green cellular networks is cell zooming. It allows adjusting the cell size according to the traffic conditions and has the potential to balance the traffic load and reduce the energy consumption, by decreasing the transmitting power to reduce cell coverage (zoom in) [5]. Additionally, multi-hop relays with lower hardware complexity, power consumption and cost, can also be used to optimise network planning (enhancing coverage) and reduce energy consumption [6]. The use of RSs allied to cell zooming can enable the design of cost-efficient and green wireless systems.

For commercial and technical reasons [7], it is critical for network operators and service providers to be able to assess, predict and possibly control their user's perceptual multimedia (e.g., voice and video) quality. The first step to reach this goal is to fully characterize and define deployment scenarios, as well as, services and applications requirements for wireless heterogeneous multi-hop networks. In this context, the ITU-T, 3GPP, WiMAX Forum and EU-MESH recommendations are merged and updated to address nowadays wireless networks requirements. The second step is enabling operators and service provider to evaluate the user's QoE according to the network state (QoS parameters). Moreover, several works have been performed on the characterization of the QoE as a function of the QoS [2], [8] and [9]. However, they only consider one QoS parameter for each application. In the framework of this thesis, a unified model for the mapping between QoS and QoE is proposed. This model considers key parameters that impact user's experience for several multimedia applications. One of the most accurate approaches to evaluate QoE is the subjective quality assessment, since the best indicator of personal quality is the one given by a human being. Therefore, QoE data should succeed where possible in combining both user experience and technical measures, for example, to provide an equation for the user experience when using a particular service with known levels of QoS [10]. The objective is to provide the network and service providers with the means to assess the contribution of the

network performance to the overall level of user's satisfaction. This mechanism allows building an effective QoE control mechanism onto measurable QoS parameters.

There is growing interest in LTE-A CA implementation. Not only it allows for superior data rates but, CA importance lays in its potential to allow real-time optimization of spectral resources and radically change spectrum management by better exploiting (aggregating) small portions of radio spectrum that would be unusable otherwise. As so, another objective of this thesis is to address CA application to answer to the increased demand for communication bandwidth, as well as, enhance wireless networks capacity, i.e., QoS and QoE. In the framework of the Portuguese scenario, e.g., available bandwidths and radio frequency bands, multi-band scheduling algorithms will be proposed to optimize average cellular capacity, service performance and user's perceived quality. Besides, CA's cost/revenue trade-off, from the operator/service provider point of view will also be addressed.

The main goals of the research from this thesis can be summarized as the follows:

- Deployment scenarios and characterization parameters for concatenated ubiquitous wireless mesh network applications:
    - Definition of deployment scenarios;
    - Definition of key parameters impacting users;
    - Definition of services and applications requirements.
- Unified model for the mapping between the QoS and QoE in multimedia applications:
    - Sub-model for gaming applications;
    - Sub-model for video applications;
    - Sub-model for web-browsing applications;
    - Sub-model for audio applications;
    - Unified model for the mapping between QoS and QoE.
- Planning and optimization of fixed WiMAX networks with relays:
    - Formulation of the signal-to-noise-plus-interference ratio in the presence and absence of RSs;
    - System capacity;
    - Supported cell/sector physical throughput;
    - Measurement-based propagation modelling for hilly rural areas at 3.5 GHz;
    - Cellular planning in actual environments, hilly rural areas.
- Energy saving and cost-revenue analyses through relay sleep modes and cell zooming:
    - Models for cost/revenue optimization;
    - Economic and environmental impact of cell zooming and RSs deployment.
- Carrier Aggregation for wireless networks capacity enhancement:
    - Definition of the LTE scenario within two non-continuous bands;
    - Multi-band scheduling for carrier aggregation;
    - Average cell SINR analysis
    - Transmitter power normalization over 800 MHz and 2.6 GHz frequency bands;
    - QoS, QoE and cost/revenue improvement through carrier aggregation.

Additionally, the work presented in this thesis is a significant part of different research European frameworks, such as the European Cooperation in Science and Technology (COST), namely COST 2100 [11], COST IC1004 [12] and COST IC0905 "TERRA" [13]. Moreover, contributions on the deployment scenarios and characterization parameters for concatenated ubiquitous wireless mesh networks applications and the unified model between QoS parameters and QoE addressed in this thesis have been developed in the context of the Portuguese project Ubiquimesh [14] and Opportunistic-CR [15]. The planning and optimization of fixed WiMAX networks with relays, energy saving aspects and cost-revenue analysis, and the common radio resource management for spectrum aggregation were developed within the framework of Planopti (Marie Curie Reintegration Grant) [16], Opportunistic-CR and CREaTION [17]. The main contributions and dissemination achieved within the scope of this thesis will be detailed in a later section.

1.3 Cellular Network Planning and Optimization

The network planning process itself is not standard for all mobile communication technologies, even though some of the steps may be common. In this thesis, the planning and optimization approach shares some key points with the network planning process from [18]. The network planning project organisation is based on the network planning roll-out process steps. The final target of the roll-out process is to deliver a new network for the operator according to the agreed requirements and applies both for individual BSs as well as for the whole network. The network planning project organisation is pictured according to the process flow from Figure 1.1.

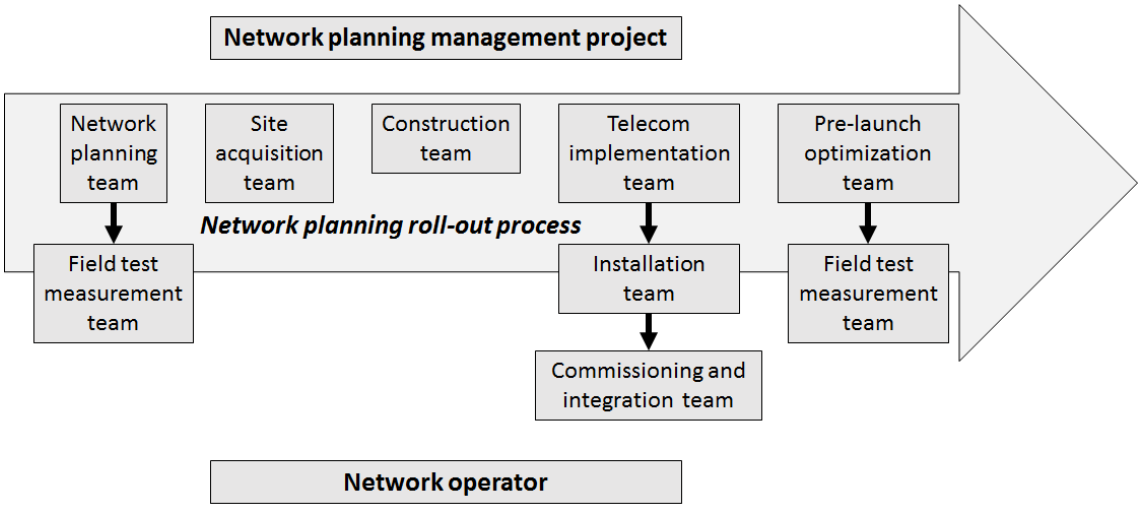

Figure 1.1 Network planning project organisation (extracted from [18]).

In this, thesis the goal is not to plan an end-to-end network, some parts of the above project organization will not be addressed, e.g., activities directly linked to the network operator (site acquisition team, construction team and telecom implementation team). Therefore, the main steps from the network planning process proposed by [18] will instead be considered, shown in Figure 1.2.

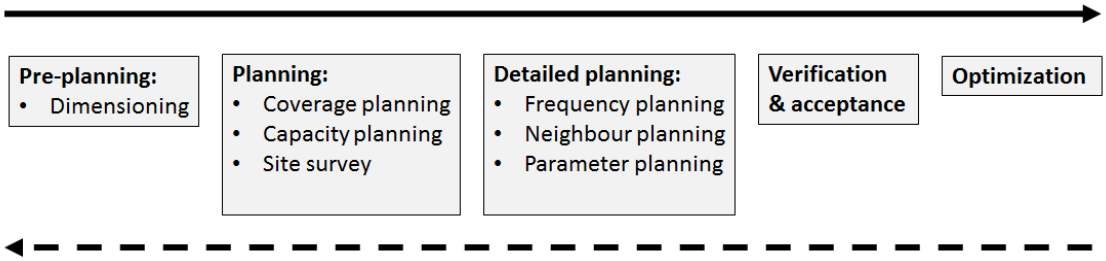

Figure 1.2 Network planning process steps (extracted from [18]).

The radio network planning process is divided into five main steps, from which four are typically performed before the network launch, i.e., pre-planning, planning, detailed planning, verification acceptance. Finally, the optimization is usually addressed after the network has been launched. After the detailed planning step, the network is ready for commercial launch, but the post-planning phase continues the process and targets the most optimal network configuration. Actually, the network planning process is a never ending cycle due to changes in the design parameters [18].

The input for the pre-planning phase is the network planning criteria. Its main activity is dimensioning, which gives the initial network configuration as a result. The first step in the planning phase is nominal planning; it provides the first site locations in the map based on input from the dimensioning phase. The process continues with more detailed coverage planning after site hunting and transmission planning and also includes capacity planning. Detailed planning covers frequency, neighbour and parameter planning. After the detailed planning the network is ready for verification and acceptance, which finishes the pre-launch activities. After the launch the activities continue with optimization. As mentioned earlier, some of these steps, such as site hunting, will not be considered; they are beyond the scope of this thesis. Furthermore in the context of the site location, i.e., the BS location considered in this work for propagation analysis was not optimized by the dimensioning phase, but rather by the limitations of the University estate and approval constraints to install the WiMAX equipment, shown in Chapter 4.

1.3.1. Pre-planning

Before the actual network planning is started, the pre-planning phase covers the assignments and preparation. As in any other field of business it is an advantage to be aware of the current market situation and competitors. The network planning criteria is considered

as an input for network dimensioning. Some of the basic inputs for dimensioning are the following ones [18]:

- Coverage requirements, the signal level with the coverage probabilities;
- Quality requirements;
- Frequency spectrum;
- Services and applications.

1.3.2. Planning

The planning phase takes the inputs from the pre-planning dimensioning. This is the basis for nominal planning, which means radio network coverage and capacity planning. The goal of the coverage planning phase is to find the optimal BSs locations. In the capacity planning phase the network capacity is allocated by combining the final coverage plan with the user density information. The detailed coverage maps for the planned area, the final site locations and the capacity plans are the outputs of the planning phase.

1.3.3. Detailed planning

Once the site location and configurations are known the detailed planning can be started. It includes frequency, adjacency and parameter planning. According to [18], planning tools are usually used in this step, as they have specific algorithms for automatic frequency planning. The tools use interference calculation algorithms aiming to minimise the co-channel and adjacent channel interference, in context of this thesis the Winprop™ tool was used. Frequency planning is a critical phase in network planning, since the number of frequencies is limited and the best possible solution must be found. Neighbour planning is usually performed with a coverage planning tool using the frequency plan information. The basic rule is to consider the neighbouring cells from the first tier of the surrounding BS [18].

1.3.4. Verification and Acceptance

The verification and acceptance is performed once the planning phase has been finished and aims to ensure optimal operation of the network. Besides fine-tuning, a verification of possible errors that might have occurred during the installation is performed. The targets to be met for network acceptance are specified by the key performance indicators found during the pre-planning phase. This radio network planning process step is not fully addressed in this thesis as no real network installation is performed, however the key performance parameters (QoS) are defined in Chapter 2 and used to evaluate the multi-band schedulers proposed in Chapter 6.

1.3.5. Optimization

Radio and network planning and optimization are a continuous process that does not end after the network has been launched. The optimization inputs are all available network

information and status. The network statistic figures, alarms and traffic itself are monitored carefully. Customer observations and opinions are also taken into account by the network optimization team. To detect and analyse potential problems at a given location, the optimization process includes both network level measurements and field test measurements. Besides, it is worth noting that, among other methodologies, like drive testing, the authors from [18] also refer MOS as a practice to measures human beings perception during the optimization process, as addressed in Chapter 3.

1.3.6. Network Coverage and Capacity Enhancement Methods

The performance of a mobile network can be seen from several perspectives:

- Capacity - Each operator owns a limited frequency band which is shared by an increasing number of network users;
- Quality - It is measured by metrics such as the carrier-to-interferer ratio (C/I);
- Coverage - Service continuity is tremendously important in a cellular network;
- Cost - Technical requirement to achieve the best quality perception from the subscriber side should be balanced with costs;
- New services - Operators cannot differentiate and gain new customers if they do not offer enhanced data services on top of high data rate technologies;
- Complexity and flexibility - Two very important criteria from an operation of the network point of view make it easy for maintenance teams to maintain the network.

All these aspects are related among them and are interdependent. Commonly, network design transits mainly through the path shown in Figure 1.3.

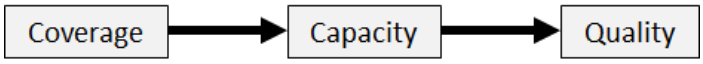

Figure 1.3 Network performance constraint evolution path (extracted from [18]).

At the first roll-out stage, the most important thing is to provide coverage. Then, when the number of subscribers starts to increase and generate more traffic, capacity becomes the main issue for the operator. When a certain maturity in terms of subscriber behaviour, coverage and capacity levels is reached for the network, the operator should improve the end user's perceived quality. To achieve the best trade-offs, especially between quality and costs, the operator tries to make use of several coverage and capacity enhancement methods [18]. In this context, the research throughout this thesis proposes methods such as RSs, cell zooming and CA for coverage and cellular capacity improvement.

Radio resource management (RRM) plays an important role in the optimization LTE-A with CA, due to the scheduling algorithm which decides among packets that are ready for transmission. Based on the scheduling algorithm which allocates Component Carriers' (CCs) resource blocks to users, as well as the traffic characteristics of the multiplexed flows, the

optimization of radio and network planning is tuned, and certain QoS requirements can be achieved. Common RRM (CRRM) refers to the set of functions that are devoted to ensure an efficient and coordinated use of the available radio resources in heterogeneous networks scenarios. A non-contiguous CA (from an upper layer point of view) and an integrated CRRM (iCRRM) entity for multiband scheduling are proposed in the framework of this thesis, where CA and CRRM functionalities are handled simultaneously in an LTE-A scenario. The proposed resource allocation (RA) assigns the user packets to the available radio resources, i.e., CCs, in order to satisfy user requirements based on integer programming optimization, or even suitability based optimization, and ensures efficient packet transport to maximize spectral efficiency.

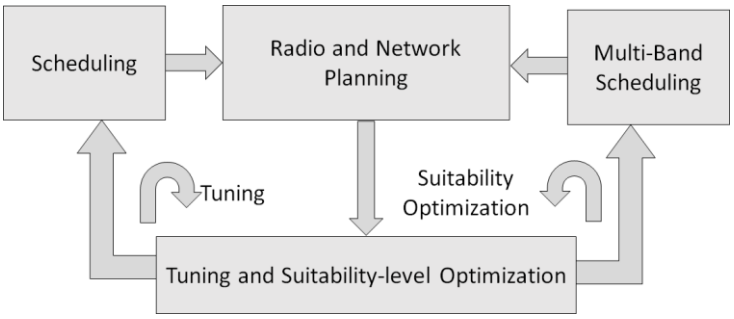

Figure 1.4 Radio and network planning optimization.

1.4 Contributions

The contributions given in this work were originates from (and financed through research grants) the Portuguese projects: Cross-Layer Optimization in Multiple Mesh Ubiquitous Networks (Ubiquimesh) [14], Opportunistic Aggregation of Spectrum and Cognitive Radios: Consequences on Public Policies (Opportunistic-CR) [15] and Cognitive Radio Transceiver Design for Energy Efficient Data Transmission (CREaTION) [17].

Besides, the research presented in this thesis has been addressed within the scope of the research European framework, Planning and Optimization for the Coexistence of Mobile and Wireless Networks Towards Long Term Evolution (PLANOPTI), Marie Curie European Reintegration Grant [16], as well as, cooperation in the field of Scientific and Technical Cooperation (COST), namely COST2100 (Pervasive Mobile Ambient Wireless Communications) [11], COST IC1004 (Cooperative Radio Communications for Green Smart Environments) [12] and COST IC0905 "TERRA" (Techno-Economic Regulatory Framework for Radio Spectrum Access for Cognitive Radio/Software Defined Radio) [13].

The research conducted in the framework of the aforementioned projects has been of particular importance for this thesis and has already been disseminated in published papers, accepted for publication or submitted to conferences proceedings, journals or book chapters.

The characterization of applications and deployment scenarios for ubiquitous concatenated multiple mesh networks was addressed in the Ubiquimesh project framework. The proposed requirements for services and applications were defined upon the analysis and update of current ITU-T, 3GPP and EU-MESH European project recommendations. This proposal accounts for the parameters that most impact the user's service quality and defines performance targets for each of those parameters according to the application type. This work was addressed in a technical report [19], the conference proceeding paper [20] and two COST actions communications, [21] and [22].

The model for the mapping between the QoS and experience for multimedia applications was developed within the Ubiquimesh project scope. This work proposes a function that characterizes the relation between a set of QoS parameters gathered within the wireless network and the corresponding QoE, which provides network and service providers a framework to evaluate user's satisfaction for gaming, video, audio a web-browsing applications. This research was addressed in a technical report [23] and conference proceedings [20] and [24].

The research conducted on the planning and optimization of fixed WiMAX networks in the presence and absence of relays was performed in the context of PLANOPTI. This work introduces cell zooming and advanced DL and UL frame structures for cellular networks with relays as key enabling technologies for capacity performance. Besides PLANOPTI, Opportunistic-CR's scope of research also included the cost/revenue trade-off and energy waste consumption reduction of the capacity performance technologies mentioned above. Within the scope of both projects field trials for the experimental characterisation of WiMAX propagation in different environments was addressed. This research activities resulted into the publication of three book chapters [25], [26] and [27], three journal papers [28], [29], [30], six conference proceeding papers [31], [32], [33], [34], [35], [36], two COST 2100 [37] and [38], and one COST IC 1004 [39] communications, and one journal paper submission [40].

Contributions given within Opportunistic-CR framework also include the transmitted power formulation for the optimization of carrier aggregation (CA) in LTE-Advanced (LTE-A) networks. This proposal accounts for a formulation to compute the transmitter power needed to cover cells of different sizes whilst maintaining the average signal to interference-plus-noise ratio (SINR) constant, and near the maximum. As such, small cell radii require lower transmitter power than their counterparts with larger radii to achieve similar average cell SINR and coverage. This research was published in conference proceeding [41], two COST communications [42] and [43], and submitted to a journal paper [47].

The proposal for an integrated CRRM entity that implements multi-band scheduling functionalities in the context of inter-band CA was addressed in the scope of the CREaTION project. The aim of the iCRRM entity is to satisfy user's QoS and QoE requirements, as well as, improve spectral efficiency through optimized inter-band scheduling. The iCRRM performance is evaluated in terms of packet loss ratio, delay, QoE, goodput (application level throughput) and a cost/revenue analysis. This research has been published in a conference

proceeding paper [44], two COST action communications [45] and [46], and is part of the work accepted for journal paper publication with minor revisions in [47], and submitted to a journal paper in [48].

A list of the publications organized chronologically and by type is given in the following tables. Table 1.1 addresses the contributions given to COST actions. Table 1.2 presents the conference proceedings paper. Table 1.3 presents the published book chapters. Finally, Table 1.4 shows journal papers.

Table 1.1 Contributions to COST actions.

Year	Title
2010	Marina Barbiroli, Claudia Carciofi, Vitorio Esposti, Franco Fuschini, Paolo. Grazioso, Doriana Guiducci, Daniel Robalo, Velez, F. J., "Characterization of WiMAX Propagation in Microcellular and Picocellular Environments", *11th Meeting of the Management Committee of COST2100 - Pervasive Mobile & Ambient Wireless Communications*, TD(10)11007, Denmark, Aalborg, June 2010.
2010	Daniel Robalo, Valeria Petrini, João Oliveira, Fernando J. Velez, Marina Barbiroli, Claudia Carciofi, Paolo Grazioso, Franco Fuschini, "Experimental characterisation of WiMAX propagation in different environments", *12th Meeting of the Management Committee of COST2100 – Pervasive Mobile & Ambient Wireless Communications*, TD(10)12030, Bologna, Italy, Nov. 2010.
2011	Daniel Robalo, Fernando J. Velez, "Characterization of Parameters for Wireless Networks Services and Applications", *3rd Meeting of the Management Committee of COST TERRA-Techno-Economic Regulatory Framework for Radio Spectrum Access for Cognitive Radio Software Defined Radio, WG1*, Brussels, Belgium, June 2011.
2012	Fernando J. Velez, João Oliveira and Daniel Robalo, Oliver Holland and Hamid Aghvami, "Energy Saving in the Optimization of the Planning of Fixed WiMAX with Relays in Hilly Terrains: Impact of Sleep Modes and Cell Zooming", *5th Meeting of the Management Committee of COST IC 1004 - Cooperative Radio Communications for Green Smart Environments*, TD(12)05025, Bristol, UK, Sep. 2012.
2012	Jessica Acevedo, Daniel Robalo and Fernando J. Velez, "Transmitted Power Formulation for the Implementation of Spectrum Aggregation in LTE-Advanced over 800 MHz and 2 GHz Frequency Bands", *6th Meeting of the Management Committee of COST TERRATechno-Economic Regulatory Framework for Radio Spectrum Access for Cognitive Radio Software Defined Radio, WG2*, Brussels, Belgium, Nov,. 2012.
2013	Daniel Robalo and Fernando J. Velez, "Wireless Networks Services and Applications Parameters Characterization and Model for the mapping between the Quality of Service and Experience for multimedia applications", *8th Meeting of the Management Committee of COST IC 1004 - Cooperative Radio Communications for Green Smart Environments*, TD(13)08069, Ghent, Belgium, Sep. 2013.
2013	Jessica Acevedo, Daniel Robalo and Fernando J Velez, "Cost/Revenue Performance of LTE Employing Spectrum Aggregation with Multi-Band User Allocation over Two Frequency Bands",*.8th Meeting of the Management Committee of COST TERRA- Techno-Economic Regulatory Framework for Radio Spectrum Access for Cognitive Radio Software Defined Radio, WG2*, Biel, Switzerland, Nov. 2013.
2014	Jessica Acevedo Flores, Daniel Robalo, Fernando J. Velez, "Transmitted Power Formulation for the Implementation of Spectrum Aggregation4in LTE-A over 800 MHz and 2 GHz Frequency Bands", *9th Meeting of the Management Committee of COST IC 1004 - Cooperative Radio Communications for Green Smart Environments*, TD(13)09079, Ferrara, Italy, Feb. 2014.
2014	Jessica Acevedo Flores, Fernando J. Velez, Orlando Cabral, Daniel Robalo, Oliver Holland, Hamid Aghvami, Filippo Meucci, Albena Mihovska, Neeli R. Prasad and Ramjee Prasad, "Cost/Revenue Performance in an IMT-Advanced Scenario with Spectrum Aggregation Over Non-Contiguous Frequency Bands", *9th Meeting of the Management Committee of COST IC 1004 - Cooperative Radio Communications for Green Smart Environments*, TD(13)09080, Ferrara, Italy, Feb. 2014.

Table 1.2 Conference proceeding papers.

Year	Title
2010	Marina Barbiroli, Claudia Carciofi, Vitorio Esposti, Franco Fuschini, Paolo. Grazioso, Doriana Guiducci, Daniel Robalo, Fernando J. Velez, "Characterization of WiMAX Propagation in Microcellular and Picocellular Environments", in *Proc. of European Conf. on Antennas & Propagation - EUCAP*, Barcelona, Spain, Apr. 2010.
2010	Frederico Varela, Pedro Sebastião, Américo Correia, Francisco Cercas, Fernando J. Velez, Daniel Robalo; "Unified Propagation Model for Wi-Fi, UMTS and WiMAX Planning in Mixed Scenarios", in *Proc. of PIMRC 2010 21st Annual IEEE International Symposium on Personal, Indoor and Mobile Radio Communications,* Istanbul, Turkey, Sep. 2010.
2010	Frederico Varela, Pedro Sebastião, Américo Correia, Francisco Cercas, Fernando J. Velez, Daniel Robalo; "Validation of the Unified Propagation Model for Wi-Fi, UMTS and WiMAX Planning", in *Proc. of PIMRC 2010 21st Annual IEEE International Symposium on Personal, Indoor and Mobile Radio Communications,* Istanbul, Turkey, Sep. 2010.
2011	Daniel Robalo, João Oliveira, Fernando J. Velez, Valeria Petrini, Marina Barbiroli, Claudia Carciofi, Paolo Grazioso, Franco Fuschini, "Experimental characterisation of WiMAX propagation in different environments", in *Proc. of EUROCON and Conftele' 2011 - International Conference on Computer as a Roll*, Lisbon, Portugal, Apr. 2011.
2011	Daniel Robalo, Fernando J. Velez, "Model for the Correlation between Quality of Service and Experience in Cognitive Radio Networks", (invited paper) in *Proc. of International Symp. on Applied Sciences in Biomedical and Communication Technologies - ISABEL-CogART,* Barcelona, Spain, Oct. 2011.
2012	Fernando J. Velez, João Oliveira, Daniel Robalo, Oliver Holland and Hamid Aghvami, "Energy Saving in the Optimization of the Planning of Fixed WiMAX with Relays in Hilly Terrains: Impact of Sleep Modes and Cell zooming", (invited paper) in *Proc. of ISWCS 2012 - The Ninth International Symposium on Wireless Communication Systems (invited Session on Green Wireless Communications)*, Paris, France, Aug. 2012.
2012	Fernando J. Velez, João Oliveira and Daniel Robalo, Oliver Holland and Hamid Aghvami, "Cost/Revenue Optimization of WiMAX Networks with Relay Power Saving Modes: Measurement-Based Scenario in a Hilly Region", in *Proc. of Globecom 2012 - Global Communications Conference Exhibition & Industry Forum*, Anaheim, CA, USA, Dec. 2012.
2013	Jessica Acevedo Flores, Daniel Robalo and Fernando J. Velez, "Transmitted Power Formulation for the Implementation of Spectrum Aggregation in LTE-A over 800 MHz and 2 GHz Frequency Bands", in *Proc. of WPMC 2013 - International Symposium on Wireless Personal Multimedia Communications*, Atlantic City, New Jersey, USA, June 2013.
2014	Jessica Acevedo Flores, Fernando J. Velez, Orlando Cabral, Daniel Robalo, Oliver Holland, Hamid Aghvami, Filippo Meucci, Albena Mihovska, Neeli Rashmi Prasad and Ramjee Prasad, "Cost/Revenue Performance in an IMT-Advanced Scenario with Spectrum Aggregation Over Non-Contiguous Frequency Bands", in *Proc. of International Conference on Telecommunications 2014 (ICT 2014)*, Lisboa, Portugal, 5-7 May 2014.
2014	Daniel Robalo, Fernando J. Velez, "A Model for Mapping between the Quality of Service and Experience for Wireless Multimedia Applications", in *Proc. of IEEE 79th Vehicular Technology Conference*, Seoul. Korea, May 2014.

Table 1.3 Book chapters.

Year	Title
2010	Fernando J. Velez, Pedro Sebastião, Rui Costa, Daniel Robalo, Cláudio Comissário, António Rodrigues, Hamid Aghvami, "Radio and Network Planning", Chapter 8 in the book *WiMAX Networks: Techno-Economic Vision and Challenges*, edited by Ramjee Prasad and Fernando J. Velez, Springer, 2010, ISBN: 978-90-481-8751-5.
2010	Fernando J. Velez, M. Kashif Nazir, Hamid Aghvami, Oliver Holland, Daniel Robalo, "System capacity", Chapter 9 in the book *WiMAX Networks: Techno-Economic Vision and Challenges*, edited by Ramjee Prasad and Fernando J. Velez, Springer, 2010, ISBN: 978-90-481-8751-5.
2010	Fernando J. Velez, M. Kashif Nazir, Ramjee Prasad, Hamid Aghvami, Oliver Holland, Daniel Robalo, "Business Models and Cost/revenue Optimization", Chapter 10 in the book WiMAX Networks: *Techno-Economic Vision and Challenges*, edited by Ramjee Prasad and Fernando J. Velez, Springer, 2010, ISBN: 978-90-481-8751-5.

Table 1.4 Journal papers.

Year	Title
2009	Pedro Sebastião, F. Velez, Rui Costa, Daniel Robalo, Cláudio Comissário and Antonio Rodrigues, "Planning and Deployment of WiMAX and Wi-Fi Networks for Health Sciences Education", *Telektronikk*, vol. 105, no. 2, pp. 173-185, 2009.
2010	Pedro Sebastião, Fernando J. Velez, Rui Costa, Daniel Robalo and António Rodrigues, "Planning and Deployment of WiMAX Networks", *WIRE - Wireless Personal Communications*, vol. 55, no.3, pp. 305-323, Nov. 2010.
2011	Fernando J. Velez, M. Kashif Nazir, Hamid Aghvami, Oliver Holland, Daniel Robalo, "Cost/Revenue Trade-off in the Optimization of Fixed WiMAX Deployment with Relays", *IEEE Transaction on Vehicular Technology*, vol. 60, no. 1, pp. 298-312, Jan. 2011.
2014	Daniel Robalo, João Oliveira Fernando J. Velez, Oliver Holland and Hamid Aghvami, "Dynamic Configuration and Optimization of WiMAX Networks with Relay Power Savings Modes: Measurement-Based Scenario in a Hilly Region", submitted to *Wireless Personal Communications*, Feb. 2014.
2014	Jessica Acevedo, Daniel Robalo, Fernando J. Velez, "Transmitted Power Formulation for the Optimization of Spectrum Aggregation in LTE-A over 800 MHz and 2 GHz Frequency Bands", accepted for publication with minor revisions *in Special Issue of the Wireless Personal Communications Journal*, July 2014.
2014	Daniel Robalo, Fernando J. Velez, "Enhanced Multi-Band Scheduling for Carrier Aggregation in LTE-Advanced Scenarios" submitted to *Special Issue on Technical advances in the design and deployment of future heterogeneous networks of EURASIP Journal on Wireless Communications and Networking*, Aug. 2014.

1.5 Structure of the Thesis

This thesis is organized into seven chapters, including this one. Chapter 2 presents an extended survey on the characterization of applications and deployment scenarios for concatenated multiple mesh networks with different technologies usage. Following this characterization, the parameters that most impact the user's service quality are identified. The following Sections present performance targets for audio, video and data applications extracted from ITU-T G.1010 recommendation, 3GPP TS 22.105 and EU-MESH, as well as detailed information on the characterization of voice and video application, defined by the WiMAX Forum Application Working Group. Finally, the proposed requirements for services and applications are defined based on the analysis and update from the previous Sections, followed by some final remarks and conclusions.

Chapter 3 proposes an innovative model for the mapping between the QoS and QoE for multimedia applications. Gaming, web-browsing, video and audio applications are considered. A unified model is proposed for all applications. MOS experiments have been considered for gaming and video applications. The model for web-browsing and audio applications considers ITU-T recommendations since no MOS results were available. The proposed MOS fittings have been verified by means of regression analysis by computing the mean square error, as wells as the coefficients of determination and correlation. These terms provide a measure of how well the model fits to experimental MOS measurements. Finally conclusions are presented and possible enhancements of the unified model are discussed.

Chapter 4 addresses the planning and optimization of fixed WiMAX networks with RSs. Section 4.2 presents the formulation for the UL and DL signal-to-noise-plus-interference ratio

in the presence and absence of RSs, considering the co-channel interference in the worst-case. Section 4.3 presents the modelling of the propagation environment by means of field trials at 3.5 GHz. The transmitter, the receiver equipment and the measurement methodology are fully described. The path loss exponent computation is defined by considering the influence of the transmitter power and gains from the antennas, as well as the influence of the inclination of the subscriber antenna, into the received power. Besides, Section 4.3 also discusses on the system capacity by introducing an innovative structure for uplink and downlink sub-frames with deployed RSs, for omnidirectional and tri-sectored BS. Section 4.4 addresses the formulation for the supported cell/sector physical throughput and shows the comparison of the equivalent supported throughput between the cells with RSs and the zoomed-out cells, $K = 3$. Section 4.6 addresses the cellular planning in the hilly terrain of Covilhã. The percentage of area not covered and supported throughput obtained from Winprop™, through ray tracing and the dominant path model, are presented for the omnidirectional and tri-sectored cases. Finally, Section 4.5 presents some final conclusions.

Chapter 5 investigates energy efficiency and economic implications in WiMAX deployments of the use of power saving modes for RSs in conjunction with cell zooming. Section 5.2 introduces the considered economic cellular models. Sections 5.3 and 5.4 present the costs hypothesis and assumptions in the presence and absence of RSs, respectively. Section 5.5 shows the economic and environmental impact of cell zooming. The power consumption parameters are presented for the RSs and both omnidirectional and tri-sectored BSs. The energy and respective cost reduction are computed, in a scenario where during the night periods and weekends, when the traffic exchanged is low, RSs are zoomed in to zero, by switching the RS equipment off, and the central BS coverage zone is zoomed out to maintain coverage. Finally, a comparison is drawn for the economic performance between omnidirectional (three carriers) and tri-sectored (one carrier/sector) BSs, in the presence of RSs and with the central BSs coverage zone zoomed out (while RSs coverage zone zooms in to zero), under the same total bandwidth, in the DL and $K = 3$. Finally, Section 5.6 draws some conclusions.

Chapter 6 addresses an integrated Common Radio Resources Management (iCRRM) entity which implements LTE-A inter-band Carrier Aggregation (CA) by performing scheduling between two Component Carriers (CCs), aiming to increasing users' quality of service and experience while improving spectral usage. To guarantee energy efficiency and comparable results for different cell radii, a formulation for the computation of the normalized transmitter power is presented. This formulation allows for obtaining a constant average cell SINR throughout different cell radii. Additionally, iCRRM may use two multi-band schedulers, the general multi-band schedulers (GMBS) operates in parallel with a classic downlink packet schedulers, in this case users may only be allocated to one carrier at the time. The enhanced multi-band schedulers (EMBS) operates on its own and may allocate users to both bands. A detailed analysis of CA performance is presented by evaluating simulation results considering the packet loss ratio, delay, goodput and quality of experience with and without CA.

Moreover, iCRRM's spatial distribution and allocation of radio resources is also analysed, i.e., the average percentage of users allocated geographically in the cell on each frequency band and the equivalent supported goodput.

Finally, Chapter 7 presents the conclusions on the research carried out throughout this thesis, as well as, some final remarks and suggestions for further research.

Chapter 2

Deployment Scenarios and Characterization Parameters for Concatenated Ubiquitous Wireless Mesh Network Applications

2.1 Introduction

The permanent evolution of wireless network technologies, with new standards that allow for increased data rates and wider coverage areas, motivates a high usage of diverse wireless network technologies, even at the level of network operators. From the network side, the replacement of cable backbone wireless solutions is becoming attractive. Besides, in zones whose access is difficult and there is no cable access yet, wireless technologies may be themselves a profitable solution. Mesh networks may allow for coverage enhancement, with very low transmitter powers, while supporting very high system capacity.

In the framework of this thesis, a survey is presented on the requirements defined by some of the major regulator parties, i.e., ITU-T and 3GPP. Moreover, the work described in this chapter was also performed within Ubiquimesh project's [14] scope, which addressed wireless ubiquitous concatenated mesh networks. The perspectives on services and applications requirements specified by EU-MESH, 7th Framework Programme Working Group (FP7 WG) European project [51] have also been considered, and recommendations from the ITU-T [49] and 3GPP [50] have also been taken into account. Some applications and characterization for video and voice encoding presented by the WiMAX Forum have also been considered. Based on this initial survey, the requirements for services and applications of ubiquitous multiple wireless mesh networks were proposed. This proposal takes into account (and merges) all previous gathered information, video and voice DL/UL were thoroughly updated according to compression and encoding information techniques provided by the WiMAX Forum [55].

The main QoS key parameters, delay, delay variation, information loss and throughput have been considered for the proposed applications characterization. Considering that next generation wireless networks should provide superior data rates, the targeted throughput, DL and UL speeds were chosen by considering the highest values provided by the ITU [49], 3GPP [50], EU-MESH [51] and the WiMAX Forum [55].

2.2 Scenarios

This Section addresses the definition of the scenarios for ubiquitous mesh networks with different technologies usage. Due to the similarities between the objectives of the FP7 WG EU-MESH and Task 1.1 of Ubiquimesh projects, these scenarios are extracted from [51]. Although in the near future it is expected to witness an increasing evolution of mesh network technologies, with an intense research and high user demand, there is however the risk of limitations of mobility support in IEEE 802.16 nodes, and the multiple uses of different 3G/4G backhaul technologies is also considered.

2.2.1. Mobile Business User Scenario

The mobile business user scenario involves access to services and applications by business users that are on the move [51]. ITU defines user mobility as the user's ability to maintain the same identity irrespective of the terminal used and its network attachment point. The key characteristic from the user point of view is seamless mobility. The user/terminal is able to change the network access point, as he/it moves, without interrupting the current service session, i.e., handovers are possible.

In the "mobile usage" case, the user is moving at a pedestrian, vehicular or train speed and has active service sessions. One can distinguish the pedestrian/vehicular case from the train case. In the first situation, as they cannot pay too much attention to the mobile device, users can use their smart-phones or PDAs for making VoIP calls or for accessing streaming audio from anywhere, and any time. In the second case, as they can work while moving, users can use their laptops (smartphones or PDA) for accessing not only the previous services but also a full range of corporate services and information, or for running real time multimedia application (video and audio). Consequently, employees, partners, suppliers and customers gain the ability to access or update critical data and complete commercial transactions through wireless devices.

The network requirements derived from this scenario are the following ones [51]:

- Efficient and scalable QoS support, including prioritization, controlled jitter and latency, and reduced packets loss for voice and multimedia traffic;
- Network traffic monitoring and tuning to provide the requested QoS by an estimation of the network's load;
- Mechanisms for secure and fast handoffs between heterogeneous networks and different operators;
- Mechanisms for (automatic) re-authentication during handover. This requirement applies particularly to the Virtual Private Network (VPN) services scenario;
- Reliability/availability, the system should be able to adapt to varying network conditions and should provide security mechanisms to ensure high reliability and availability;

- Scalability;
- Cost effectiveness.

2.2.2. Nomadic Business User Scenario

Nomadic businesses users are people moving from place to place, who require information exchange and communication services available for business purposes when they stop moving [51]. In this scenario, users have to suspend an application or session and resume it when they connect to a new access point at the next location.

Whilst nomadic business users increasingly need access to their corporate networks, it is the small and medium sized businesses that recognise the immediate benefit. Many of these businesses are either being operated from home, or are businesses with customers, premises and collaborators in multiple urban locations.

The network requirements share most of the key points with the previous scenario and are listed below [51]:

- Efficient and scalable QoS support, including prioritization, controlled jitter and latency and improved loss packets for voice and multimedia traffic;
- Network traffic monitoring and tuning to provide the requested QoS by an estimation of the network's load;
- Mechanisms for fast (automatic) re-authentication between different operators. This requirement applies particularly to the VPN services scenario;
- Reliability/availability, the system should be able to adapt to varying network conditions and should provide security mechanisms to ensure high reliability and availability;
- Scalability;
- Cost effectiveness.

2.2.3. Gaming User Scenario

Online games are played over some form of computer network, typically on the Internet. Online gaming offers both the ability to play with other users (co-op or competitive multiplayer) or alone (single-player) [51].

There are multiple online games types, the most well-known are as follows:

- First person shooter games;
- Real-time strategy games;
- Massively multiplayer games, including role playing games, social games etc.

Cross platform online games are not usual but some exist, they allow consoles (Xbox, PlayStation or Nintendo) or PC users to connect to the game. Users playing online games need a broadband connection with adequate throughput, low latency and jitter.

The network requirements for this scenario are [51]:

- low delay and low jitter;
- higher uplink rates;
- predictable QoS.

2.2.4. Fixed Home User – Leisure Activity Scenario

Mesh networks can serve the typical needs of the Internet user at home. However, the home usage depends on the habits from each person. One the one hand, the average low usage level is the occasional user who sends and receives mails as well as browses the web and sometimes concludes e-commerce transactions, not necessarily on a daily basis. On the other hand, an advanced user has increased requirements in terms of performance and traffic load. The services he is using go far beyond the web, and include Voice over IP (VoIP) telephony, sharing of multimedia content, peer-to-peer (P2P), participation into online communities, etc. The assumed user scenario is the following [51]:

1) The user arrives home after a vacation. As soon as he enters his apartment, his mobile phone switches from Global System for Mobile (GSM) network to his residential Wireless Fidelity (WiFi) Access Point and logs-in to his own Session Initiation Protocol (SIP) server/gateway. The message waiting indicator on his phone blinks, after all these days of absence he has a lot of messages stored in his telephone appliance;
2) The user is utilizing a GSM/WiFi phone with a SIP telephony client. He has also installed at home an IP telephony appliance and has a subscription to a VoIP provider. The connection of this appliance to the VoIP provider needs VoIP class QoS;
3) He turns on his internet stereo and tunes to some jazz music before browsing his voice messages. His stereo utilizes a smart P2P client that at the same acts as a relay for other users. His music provider is employing P2P networking in order to both reduce his own infrastructure costs and at the same time provide better quality to the end users;
4) He fires up his computer to check his social networking website. He decides to update his blog about his vacation. While writing, he uploads photos and videos from his camera to accompany the text.

The network requirements for this scenario are listed below [51]:

- Efficient and scalable QoS support;
- Availability;
- Scalability;
- Cost-effectiveness.

2.2.5. Fixed Home User – Entertainment Activity Scenario

Broadband access in fixed environments is increasingly utilised for activities related to entertainment, mainly music, television over IP and video (streaming or on demand) [51]. Both the technological and market trend lead the way towards increased penetration of triple-play services. A usage scenario can include the case of the fixed home in which [51]:

- The user has the necessary IP-enabled multimedia equipment (Set-Top-Box, STB) at his home to view videos, TV programmes and listen to music;
- The user has on-demand access to multimedia (movies, music, etc.) content through content providers;
- The user has access to streaming content and time-shifting viewing capabilities.

The network requirements derived from this scenario are [51]:

- High DL speeds, with prioritization and controlled jitter;
- Efficient and scalable QoS support;
- Availability;
- Scalability;
- Cost-effectiveness.

2.2.6. Tourist/Attraction Visitor Scenario

The tourist info system/attraction visitor scenario delivers services and free (or low cost) public access based on the location information and the user personal profile [51]. It also allows people to share their multimedia files (photographs, video, text, etc.) with locations on electronic maps with other users. A user can add pictures to a certain point of the map by clicking on the map and browsing the image files corresponding to this location. The user can dynamically add, modify, or delete comments on a certain multimedia file, change its permission, and rate its content. He can search for multimedia files using criteria based on location and rating. The local user can view the files, reviews and rates included in the response of another person.

Several examples of services proposed to the user are as follows [51]:

- Multimedia content (music, photo or video) sharing both synchronously and asynchronously;
- Location-based on-demand services: nearby points of interest, search engines (transportation, restaurant, events, weather), travel directions, location discovery and localized maps;
- Proximity-based notification (push or pull). The latter includes push services such as targeted advertising (i.e., events) or automatic airport check-in, and push/pull facilities like common profile matching (i.e., ad hoc grouping for visiting an exhibition) or buddy list;

- Proximity-based actuation (push or pull). These services concern payments based upon proximity, like electronic toll collection.

The tourist/attraction visitor scenario is a very relevant example of context-aware application for both nomadic/mobile users. The context variables that play an important role in this scenario are the following [51]:

- Interest - the personal interest of the user that direct the search for relevant points of interest and events;
- Location - to find nearby points of interest;
- Visiting history - information about places that the user has already visited before.

From the user perspective the requirements for this scenario are [51]:

- Ubiquitous access - the network should be easily accessible from everybody;
- Access anytime/anywhere - network access is assured at all times and from all locations;
- User mobility.

The network perspective requirements are listed below [51]:

- User positioning - the system should autonomously detect the user position;
- High UL speed - the system should support the transmission of large quantities of data;
- Resilience to operational anomalies and security attacks, as it should work in a multi-operator environment;
- High availability;
- Scalability;
- Cost-effectiveness.

2.2.7. Video Surveillance/Home Monitoring Scenario

Wireless networks can also address video surveillance. To better elaborate this remark, one can consider the following example: assume a large apartment house, 6 floors, 3 stairways and entrances, underground parking garage. Most of the apartments are owned by the inhabitants. The owners deployed a new surveillance, monitoring equipment based on a new mesh network environment. The preliminary requirements of the owners include the following [51]:

- They need a cheap solution, therefore they want to save costs on wires;
- An operator will be contracted to build and maintain the mesh network;
- A large number of cameras are needed to provide enough coverage to track illegal activities;

- They want a modern, digital system, no matter how the equipment works; it has to be digital, widely reachable, digitally achievable, etc.;
- Digital recordings use high bandwidth to provide quality, 24 fps, video resolution (e.g., 640x480), multiple (~30) cameras;
- For cost savings, a group of owners will be selected as administrators of the system. These owners will be responsible to look back previous recordings or watch for real-time events if special conditions occur. The members of the administrative group might change in time, therefore a flexible solution is needed;
- Some of the administrators want to be able to watch for events in real time through the internet from their workplace;
- An official security firm will be contracted to lookout for security events with the usage of combined information of the video surveillance, fire protection and burglar alarm system of the house. For this purpose, high speed connectivity with high upload rate should be provided by the house;
- Personnel of the security firm will patrol in the area and check the contracted buildings if needed. During the patrol, the personnel should have access to the camera video feed of any of the protected houses;
- In emergency conditions, the administrators of the system should be able to access the surveillance system through mobile computers throughout the house;
- At some places in the house, particularly in the underground garage, there is no GSM/3G coverage. The owners or administrators still want to get access to the internet and also to VoIP providers, therefore in emergency situations, they can report the event (to official emergency service, or just to the other administrators, local personnel, or contracted security firm) from every place in the house. (e.g., by WiFi based VoIP phones);
- High quality images from the cameras need high bandwidth for storing and for real-time delivery to remote and local users. This bandwidth is "upload" direction from the internal network.

To achieve owner's requirements, wireless mesh network architecture can be established, with the following features and characteristics [51]:

- Mesh routers are set up at every floor, they are interconnected through wireless links;
- The network is built and maintained by a network operator. The operator provides access to the mesh network and the internet. The operator also provides the necessary security services, such as authorized access to the network resources;
- The mesh network operator provides services in multiple houses in the area, which are interconnected to each other providing extra bandwidth for mesh-internal resources, such as the surveillance system of the different houses;

- Every camera uses IP protocol to deliver pictures and they are connected to the next access point by wire or wireless manner;
- Central servers (or PC computers) collect and store the incoming information through the mesh network;
- The mesh network provides mobility. The security personnel of the security services company can access any of the video streams of any of the nearby houses. The video quality might be very high, especially in the houses that joined into a single mesh network in the area;
- Every flat owner can connect to the mesh network, the administrators are allowed to watch the real-time streams and stored recordings, the reconfiguration of the administrators is easy;
- The network is highly resilient. The lack a single mesh router, or a problem on a separate internet gateway does not harm the stability of the service, therefore it is more likely to be protected against direct attacks and occasional failures;
- The administrators with notebooks and VoIP based phones can roam through the house and are connected to the network, to the surveillance system and to the VoIP based phone service constantly.

2.2.8. Mobile Commerce Scenario

The term m-commerce refers to a set of applications offered to mobile users that allow them to buy goods and services using their handheld devices through wireless network access [51].

Some examples of m-commerce applications include mobile ticketing, mobile coupons, information services, fleet-tracking, etc. These applications require ubiquitous Internet access, however nowadays this is still quite expensive for the general public. Hence, m-commerce applications are currently mainly used by business users only. One of the main advantages of mesh networks is that they can provide ubiquitous Internet access at a reduced cost. Therefore, mesh networks can foster the wider deployment and usage of m-commerce applications. The following m-commerce usage scenarios are specific examples [51]:

- Mobile ticketing - The owner of a smart phone wants to buy a cinema ticket. The cinema complex provides its program through location based services. Thus, the customer does not have to search for the webpage of the cinema. Without staying in a queue at the box office, she selects the show that she is interested in, and buys the ticket using her phone and her wireless internet access. The cinema can later validate the customer's ticket using inexpensive WiFi connections at the gates;
- Mobile coupons - A chain of department stores wants to attract customers in its shops. In order to achieve that, it may disseminate electronic coupons near to its shops through the wireless mesh network. The prospective customers walking near to one of the shop receive the electronic coupons in their handhelds. When they enter

into any shops of the chain, they can validate their coupons. The chain of department stores can administrate the coupon dissemination in a centralized way and determine at which access points it wants to broadcast coupons. On the one hand, the mesh network provider can charge the chain for the usage of each access point. On the other hand, the chain can select the access points where the coupons are disseminated, which can be a larger area than the territory of the shops;

- Information services - Mobile users can receive a wide variety of information services. The services can be location based, namely, local traffic information, weather forecast, news, etc.;
- Fleet-tracking - The companies which can gain the most from the multiple mesh networks are the dispatch-rider companies. Due to the fleet-tracking and ever-online possibilities of the EU-MESH network, the companies can follow where the employers are and give new destinations for the better utilization of resources. The companies can detect and take advantage of special situations. For instance let's imagine a distribution company with two cars; the company can choose the vehicle closest to the destination to perform a delivery. In addition, the drivers can call each other at a flat rate using VoIP services.

The user and network requirements derived from this scenario are the following [51]:

- Privacy, no outsider or even none of the operators should be aware who buys what, what they are interested in, etc.;
- Confidentiality and integrity of payment messages, as well as the content of the m-commerce services;
- Efficient and scalable QoS support. This includes prioritization, controlled jitter and latency and improved loss packets for multimedia traffic;
- Network traffic monitoring and tuning to provide the requested QoS by an estimation of the network's load;
- Mechanisms for secure and fast handoffs between heterogeneous networks and different operators during a transaction;
- Mechanisms for (automatic) re-authentication during handover;
- Reliability/availability, the system should be able to adapt to varying network conditions and should provide security mechanisms to ensure high reliability and availability;
- Scalability;
- Cost effectiveness.

2.3 Key Parameters Impacting the User

ITU has already identified the parameters that most impact the users in [49]. This knowledge is necessary to provide adequate user QoS for different services. A typical user is not concerned with how a particular service is implemented. However, the user is interested in comparing the same service offered by different providers in terms of universal, user-oriented performance parameters [49]. According to the ITU, the main parameters impacting the user QoS are the delay, delay variation and information loss and are defined, according to [49], as follows:

Delay - delay manifests itself in a number of ways, including the time taken to establish a particular service from the initial user request and the time to receive specific information once the service is established. Delay has a very direct impact on user satisfaction depending on the application, and includes delays in the terminal, network, and any servers. Note that from a user point of view, delay also takes into account the effect of other network parameters such as throughput;

Delay variation - delay variation is generally included as a performance parameter since it is very important at the transport layer in packetized data systems due to the inherent variability in arrival times of individual packets. However, services that are highly intolerant of delay variation will usually take steps to remove (or at least significantly reduce) the delay variation by means of buffering, effectively eliminating delay variation as perceived at the user level (although at the expense of adding additional fixed delay);

Information loss - information loss has a very direct effect on the quality of the information finally presented to the user, whether it is voice, image, video or data. In this context, information loss is not limited to the effects of bit errors or packet loss during transmission, but also includes the effects of any degradation introduced by media coding for more efficient transmission (e.g. the use of low bit-rate speech codecs for voice).

2.4 Performance Considerations for Different Applications

Applications are generally classified by four different categories, audio, video, data and background, which, in turn, can be divided into various services, whose levels of quality are defined by the ITU. Additionally, this thesis considers a fifth category, the context-based information, inspired by EU-MESH.

2.4.1. Audio

The minimum quality for audio services is similar to ordinary telephony, i.e. the quality that allows a reasonable ease for understanding speech. However, for most audio services, the quality objectives are generally much higher, ranging from a good comfort for listening to speech to the highest quality in reproducing music or other sounds. A general

classification of audio into five quality levels, and a mapping to various services is given in [52], as shown below:

Conversational voice - Requirements for conversational voice are heavily influenced by one-way delay. In fact, there are two distinct effects of delay. The first is the creation of echo in conjunction with two-wire to four-wire conversions or even acoustic coupling in a terminal. This begins to cause increasing degradation to voice quality for delays of the order of tens of milliseconds, and echo control measures must be taken at this point (provision of echo cancellers, etc. [53]). The second effect occurs when the delay increases to a point where it begins to impact conversational dynamics, i.e., the delay in the other party responding becomes noticeable. This occurs for delays of the order of several hundred milliseconds [54]. However, the human ear is highly intolerant of short-term delay variation (jitter). As a practical matter, for all voice services, delay variation due to variability in incoming packet arrival times must be removed with a de-jitterizing buffer. Requirements for information loss are influenced by the fact that the human ear is tolerant to a certain amount of distortion of a speech signal. In IP-based transmission systems a prime source of voice quality degradation is due to the use of low bit-rate speech compression codecs and their performance under conditions of packet loss;

Voice messaging - Requirements for information loss are essentially the same as for conversational voice (i.e., dependent on the speech coder), but a key difference here is that there is more tolerance for delay since there is no direct conversation involved. The main issue therefore becomes one of how much delay can be tolerated between the user issuing a command to replay a voice message and the actual start of the audio. There is no precise data on this, but based on studies related to the acceptability of stimulus-response delay for telecommunications services, a delay of the order of a few seconds seems reasonable for this application. In fact, a distinction is possible between recording and playback, in that user reaction to playback is likely to have the more stringent requirement;

Streaming audio - is expected to provide better quality than conventional telephony, and requirements for information loss in terms of packet loss will be correspondingly tighter. However, as with voice messaging, there is no conversational element involved and delay requirements for the audio stream itself can be relaxed, even more so than for voice-messaging, although control commands must be dealt appropriately, such as in command/control, shown in Table 2.2.

2.4.2. Video

Video quality is a measure of the ability of a video transmission system to accurately reproduce moving scenes. Video services quality objectives are generally expressed in terms of spatial and temporal resolution. However, other parameters may also be relevant (e.g. distortion, signal loss or errors). A general classification of video into six levels of quality is proposed in [52], and a mapping to various services is given in below:

Videophone - as used here implies a full-duplex system, carrying both video and audio and intended for use in a conversational environment. As such, in principle the same delay requirements as for conversational voice will apply, i.e., no echo and minimal effect on conversational dynamics, with the added requirement that the audio and video must be synchronised within certain limits to provide "lip-synch". Once again, the human eye is tolerant to some loss of information, so that some degree of packet loss is acceptable depending on the specific video coder and amount of error protection used. It is expected that the latest MPEG-4 video codecs will provide acceptable video quality with frame erasure rates up to about 1 %;

One-way video - The main distinguishing feature of one-way video is that there is no conversational element involved, meaning that the delay requirement will not be so stringent, and can follow that of streaming audio;

Taking into account the above considerations, performance targets for audio and video applications are shown in Table 2.1.

2.4.3. Data

From a user point of view, a prime requirement for any data transfer application is to guarantee essentially zero loss of information. At the same time, delay variation is not generally noticeable to the user, although there needs to be a limit on synchronisation between media streams in a multimedia session, e.g. audio in conjunction with a white-board presentation. The different applications therefore tend to distinguish themselves on the basis of the delay which can be tolerated by the end-user from the time the source content is requested until it is presented to the user. The description of data services is given below:

Web-browsing - In this category one refers to retrieving and viewing the HyperText Markup Language (HTML) component of a Web page, other components, e.g., images, audio/video clips are dealt with under their separate categories. From the user point of view, the main performance factor is how quickly a page appears after it has been requested. Delays of several seconds are acceptable, but not more than about ten seconds;

Bulk data - This category includes file transfers, and is clearly influenced by the size of the file. As long as there is an indication that the file transfer is proceeding, it is reasonable to assume somewhat longer tolerance to delay than for a single Web-page;

High-priority transaction services (e-commerce) - The main performance requirement here is to provide a sense of immediacy to the user that the transaction is proceeding smoothly, and a delay of no more than a few seconds is desirable;

Command/control - Clearly, command/control implies very tight limits on allowable delay, much less than a second. Note that a key differentiator from conversational voice and video services with similar low delay requirements is the zero tolerance for information loss;

Still image - This category includes a variety of encoding formats, some of which may be tolerant to information loss since they will be viewed by a human eye. However, given that even single bit errors can cause large disturbances in other still image formats, it is

argued that this category should in general have zero information loss. However, delay requirements for still image transfer are not stringent and may be comparable to that for bulk data transfer, given that the image tends to be built up as it is being received, which provides an indication that data transfer is proceeding;

Interactive games - Requirements for interactive games are obviously very dependent on the specific game, but it is clear that demanding applications will require very short delays in the order of a fraction of a second, consistent with demanding interactive applications;

Telnet - Telnet is included here with a requirement for a short delay of a fraction of a second in order to provide essentially instantaneous character echo-back;

E-mail (server access) - Electronic mail (e-mail) is generally thought to be a store and forward service which, in principle, can tolerate delays of several minutes or even hours. However, it is important to differentiate between communications between the user and the local e-mail-server and server-to-server transfer. When the user communicates with the local mail server, there is an expectation that the mail will be transferred within a few seconds;

Instant messaging - Instant messaging primarily relates to text, but can also include audio, video and image. In any case, despite the name, it is not a real-time communication in the sense of conversational voice, and delays of several seconds are acceptable.

2.4.4. Background Applications

The only requirement for this type of application is that essentially error free information should be delivered to the user. However, there still is a delay constraint since, for any practical purpose, data is useless if it is received too late. The following services belong to the background applications list:

Fax – Facsimile (Fax) is included in this category since it is not normally intended to be an accompaniment to highly interactive real-time communication. Nevertheless, for so-called "real-time" fax there is an expectation in most business scenarios that a fax will be received within about 30 seconds. Delay for store and forward fax can be much higher. Note that fax does not require zero information loss;

Low priority transaction services - An example in this category is Short Message Service (SMS). Tens of seconds are an acceptable delivery delay value;

E-mail (server-to-server) - This category is included for completeness, since as mentioned earlier; the prime interest in e-mail is in the access time;

Usenet - It is a world-wide distributed discussion system. It consists of a set of "newsgroups" with names that are classified hierarchically by subject. "Articles" or "messages" are "posted" to these newsgroups by people on computers with the appropriate software. These articles are then broadcast to other interconnected computer systems via a wide variety of networks. This is a very low priority service, with corresponding relaxed delay requirements. However, it is desirable that messages are received by the user in the order that they are posted, to avoid seeing a reply prior to the original message.

Taking into account the above considerations, performance targets for data applications are summarised in Table 2.2.

2.4.5. Context-based Information

As mentioned earlier, besides the previous applications defined by the ITU, this Ph.D. thesis considers a fifth type, the context-based information application, which belongs to the location dependent services category. It includes services which are expected to play a significant role in emerging ubiquitous broadband access networks. The context-based information scenario was previously addressed in Section 2.2.6 (tourist/attraction scenario). The application performance targets are addressed in Section 2.6 and their description is listed below:

Location-based multimedia broadcast – Examples of this service is the broadcast of nearby points of interest, search engines (transportation, restaurant, events, and weather), travel directions, location discovery and localized maps;

Location-based interactive multimedia – This service shares similarities with the previous one, only the type of data broadcasted changes, i.e., music, photos or video;

Location-based on demand – in this case, only the type of information beforehand select by the user is broadcasted to him;

Alert/notification advertisement – This service includes push services such as targeted advertising (i.e., events, spots) or automatic airport check-in, and push/pull facilities like common profile matching (i.e., ad hoc grouping for visiting an exhibition) or buddy list;

Personalized content – This category includes the sharing of user's multimedia content both synchronously and asynchronously.

2.5 ITU-T and 3GPP Performance Targets

This Section presents the performance targets according to the ITU-T G.1010 [49] recommendation cross-referenced with the 3GPP TS 22.105 [50]. Furthermore, both consider the characterization of specific QoS parameters, i.e., the packet loss ratio (PLR), frame erasure rate (FER), bit error rate (BER), as shown in Table 2.1 and Table 2.2.

Table 2.1 Performance targets for audio and video applications (extracted from [49] and [50]).

Medium	Application	Degree of symmetry	Typical data rates [kbps]		Key performance parameters and target values			
			ITU	3GPP	One-way delay	Delay variation	Information loss[2]	Other
Audio	Conversational voice	Two-way	4-64	4-25	<150[1] ms preferred <400[1] ms limit	<1 ms	<3 % PLR	
	Voice messaging	Primarily one-way	4-32	4-13	<1 s for playback <2 s for record	<1 ms	<3 % PLR	
	High quality streaming audio	Primarily one-way	16-128[3]	5-128	< 10 s	<<1 ms	<1 % PLR	
Video	Videophone	Two-way	16-384	32-384	<150[4] ms preferred <400[4] ms limit		<1 % PLR	Lip-synch: <80 ms
	One-way	One-way	16-384		< 10 s		<1 % PLR	

[1] Assumes adequate echo control.
[2] Exact values depend on specific codec, but assumes use of a packet loss concealment algorithm to minimise effect of packet loss.
[3] Quality is very dependent on codec type and bit-rate.
[4] These values are to be considered as long-term target values which may not be met by current technology.

Table 2.2 Performance targets for data applications (extracted from [49] and [50]).

Application	Degree of symmetry	Typical amount of data (ITU)	Data Rate (3GPP)	Key performance parameters and target values		
				One-way delay (Note)		Information loss
				ITU	3GPP	
Web-browsing- HTML	Primarily one-way	~10 kB		Preferred < 2 s /page Acceptable < 4 s /page		Zero
Bulk data transfer/retrieval	Primarily one-way	10 kB-10 MB	<< 84 kbps	Preferred < 15 s Acceptable < 60 s	< 10 s	
Transaction services - high priority e.g. e-commerce, ATM	Two-way	< 10 kB		Preferred < 2 s Acceptable < 4 s		
Command/control	Two-way	~ 1 kB		< 250 ms		
Still image	One-way	< 100 kB		Preferred < 15 s Acceptable < 60 s	< 10 s	
Interactive games	Two-way	< 1 kB	< 60 kbps	< 200 ms	< 75 ms preferred	ITU: Zero 3GPP: <3 % FER preferred, < 5 % FER limit
Telnet	Two-way (asymmetric)	< 1 kB		< 200 ms	< 250 ms preferred	Zero
E-mail (server access)	Primarily one-way	< 10 kB		Preferred < 2 s Acceptable < 4 s		Zero
E-mail (server to server transfer)	Primarily one-way	< 10 kB		Can be several minutes		Zero
Fax ("real-time")	Primarily one-way	~ 10 kB		< 30 s/page		<10^{-6} BER
Fax (store & forward)	Primarily one-way	~ 10 kB		Can be several minutes		<10^{-6} BER
Low priority transactions	Primarily one-way	< 10 kB		< 30 s		Zero
Usenet	Primarily one-way	Can be 1 MB or more		Can be several minutes		Zero

Note – In some cases, it may be more appropriate to consider these values as response times.

2.6 EU-MESH Services and Applications Requirements

The European project EU-MESH has also defined services and applications requirements. This data is also based on ITU-T and 3GPP recommendations [51]. For comparison and additional information purposes EU-MESH's characterization is provided in Table 2.3 and Table 2.4.

Table 2.3 EU-MESH Requirements for Internet, conversational and streaming services [51].

Applications	DL/ UL traffic ratio	DL speed [kbps]	UL speed [kbps]	Interactive	Performance parameters			Transmission mode
					One-way delay	Delay variation	Loss ratio	
Basic Internet Services								
Web browsing	>>1	>500	4-25	Yes	<2 s/page (acceptable <4 s/page)		0%	Unicast
E-mail	1	>500	>500	No	<2 s (acceptable < 4 s)		0%	Unicast
File transfer	>>1	>1000	4-25	Yes	<15 s (acceptable < 60 s)		0%	Unicast
Telnet	1	4-25	4-25	Yes	<250 ms		0%	Unicast
Conversational Services								
VoIP, tele-conferencing	1	30-50	30-50	Yes	< 150 ms (limit <400ms)	<1 ms	<3 %	Unicast/ multicast
Video-telephony/ video-conferencing	1	32-384	32-384	Yes	< 150 ms (limit <400 ms)	<1 ms	<1 %	Unicast/ multicast
Instant messaging (IM)	1	4-25	4-25 kbps	Yes	<250 ms		0%	Unicast
Online chatting	1	4-25	4-25	Yes	<250 ms		0%	Unicast
Streaming Services								
IPTV	>>1	1-3 Mbps		No	<10 s	<2 ms	<1 %	Broadcast
Mobile TV	>>1	28-512		No	<10 s	<2 ms	<1 %	Broadcast
VoD (SD)	>>1	1-3 Mbps	<8	Yes	<10 s	<2 ms	<1 %	Unicast
VoD (HD)	>>1	6-10 Mbps	<8	Yes	<10 s	<2 ms	<1 %	Unicast
On-demand streaming media (MoD)	>>1	32-384	<8	Yes	<10 s	<2 ms	<1 %	Unicast
Internet radio	>>1	16-64			<10 s	<2 ms	<1 %	Broadcast
Video surveillance	>>1	32-384	<8	Yes	<2 s	<2 ms	<1 %	Unicast

Table 2.4 EU-MESH Requirements for interactive, multimedia and context-based services [51].

Applications	DL/ UL traffic ratio	DL speed	UL speed	Interactive	Performance parameters		Location-dependence	Transmission mode
					One-way delay	Loss ratio		
Interactive Services								
Interactive gaming	1	4-25 kbps	4-25 kbps	Yes	<250 ms	0%	No	Unicast
Real-time gaming	1	32-64 kbps	32-64 kbps	Yes	<75 ms	0%	No	Unicast
Voice mail	1	30-50 kbps	4-25 kbps	Yes	<2 s	<3%	No	Unicast
Collaborative working	>>1	>500 kbps	4-25 kbps	Yes	<2 s/transact.	0%	No	Unicast
ASP services	>>1	>500 kbps	4-25 kbps	Yes	<2 s/transact.	0%	No	Unicast
E-commerce	>>1	>500 kbps	4-25 kbps	Yes	<2 s/transact.	0%	No	Unicast
Control of remote devices	1	<28 kbps	<28 kbps	Yes	<10 s	0%	No	Unicast
Multimedia Sharing								
Peer-to-peer file sharing	1	>500 kbps	>500 kbps	Yes	<15 s (acceptable <60 s)	0%	No	Unicast
User-created content sharing	<1	32-64 kbps	>500 kbps	Yes	<2 s/upload	0%	No	Unicast
Context-based Information Services								
Location-based multimedia broadcast	>>1	32-384 kbps		No	<10 s	<1%	Yes	Broadcast
Location-based interactive multimedia	>>1	32-384 kbps	<8 kbps	Yes	<10 s		Yes	Unicast
Location-based on demand services	>>1	32-384 kbps	<8 kbps	Yes	<10 s	<1%	Yes	Unicast
Alert/notification, advertisement services	>>1	<28 kbps		No	<10 s	0%	Yes	Multicast
Presence-based applications	>>1	<28 kbps	<28 kbps	Yes	<10 s	0%	Yes	Unicast
Personalized content	>>1	32-64 kbps	<8 kbps	Yes		0%	Yes	Unicast

2.7 WiMAX Forum Application Working Group Views

The WiMAX Forum, more specifically the WiMAX Forum Application Working Group (AWG) has also characterized traffic models for simulation purposes of five application classes, as shown in Table 2.5.

The AWG defined these five classes of applications perceived by service providers as priority revenue-generating applications. These applications are characterized in terms of end-user performance requirements such as bandwidth, jitter, latency as well as network features such as QoS, security, reliability, and availability. These five classes of applications from a user perspective are the following [56]:

Class 1: Interactive Gaming: Low bit rate, real time, very bursty, asynchronous, asymmetric and interactive;

Class 2: VoIP and Video conferencing: Low to moderate bit rate, real time, synchronous, symmetric and interactive;

Class 3: Streaming Media: Low to high bit rate, non-real time, low jitter, synchronous, asymmetric and non-interactive;

Class 4: Instant Messaging, Web Browsing (Basic Internet Applications): Low to moderate bit rate, no information loss, asynchronous, asymmetric, moderate delay and interactive;

Class 5: File transfers, Media download: Low to high bit rate, no information loss, low priority, non-real time, asynchronous, asymmetric.

Table 2.5 WiMAX Application Classes, extracted from [55].

Class	Application	Bandwidth Guideline		Latency Guideline		Jitter Guideline	
1	Multiplayer Interactive Gaming	Low	50-85 kbps	Low	< 150 ms	Low	< 100 ms
2	VoIP & Video Conference	Low	4-384 kbps	Low	< 150 ms	Low	< 50 ms
3	Streaming Media	Low to High	5 kbps to 2 Mbps	N/A		Low	< 100 ms
4	Web Browsing & Instant Messaging	Moderate	10 kbps to 2 Mbps	N/A		N/A	
5	Media Content Downloads	High	> 2 Mbps	N/A		N/A	

Table 2.6 shows the types of subscribers, application-session attempts per application per day, and application-mix ratio among eighteen applications categorized in five application classes defined above. The application-mix ratio represents the distribution of applications that users will most likely use [58]. Moreover, Table 2.6 also shows three types of subscribers: consumer, enterprise, and machine. It assumes that 64 % of the total human subscribers are consumers, and the rest of the human subscribers are enterprise subscribers. Table 2.6 considers two different categories of mobile terminals that influence traffic and symmetry. Professionals tend to use terminals with high-resolution screens (high-complexity terminals) such as laptops and high-end PDAs for multimedia, where the accuracy and detail of the information is crucial. On the other hand, consumer subscribers have more interest in small, lightweight terminals, for which a high-resolution screen is not relevant. However, some exceptions may occur, e.g., when a consumer (with a small device) sends a photo to someone in the fixed network (e.g., as an e-mail attachment). Here, the recipient has a high-resolution screen and printer and so wants the picture at high resolution. The size and resolution of the screen significantly affect the data volume of the picture or video media intended for it.

A more in depth characterization of each class will not be presented in this thesis, however WiMAX Forum has voice and video applications extremely detailed and can provide additional information useful for the proposal of wireless mesh networks applications. Hence, for this purpose, classes 2 and 3 will be further detailed.

Table 2.6 Application mix ratio and subscriber distribution, extracted from [57].

Class #	WiMAX AWG class	Packet data applications	% of Subscribers actively using applications			Consumer (% of total subscribers)		Enterprise (% of total subscribers)		% of total machines
						64%		36%		100%
						Laptop PC	Smaller device	Laptop PC	Smaller device	
						30%	70%	70%	30%	
			Consumer	Enterprise	Machine	No. sessions/day/ subscriber				
1	Internet gaming	Quake II	25	5	0	0.15	0.15	0.05	0.05	0
		World of Warcraft	25	5	0	0.15	0.15	0.05	0.05	0
		Xbox TimeSplitter 2	25	5	0	0.15	0.15	0.05	0.05	0
		ToonTown	25	5	0	0.15	0.15	0.05	0.05	0
		VoIP	100	100	0	5.71	5.71	4.44	4.44	0
2	VoIP/Video Conference	Video Conference	50	100	0	0.30	0.30	0.27	0.27	0
		PTT	20	20	0	0.10	5.00	0.10	5.00	0
		Music/speech	100	100	0	0.08	0.08	0.12	0.12	0
3	Streaming media	Video clip	50	100	0	1.10	1.10	1.50	1.50	0
		Movie streaming	100	100	0	0.20	0.20	0.12	0.12	0
		MBS	100	0	0	1.00	1.00	0.10	0.10	0
		IM	100	100	0	7.26	7.26	7.26	7.26	0
		Web browsing	100	100	0	5.00	2.00	5.00	2.00	0
4	Information technology	E-mail (POP3)	50	50	0	0.65	0.65	1.50	1.50	0
		E-mail (IMAP)	50	50	0	0.65	0.65	1.50	1.50	0
		Telemetry	0	0	100	0.00	0.00	0.00	0.00	24
5	Media content download/ backup	FTP	50	100	0	2.00	0.10	2.00	0.10	0
		P2P	30.0	0.0	0.0	0.30	0.30	0.00	0.00	0

2.7.1. VoIP Traffic Model (Class 2)

There are a variety of encoding schemes for voice (i.e., G.711, G.722, G.722.1, G.723.1, G.728, G.729, and AMR) that result in different bandwidth requirements. Including the protocol overhead, it is very common for a VoIP call to require between 5 kbps and 64 kbps of bi-directional bandwidth.

The Adaptive Multi-Rate (AMR) codec is the most important vocoder in wireless applications being the newest vocoder for the existing GSM networks and it has been adopted

as a mandatory speech codec speech processing function in Universal Mobile Telecommunication System (UMTS).

2.7.2. Video Conference Traffic Model (Class 2)

Video conferencing has differing bandwidth requirements for the audio and the video components. For example, the audio component of a video-conference requires between 16 and 64 kbps and the video component of a video-conference requires between 320 kbps and 1 Mbps. The typical sustainable send/receive throughput requirements ranges from 32 kbps to 1 Mbps. A typical business-quality videoconference runs at 384 kbps and can deliver TV-quality video at 25 to 30 frames per second.

H.264 is the next-generation video compression technology in the MPEG-4 standard, and it can match the best possible MPEG-2 quality at up to half the data rate. H.264 also delivers excellent video quality across the entire bandwidth spectrum from 3G to High Definition (HD) and everything in between (from 40 kbps to upwards of 10 Mbps). HD MPEG-2 content at 1920x1080 traditionally runs at 12-20 Mbps, while H.264 can deliver 1920x1080 content at 7-8 Mbps at the same or better quality. H.264 provides Digital Versatile Disc (DVD) quality at about half the data rate of MPEG-2. Because of this efficiency H.264 stands to be the likely successor to MPEG-2 in the professional media industry.

MPEG compressed videos are composed of pictures (frames) that are separated into three different types: I, B, and P. I frames are intra-frames that encode the current picture, while B and P frames interpolate from previous and future frames. When transmitted over an IP network, these frames are segmented into one or more IP packets. For a mobile device, the MPEG encoder may not generate B frames and the distance between I frames could be longer than 10 seconds.

The H.264 surpasses H.261 and H.263 in terms of video quality, effective compression and resilience to transmission losses, giving it the potential to halve the required bandwidth for digital video services over the Internet or 3G Wireless networks. H.264 is likely to be used in applications such as Video Conferencing, Video Streaming, Mobile devices, Tele-Medicine etc. Current 3G mobiles use a derivate of MPEG-4.

Based on the compression efficiency and market acceptance as described above, MPEG-4 has been selected for the video codec. The estimated values, for the parameters to model a video stream, vary from one trace to another. In this model two different resolutions for the display were considered: 176x144 for a small device and 320x240 for a large device. The required bandwidth for the uncompressed video stream with 176x144 pixels and 8-bit colour depth is about 7.6 Mbps and with 320x240 pixels and 8-bit colour depth is about 23 Mbps. Table 2.7 presents a summary of the details assumed for the two resolutions from the WiMAX Forum Video Conference Traffic Model.

Table 2.7 Video Conference Traffic Model [55].

Display size	**176x144**	**320x240**
Colour depth (bit)	8	8
Subsampling method	4:1:1	4:1:1
Mean BW for Uncompressed stream	7.6 Mbps	23 Mbps
Compression ratio	13.95	13.95
Mean BW for compressed stream	0.54 Mbps	1.65 Mbps

2.7.3. MPEG traces

The authors of [59] studied MPEG-4 encoded videos and provide a statistical analysis of them. An overview of the compression and encoding techniques are presented for MPEG-4 and a detailed analysis of the video traces is provided. Table 2.8 presents an overview of the statistical properties of the generated MPEG-4 traces. The compression ratio is defined as the ratio of the size of the entire uncompressed YUV video sequence (in bit) to the size of the entire MPEG-4 compressed video sequence (in bit). The YUV information was grabbed at a frame rate of 25 frames/sec in the QCIF format, i.e., a luminance resolution of 176x144 picture elements and 4:1:1 chrominance subsampling at a colour depth of 8 bits.

Table 2.8 Overview of frame statistics of MPEG-4 traces [58].

Quality	**Trace**	**Compression Ratio YUV:MP4**	**Mean Frame size (Kbyte)**	**Mean bit rate (kbps)**
High	Jurassic Park I	9.92	3.80	770
	Silence of the Lambs	13.22	2.90	580
	Star Wars IV	27.62	1.40	280
	Mr. Bean	13.06	2.90	580
	First Contact	23.11	1.60	330
	From Dusk Till Dawn	11.16	3.40	680
	The Firm	24.53	1.50	310
	Formula 1	9.10	4.20	840
	Soccer	6.87	5.50	1100
	ARD News	10.52	3.60	720
	ARD Talk	13.95	2.70	540
	N3 Talk	13.76	2.80	550
	Office-Cam	19.16	2.00	400
Medium	Jurassic Park I	28.40	1.30	270
	Silence of the Lambs	43.43	0.88	180
	Star Wars IV	97.83	0.39	80
	Mr. Bean	41.34	0.92	180
	First Contact	70.56	0.54	110
	Formula 1	26.11	1.50	290
	Office-Cam	68.13	0.56	110
Low	Jurassic Park I	49.46	0.77	150
	Silence of the Lambs	72.01	0.53	110
	Star Wars IV	142.52	0.27	53
	Mr. Bean	66.60	0.57	110
	First Contact	110.94	0.34	69
	Formula 1	43.51	0.87	170
	Office-Cam	84.20	0.45	90

The average number of bits per pixel in 4:1:1 subsampling is 8 x 4/4, or 12 bits per pixel on average. QCIF format was selected because the focus of study was for the evaluation

of wireless networking systems and expecting that hand-held wireless device will be typically has a screen size that corresponds to the QCIF video format. Comparing encodings at different quality levels, the lower quality encoding achieves higher compression ratios, as is to be expected. For the low quality encoding the quantization parameters were fixed at 10 for I frame, 14 for P frames, and 18 for B frames. For the medium quality encoding the quantization parameters for all three frame types were fixed at 10. For the high quality encoding the quantization parameters for all three frame types were fixed at 4 [60].

2.7.4. Music/Speech Traffic Model (Class 3)

Listening tests have attempted to find the best-quality lossy audio codecs at certain bit rates. At high bit rates (>128 kbps), most people do not hear significant differences among most audio codecs. What is considered "Compact Disc (CD) quality" is quite subjective; for some 128 kbps MP3 is sufficient, while for others 200 kbps or higher MP3 is required. Though proponents of newer codecs such as WMA and RealAudio have asserted that their respective algorithms can achieve CD quality at 64 kbps, listening tests have shown otherwise. However, these codecs quality at 64 kbps is definitely superior to MP3 at the same bit rate.

MP3, which was designed and tuned for use alongside MPEG-1/2 Video, generally performs poorly on monaural data at less than 48 kbps or in stereo at less than 80 kbps. Because MP3 is a lossy format, it is able to provide a number of different options for its "bit rate", that is, the number of bits of encoded data that are used to represent each second of audio. Typically, rates chosen are between 128 and 320 kbps. By contrast, uncompressed audio as stored on a compact disc has a bit rate of 1411.2 kbps (16 bits/sample × 44100 samples/second × 2 channels). For average signals with good encoders, some listeners accept the MP3 bit rate of 128 kbps and the CD sampling rate of 44.1 kHz as near enough to compact disc quality for them, providing a compression ratio of approximately 11:1.

2.8 Proposed Requirements for Services and Applications

The previous Sections have shown services and application description from the ITU [49], 3GPP [50], EU-MESH European project [51] and the WiMAX Forum [55]. The goal is to merge and update all recommendations/documents, to provide a wireless mesh networks services and applications characterization, in the context of the Ubiquimesh project. Additionally, video and voice DL/UL were thoroughly updated according to compression and encoding techniques provided by the WiMAX Forum. The trend of wireless technologies has been to provide higher throughputs and QoS. Considering that next generation wireless networks will continue to provide superior data rates, the DL and UL speeds were chosen, whenever possible, by considering the highest value from the gathered applications requirements.

Table 2.9 Applications and services requirements.

Service	Typical data rates [kbps]		Interactive [51]	Key performance parameters			Transmission mode [51]
	DL	*UL*		*One-way delay*	*Delay variation*	*Information loss*	
Audio							
VoIP, tele-conferencing	5-64[1] [55]		Yes	<150 ms (limit <400 ms) [49] [50] [55]	<1ms [49] [50] [55]	<3 % [49] [50]	Unicast/ multicast
Internet radio	16-64 [51]	N.A.	No	<10 s [51]	<2 ms [50]	<1 % [51]	Broadcast
Voice mail	30-50 [51]	4-25	Yes	<2 s [51]	N.A.	<3 % [51]	Unicast
Video							
Video-telephony/confer.	32 to 1024[1] (Typical = 384) [55]		Yes	< 150 ms (limit <400 ms) [49] [50] [55]	<1 ms [49] [50] [55]	<1 % [49] [51]	Unicast/ multicast
IPTV	1024-3072 [51]	N.A.	No	<10 s [51]	<2 ms [50]	<1 % [51]	Broadcast
Mobile TV	28-512 [51]						
VoD (SD)	1024-3072 [51]	<8 [51]	Yes				Unicast
VoD (HD)	7168-10240[2] [55]						
On-demand streaming media	32-384 [51]						
Video surveillance				<2 s [51]			
Data							
Real-time gaming	32-64 [51]		Yes	<75 ms [50] [51]	N.A.	0 % [51]	Unicast
Interactive gaming	4-25 [51]			<150 ms [55]			
Collaborative working	>500 [51]	4-25 [51]		<2 s/transact. [51]			
ASP services							
E-commerce							
Control of remote devices	<28 [51]			<10s [51]			
Peer-to-peer file sharing	>500 [51]			<15 s (acceptable <60 s) [51]			
User-created content sharing	32-64 [51]	>500 [51]		<2 s/upload [51]			
Web browsing	10 to 2048 [51]	4-25 [51]		<2 s/page (acceptable<4 s/page) [49] [51]			
E-mail (server access)	>500 [51]			<2 s (acceptable <4 s) [49] [51]			
File transfer	>2048 [51]	4-25 [51]		<15 s (acceptable <60 s) [51]			
Telnet	4-25 [51]			<200 ms [49]		0 % [50] [51]	
Instant messaging (IM)				250 ms [51]		0 % [51]	
Background							
Online chatting	4-25 [51]		Yes	250 ms [51]	N.A.	0 % [51]	Unicast
Fax ("real-time")	N.A.			<30 s/page [49]		<10^{-6} BER [49]	
Usenet	N.A.			Can be several minutes		0 % [49]	Broadcast
Context-based Information [51]							
Location-based multimedia broadcast	32-384	N.A.	No	<10 s	NA	<1 %	Broadcast
Location-based interactive multimedia		<8	Yes			N.A.	Unicast
Location-based on demand						<1 %	
Alert/notification, advertisement	<28	N.A.	No			0 %	Multicast
Presence-based applications		<28	Yes				Multicast
Personalized content	32-64	<8		NA			Unicast

[1] Depends of encoding schemes
[2] H.264 video compression

2.9 Conclusions

This chapter described deployment scenarios, as well as, application characterization proposed for wireless mesh networks in a multiple concatenated network environment. The main recommendations from regulators bodies, e.g., ITU-T and 3GGP, were considered and key elements proposed by a major European project, i.e., EU-MESH were assumed. Rather than developing new and distinct sets of deployment scenarios it is assumed that, for a better iteration and perhaps acceptance of the remaining international scientific community, one should rather assume the previously mentioned recommendations and assumptions from EU-MESH.

Scenarios and characterization parameters extracted from the EU-MESH were addressed and features of eight scenarios were defined. The main network and users requirements are identified as follows:

- The mobile business user scenario involves access to services and applications by business users that are always on the move;
- The nomadic business scenario considers people moving from place to place, that require information exchange and communication services available for business purposes when they stop moving;
- The gaming user scenario addresses users playing online games with the need for a broadband connection with adequate throughput, low latency and jitter;
- The fixed home user-leisure activity scenario considers the typical needs of the Internet occasional user at home with low usage levels, which sends and receives mails as well as browses the web;
- The fixed home user-entertainment activity scenario addresses mesh networks supporting increased activities related to entertainment, mainly music, television over IP and video;
- Tourist/attraction visitor scenario delivers services and free public access based on the location information and the user personal profile;
- The video surveillance/home monitoring scenario considers the deployment of surveillance, monitoring equipment based on a new mesh network environment;
- The mobile commerce scenario refers to a set of applications offered to mobile users that allow them to buy goods and services using their handheld devices through wireless network access.

The main key parameters impacting users according to ITU-T, i.e., delay, delay variation and information loss were defined and characterized. Moreover, ITU-T performance considerations for audio, video data and background applications were identified. Audio applications are classified into three types: conversational voice, voice messaging and streaming audio. Conversational voice requirements are heavily influenced by one-way delay. Voice messaging requirements for information loss are essentially the same as for

conversational voice. The main difference is higher tolerance for delay given that there is no direct conversation involved. Streaming audio should provide the lowest packet loss of this category; however as with voice messaging, there is no conversational element involved and delay requirements for the audio stream itself can be higher. Video applications are classified as videophone and one-way video. Videophone implies a full-duplex system and the same delay requirements as for conversational voice. Some degree of packet loss is acceptable depending on the specific video coder and amount of error protection used. The main distinguishing feature of one-way video is the absence of conversational elements, meaning that the delay requirement will not be so stringent, and can follow that of streaming audio. The requirements for data transfer applications are to guarantee a minimal loss of information. Delay variation is not generally noticeable to users; nevertheless data applications are distinguished according to the delay which can be tolerated by the end-user. The last category is background applications. The only requirement for this type of applications is that information should be delivered to the user essentially error free. However, there is still a delay constraint, since data is effectively useless if it is received too late for any practical purpose.

ITU-T G.1010 recommendation, 3GPP TS 22.105 and EU-MESH performance targets for audio, video and data applications were gathered to identify similarities and differences between them.

Moreover, regarding the characterization of voice and video application, detailed information provided by WiMAX's Forum Application Working Group was considered. The objective was to present the throughput requirements for voice and video applications according to employed compression technology. Five classes of applications from a user perspective were defined and characterized; interactive gaming, VoIP and video conferencing, streaming media, basic Internet applications and file transfer/media download. This classification for the applications allowed appraising the importance of audio/video compression techniques. Audio encoding schemes and video compression play a major role in throughput requirements. Furthermore, information on video data rates requirements is provided according to the display size of user's terminals. This information can be valuable for several purposes, such as the characterisation of applications on different radio access technologies, i.e., different available data rates, an important factor in multiple concatenated wireless networks.

Finally, considering the analysis and updating the recommendations from ITU-T, 3GPP, EU-MESH and WiMAX Forum AWG a new services and applications requirement was proposed. Video and voice DL/UL were thoroughly restructured according to compression and encoding techniques. The main QoS key parameters defined by the ITU, delay, delay variation and information loss have been considered for the proposed application characterization. Besides, considering that next generation wireless networks should provide superior data rates, the targeted throughput, DL and UL speeds, were selected, whenever possible, considering the highest value proposed by the above entities. Similarly, for some applications,

e.g., interactive gaming and telnet, it was chosen to adopt the lower values of the ITU-T one-way delay. The remaining application characterization subscribe to one or more information source, i.e., ITU, 3GPP, EU-MESH or WiMAX Forum. It was found that the most complex application characterizations are the ones involving voice and most of all video communication, given that data rate requirements depend on the used encoding scheme. The overall final proposal is a mix of the mentioned regulators bodies and European project recommendations, considering the optimal key parameters values provided from this group.

Chapter 3

Generic Unified Model for the Mapping between the Quality of Service and Experience in Multimedia Applications

3.1 Introduction

With recent growth of mobile services and applications, operators success depends on how good the Quality of Service (QoS) is and whether it meets the end user's expectations or Quality of Experience (QoE). With the increased competition, improving the quality of the offered services as perceived by the users (QoE) becomes very important as well as a significant challenge to the service providers with a goal to minimize the customer churn yet maintaining their competitive edge [61]. Thus, it is critical for network operators and service providers to be able to assess, predict and possibly control the end-to-end perceptual multimedia (e.g., voice and video) quality for commercial and technical reasons [62].

However, QoS measurements are generally defined in terms of network delivery capacity and resource availability but not in terms of the satisfaction to the end-user. QoE is very subjective in nature and is composed by parameters such as cost, reliability, availability, usability, and fidelity. Hence, the most accurate approach to evaluate the QoE is the subjective quality assessment, since there is no better indicator of personal quality then the one given by a human being. This assessment is essentially a subjective measurement of the network performance at the service level, i.e., QoS parameters, from the user's point of view. It is important that QoE is expressed in relation to the networks and equipment that influence user behaviour and result in a certain level of satisfaction. Therefore, QoE data should succeed where possible in combining both user experience and technical measures; for example, to provide an equation for the user experience when using a particular service with known levels of QoS [63].

It is therefore important to provide a framework for the correspondence between system service parameters and the QoE for different backhaul and access networks. For such purpose, QoS metrics gathered from various parts of the network must be mapped onto QoE targets, facilitating the inclusion of the end-user perception into the QoE model. The process to obtain the mapping between QoS and QoE, for each type of application, involves the identification of the relationship between QoS performance and its effects onto QoE.

In this work, a function is proposed to characterize the relation between a set of QoS parameters and the corresponding QoE, providing network and service providers a framework to evaluate user's satisfaction. The novelty of the proposed approach is to introduce a unified model for multimedia applications. The following four types of application are considered:

gaming, video, web-browsing and audio. As so, the final model is formed by considering fittings obtained for every individual application. Some are based on Mean Opinion Score (MOS) measurements available in the literature (or provided by other researchers). The remaining, for which MOS values could not be obtained, are achieved with some well-known ITU-T recommendations, namely ITU-T G.1030 and G.107, which in turn, are also based on MOS experiments. Regression analysis was performed by means of computing the mean square error, correlation coefficient, and coefficient of determination. These parameters characterize how well the model fits to the experimental results and ITU-T recommendations.

3.2 Gaming Applications

In the framework of online gaming, several studies have been performed on the impact of network impairments affecting the user's QoE [64], [65] and [66]. In [66], the authors provide a study on three First Person Shooter (FPS) games (Alien Arena, Halo, and Unreal Tournament) and investigate the corresponding network robustness. The research shows in detail how each QoS parameter, i.e., delay, loss and jitter, affects the QoE. It is shown that, even for the same type of game the QoS requirement can be very different due to their variety in game design, scene complexity, game pace, game rules, playing strategy, and so on, this why slower paced games tend to be less sensitive to network impairments. Additionally, in [67], the authors performed experiments on real-time multiplayers driving games whilst studying the impact of delay. It was found and shown how this network parameter impacts the quality and playability of the game. Unfortunately, such as in the previous work, no model was proposed for the mapping or correlation between QoS parameters and the QoE value.

In the world of online gaming, as not all games have the same interactions and gameplay, latency does not affect all games equally. For example, one FPS may have intense one-on-one combat with high precision weapons, while another may require strategic movement of teams of players and less frequent combat with lower precision weapons or even vehicles. In the play phase, the player actions can be significantly impaired by latency [68]. As not all player actions are equally tolerant to latency, some rapid actions such as shooting at a moving target are greatly impacted by the delay. However, in a strategy game, selecting troops and moving them across the world is less affected by delay. In these circumstances, it is not feasible to consider a generic model that would consider all types of game, especially when one considers the amount of MOS campaigns required to fully evaluate the user's quality assessment. The model proposed in the framework of this thesis considers a FPS game is considered, i.e., one of the most delay sensitive type of games. It is assumed that, if the estimated value for the QoE is above the minimum user requirement, it is possible to infer that other types of game will be above this QoE value (given that they are less delay sensitive). This approach should deliver service providers a tool to assess if network conditions are within the required quality to guarantee gaming services.

The unified model is divided into four sub-models, one for each application. The proposal for the sub-model for gaming is based on the MOS measurements from [69]. The performed campaign emulates the delay (in the form of ping) and jitter (the variance in packet arrival times at the destination) during subjective experiments. Technical details on the network emulator (Netem) can be found in [69], as well as the range of variation for the QoS parameters considered during the trials.

During two test sessions, six gamers simultaneously played Quake IV in a Free-For-All (FFA) setting. All players had prior experience with FPS games. The FFA setting is one of the most popular FPS game modes, in which players constantly engage in battles to collect the most frags (kills) during a certain time limit. This mode is particularly suited for the experiment, as it is combat oriented and different from, for example, team games, which have a more strategic aspects. The simulation of each Netem scenario lasted five minutes. After this time period, the gamers were asked to give their opinion on the gaming quality. They were able to select one of the following five values for the opinion score, motivated by the ITU-T ACR scale [70]:

- 5: Excellent gaming quality;
- 4: Good gaming quality;
- 3: Fair gaming quality;
- 2: Poor gaming quality;
- 1: Bad gaming quality.

During the experiment, the gaming server kept track of all kills and deaths of the participating players. The purpose was to identify a relation between these objective performance measures and the chosen impairment factors. The gaming test setup consisted of 6 clients PC's which were all connected to the gaming server through a Gigabit switch. The Netem network emulator was placed between the switch and the server. Both the gaming clients and the dedicated server were running the latest version of Quake IV at the time (v1.1).

Each player has to assess a total of 33 experimental scenarios. The scenarios included both network impairment caused by a single factor, as well as impairment consisting of a combinations of the ping, p, and jitter, j, in ms, and the loss, ρ, in percentage.

The results for these experiments were provided by Robert Kooij, one of the authors of the Muse G-Model [71]. A sample of 20 MOS results is presented in Table 3.1, the column "Average MOS" represents the average of each gamer/user MOS.

The equation that better fits to MOS experimental measurements must be found. For this first case, the mathematical process used to attain the sub-model will be presented more thoroughly. In this process of finding the equation that better fits to the MOS experimental measurements, several regressions have been tested, the validation of these regressions is performed by evaluating the coefficient of determination (R^2), coefficient of correlation (R) and the Mean Square Error (MSE), Table 3.2 presents the evaluation of these fits.

Table 3.1 Sample of 20 results obtained during experimental gaming MOS trials.

Sample	ping [ms]	jitter [ms]	loss [%]	Average MOS
1	80	10	20	3.1667
2	0	40	0	3.4167
3	0	0	5	4.3333
4	160	20	10	2.2500
5	0	0	0	4.0000
6	20	20	0	3.4167
7	0	160	0	1.0833
8	320	0	0	1.7500
9	0	20	0	4.1667
10	80	20	5	3.5000
11	320	80	0	1.1667
12	100	20	20	2.6667
13	40	0	0	3.6667
14	0	40	0	3.3333
15	0	80	0	2.1667
16	0	0	2	4.0000
17	160	40	10	2.0833
18	0	80	0	2.1667
19	20	0	0	4.5000
20	320	40	5	1.4583

Table 3.2 Sample of results obtained during the fitting of the experimental gaming MOS.

Goodness	Linear	2º poly.	3º poly.	4º poly.	5º poly.	6º poly.	7º poly.
R^2	0.8978	0.9232	0.9288	0.9310	0.9336	0.9387	0.9387
R	0.9475	0.9608	0.9638	0.9649	0.9662	0.9689	0.9689
MSE	0.1256	0.0943	0.0874	0.0847	0.0815	0.0752	0.0753

Additionally, Figure 3.1 shows the MOS as a function of the number of samples and the expected value according to a linear and a sixth degree polynomial equation.

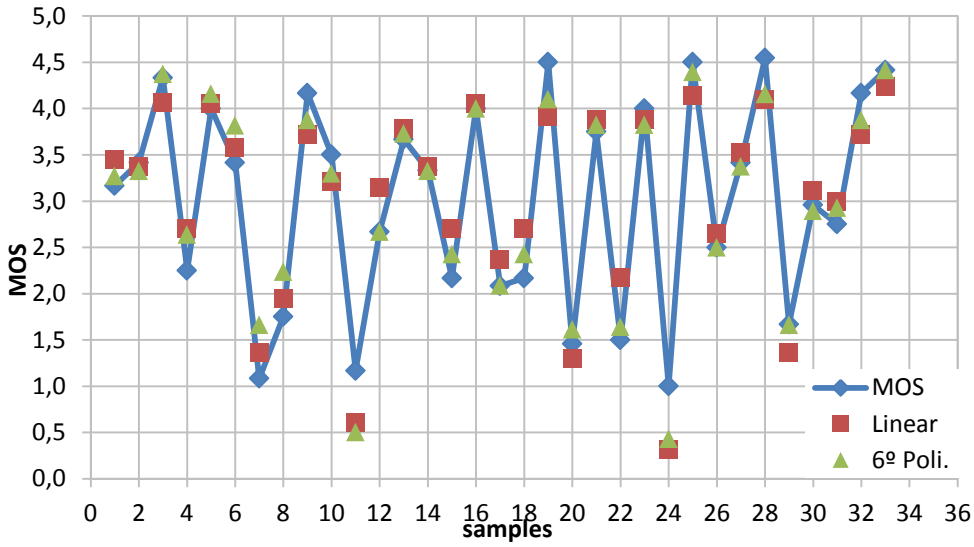

Figure 3.1 MOS results as a function of the number of samples.

Figure 3.1 also illustrates the somehow inconsistent behaviour of the MOS results, this shows why exponential and logarithmic regressions failed to provide proper fittings, thus only polynomial equations can approach the comportment of the experimental MOS results. If only one parameter was considered (when the interference of all other parameters is null), such as the ping represented in Figure 3.2 the regression could, in this case, be simplified to an exponential regression, also shown in Figure 3.2. It is the added complexity of multiple QoS parameters that forces to use polynomial fittings.

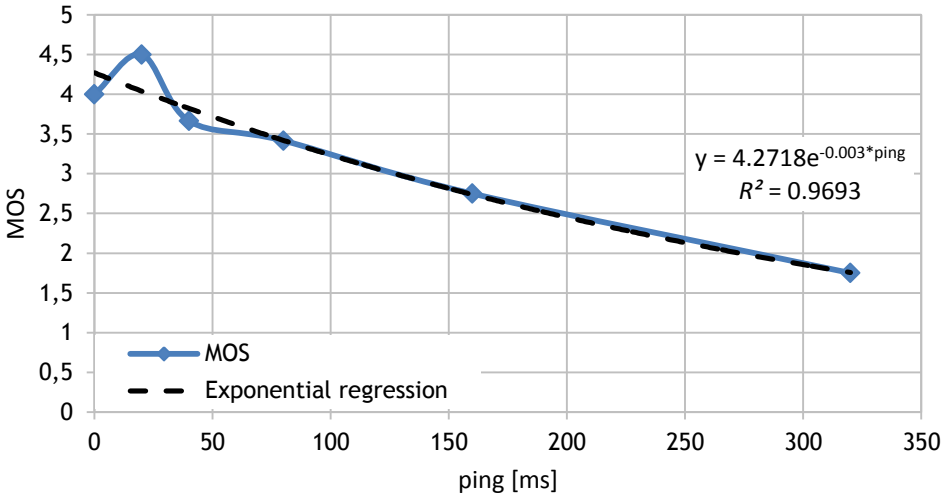

Figure 3.2 Variation of the MOS considering only the interference of the ping.

From the analysis of Table 3.2 it can be can verified that the sixth degree polynomial equation provides the best compromise between complexity and goodness of fit, the seventh polynomial regression only provide fringe benefits. As so, the selected sixth degree polynomial equation is given by:

$$\begin{aligned} MOS = {} & 4.16031 + 0.0349952 \times p - 0.104905 \times j - 0.267622 \times \rho - 0.00315486 \times p^2 \\ & + 0.011092 \times j^2 + 0.119224 \times \rho^2 + 7.84 \times 10^{-5} \times p^3 - 0.00048113 \times j^3 \\ & - 0.0135847 \times \rho^3 - 8.48647 \times 10^{-7} \times p^4 + 9.07 \times 10^{-6} \times j^4 \\ & + 0.000412947 \times \rho^4 + 3.92 \times 10^{-9} \times p^5 - 7.51346 \times 10^{-8} \times j^5 \\ & + 3.90407 \times 10^{-6} \times \rho^5 - 6.0582 \times 10^{-12} \times p^6 + 2.16813 \times 10^{-10} \times j^6 \\ & - 1.87 \times 10^{-7} \times \rho^6 \end{aligned} \tag{3.1}$$

The goodness of this fit can be verified by the values of R, R^2, and the MSE, presented in Table 3.1. In this first case, the achieved results are the following, R = 0.9689, R^2 = 0.9387 and MSE = 0.0752. It can be observed that, for this regression, the coefficients R and R^2 are very close to 1 while the MSE is near 0.

3.3 Video Applications

A multitude of studies have been performed on the assessment of QoE for streaming video applications [72], [73] and [74]. However, these research activities have not produce a true model for the correspondence between service level QoS parameters and the subjective user's quality assessment. Instead, one considers parameters such as frame rate, initial buffering time, mean rebuffering duration and rebuffering frequency. From a network point of view, these parameters are not easily measurable, i.e., they are not network service or QoS parameters. Hence, the model for QoE proposed in this work cannot incorporate the above mentioned parameters.

In the determination of video perceptual quality, approximating the user's perception of picture quality in real-time via image processing algorithms is a complex procedure, requiring significant processing power [75]. As a consequence, it is not feasible to consider parameters like colour of shape distortion or even I-P-B frame drops for MPEG compressed videos. Network-level connection quality indicators, such as packet loss, jitter or delay can be easily measured by the user terminal and monitored by the wireless network provider. Moreover, the network provider can employ numerous mechanisms at network level in order to optimize the access network and compensate for such impairments. What is needed to address is the impact of this optimization on the user-perceived quality, whose improvement should be the ultimate goal [75]. Consequently, it would be desirable to associate the QoS indicators to the actual QoE level, as perceived by the viewer, facilitating to instantaneously provide an estimation of the viewed picture quality whilst achieving the actual optimization of the network-service chain at any moment [75]. Additionally, previous research on dynamic control scheme for streaming video [76] also focuses on the mapping of QoS parameters to achieve reliable and consistent end-to-end video.

This work considers the MOS measurements performed in [77]. The setup for this experiment is shown in Figure 3.3.

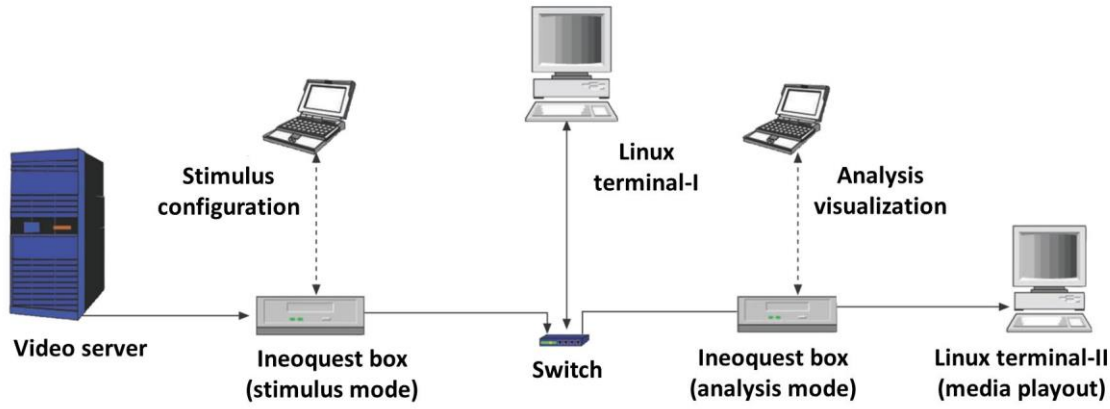

Figure 3.3 Sequences for the video the metric tests (extracted from [77]).

The topology consists of a video server that initiates a push-based stream onto the network. The server can encode a video stream at various bitrates and frame rates. The server is connected to an IneoQuest (IQ) Sigulus G1-T box configured in the stimulus mode. In this mode the IQ can generate impairments to the flow by inducing loss, delay, or jitter. The flow is streamed to another IneoQuest G1-T configured in the *analysis and playback mode*. The stream is then passed onto a destination (Terminal-II) for visualization, additional information on the experimental setup can be found in [77].

Similarly to the case of gaming, several fittings have been performed. A sample of the obtained results can be verified in

Table **3.3**.

Table 3.3 Sample of results obtained during the fitting of the experimental video MOS

Goodness	Linear	2º poly.	3º poly.	4º poly.	5º poly.	6º poly.	7º poly.
R^2	0.4495	0.4833	0.5430	0.6302	0.7154	0.8379	0.8611
R	0.6705	0.6952	0.7369	0.7939	0.8458	0.9154	0.9280
MSE	0.6677	0.6267	0.5544	0.4485	0.3452	0.1966	0.1685

It can be found that the more complex seventh degree polynomial only provides a fringed improvement over the simpler sixth degree polynomial equation (compared to previous regressions). For this reason, the sixth degree polynomial fitting will be chosen for the unified model:

$$\begin{aligned} MOS = {} & 3.21779 + 0.00266916 \times b_{rate} - 10.4811 \times \tau - 20.9894 \times \rho - 5.8875 \times 10^{-6} \times {b_{rate}}^2 \\ & + 40.3305 \times \tau^2 + 166.121 \times \rho^2 + 1.449 \times 10^{-8} \times {b_{rate}}^3 - 42.493 \times \tau^3 \\ & - 730.016 \times \tau^3 - 4.2939 \times 10^{-12} \times {b_{rate}}^4 + 18.3884 \times \tau^4 \\ & + 1764.47 \times \rho^4 - 2.29851 \times 10^{-15} \times {b_{rate}}^5 - 3.48213 \times \tau^5 \\ & - 2069.09 \times \rho^5 + 8.08679 \times 10^{-19} \times {b_{rate}}^6 + 0.237418 \times \tau^6 \\ & + 903.102 \times \rho^6 \end{aligned} \tag{3.2}$$

where τ is de delay in ms, ρ is the percentage of loss and b_{rate} is the bitrate, in kbps. The goodness of fit is confirmed by R = 0.9154, R^2 = 0.8379 and the MSE = 0.1966. It can be verified that the coefficients R and R^2 are very close to 1 while the MSE is near 0.

3.4 Web-browsing Applications

In web-browsing, it has been widely recognized that end-user waiting time is the key predominant aspect for QoE, in contrast to service quality in audio and video quality, where psychoacoustic and psycho-visual phenomena are dominant. The longer users have to wait for the web page to arrive (or transactions to complete), the more dissatisfied they tend to become with the service [78]. A study has been performed in [79] on the impact of transfer

times for web-browsing. This study characterizes user's behaviour when network performance decreases, causing the increase of page transfer times. Similarly, the authors from [80] present results concerning the user's cancelation rate as a function of response times. Related works [81], [82] have also shown that the utilization of MOS evaluation is the standard regarding assessment methodologies for web-browsing QoE.

As it was not possible to obtain MOS experiments results for web-browsing, the data available by the ITU-T G.1030 recommendation [83] were used instead. This recommendation provides a model for mapping the response and downloads times, as measured in the network or calculated from the HTTP transaction time to the perceived quality of a web-browsing session. The scope of the model is currently limited to web browsing sessions. The first step is a search request followed by the display of the web page. According to ITU-T G.1030, the correlation between the performed experiments and the one from the recommendation are superior to 0.9. The model is based on experiments where the response and download times in a web-browsing session have been manipulated [84] and [85].

The model from the G.1030 recommendation describes the relation between the different response and download times within web-browsing sessions and the corresponding perceived web-browsing quality, for a given maximum session time, within a certain network and system configuration. The model is applicable to a wide range of network and system configurations, as well as to web-browsing services for a wide variety of users. The subjective experiments mimicked as closely as possible a real-life web-browsing experience. Three subjective web-browsing experiments with time-scales of around 6, 15, and 60 seconds were considered in this recommendation, representing fast, moderate and slow network contexts, respectively. During each session, a subject initially requests a search page, and finally retrieves the requested web page. Figure 3.4 shows the session time-line.

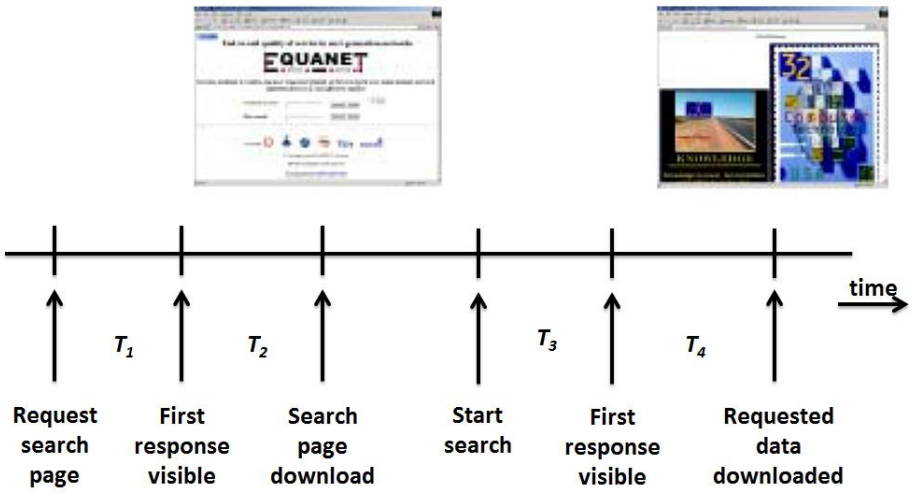

Figure 3.4 Time-line for the web-browsing application: T_1 is the non-interactive response time, T_2 is the non-interactive download time, T_3 and T_4 are the equivalents for the interactive part (extracted from [83]).

The first two time intervals, T_1 and T_2, represent the non-interactive response and download times of the search page. The second two time intervals, T_3 and T_4, represent the interactive response and download times of the result page.

A general mapping from session time to web-browsing quality is built by defining minimum (*Min)* and maximum (*Max)* session times whilst using a logarithmic interpolation between these extreme session times. It has been also found that for naive and expert users, a more advanced model for the prediction of the subjective quality may be constructed by considering that, for shorter duration sessions, the last download time, T_4, has a more severe impact on the final perceived web browsing quality than the other response and download times (T_1, T_2, T_3). Table 3.4 gives the weight factors for each download time. T_1, T_2, T_3 and T_4 have to be weighted in order to get a weighted session time that has the highest correlation with the subjectively determined MOS values, as follows:

$$WeightedST = WT_1 \times T_1 + WT_2 \times T_2 + WT_3 \times T_3 + WT_4 \times T_4 \tag{3.3}$$

The equation for the logarithmic interpolation is the following:

$$MOS = \frac{4}{\ln\left(\frac{Min}{Max}\right)} \times \left[\ln(WeightedST) - \ln(Min)\right] + 5 \tag{3.4}$$

Table 3.4 Optimal model weighting T_1, T_2, T_3 and T_4 with the associated model correlations between objective timing and subjective MOS results (extracted from [84])

Type of usage	WT_1	WT_2	WT_3	WT_4	*Min*	*Max*	Correlation
6 s expert	0.56	0.84	0.80	1.80			0.97
6 s naïve	0.37	0.40	0.60	2.63			0.93
6 s overall	**0.47**	**0.60**	**0.71**	**2.22**	**0.62**	**13.5**	**0.95**
15 s expert	0.63	0.77	1.11	1.49			0.98
15 s naive	0.48	0.70	0.88	1.95			0.96
15 s overall	**0.54**	**0.72**	**0.98**	**1.76**	**0.81**	**39**	**0.97**
60 s expert	0.84	0.77	1.22	1.18			0.99
60 s naive	0.64	1.01	1.12	1.24			0.98
60 s overall	**0.73**	**0.90**	**1.16**	**1.22**	**2.22**	**151**	**0.98**

The ITU-T G.1030 recommendation further establishes three advanced models by using the best overall weights in combination with the following mappings from weighted session time to perceived browse quality, in terms of the mean opinion score, clipped between 1 and 5. For short duration sessions the MOS is given by:

$$MOS = 4.38 - 1.30 \times (WeightedST) \tag{3.5}$$

For medium duration sessions:

$$MOS = 4.79 - 1.03 \times (WeightedST) \tag{3.6}$$

For long duration sessions

$$MOS = 5.76 - 0.948 \times (WeightedST) \tag{3.7}$$

In the context of this research, from a network or operator point of view, it is not feasible to analyse user's web-browsing traffic load to obtain T_1, T_2, T_3 and T_4. Besides, when the session times are shorter, the last download time, T_4, has a higher weight on the finally perceived quality than the other response and download times, T_1, T_2 and T_3. Hence, one is able to conclude that from the user point of view, the main performance factor is how quickly a page appears after it has been requested. Additionally the time intervals are backbone delay sensitive and changes in rate do not have noticeable impact on their variation, whereas T_4 relies on the transmission rate of the Internet access connection. Moreover, by analysing Figure 3.4 it can be concluded that T_4 is the time required to open the user desired web page.

With the above considerations in mind, it can be concluded that T_4 is the ratio between the requested amount of *data* (page), in kb, and the available network bitrate, b_{rate}, in kbps:

$$T_4 = data / b_{rate} \tag{3.8}$$

Two simplifications are assumed, on the one hand only the session time with the highest weight are considered, i.e., with interactive response time T_4. On the other hand, only medium duration sessions are addressed, i.e., 15 seconds. The MOS is then given by:

$$MOS = 4.79 - 1.03 \times \ln\left(WT_4 \times data / b_{rate}\right) \tag{3.9}$$

By replacing WT_4 by the value extracted from Table 3.4, one obtains:

$$MOS = 4.79 - 1.03 \times \ln\left(1.76 \times data / b_{rate}\right) \tag{3.10}$$

Finally, equation (3.10) provides a relation between objective service conditions (or QoS) and objective user perception (or QoE). By using ITU-T G.1030 recommendation it can be estimated that the correlation value, R, is approximately 0.9. Additionally, Figure 3.5 depicts the MOS fitting with transferred data and b_{rate} for web-browsing application.

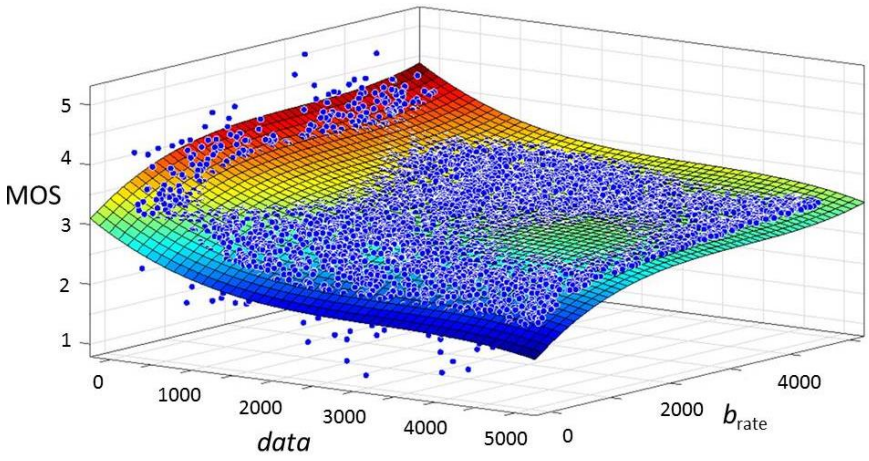

Figure 3.5 MOS fitting as a function of the transferred data and b_{rate} for web-browsing application.

3.5 Audio Applications

Several research activities have been performed in the assessment of audio QoE. Most contributions have been based on the popular ITU-T E-Model. In [86], a dedicated nonintrusive parametric QoE model for conversational quality based on the E-model approach was proposed. This model focuses on complex live discussion (numerous contributors from multiple locations) rather than simple outside broadcast (e.g. sports commentary) due to the challenging applications in Audio Contribution over IP (ACIP). In [87], a non-intrusive model for VoIP quality assessment was proposed. The new methodology is based on nonlinear regression models for G.729, G.723.1, AMR, and Internet Low Bitrate Codec (iLBC) audio codecs, and considers two main network impairments: packet loss and end-to end delay. The regression can be adjusted to the desired audio codec by defining 10 parameters in the fitness equation. The method exploits the intrusive algorithm Perceptual Evaluation of Speech Quality (PESQ), and a combined PESQ/E-model structure, to provide a perceptually accurate prediction of voice quality non-intrusively, which avoids time-consuming subjective tests [87].

In this work, for audio applications, one considered the well-known ITU-T E-Model from the G.107 recommendation [88]. The E-model assesses the combined effects of varying transmission parameters that affect the conversation quality of narrow band telephony. The E-model is based on the assumptions that transmission impairments can be transformed into psychological factors and psychological factors on the psychological scale are additive. The result of any calculation with the E-model, in a first step, is a transmission rating factor R_f, which combines all transmission parameters relevant for the considered connection. This rating factor is computed by [88]:

$$R_f = R_0 - I_s - I_d - I_e + A \tag{3.11}$$

where R_0 represents the basic signal-to-noise ratio, including noise sources such as circuit noise and room noise. The factor I_s is a combination of all impairments which occur more or less simultaneously with the voice signal. Factor I_d represents the impairments caused by delay. The effective equipment impairment factor I_e represents impairments caused by low bitrate codecs, it also includes impairment due to randomly distributed packet losses. The advantage factor A allows for the compensation of impairment factors when the user benefits from other types of access. The term R_0 as well as the I_s and I_d values, are subdivided into further specific impairment values. By considering the default values for these parameters, R_f is given by [88]:

$$R_f = 93.2 - I_d - I_e \tag{3.12}$$

For $0<R_f<100$ the dependence between R_f and MOS, defined by the ITU, is the following one:

$$MOS = 1 + 0.0035 \times R_f + R_f \times (R_f - 60) \times (100 - R_f) \times 7 \times 10^{-6} \tag{3.13}$$

The delay impairment factor, I_d, represents all impairments due to delay of voice signals, and includes impairments due to listener echo, talker echo and absolute delay, defined by [88]:

$$I_d = I_{dte} - I_{dle} - I_{dd} \tag{3.14}$$

The factor I_{dte} gives estimation for the impairments due to talker echo. The factor I_{dle} represents impairments due to listener echo and I_{dd} characterizes the impairment caused by too-long absolute one-way mouth-to-ear delay, T_a. The delay associated with listener echo is T_r, the round trip delay in the four-wire loop and the delay related with Talker Echo is T. Assuming IP-based voice applications the delay can be defined as [89]:

$$\tau = T_a = T = {}^{T_r}\!/_{2} \tag{3.15}$$

Equation (3.14), i.e., I_d, can be re-written as a function of the one-way delay in ms, τ, by means of the curve fitting provided by [89]:

$$I_d = 0.024d + 0.11(\tau - 177.3) \times H(\tau - 177.3) \tag{3.16}$$

where H(x) is the Heaviside or step function.

In order to reach a more accurate fit to the curve from G.107, a sixth degree polynomial fit function is provided [90]:

$$I_d = 1.618\times10^{-13}\times\tau^6 - 1.765\times10^{-10}\times\tau^5 + 6.447\times10^{-8}\times\tau^4 - 8.211\times10^{-6}\times\tau^3 + 0.0002315\times\tau^2 + 0.0352\times\tau - 0.02434 \quad (3.17)$$

Given a set of measured I_e values for a codec, its model can then derive by using regression techniques, without the need for subjective tests. For the AMR codec, Figure 3.6, the MOS (PESQ) vs. packet loss rate can be obtained by averaging over 30 different packet loss locations, in order to remove the influence of these locations [90].

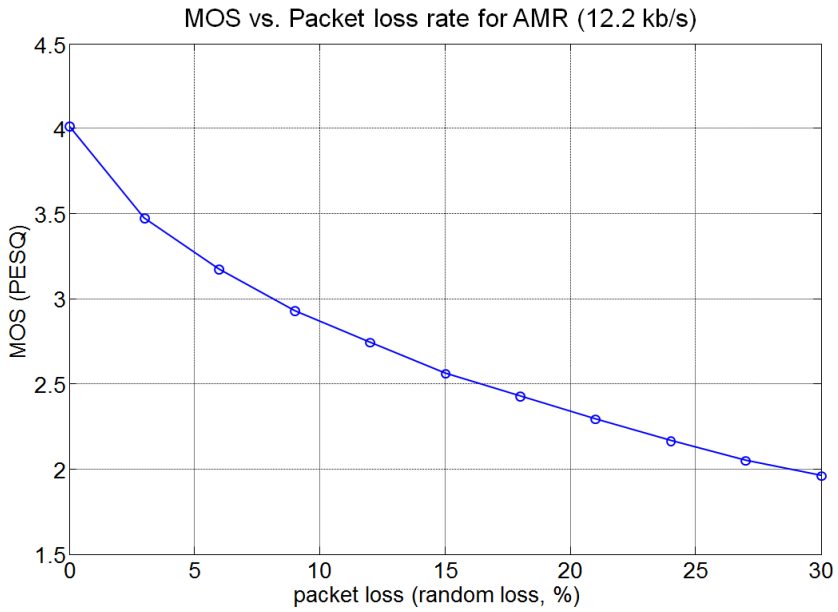

Figure 3.6 MOS vs. packet loss rate ρ for AMR codec (extracted from [91]).

Additionally, the MOS for one packet loss rate is obtained by averaging all speech samples (a total of 16 samples, consisting of 8 males and 8 females), so that the influence of gender is removed [90]. The reference speech database was taken from the ITU-T data set [91]. The relation between the MOS and packet loss rate can be converted to the equipment impairment, I_e, vs. packet loss rate by considering the following third degree polynomial fitting:

$$R_f = 3.026\times MOS^3 - 25.314\times MOS^2 + 87.06\times MOS - 55.336 \quad (3.18)$$

By considering only the equipment impairment, R_f can be converted to I_e as follows:

$$I_e = R_0 - R_f \quad (3.19)$$

Finally, a logarithm fitting function, similar to the one from [89], can be derived through curve fitting:

$$I_e = 16.68 \times \ln(1 + 0.3011 \times \rho) + 14.96 \tag{3.20}$$

where ρ is the packet percentage loss.

The MOS versus packet loss and delay may now be obtained by replacing equations (3.17) and (3.20) in (3.12) and computing the MOS by considering equation (3.13) as shown in Figure 3.7.

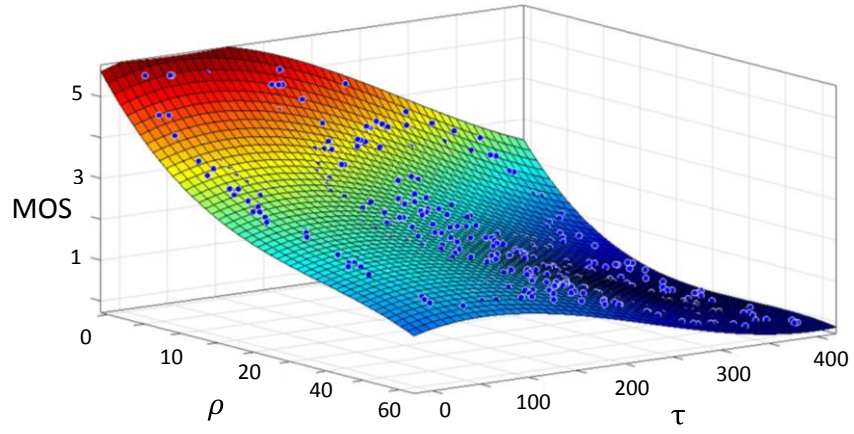

Figure 3.7 MOS fitting as a function of packet loss and delay for audio applications.

To simplify (3.13) the equation that best fits the obtained data and achieved a simpler third degree equation was computed:

$$\begin{aligned} MOS = {} & 3.657 - 0.1345 \times \rho - 0.003303 \times \tau - 0.004012 \times \rho^2 - 3.275 \times 10^{-5} \times \tau^2 \\ & - 4.564 \times 10^{-5} \times \rho^3 + 4.414 \times 10^{-18} \times \tau^3 \end{aligned} \tag{3.21}$$

The goodness of this fit is guaranteed by the obtained values of the coefficients R and R^2, 0.9921 and 0.9842, respectively, while the MSE is 0.0009633.

3.6 Unified Model

In nowadays competitive market, as the user satisfaction is becoming a crucial factor for the success of telecommunication companies, to make a generic and global QoE model available is very important. The unified model is obtained by mathematically integrating the fitness obtained for each application, equation (3.22).

$$
\begin{aligned}
QoE(QoS) = {} & a_0 + A_1(0.035p - 0.105j - 0.003p^2 + 0.011j^2 + 7.84\times10^{-5}p^3 - 48.113\times10^{-5}j^3 \\
& - 8.486\times10^{-7}p^4 + 9.07\times10^{-6}j^4 + 3.92\times10^{-9}p^5 - 7.513\times10^{-8}j^5 - 6.058\times10^{-12}p^6 \\
& + 2.168\times10^{-10}j^6) + A_2(-26.6916\times10^{-4}b_{rate} - 5.888\times10^{-6}{b_{rate}}^2 + 1.449\times10^{-8}{b_{rate}}^3 \\
& - 4.294\times10^{-12}{b_{rate}}^4 - 2.299\times10^{-15}{b_{rate}}^5 + 8.087\times10^{-19}{b_{rate}}^6) \\
& + A_3\left(4.79 - 1.03\ln\left(1.76\times {data}/{b_{rate}}\right)\right) + A_4(a_1\rho + a_2\rho^2 + a_3\rho^3 + a_4\rho^4 + a_5\rho^5 + a_6\rho^6) \\
& + A_5(a_7\tau + a_8\tau^2 + a_9\tau^3 + a_{10}\tau^4 + a_{11}\tau^5 + a_{12}\tau^6)
\end{aligned}
\tag{3.22}
$$

Table 3.5 presents the variables to be replaced in the final equation, according to the selected application to compute the expected QoE. A_1, A_2, A_3, A_4 and A_5 are Boolean variables used to select the QoS parameters impacting the QoE. The performed regression analysis validates the final model by means of the goodness of fit obtained for all multimedia applications, i.e., R, R^2 and MSE. The accuracy of the model can still be improved by considering further MOS experimental results, i.e., with other QoS parameters, and additional MOS values for web-browsing and audio applications.

Table 3.5 Variables to be replaced in the final equation, according to the selected application to compute the expected QoE.

	Gaming	Video	Web	Audio
a_0	4.16	3.215	4.79	3.657
A_1	1	0	0	0
A_2	0	1	0	0
A_3	0	0	1	0
A_4	1	1	0	1
A_5	0	1	0	1
a_1	-0.268	-20.989	0	-0.135
a_2	0.119	166.121	0	-4.012×10^{-3}
a_3	-0.014	-730.016	0	-4.564×10^{-5}
a_4	41.295×10^{-5}	1764.47	0	0
a_5	3.9×10^{-6}	-2069.09	0	0
a_6	-1.87×10^{-7}	903.102	0	0
a_7	0	-10.481	0	-0.003303
a_8	0	40.331	0	-3.275×10^{-5}
a_9	0	-42.493	0	4.414×10^{-8}
a_{10}	0	18.388	0	0
a_{11}	0	-3.482	0	0
a_{12}	0	0.237	0	0

This pioneering single equation for multiple multimedia application is provided to build an effective QoE control mechanism onto measurable QoS parameters for multimedia networks, i.e., for improving packet scheduling in mesh and or cognitive radio (CR) networks. In particular, when considering the additional delay and possible packet loss induced by spectrum mobility in CR networks (when a secondary user migrates or as to vacate a primary user spectrum) the model facilitates to verify their impact on the achieved user QoE, explicitly for delay-sensitive applications, such as interactive gaming.

3.7 Conclusions

Next generation networks are bound to provide various multimedia services. The QoE concept is introduced in these networks to describe the satisfaction of subscriber's quality requirements. Thus, QoE evaluation is becoming critical to operators to guarantee their clients degree of satisfaction in nowadays competitive market. To evaluate the QoE it is important to create a strategy to instantly measure it. This will give operators some sense of the contribution of the network performance to the overall level of user's satisfaction, and enable them to interact with it. There are many network related features (QoS parameters) that affect the way users perceive their experience, i.e., their subjective usage involvement. In such context, the goal of this work is to propose a mapping model between quality of service parameters and the user's quality of experience. The objective is to provide network and service providers a tool to evaluate their user's satisfaction. The four main type of applications, gaming, web-browsing, video and audio are addressed. MOS experiments have been considered for gaming and video applications. The model for web-browsing and audio applications considers ITU-T recommendations since no MOS results were available.

The fittings were validated by means of regression analysis by computing the mean square error, and the coefficients of determination and correlation. These terms provide a measure of how well the model fits to experimental MOS measurements. It has been shown that the values for the coefficient of determination between the model for MOS and the available data (either experimental values or the ones from ITU-T G.107 recommendation) are R^2 = 0.9387, 0.9842 and 0.8379 for gaming, audio and video, respectively. The computed mean square error is approximately zero in all the cases.

Additionally, one believes that, with additional MOS measurements, this model can certainly be enhanced. QoE is so subjective in nature that the more experimental MOS results are made available, the more accurate would be the computed trend; hence a more precise estimation of QoE would be inferred. The considered experimental MOS results have been obtained from different networks and conditions (trials), it is also thought that the model can also benefit from obtained MOS in a more controlled environment, i.e., MOS experiments performed in the same networks (conditions) for all multimedia applications. On a positive note, the variety of network conditions allows for inferring a broader set of conditions and thus a wider user's quality assessment. Moreover, as games have greatly evolved along the last few years, and although MOS measurement for FPSs were considered (one of the most delay sensitive type of games), it can be expected that nowadays games, created with advanced programming techniques, which provides a higher tolerance to network latency, as well as a variety in game design, scene complexity, game pace, and so on, will better portray today's users experience.

Chapter 4

Planning and Optimization of Fixed WiMAX Networks with Relays

4.1 Introduction

In the context of Worldwide Interoperability for Microwave Access (WiMAX) planning, research on the variation of the Carrier-to-Noise-Plus-Interference Ratio (CNIR) with different system parameters is of fundamental importance. The goal is to provide access to mobile users in the cell, while guaranteeing the quality of the received signal in both the uplink (UL) and downlink (DL), even for users at the cell edge. As resources, e.g., frequency channels, need to be reused in different geographical zones, the impact of interference among co-channel cells needs to be evaluated in both link directions. As there are limitations in both UL and DL, techniques such as sub-channelization need to be applied to reduce the impact of the noise on the link performance. However, only mobile WiMAX will allow for sub-channelization in the DL while fixed WiMAX only allows for it in the UL, and may cause a degradation of performance (mainly owing to the extra noise caused by the largest bandwidth). For cellular planning purposes, the UL and DL CNIRs from/at the wireless Subscriber Station (SS) are very important parameters. From a detailed analysis of its variation with the coverage and reuse distances for different modulation and coding schemes (MCS), an evaluation of the possible reuse patterns can be performed.

Besides, in the optimization of cellular planning for fixed WiMAX, the use of RSs reduces the necessary extent of wire-line backhaul, improving coverage significantly whilst achieving a competitive system throughput. Moreover, RSs have a much lower hardware complexity, and using them can significantly reduce the system deployment cost, as well as, its energy consumption. Consequently, in [92] and [93] frequency reuse topologies were explored for bi-dimensional space (2D) broadband wireless access topologies in the absence and presence of RSs, and the basic limits for system capacity and cost/revenue optimization have been discussed. The identification of these fundamental limits involves the study of the variation of the CNIR as a function of the coverage and reuse distances, considering propagation models and different modulation and coding schemes.

In this work, propagation modelling through experimental measurements is addressed in detail, and the Dominant Path (DP) model and Ray Tracing (RT) propagation functionalities are simultaneously considered in the cellular planning tool simulations. Analytical results for the CNIR versus distance and maximum supported throughput were obtained, with the results from cellular planning exercises being achieved using Winprop™ for WiMAX deployments, with and without RSs, in the zone of Covilhã, Portugal, a very hilly region. Different MCSs are considered, and cellular planning exercises are performed for frequency reuse pattern $K = 3$.

RS backhauling is supported through dedicating specific sub-frames within the radio transmissions to that purpose. Besides BS-to-SS communications, BS-to-RS and RS-to-SS communications are also guaranteed. Moreover, it is noted that there is usually less traffic load in the UL direction in wireless multimedia communications, leading to a 1:5 asymmetry factor between UL/DL being appropriate.

Despite the above, as considerable resources are needed for BS-to-RS communication, some configurations with no RSs, e.g., with tri-sectored BSs, may still lead to better efficiency in theoretical terms. If there were no coverage difficulty, topologies with no RSs would consequently still have a higher throughput performance. However, this is not always the case, and a detailed analysis of the achieved throughput versus coverage in the presence of interference is essential to understand the pros and cons of using RSs in practical terms.

4.2 Carrier-to-Noise-plus-Interference Ratio

4.2.1. Carrier-to-Noise-plus-Interference Ratio without Relays

If Frequency Division Duplexing (FDD) is used, in fixed WiMAX, worst-case situations occur in the DL when the BS of the central cell transmits to the most distant SS, located at the cell edge, whilst receiving interference from the BS of the six co-channel cells of each ring of interference, Figure 4.1.

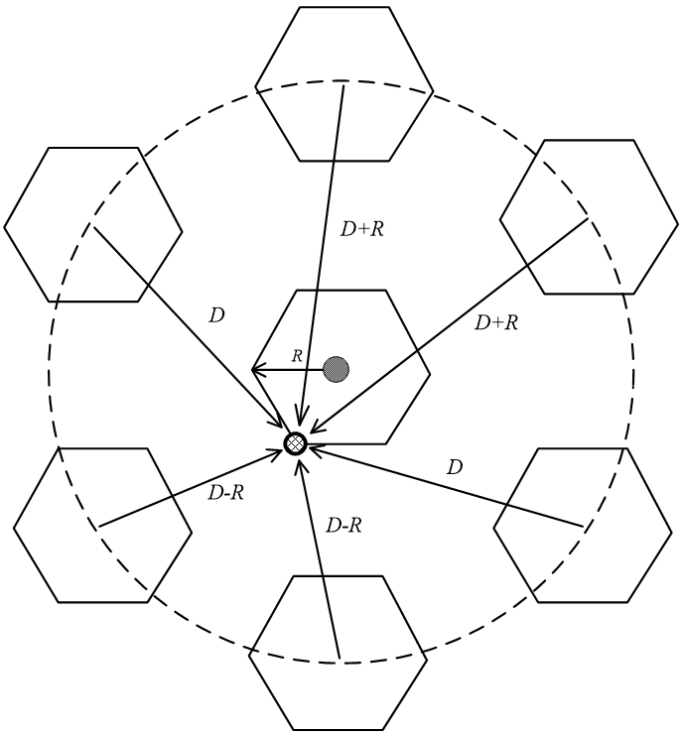

Figure 4.1 Co-channel interference in the worst-case for the DL (extracted from [94]).

In the UL, the worst-case situation occurs when the SS is transmitting to the BS from the cell boundary while interfering mobiles are at the interfering cells edge (in the region closest to the central cell), Figure 4.2. When sectorization is considered the number of interfering cells is decreased, and system capacity increases.

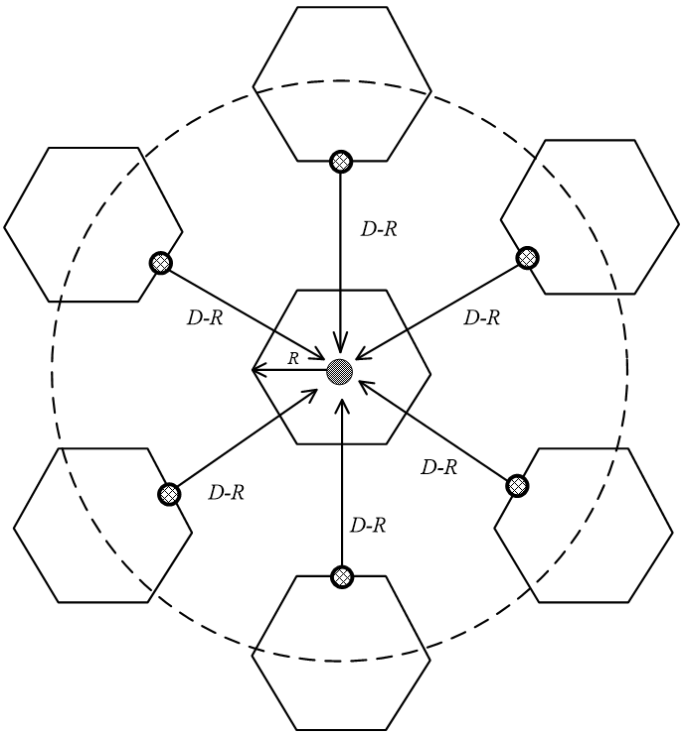

Figure 4.2 Co-channel interference in the worst-case for the UL.

If one considers the interference-to-noise ratio, defined by:

$$M = I/N \tag{4.1}$$

The equation for the carrier-to-noise-plus-interference ratio (*CNIR*) to be considered in the dimensioning process is the following:

$$\frac{C}{(N+I)} = \left(\frac{C}{N}\right)_{\min} \tag{4.2}$$

According to [94] equation (4.2) can be written in the two following ways:

$$\frac{C}{N} = \left(\frac{C}{N}\right)_{\min} (1+M) \tag{4.3}$$

and:

$$\frac{C}{I} = \left(\frac{C}{N}\right)_{\min} \left(1 + M^{-1}\right) \tag{4.4}$$

In (4.2) one is using the model for CNIR from [95], and one is assuming that the weights for the noise and the interference are the same.

From equation (4.3) one obtains the following equation for the interference-to-noise ratio:

$$M(R) = \frac{(C(R)/N)}{(C/N)_{\min}} - 1 \tag{4.5}$$

where $C(R) = P_R(R)$ is computed by the modified Friis formula considering urban environments, i.e., with $\gamma = 3$, the assumption considered in this section for urban environments.

The values of $M(R)$ are proportional to the interference that is still possible to tolerate for a coverage distance R while (still) agreeing with the quality requirements for a given modulation and coding scheme.

With a hexagonal cellular topology, in the DL, as shown in Figure 4.1, as the distance associated with interference is D, i.e., the reuse distance itself, the carrier-to-interference ratio can be given by:

$$\frac{C}{I} = \frac{1}{2(r_{cc}+1)^{-\gamma} + 2r_{cc}^{-\gamma} + 2(r_{cc}-1)^{-\gamma}} \approx \frac{{r_{cc}}^{\gamma}}{6} \tag{4.6}$$

where r_{cc} is the co-channel reuse factor, given by:

$$r_{cc} = D/R \tag{4.7}$$

For the UL, as shown in Figure 4.2, the carrier-to-interference ratio is given by:

$$\frac{C}{I} = \frac{(r_{cc}-1)^{\gamma}}{6} \tag{4.8}$$

By replacing (4.6) into (4.4), it is therefore possible to obtain the following equation for the reuse factor in the DL:

$$r_{cc} = \sqrt[\gamma]{6 \cdot \left(1 + M^{-1}\right) \cdot \left(C/N\right)_{\min}} \tag{4.9}$$

In turn, for the UL, by replacing (4.8) into (4.4), one obtains the following equation:

$$r_{cc} = \sqrt[\gamma]{6 \cdot \left(1 + M^{-1}\right) \cdot \left(C/N\right)_{\min}} + 1 \tag{4.10}$$

It is also worthwhile to note that, for hexagonal reuse geometries, the reuse pattern is given by:

$$K = \frac{r_{cc}^{\,2}}{3} \tag{4.11}$$

As a horizontal asymptote arises in the analysis of the curves from r_{cc} as a function of the coverage distance, R, it is important to present its computation.

To compute the horizontal asymptote in the chart of $r_{cc}(R)$, one has to consider that $R \to 0$. From (4.5), if $R \to 0$ then $M \to +\infty$, and $M^{-1} \to 0$. On the one hand, for the DL, in the limit, one obtains:

$$\lim_{R\to 0} r_{cc} = \sqrt[\gamma]{6 \cdot \left(C/N\right)_{\min}} \tag{4.12}$$

On the other, for the UL, also in the limit, one obtains:

$$\lim_{R\to 0} r_{cc} = \sqrt[\gamma]{6 \cdot \left(C/N\right)_{\min}} + 1 \tag{4.13}$$

By considering (4.11), it is straightforward to conclude that, for each propagation exponent value, the reuse pattern K only depends on the MCS through the value of the corresponding minimum carrier-to-noise ratio (or Carrier-to-Noise-Plus-Interference Ratio), and on the cellular interference geometry, either UL or DL.

While the asymptotic reuse factor is associated with the upper bound for system capacity, the maximum coverage distance is associated with the carrier-to-interference-plus-noise ratio at the cell edge when the interference is null. Since the interference-to-noise ratio, M, represents the interference that can still be tolerated for a given R, in the limit, the maximum coverage distance for which no extra interference is tolerated is obtained when $I(R) \to 0$, i.e., when $M(R) \to 0$ (meaning that $M_{[\mathrm{dB}]} \to -\infty$). Hence, the vertical asymptotes for the $M(R)$ and $r_{cc}(R)$ charts are given by:

$$R_{asymptote} = R_{M\to 0} \tag{4.14}$$

and are obtained by solving the following equation:

$$M(R) = \frac{(C(R)/N)}{(C/N)_{\min}} - 1 = 0 \tag{4.15}$$

or, in a simplified way:

$$C(R)/N = \left(C/N\right)_{\min} \tag{4.16}$$

By comparing this equation, valid only when $M \rightarrow 0$, with equation (4.3), one concludes that the approach of only considering the carrier-to-noise ratio constraints to determine the coverage distance, R, is inadequate in systems where interference is relevant, as equation (4.16) corresponds to a null interference-to-noise ratio, M. If a cellular system had been dimensioned this way there would not be an extra margin for interference, represented by $M = I/N$. Finally, it is important to highlight that the maximum coverage distance corresponding to the vertical asymptote, $R_{asymptote}$, for a given propagation exponent, depends not only on the modulation and coding scheme but also on the noise power, N, this is the reason why the reduction of the value of the noise power through sub-channelization, i.e., through the reduction of the radio frequency bandwidth, is so important.

With omnidirectional antennas, the worst-case for interference geometry corresponds to the case where the SS in Figure 4.3 is at the cell edge, hence $d = R$. The carrier-to-interference ratio in the DL is given by (4.6).

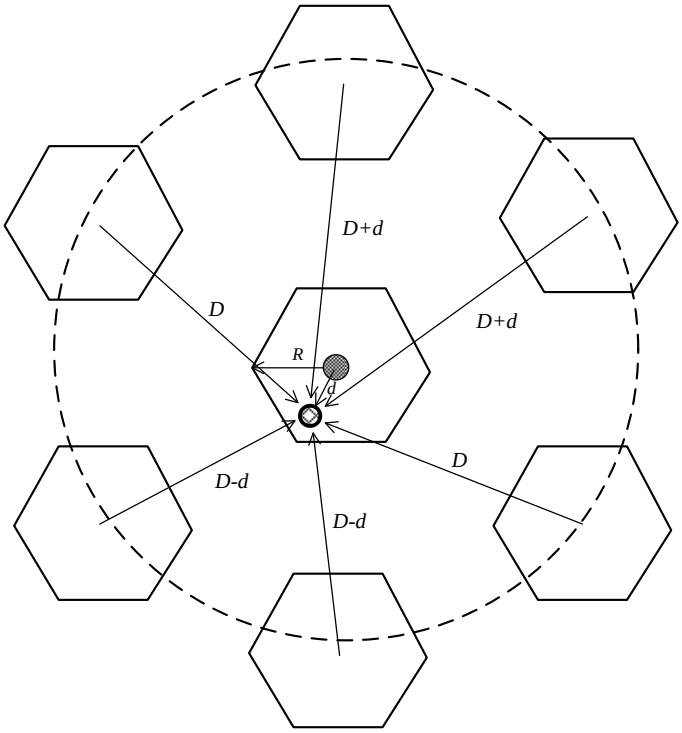

Figure 4.3 Co-channel interference in the worst-case for the UL.

With tri-sectored cells (120º sectors), equation (4.6) becomes [96]:

$$C/I = \frac{1}{(r_{cc}+0.7)^{-\gamma} + (r_{cc}-0.22)^{-\gamma}} \tag{4.17}$$

which is valid for both links. Note that in the omnidirectional case, the equation for the carrier-to-interference ratio in the UL results from the respective reuse geometry, where interferers are all at a distance D-0.866R from the central cell BS. This is given by:

$$C/I = \frac{(r_{cc} - 0.866)^{\gamma}}{6} \tag{4.18}$$

The above equations only consider the first tier of co-channel interference: this assumption is generally only valid if a high propagation exponent value is used. If lower propagation exponent values considered, interference to at least the second tier needs to also be addressed, as discussed in [95]. To satisfy this requirement, e.g., in equation (4.6), terms proportional to $2\cdot(2r_{cc}+1)^{-\gamma}$, $2\cdot r_{cc}^{-\gamma}$ and $2\cdot(2r_{cc}-1)^{-\gamma}$ need to be added to the denominator.

The differences caused by the presence of sub-channelization and sectorization can be interpreted by analysing the curves for CNIR as a function of the co-channel reuse factor, r_{cc}, with R as a parameter. To produce these curves, the power of the carrier is obtained by computing the power received by an SS at a distance R from the BS, while the computation of the interference depends on the UL and DL configuration, and also on the use of sectorization. This can be computed for a fixed R by making the same considerations for frequency reuse as in equations (4.6), (4.17) and (4.18). For the sake of simplicity, the modified Friis equation is considered with different values of the propagation exponent, γ, depending on the environment (γ = 3 is considered in many numerical examples, as it may be suggested from the experimental work in a suburban area from [97]). The noise power is computed by using the following equation:

$$N_{[dBW]} = -204 + 10 \cdot \log\left(b_{rf[Hz]}\right) \tag{4.19}$$

where b_{rf} is the channel radio frequency bandwidth. In the sub-channelization case, b_{rf} should be divided by 16, the number of sub-channels.

From these curves for the achievable CNIR as a function of r_{cc}, by considering the values of $CNIR_{min}$, it is straightforward to obtain the maximum supported physical throughput at the cell edge (distance R, or cell radius) in a simplified way, by considering that users are uniformly distributed on the cell but not considering the mixture of services and applications and the exact details for the corresponding "multiplexing" characteristics. For hexagonal-shaped cells, K = 1, 3, 4, and 7 correspond to reuse factors r_{cc} = 1.732, 3.000, 3.464, and 4.583, respectively.

4.2.2. Interference-to-Noise Ratio and Reuse Pattern

By using (4.5), one obtains the chart for the interference-to-noise ratio without sub-channelization from Figure 4.4, which is valid both for the UL and DL. The propagation exponent considered for the modified Friis model is $\gamma = 3$.

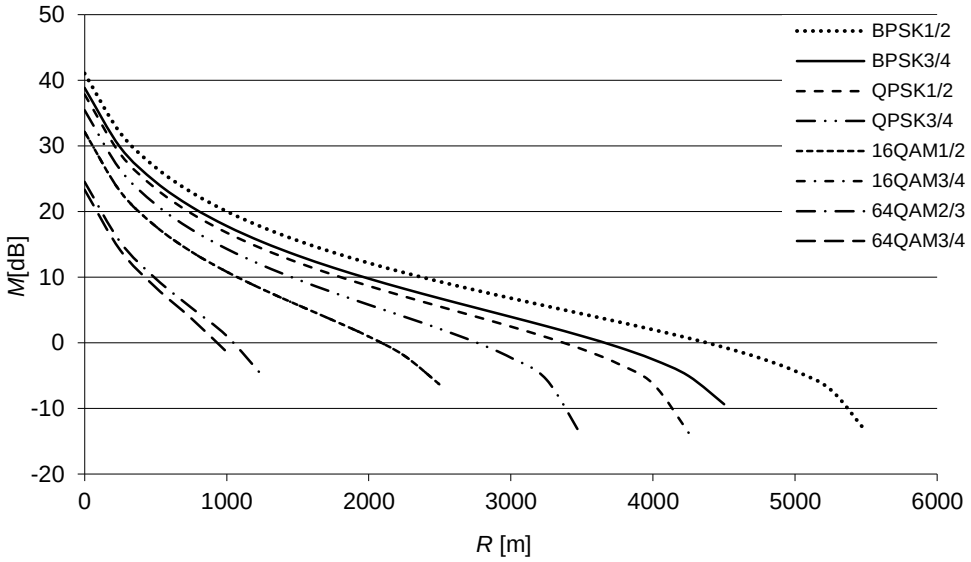

Figure 4.4 Interference-to-noise ratio without sub-channelization.

The modified Friis propagation model with $\gamma = 3$, transmitter power P_t = -2 dBW, and transmitter and receiver antenna gains G_t = 17 dBi and G_r = 9 dBi, respectively, are considered. The radio frequency bandwidth, the noise figure and the frequency are b_{rf} = 3.5 MHz, N_f = 3 dB, and f = 3.5 GHz, respectively. Table 4.1 presents the corresponding values for the vertical asymptote without sub-channelization, $R_{asymptote}$. It is observed a relevant decrease of the values for the vertical asymptote (maximum coverage distance) as the MCS level increases, which is compatible with the lowest values for C/N_{min}.

Table 4.1 Values for the vertical asymptote without sub-channelization.

Level	*MCS*	$R_{asymptote}$ [m]
1	BPSK $^{1/2}$	5814.86
2	BPSK $^{3/4}$	4911.41
3	QPSK $^{1/2}$	4548.55
4	QPSK $^{3/4}$	3783.32
5	16-QAM $^{1/2}$	2936.79
6	16-QAM $^{3/4}$	2368.86
7	64-QAM $^{2/3}$	1638.85
8	64-QAM $^{3/4}$	1494.65

Moreover, by applying (4.9) and (4.11) to the DL one obtains the charts for $r_{cc}(R)$ and $K(R)$ shown in Figure 4.5 and Figure 4.6, respectively.

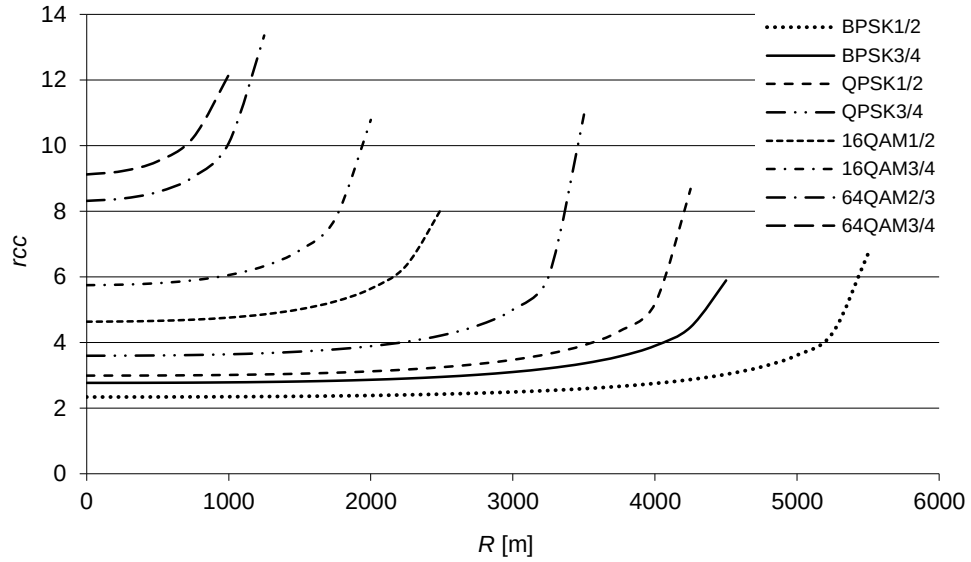

Figure 4.5 Reuse co-channel factor as a function of the coverage distance with MCS level as a parameter, in the DL without sub-channelization.

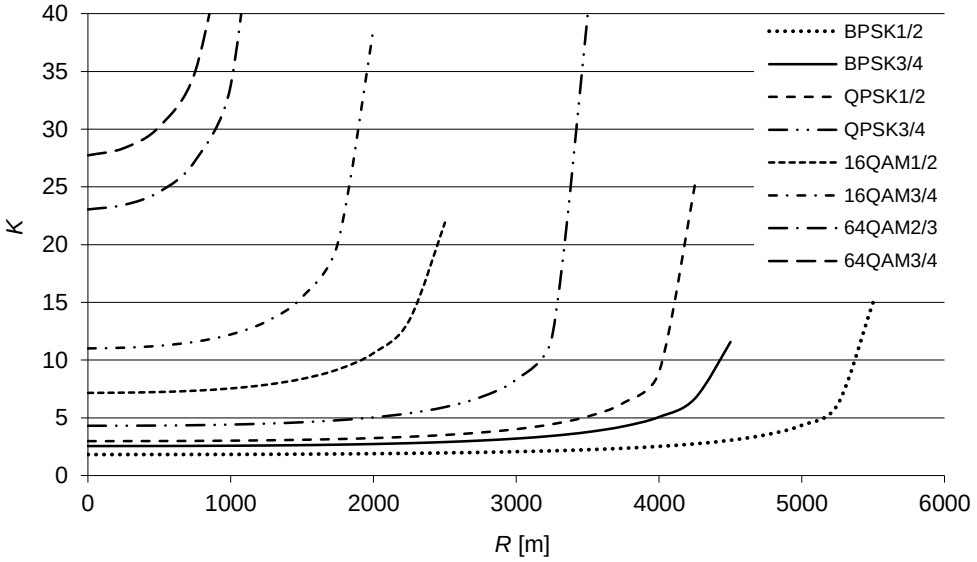

Figure 4.6 Reuse pattern as a function of the coverage distance with MCS level as a parameter, in the DL without sub-channelization.

By considering a reuse pattern K = 7 it is possible to use a maximum MCS level of 4, i.e., QPSK ¾, for $R \leq$ 2.7 km, and a maximum MCS level of 5, i.e., 16-QAM ½, for coverage distances lower than 1.2 km.

Figure 4.7 presents the results for the UL, which are worst since they correspond to higher values for the reuse pattern. In the UL without sub-channelization, for a reuse pattern

K = 7, only a low order MCS is achievable, i.e., QPSK ¾, up to a coverage distance of 2 km. It is verified that it is not possible to use 16-QAM ½, as it was in the DL.

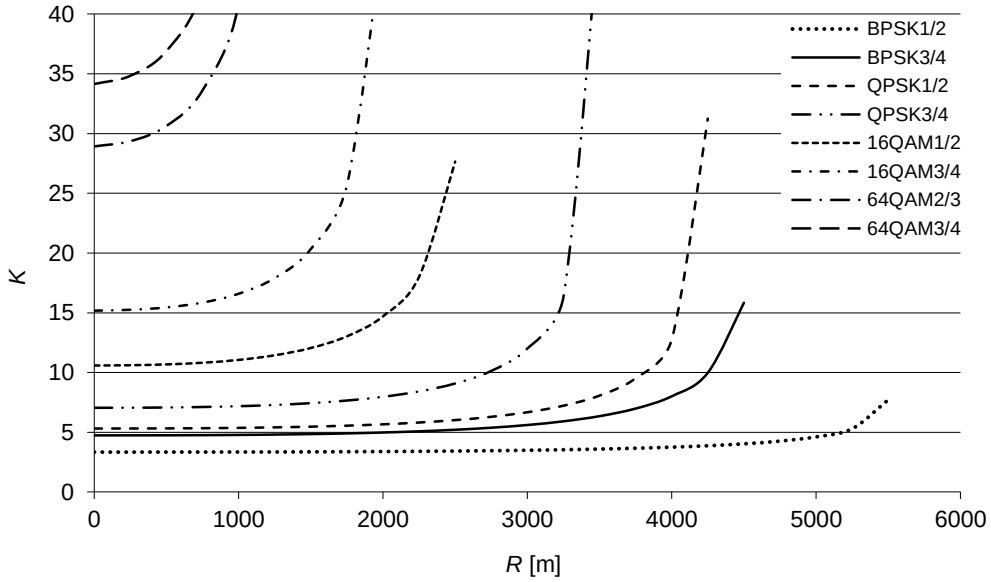

Figure 4.7 Reuse pattern as a function of the coverage distance with MCS level as a parameter, in the UL without sub-channelization.

It is therefore important to address techniques for the improvement of system capacity and coverage range. As sub-channelization is an optional feature in the IEEE 802.16-2004 UL, one explored its impact on the achieved MCS. Differently from the mobile version of WiMAX, IEEE 802.16-2004, based on Orthogonal Frequency division Multiplexing Physical (OFDM-PHY) does not support sub-channelization in the DL. For the UL, the use of sub-channelization limits the SS transmissions to 1/16 of the bandwidth assigned to the communication through the BS. The standard defines 16 sub-channels, and 1, 2, 4, 8 or all sets of sub-channels can be assigned to a SS, and each subscriber may use a different MCS in a more permanent way as far he/she is using a different sub-channel.

Nevertheless, in the DL, as the MCS can be chosen at burst level, there is also the flexibility of using different MCS by different users (even without sub-channelization), as they are served by different consecutive bursts within a frame.

By using (4.5) and (4.10) one obtains the charts for $M(R)$ and $K(R)$ from Figure 4.8 and Figure 4.9, respectively. Table 4.2 presents the new values for the vertical asymptotes, which are clearly higher than the ones without sub-channelization (more than twice the value). In this case, with 16 sub-channels, the variation of the noise power is $10 \cdot log(1/16)$ = -12 dB, providing an enhancement of 12 dB in the link budget. By comparing the evolution of $K(R)$ from Figure 4.9 with the case without employing sub-channelization there is no decrease in the reuse pattern, as a consequence, there is no direct increase in system capacity for the lowest values of R (only the achievable coverage distances are increased). For K = 7, the

achievable MCS is QPSK ¾. However, the achievable coverage distance increases from 2 to 5 km, approximately.

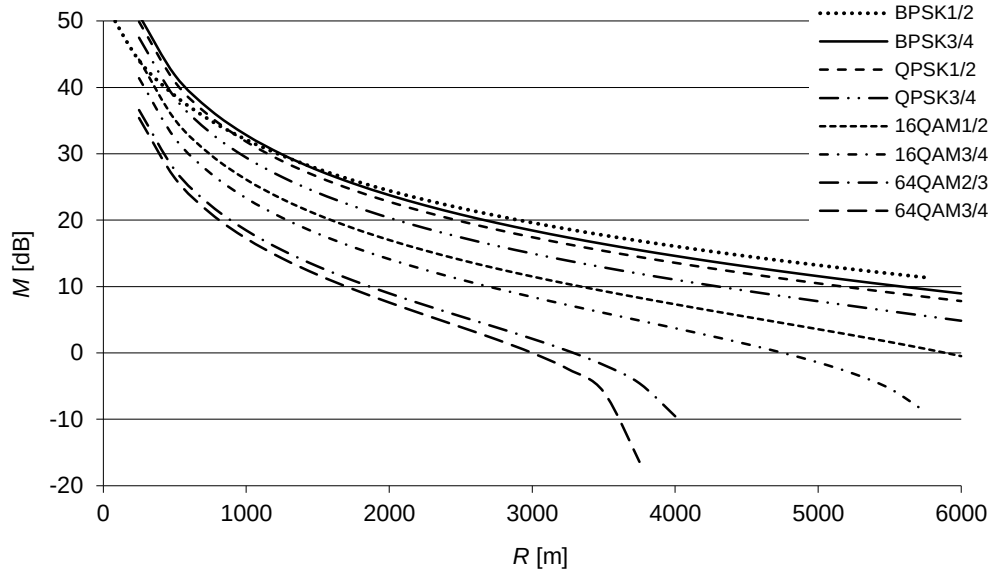

Figure 4.8 Interference-to-noise ratio with sub-channelization, valid for both links.

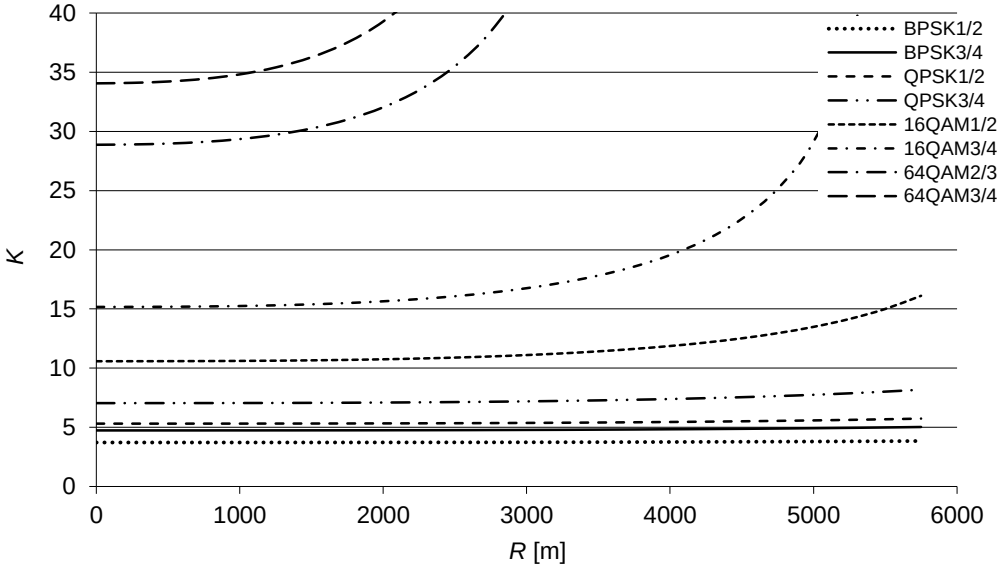

Figure 4.9 Reuse co-channel as a function of the coverage distance with MCS level as a parameter, in the UL with sub-channelization.

It is a worth noting that, in this case, the QPSK ½ MCS may be used up to a coverage distance of 6 km. In order to achieve higher system capacity the use of sectorization is suggested. The use of 120º sectorial BS antennas is adopted, i.e., one proposes the use of tri-sectored antennas.

Table 4.2 Values for the vertical asymptote with sub-channelization.

Level	*MCS*	$R_{asymptote}$ [m]
1	BPSK $^{1/2}$	14652.51
2	BPSK $^{3/4}$	12375.98
3	QPSK $^{1/2}$	11461.63
4	QPSK $^{3/4}$	9533.36
5	16-QAM $^{1/2}$	7400.25
6	16-QAM $^{3/4}$	5969.16
7	64-QAM $^{2/3}$	4129.65
8	64-QAM $^{3/4}$	3766.28

By inverting both members from (4.4) while using the formula for *C/I* from [97], one obtains:

$$\left[(r_{cc}+0.7)^{-\gamma}+(r_{cc}-0.22)^{-\gamma}\right]-\frac{1}{(1+M^{-1})\cdot(C/N)_{\min}}=0 \tag{4.20}$$

which is valid both for UL and DL. The minimum reuse factor required for such a tri-sectorial system may be obtained by solving this equation in order to r_{cc} while obtaining the reuse pattern through the use of (4.11). Note that, for the omnidirectional case, the usual assumptions for interference coming from six sources of interference were used in the computations. Although one only has considered one ring of interference some care would be needed if lower propagation exponents were used.

Figure 4.10 shows the variation of the reuse pattern, *K*, with the coverage distance, *R*. As no sub-channelization is considered in this case, the vertical asymptotes are the ones from Table 4.1. It is observed that, with sectorization, a clear improvement is obtained in the reuse pattern results in comparison with the ones previously presented, as reuse patterns suffer an important reduction. For *K* = 7 it is now possible to consider level 6 MCS, i.e., 16-QAM ¾, up to *R*~1.5 km, overcoming the level 5 MCS without sectorization. While 16-QAM ¾ can be used for coverage distances up to 1.5 km, 16-QAM ½ may be used up to *R* ≈ 2.2 km. With the QPSK ½ and QPSK ¾ MCSs it is possible to achieve *K* = 7 for coverage distances up to approximately 4.1 and 3.3 km, respectively.

The use of sub-channelization enables to increase the coverage distance while the use of sectorization increases the achievable system capacity (through the decrease of the reuse pattern). It is therefore worthwhile to explore the simultaneous use of sub-channelization and sectorization. Figure 4.11 presents the variation of the reuse pattern with the cell coverage distance for this new case, only possible in the UL for fixed WiMAX. Larger coverage distances are possible together with lower reuse distances. With *K* = 7, it is possible to achieve the 16-QAM ¾ MCS (level 6) up to *R* = 4.3 km, while the achievable MCS is 16-QAM ½ (level 5) up to a coverage distance of 6.0 km. In this case, with *K* = 3, lower order MCSs, e.g., BPSK ½, BPSK 3/4, QPSK ½, or QPSK ¾, are perfectly achieved up to coverage distances larger than 6.0 km.

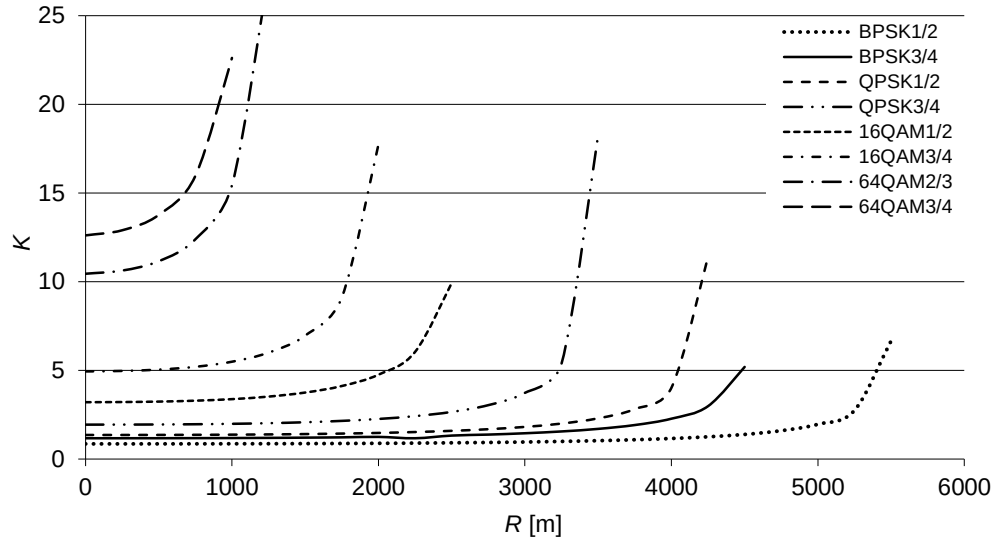

Figure 4.10 Reuse pattern as a function of the coverage distance with MCS level as a parameter, in the UL with sectorisation, but without sub-channelization.

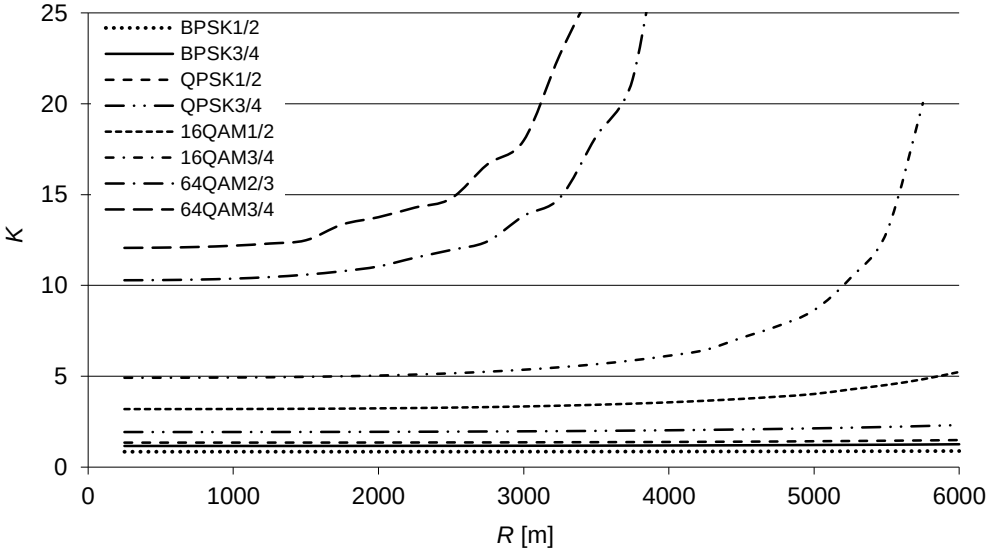

Figure 4.11 Reuse pattern as a function of the coverage distance with MCS level as a parameter, in the UL with sectorisation and sub-channelization.

The reduction of the reuse pattern directly corresponds to an increase in system capacity (but not in the cellular coverage). However, it indirectly contributes to an increase in system capacity as higher level MCSs are made available into outer cell coverage rings through the use of adaptive MCSs.

One issue that is left for further study is the dependence of these results on the propagation exponent, γ. For example, if the propagation exponent decreases the value of the coverage distance asymptote will increase but the asymptotic value for the reuse factor, r_{cc}, will also increase, corresponding to a reduction on the supported system capacity by each MCS.

4.2.3. Carrier-to-Noise-plus-Interference Ratio and co-channel Reuse Factor

To better understand the changes caused by sub-channelization (16 sub-channels) and sectorization it is worthwhile to plot the CNIR curves as a function of the reuse factor, r_{cc}, with R as a parameter. To produce these curves the power of the carrier is obtained by computing the power received by an SS at a distance R from the BS while the computation of the interference depends on the UL and DL configuration and on the use of sectorization as well. It can be computed, for a fixed R, by making the same considerations for the reuse as assumed for equations (4.6), (4.8) and (4.20). Although IEEE 802.16-2004 cannot use sub-channelization in the DL, one important comparison is between absence and presence of sub-channelization in the UL. Another important case is the simultaneous use of sub-channelization and sectorization. Figure 4.12 shows CNIR as a function of r_{cc} with R as a parameter for the UL for each MCS.

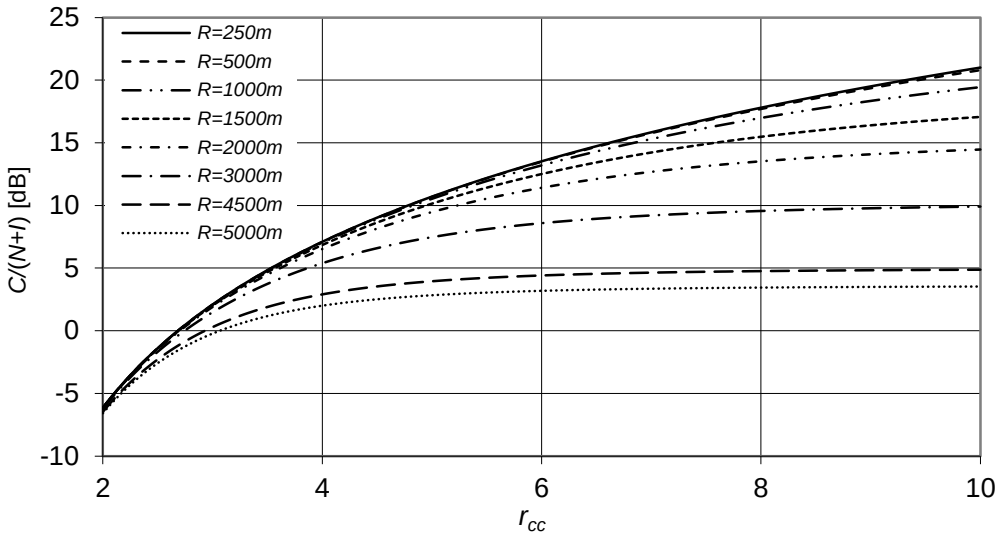

Figure 4.12 CNIR as a function of r_{cc} with R as a parameter, in the UL, no sub-channelization.

It is clear that for r_{cc} = 4.58, i.e., K = 7, values of CNIR are always lower than 8.9 dB while for coverage distances larger than 2 km it decreases considerably.

Figure 4.13 presents the results for CNIR as a function of r_{cc}, in the UL with sub-channelization. Improvements are only evident for the longest coverage distances, i.e., with sub-channelization the main improvement is on the coverage. If sectorization is applied alone then the values for CNIR at r_{cc} = 4.58 will be higher.

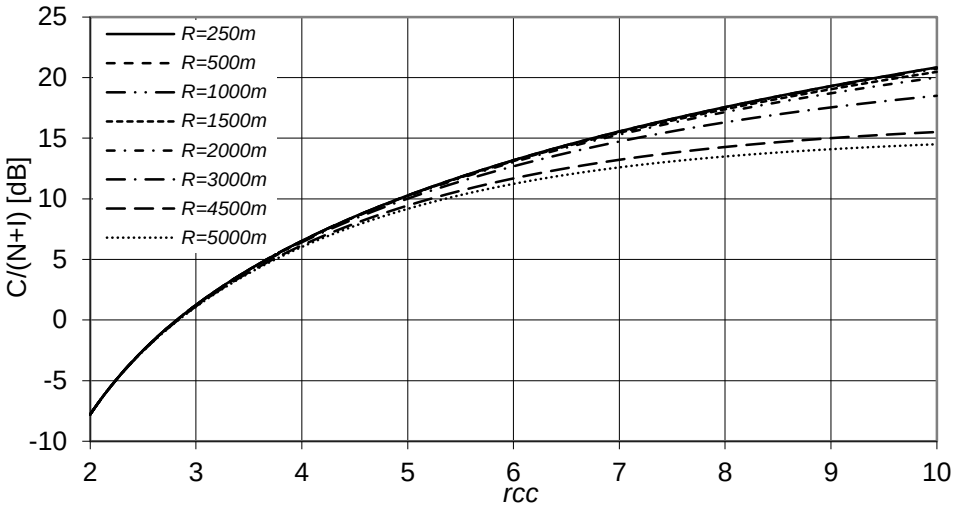

Figure 4.13 CNIR as a function of r_{cc}, with R as a parameter, in the UL with sub-channelization.

However, a truly improvement for coverage distances up to 3 km (not only 2 km anymore) requires both sectorization and sub-channelization for the UL, as CNIR exceeds 15 dB, as shown in Figure 4.14. This leads to a clear confirmation of the need for the simultaneous use of both improvement techniques.

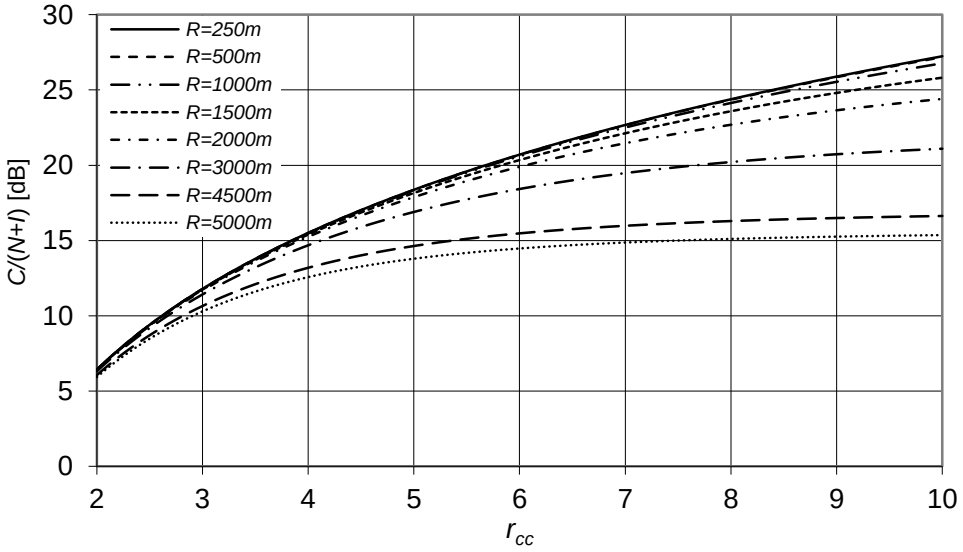

Figure 4.14 CNIR as a function of r_{cc}, with R as a parameter, in the UL with sub-channelization and sectorization.

4.2.4. Carrier-to-Noise-plus-Interference Ratio with Relays

For the DL there are three different cases that need to be individually analysed:

1. **BS to SS**: BS to SS communication is the simple case, shown in Figure 4.15. While the power of the received carrier is computed for a distance *d*, the distances assumed for the computation of co-channel interference are maintained, i.e., $r_{cc}\cdot(R\text{-}1)$ for the UL and ~$r_{cc}\cdot R$ for the DL. In the tri-sectored case, the power of the received carrier is also computed for a distance *d*. However, in the computation of co-channel interference the following formulation stands:

$$C/I = \frac{d^{-\gamma}}{(r_{cc}\cdot R + 0.7\cdot d)^{-\gamma} + (r_{cc}\cdot R - 0.22\cdot d)^{-\gamma}} \tag{4.21}$$

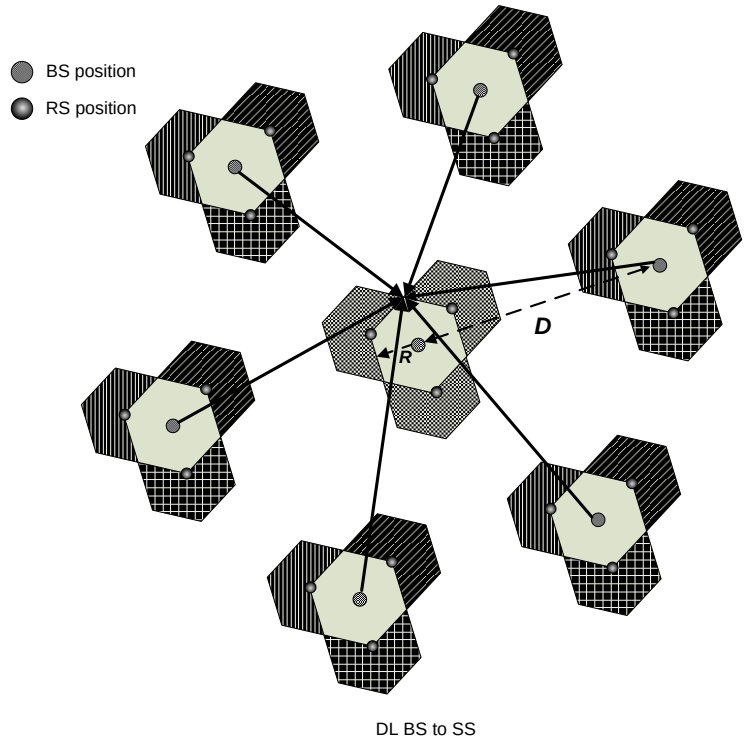

Figure 4.15 DL Scenario.

2. **BS to RS**: In the case of BS to RS communication one assumes that RSs are using directional antennas of 120 two BSs, Figure 4.16. This ultimately effects and enhances the *C/I* by a significant amount as shown in the later discussion. Therefore, $(D+\beta R)^{-\gamma}/R^{-\gamma} = (r_{cc}+\beta)^{-\gamma}$ has a coefficient 2 while $\beta = 1$ and *C/I* is given by:

$$\frac{C}{I} = \left(\frac{1}{2(r_{cc}+1)^{-\gamma}}\right) \tag{4.22}$$

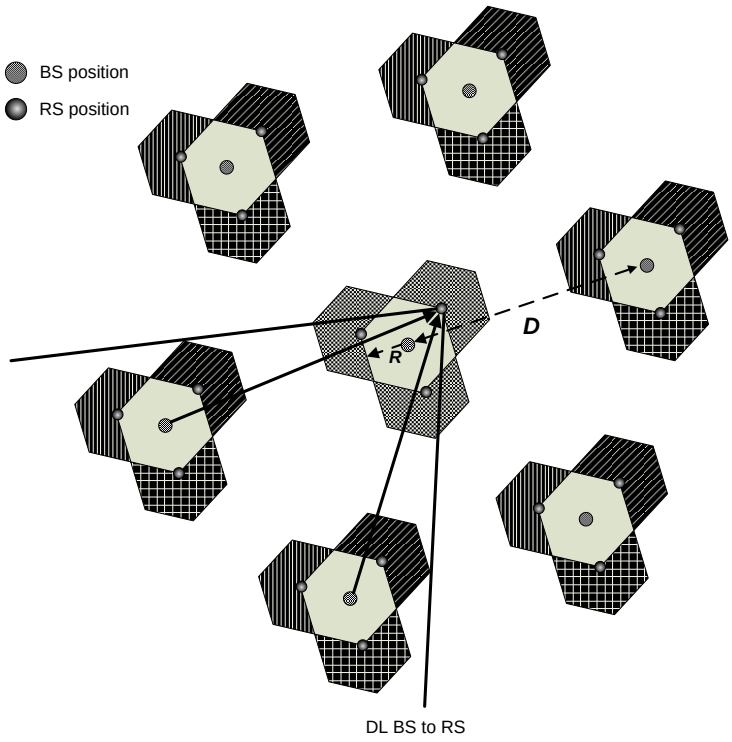

Figure 4.16 DL Scenario with 120 ° RS sectorial antennas and 240º RS sector coverage area.

3. **RS to SS:** In the case of RS to SS, the SS receives interference from four neighbouring RSs, Figure 4.17. The distances between cell centres, RS and SS shown in Figure 4.15, measured by using Autocad 2008 in a worst case situation where RS is at the edge of the coverage area. On the basis of measured distances the coefficients β (adjustment coefficient for worst case SS position in the cell with relays) of R, in$(D+\beta R)^{-\gamma}$, are calculated as given below [98]:

$$D = 3R\sqrt{3} = 519.615242 \text{ m} \tag{4.23}$$

for

$$R = 100 \text{ m} \tag{4.24}$$

There are two RS at 435.8899 m from the envisaged SS:

$$\frac{435.8899 - 519.615242}{100} = -0.83725342 \tag{4.25}$$

There is one RS at 529.1503 m from the SS:

$$\frac{529.1503 - 519.615242}{100} = 0.09535058 \tag{4.26}$$

and one at a distance 608.2763 m:

$$\frac{608.2763 - 519.615242}{100} = 0.88661058 \tag{4.27}$$

Hence, C/I is given by [98]:

$$\frac{C}{I} = \frac{R^{-\gamma}}{2(D-0.8372R)^{-\gamma} + (D+0.09535R)^{-\gamma} + (D+0.8866R)^{-\gamma}} \tag{4.28}$$

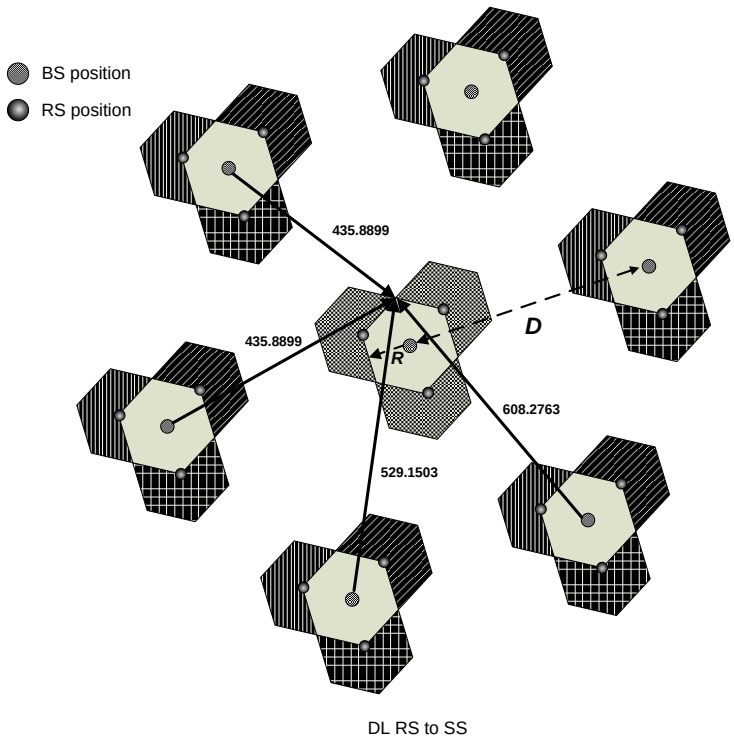

Figure 4.17 Distances from the RS interferers to the SS.

For the UL there are also are three different cases that need to be individually analysed:

1. **From SS to BS:** In case of SS to BS there is interference from six surrounding SS. Thus carrier-to-interference ratio is given by:

$$\frac{C}{I} = \frac{(r_{cc} - 0.866)^{\gamma}}{6} \tag{4.29}$$

2. **From RS to BS:** In this case it is assumed that RS antennas are 120^0 sectored. Thus, the BS at the central cell only receives interference from two RS, at distance *D*+*R*, as shown in Figure 4.18 and Figure 4.19. The carrier-to-interference ratio is given by:

$$\frac{C}{I} = \frac{(r_{cc}+1)^{\gamma}}{2} \tag{4.30}$$

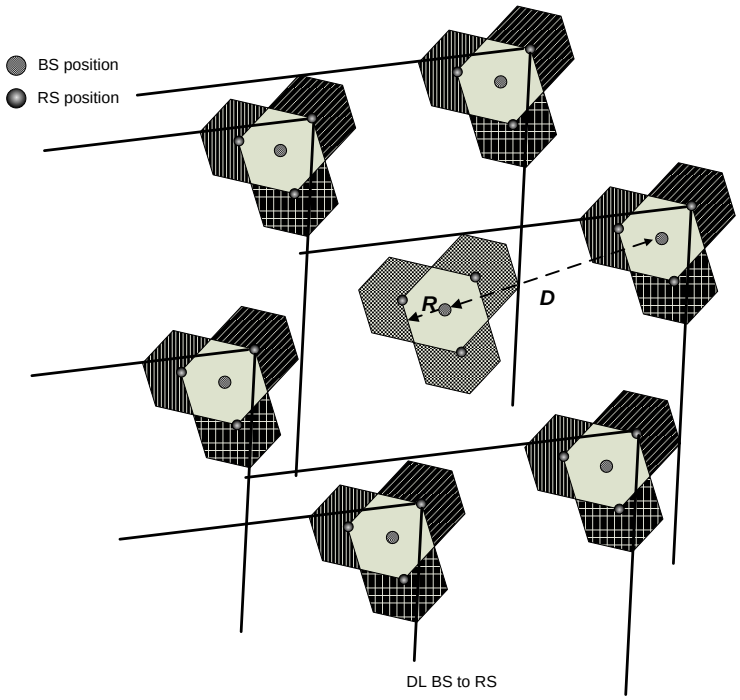

Figure 4.18 Decrease of the co-channel interference by using directional antennas at RS.

3. **From SS to RS:** In this case RS receives interference from four SSs in neighbouring cells. By using the same procedure to measure the distances between cell centres, RS and SS, the following values were obtained for the coefficients *B* of *R*: -0.8761, -0.82776, -0.80762. As a consequence, *C*/*I* is given by:

$$\frac{C}{I} = \frac{R^{-\gamma}}{2(D-0.8761R)^{-\gamma} + (D-0.082776\,R)^{-\gamma} + (D-0.80762\,R)^{-\gamma}} \tag{4.31}$$

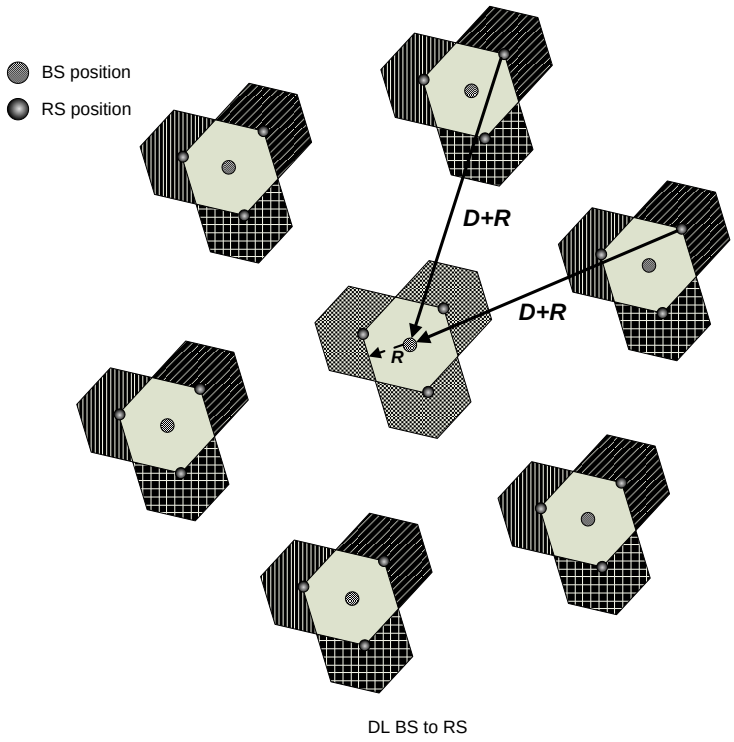

Figure 4.19 Distances from RS to BS in the UL.

4.3 System Capacity

4.3.1. Modelling of the Propagation Environment

The WiMAX propagation has been characterized in different operating situations by means of field trials at 3.5 GHz. The measurement campaigns have been conducted in a suburban cell in Covilhã, Portugal. The setup for the field trials was based on an Alvarion BreezeMAX 3000 micro Base Station (μBS). During these experiments, the Alvarion outdoor data unit (ODU) was operating at 3551.75 MHz (DL) and 3451.75 MHz (UL), with a maximum transmitter power of 28 dBm. For the μBS, a 10 dBi omnidirectional antenna is considered, installed 28 m above ground level, at the top of a 7 m pole on the rooftop of the Health Science Faculty (HSF) of the University of Beira Interior.

A summary of the equipment parameters considered during the field trials is presented in Table 4.3.

Table 4.3 Transmitter/receiver parameters for the field trials setup.

Parameter	Value
b_{rf}	3.5 MHz
f	3.5 GHz
f_{DL}	3551.75 MHz
f_{UL}	3451.75 MHz
P_t	-2 dBW
G_t	10 dBi (BS)
BS antenna height	28 m
G_r	10 dBi
receiver antenna height	2.3 m

Instead of a SS, a Rohde & Schwarz FSH8 portable spectrum analyser was used during the trials. In order to measure the received power at different locations, another 10 dBi omnidirectional antenna, connected to the spectrum analyser, was installed on the rooftop of the car, approximately 2.3 m above ground level, shown in Figure 4.20. Geo-referencing was provided by a Global Positioning System (GPS) receiver. The frequency range of the spectrum analyser covers 9 kHz to 8 GHz, with a sensitivity of -160 dBm. The sweep time can be configured between 200 μs and 100 s. The spectrum analyser measured channel power received at the antenna in the considered frequency band using the "channel power measurement" option.

Figure 4.20 Measurement campaigns μBS setup and measurement equipment.

In order to improve the acquisition methodology, instead of roaming the city at vehicular speed not exceeding 40 km/h (the approach from [99]), the car was stopped approximately every 30-50 m to acquire the channel power several times at a steady position. Aside from the spectrum measurement accuracy improvements, this method provides an increased confidence to the geo-referring process. GPS receivers have a margin of error usually of few meters, which increases whenever the receiver is moving. Additionally, to

further improve the spectrum analyser measurement accuracy, the value of its sweep was increased, i.e., the number of channel power measurements. From the chart of the repeatability/error as a function of the number of samples, extracted from [100], one obtains the acquisition parameters for different sweep times for the measurements campaign performed during autumn 2011 and spring 2012, as shown in Table 4.4. In the latter measurements the spectrum analyser was reconfigured to increase its sensitivity by setting the resolution bandwidth to 100 Hz and the video bandwidth to 10 Hz. As a consequence, it was possible to measure received power values lower than -90 dBm.

Table 4.4 Spectrum analyser acquisition parameters.

Parameter	Autumn 2011	Spring 2012
Sweep time [ms]	20	772
Number of data acquisitions	3	5
Duration of each acquisition [s]	5	25
Number of samples	750	162
Repeatability (or error) [dB]	± 0.45	± 1.00

Table 4.4 also presents the repeatability for a given number of samples [100]. For example, a repeatability of ± 0.45 dB means that the measured value lies within a range of ± 0.45 dB from the true value, with a confidence level of 99 % [100]. It was also verified that the histogram of the 80 measurements taken in a single location from Figure 4.21 follows a Gaussian distribution with a confidence level of 95 %, with expectation μ = -73.08 dBm (location of the peak) and standard deviation σ = 0.711 dB.

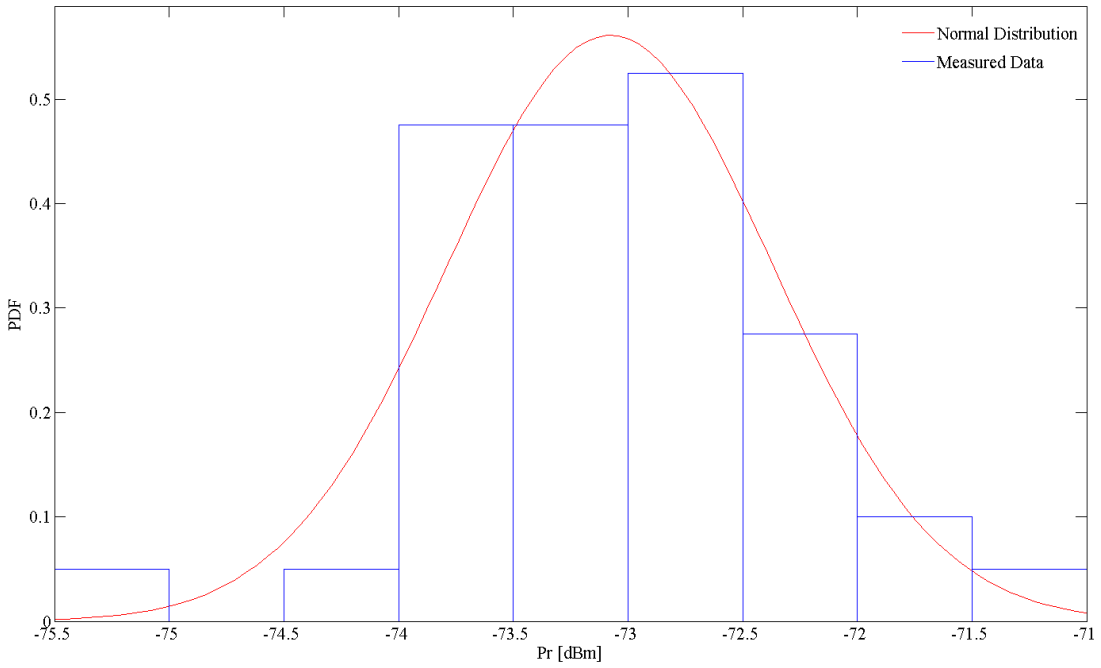

Figure 4.21 Distribution of the terminal received power (dBm) for a measurement point taken in Covilhã. The superimposed Gaussian curve (in dB) suggests this terminal received power ensemble is approximately log-normal.

4.3.2. Measurements Results and Curve Fitting

During the autumn of 2011 measurements, from the several routes that were followed, the straightest path moving away from the BS was selected. From the results, an adequate fit to the SUI-C model [101] was achieved for distances up to 900 m with low density of trees (and other foliage). In the spring of 2012, a substantial increase of the foliage and even the existence of additional vegetation (as the trees had grown) were observed. Then, the curve for the measurements of the received power (and the resulting path loss, PL) in the same range of distances fitted the SUI-A model [101]. For larger distances (up to 1670 m), the influence of the foliage near the HSF was negligible. Figure 4.22 shows the variation of the measured and the modified Friis path loss with the distance (varying from 1.30 to 1.67 km) in the latter case.

Field trial measurements provide the value of the received power. To compute the path loss one has to consider the influence of the transmitter power and gains from the antennas, as well as the influence of the inclination of the subscriber antenna, into the received power. As mentioned above, the transmitter power is a known value. However, to subtract the antenna gains one has to consider the influence of the antenna vertical (or elevation) radiation pattern. Note that the horizontal radiation (or azimuth) pattern from the antenna is omnidirectional.

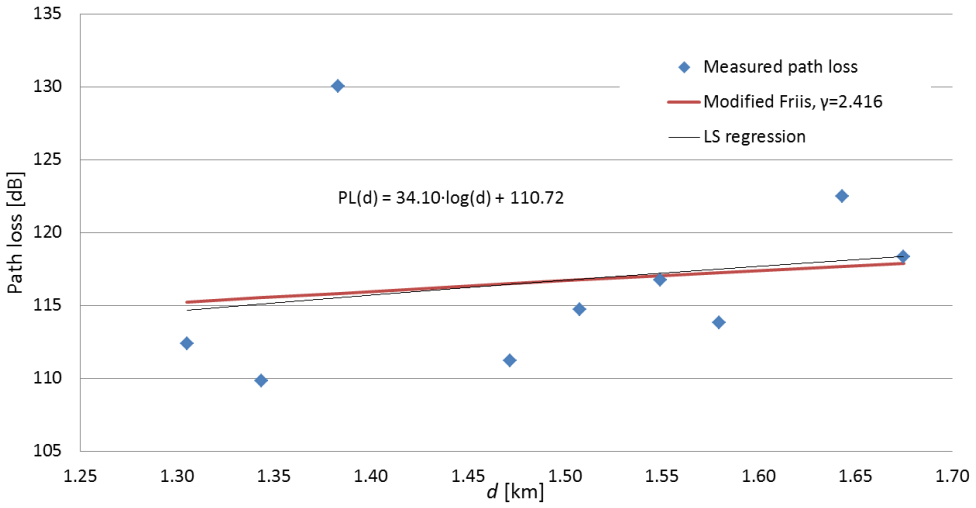

Figure 4.22 Measured and modified Friis (γ = 2.416) path loss curve.

As it is shown in Figure 4.23, different angles of incidence (or take-off angles), φ_1, provide different values for the antenna gain. The maximum values of the antenna gain occur from values of φ_1 between -10° (350°) and 10°, and 170° and 190°. When the incidence beam moves away from the horizontal plane the antenna gain diminishes.

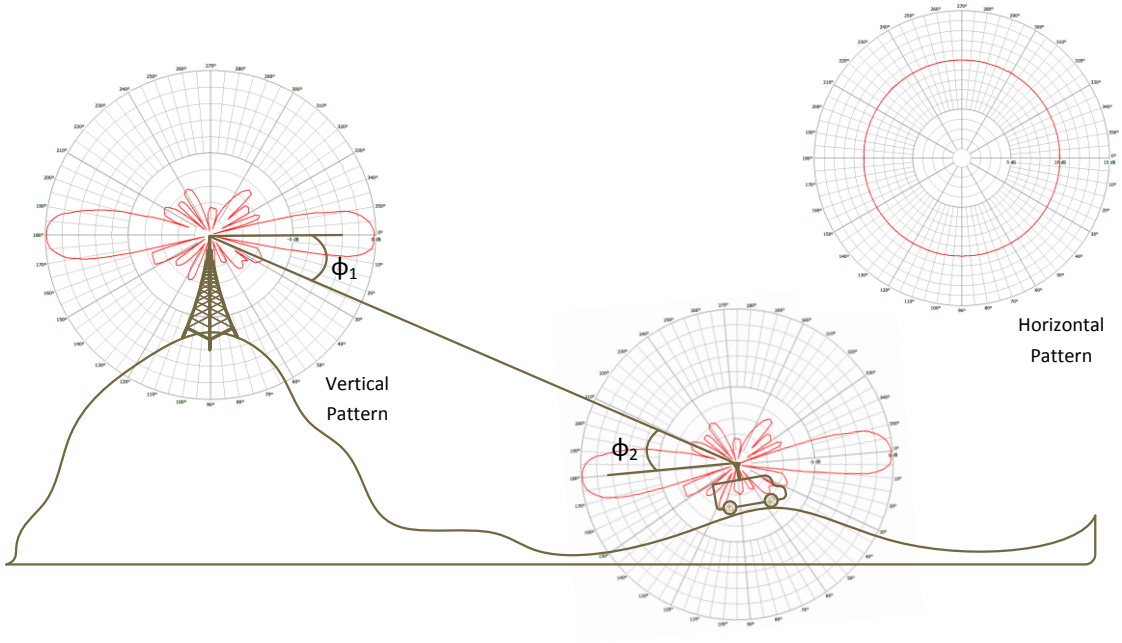

Figure 4.23 Influence of the angles of incidence and arrival in the computation of the path loss.

During the field trials, it was found that φ_1 varied between 2.5º and 24º, which correspond to a decrease in the antenna gain between 1.81 and 2.23 dB, respectively. Additionally, the angle of arrival, φ_2, between the subscriber station and the BS antenna was also considered.

The terrain slope is also responsible for changes in the antenna gain, i.e., the angle of arrival, φ_2, also incorporates de terrain slope. It is positive or negative when the car is going uphill or downhill, respectively, or null, when the trajectory is on flat terrain. The angle of arrival is determined through an approach similar to the one considered to determined φ_1. It has been found that φ_2 varied between -1.1º and 5.4º. As a consequence of this analysis, it was found that φ_1 and φ_2 are responsible for losses up to 4 dB. This formulation methodology enables to compensate for the antennas gains at different incident angles.

By comparing the results with known path loss models through least-square (LS) regression, a fit to the modified Friis model was achieved with a propagation exponent, y, varying from 2.416, in the case shown in Figure 4.22, to y = 2.55, in other field trials.

4.3.3. Assumptions

To guarantee WiMAX communications with no coverage gaps near the cell edge (i.e., to enable Binary Phase Shift Keying (BPSK) with ½ MCS, the lowest order MCS, as shown in Table 4.5), the value of the CNIR must be higher than 3.3 dB throughout the cell [92], [93] yielding a physical throughput of just 1.41 Mbps. Here, the radio frequency bandwidth, noise figure, and frequency are b_{rf} = 3.5 MHz, NF = 3 dB, and f = 3.5 GHz, respectively [92].

Table 4.5 *CNIRmin*, physical throughput and *AuxFactor* for different values of the MCS ID for the communications to the SSs at the RS coverage zone.

ID	MCS	*CNIRmin* [dB]	Physical thr. [Mbps]	*AuxFactor*(d)
1	BPSK ½	3.3	1.41	1.41/5.64
2	BPSK ¾	5.5	2.12	2.12/5.64
3	QPSK ½	6.5	2.82	2.82/5.64
4	QPSK ¾	8.9	4.23	4.23/5.64
5	**16-QAM ½**	**12.2**	**5.64**	**1**
6	16-QAM ¾	15.0	8.47	1
7	64-QAM ⅔	19.8	11.29	1
8	64-QAM ¾	21.0	12.27	1

In line with the lessons learned from the performed measurements, the modified Friis propagation model is assumed. Assumptions for the values of different parameters are P_t = -2 dBW, γ = 2.416 in suburban areas G_{BS} = 10 dBi, and G_{SS} = 9 dBi for BS-to-SS and SS-to-BS communications [92], and P_t = -2dBW, G_{RS} = 17 dBi for RS-to-SS communications, while G_{BS} = 10 dBi and G_{RS} = 28 dBi for BS-to-RS and RS-to-BS communications respectively. The difference between the receiver gains for the RS/BS and the RS/SS (or BS/SS) communications is justified by the use of a directional antenna in the RS, pointing directly towards the central BS, this antenna has a gain, G_{RS}, of ~28 dBi [92]. A summary of these parameters is presented in Table 4.6.

Table 4.6 Parameters for the analysis of the system capacity.

Parameter	Value
b_{rf}	3.5 MHz
f	3.5 GHz
f_{DL}	3551.75 MHz
f_{UL}	3451.75 MHz
P_t	-2 dBW
BS antenna height	28 m
Receiver antenna height	2.3 m
G_{BS}	10 dBi (BS-to-SS and BS-to-RS)
G_{SS}	9 dBi (SS-to-BS)
G_{RS}	17 dBi (RS-to-SS)
G_{RS}	28 dBI (RS-to-BS)

The worst-case interference scenario is considered, where the mobile is at the cell edge and the co-channel interference is the highest. On the one hand, the worst-case DL interference scenario occurs when the BS of the serving cell transmits to the SS at the cell edge, using a channel (or sub-channel) on which the SS is also receiving interference from the BSs of the six co-channel hexagonal neighbouring cells Figure 4.1. On the other hand, for the UL, the worst-case interference scenario occurs when the SS is transmitting to the BS from the cell edge, and interfering SSs are at the cell edge at the closest distance from the central/serving cell, Figure 4.2.

In the considered multihop context, with K = 3, a cell is composed by the central coverage zone, served by the BS, and three 240º sector coverage zones, served by individual RSs (RS_1, RS_2 and RS_3), as shown in Figure 4.24.a). While the BS antenna may be either omnidirectional or sectored (120º sectors) RS antennas for BS communication are considered

to be directional, e.g., 120º sectored or narrower beamwidth ones), to reduce the received interference from BSs and facilitate non-overlapping coverage with the central zone of cell.

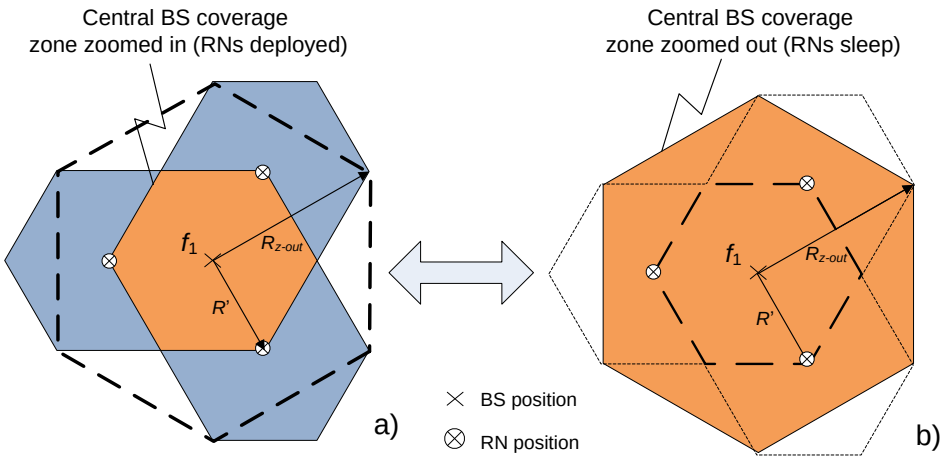

Figure 4.24 a) BS, RS and respective "hexagonal" coverage areas, b) central coverage zone zooms out when RSs sleep.

Although BS backhaul is assured in the usual terms for mobile communications, e.g., cable or micro-wave radio link, RS backhauling is supported by using special and specific sub-frames within the radio channel created for that purpose. The duration of each sub-frame is 5 ms [92]. This proposal on frames is inspired by the sub-frame structure from [102] and explores the inclusion of RS DL traffic/communications from RS to SS into the UL frequency sub-frame only considering single-hop between the RS and SSs, differently from the proposal for IEEE 802.16j from [103], which enables multihop. However, note that there may be some similarities between the sub-frame structure proposed here and the frame with transparent relaying in IEEE 802.16j. With transparent relaying, the RSs do not forward framing information, hence do not increase the coverage of the wireless system, the main use of this mode is to facilitate capacity increase within the cell. The considered type of RS is of lower complexity, and only operates in a centralized scheduling mode and for topology up to two hops.

The aforementioned mode assumes that the RSs have some small buffering capability, such that multiple hops via the RS can be scheduled in different frames. For example, data can be transmitted from the BS to the RS in one frame, and the same data can be forwarded from the RS to the SS in the subsequent frame. These assumptions for the frame are also inspired by the IEEE 802.16-2004 frames, which consist of two sub-frames, operating in the FDD mode, where the DL and the UL are transmitted simultaneously. Although the considered version of fixed WiMAX originally used FDD, this proposal implies that Time Division Duplexing (TDD) needs to be additionally supported (over the FDD frame structure) for RS-to-SS communications.

Besides, the proposal for DL and UL frequency sub-frames from Figure 4.25.a) and b) (the cases of omnidirectional and tri-sectored BS antenna) assumes an asymmetry factor of 1:5 between the UL and DL. The advantage of using RSs arises from the fact the co-channel interference now comes from cells at a larger distance [93]. The improvement of the present tri-sectored frame, relatively to the frame for the omnidirectional cells proposed in Figure 4.25.a) [92], [93], corresponds to the increase of the throughput in the area covered by the RSs by a factor of the number of sectors, N_{sec}, as there is a carrier assigned to each sector. The N_{sec} increase takes place in both DL and UL, due to the use of a more favourable frame format.

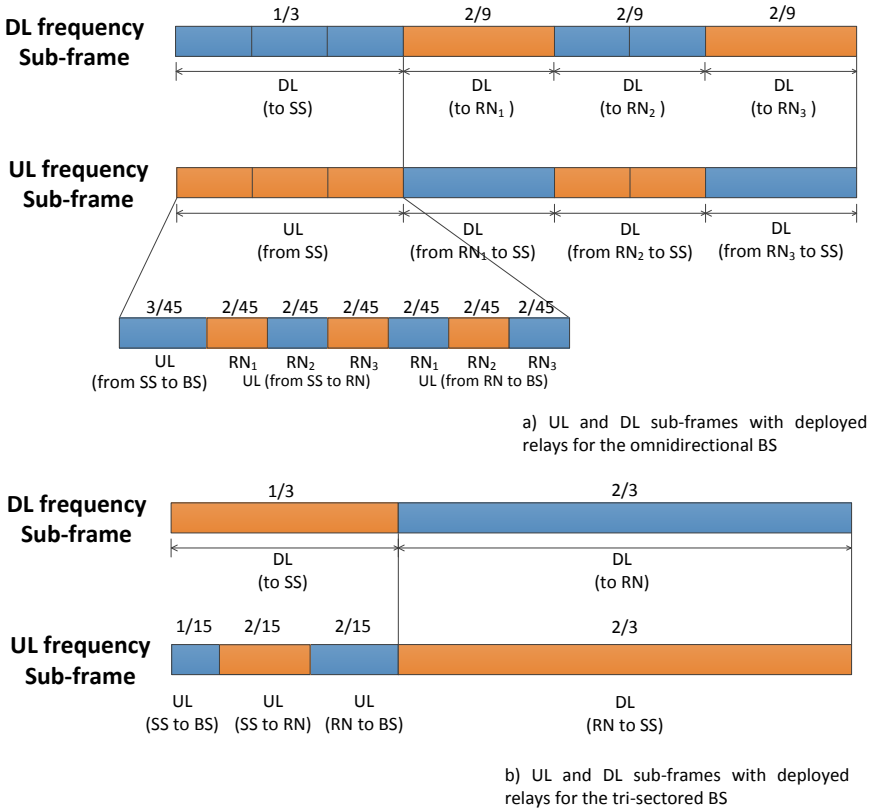

Figure 4.25 Structure for UL and DL sub-frames with deployed RSs, a) omnidirectional BS, b) the tri-sectored BS.

The assumed type of RS is not standardized and available yet but this structure for frequency sub-frames is flexible enough to accommodate changes in the relay topology (e.g., facilitating the inclusion of mobile RSs), as RSs and SSs already incorporate TDD in the UL frequency sub-frame.

4.3.4. Supported Cell/Sector Physical Throughput

4.3.4.1. Implicit Function Formulation

The assessment of the supported cell/sector physical throughput (per transceiver), R_b, as a function of the distance, d, produces a staircase-shaped curve indicating that higher maximum achievable throughputs are supported near the centre of the cell, shown in Figure 4.26 (where R is the cell radius). As the throughput is not constant over the whole coverage area, for cellular planning proposes, the supported throughput is obtained by computing the average supported throughput in the cell. As stated previously, in contrast to [105], [106] worst-case scenarios for interference geometry are considered here.

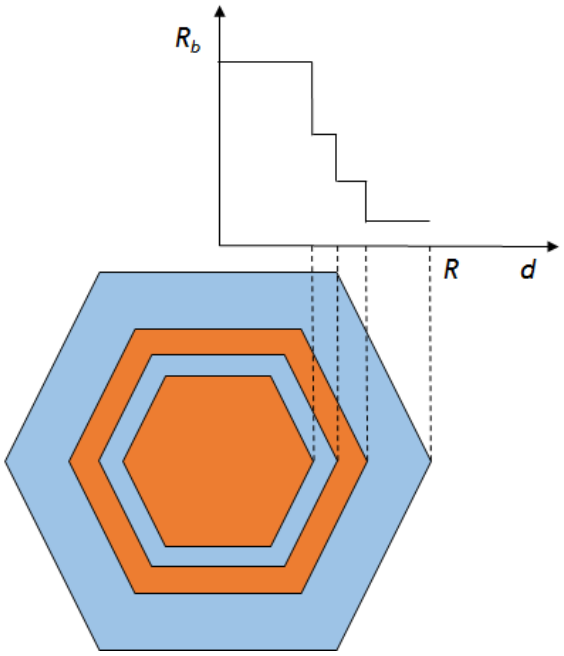

Figure 4.26 Areas of the coverage rings where a given value of physical throughput is supported.

There are J different coverage rings in each coverage zone, each supporting a different MCS (for instance, J = 4 in Figure 4.26). The distances that correspond to the steps between consecutive MCS are represented by d_j, j = 1, 2, …, J. Here one denotes the order of the MCS as MCS_j. The number of different coverage rings is given by:

$$J = MCS_{1^{st}} - MCS_{last} + 1 \tag{4.32}$$

where MCS_{1st} and MCS_{last} represent the MCS for the 1st and last coverage rings, respectively.

If only one frequency channel is considered per cell, the supported throughput is obtained as [96]:

$$R_{b-\sup} = \frac{\iint_{O} R_b(d,R,K)dxdy}{\frac{3\sqrt{3}}{2}\cdot R^2} = \frac{\sum_{j=1}^{J}\left(\frac{3\sqrt{3}}{2}\cdot\left(d_j^2 - d_{j-1}^2\right)\cdot\left(R_b\right)_{MCS_{1^{st}}+1-j}\right)}{\frac{3\sqrt{3}}{2}\cdot R^2} \tag{4.33}$$

where the 2D integral is performed over the hexagonal shape of the cell. It is computed by weighting the supported physical throughput in each concentric coverage ring by the size of the ring where that value is supported. The contribution of each of the transmission modes is thus considered.

MCS_1^{st}, MCS_2^{nd}, …, MCS_J^{th} can be obtained in the following way:

$$MCS_j\left(CNIR_{[dB]}\right) = \begin{cases} 0, & CNIR < 3.3 \\ 1, & 3.3 \le CNIR < 5.5 \\ 2, & 5.5 < CNIR < 6.5 \\ 3, & 6.5 < CNIR < 8.9 \\ 4, & 8.9 < CNIR < 12.2 \\ 5, & 12.2 < CNIR < 15.0 \\ 6, & 15.0 < CNIR < 19.8 \\ 7, & 19.8 < CNIR < 21.0 \\ 8, & CNIR > 21.0 \end{cases} \tag{4.34}$$

where j represents the coverage ring, $CNIR_{[dB]} = 10\cdot\log(\text{cnir})$, and $MCS_k = 0$ means that there is not enough coverage in that part of the cell (or coverage ring), in this case, the system will not be viable. Besides, if $l = MCS_j$, one can represent the physical throughput corresponding to each MCS, $l = 0, 1, \ldots, 8$, as:

$$\left(R_b\right)_l = \begin{cases} 0, & l = 0 \\ 1.41, & l = 1 \\ 2.12, & l = 2 \\ 2.82, & l = 3 \\ 4.23, & l = 4 \\ 5.64, & l = 5 \\ 8.47, & l = 6 \\ 11.23, & l = 7 \\ 12.27, & l = 8 \end{cases} \tag{4.35}$$

$CNIR(R_b)$ is not a bijective function. Therefore, the value of CNIR that corresponds to a given R_b is the minimum value of $CNIR$, i.e., $CNIR_{min}$, that supports a given throughput R_b. Hence $d_0 = 0$, and

$$d_j = cnir^{-1}\left(\min\left(CNIR\left(\left(R_b\right)_{MCS_{1^{st}}+1-j}\right)\right)\right) \tag{4.36}$$

Figure 4.27 presents the correspondence between the CNIR vs. propagation distance curve and the stepwise function that represents the $CNIR_{min}$ threshold for each MCS vs. R_b. Figure 4.27 illustrates how the mapping between $CNIR$ and supported physical throughput relates to step distances between consecutive MCS d_J, d_{J-1}, d_{J-2},…

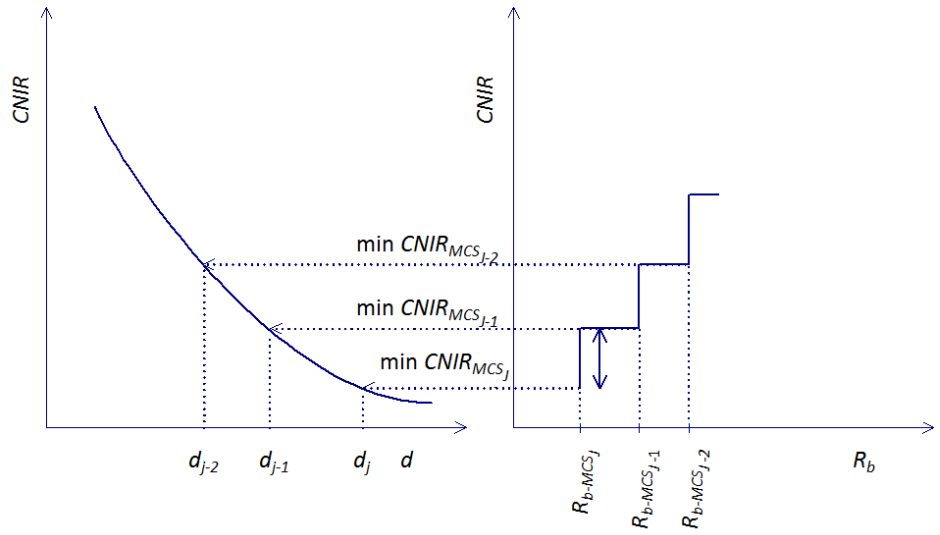

Figure 4.27 Correspondence between the physical throughput for rings *J*, *J*-1, *J*-2, …, and the minimum *CNIRs* of consecutive MCS that map to step distances d_J, d_{J-1}, d_{J-2}, ….

In the context of the experimental work performed within the Instituto de Telecomunicações research group, results have fitted the modified Friis equation to some ranges of coverage distances in Fixed WiMAX [97]. According to the modified Friis equation, the received power is given by:

$$p_r(d) = \frac{p_t \cdot g_t \cdot g_r \cdot \lambda^2}{(4\pi)^2 d^\gamma} \tag{4.37}$$

where $0 \leq d \leq R$, λ is the wavelength, P_t, G_t and G_r (the latter ones are in dB), and γ is the propagation exponent.

4.3.4.2. Physical throughput with relays and cell zooming

With the frame format proposed for the tri-sectorial BS, communications using a given frequency carrier are only from/to a sector and a RS. In the omnidirectional case (number of sectors N_{sec} = 1), the central zone BS provides shared access to/from three RSs within the same frequency carrier. Hence, to obtain the supported throughput, the contribution from the central cell results from multiplying the sector supported throughput by N_{sec}. Although the considered cells with three RSs are formed by one central hexagonal coverage zone plus three 240º RS zones, with radius *R'* each, as shown in Figure 4.24.a), as the RS coverage zones form 240º sectors the cells have an equivalent area corresponding to three omnidirectional (360º) coverage zone with radius *R'*. The equivalent supported throughput in a hexagonal coverage zone (or cell) with an area of $(3\sqrt{3}/2)\cdot R'^2$ is therefore given as follows:

$$\left(R_{b-\sup}\right)_{equiv} = \frac{R_{b-tot}}{3} = \frac{N_{\sec} \cdot R_{b-central} + 3 \cdot R_{b-RS-zone}}{3} = \\ = \frac{1}{2} \cdot N_{\sec} \cdot R_{b-central-norm} + R_{b-RS-zone} \tag{4.38}$$

where $R_{b\text{-}tot}$ is the total throughput in the multihop cell (formed by the central plus RS zones), $R_{b\text{-}central}$ is the computed throughput in the central coverage zone and $R_{b\text{-}RS\text{-}zone}$ is the computed throughput in the RSs coverage zone. $R_{b\text{-}central\text{-}norm}$ = 2/3 $R_{b\text{-}central}$ and represents the throughput as 2/3 of the areas of the central coverage zone assuming uniform user traffic distribution (over an area equal to the one from each RS zone). The use of sectored cells corresponds to N_{sec} increase in both DL and UL traffic from/to the BS, due to the use of a more favourable frame format.

The approach from [92] and [93] has been considered to compute the CNIR, corresponding to worst-case situations on the edge of the cell, where higher co-channel interference takes place, due to the proximity between co-cells. The physical throughput, $R_{b[\text{Mbps}]}$, was computed according to its correspondence to the values of CNIR from Table 4.5, yielding a stepwise behaviour that comes from the correspondence between $CNIR_{min}$, in dB, and the physical throughput for each MCS. By weighting the physical throughput achieved in each concentric cell coverage ring (or coverage area) by the size of the ring, Figure 4.26, the contribution from each transmission mode (or MCS) is included in the previous implicit function to obtain the average supported throughput.

In practice, the throughput at a distance d from the RS, $R_b(d)$, depends on the supported modulation and coding scheme (MCS), and is given by [93]:

$$R_b(d) = \frac{2}{9} N_{Sec} \times R_b(R) \times AuxFactor(d) \tag{4.39}$$

where d is the distance to the RS and $R_b(R)$ is the maximum throughput at the edge of the central coverage zone, at a distance R from the BS and N_{sec} is the number of sectors of the central coverage zone (N_{sec} = 1 or 3 in the omnidirectional or tri-sectored cases, respectively). $AuxFactor(d)$ represents the reduction of the throughput at a distance d relatively to the throughput at the centre of the RS coverage zone and is given in Table 4.5 (example for a 16-QAM ½ MCS at the central of the coverage zone).

For this example, Table 4.5 shows the values for $AuxFactor(d)$ if the MCS ID that may be guaranteed for the $CNIR(d)$ from the RS coverage area is within the range 1-8. The 16-QAM ½ MCS is shown in bold in Table 4.5. In practice, if the MCS supported at a distance d from the RS is higher than or equal to the one supported in the BS-to-RS link (16-QAM ½ in this example) in the omnidirectional case, the throughput for RS will be 2/9 $R_b(R)$; otherwise, the throughput will be 2/9 $(R_{b\text{-}sup})_{RS}$.

Additionally, when one considers the supported throughput according to the omnidirectional and tri-sectored BS sub-frames, it can be found that:

- The central BS throughput, BS to SS, is supported by 1/3 of the frame structure, so the DL throughput is obtained by multiplying the total obtained throughput by 1/3 in both the omnidirectional and the tri-sectored case.
- For the throughput from the BS to the RS (DL) and, from the RS to the SS (downlink at the UL frame), 2/9 and 2/3 of the frame structure are assigned for the omnidirectional and tri-sectored BS, respectively. As such, the throughput is obtained by multiplying these factors of 2/9 and 2/3 by the total obtained throughput.
- For the supported UL throughput from the SSs to the BS in the central coverage area, 3/45 = 1/15 of the frame structure is assigned to the UL, so the UL throughput is obtained by multiplying the total obtained throughput by 3/45 (or 1/15) in both the omnidirectional and the tri-sectored case.
- For the supported UL throughput from the SS to the RS, 2/45 and 2/15 of the frame structure are assigned for the omnidirectional and tri-sectored BS, respectively. As such, the throughput is obtained by multiplying the total obtained throughput by 2/9 and 2/3, for the omnidirectional and tri-sectored BSs, respectively.

Since the RS antennas are directional, the omnidirectional BS only receives interference from two RS at distance $D+R$. At the RS it is only possible to achieve a throughput of 2/45 $(R_{b\text{-}sup})_{SS}$ for the omnidirectional BS and 2/15 $(R_{b\text{-}sup})_{SS}$ for the tri-sectored BS, where $(R_{b\text{-}sup})_{SS}$ refers to the supported throughput from the SS to RS. This traffic will only reach the BS if the RS to BS radio link supports such a value of throughput.

Figure 4.28 shows results for the equivalent supported throughput as a function of R' and $R_{z\text{-}out}$ for the DL, K = 3 and the absence/presence of RSs, where two different horizontal axis are represented. While R' is the coverage distance for the central and RS coverage zones, $R_{z-out} = \sqrt{3}R'$ is the radius for the zoomed out cell, as shown in Figure 4.24.b). BSs with omnidirectional and tri-sectored antennas were considered whilst first assuming that the frame format is not adaptively adapted in the absence of RSs.

For omnidirectional BSs antenna, in the absence of RSs, it was not possible to obtain the curve for the supported throughput for K = 3, as the cell is not totally covered with at least the BPSK ½ MCS, corresponding to CNIR ≥ 3.3 dB. The curves for the cell throughput reach 0 Mbps for distances lower than the coverage distance, e.g., the non-covered zone is ~7 % for $R_{z\text{-}out}$ = 2000 m. In the presence of RSs, the supported throughput is very low for omnidirectional BS antennas (approximately 2.5 Mbps). However, with tri-sectored BS antennas (1 carrier/sector), as the interference is decreased, the supported throughput reaches circa 6.7 Mbps in the absence of RSs and more than 8.5 Mbps in the presence of RSs. When the RSs are switched-off, if the frame format needs to be kept, there is a partial loss of capacity (as the part of the sub-frame dedicated to communication with RSs is being wasted).

Until now, it is assumed that only one carrier was used per cell per sector, i.e., the total bandwidth is 3×3.5 = 10.5 MHz and 3×3.5×3 = 31.5 MHz, for omnidirectional and tri-

sectored cells, respectively. However, in the omnidirectional case the operator is able to use three carriers, which results in 3×10.5 = 31.5 MHz (total bandwidth). As a consequence, although the total throughput is obtained by multiplying the cell/sector throughput by three because there are three available carriers, in the omnidirectional case, and three sectors in the "zoomed out" cell with one carrier each, in the tri-sectored case), one still needs to consider the effect of the DL sub-frame format in the resulting supported throughput, i.e., a factor of 1/3 in both cases [93], yielding to an overall multiplying factor of 1.

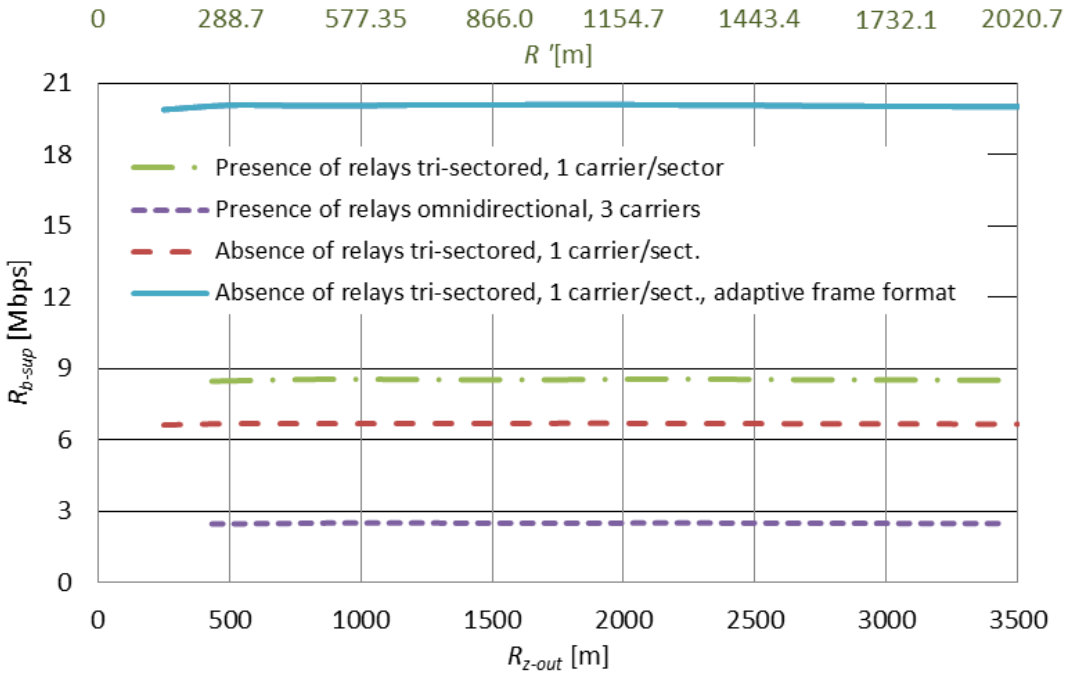

Figure 4.28 Comparison of the equivalent supported throughput between the cells with relays and the zoomed-out cells, K = 3.

For tri-sectored BS antennas, is has also been considered the possibility of adaptively adapt the frame format when the RSs are switched-off and only the BS equipment remains active. In this unlikely possibility [92], the theoretical supported throughput would reach ~20 Mbps. This improvement leads to a theoretical advantage for the topologies with no RSs that may possibly compensate the better/more regular coverage achieved in topologies with RSs. The supported throughput is used in Chapter 5 to calculate the revenues and profits.

4.4 Cellular Planning in Actual Environments

Covilhã, Portugal is located on a very hilly terrain at the bottom of Serra da Estrela, a 2000 m mountain, leading to very challenging cellular planning. The Winprop™ simulations were performed by considering the Dominant Path (DP) model and Ray Tracing (RT) propagation functionality with several reflections while neglecting diffraction. Furthermore,

Winprop™ simulations have been using a detailed 553527 pixels database for urban building data of the city of Covilhã, with 2528 buildings and a total area is 7.79 km^2, as shown in Figure 4.29. It is a worth noting that the pixel database uses rectangular coordinates from Hayford-Gauss-Lisboa of the Portuguese Army surveying Institute (Instituto Geográfico do Exército, IGeoE) coordinate system, with a resolution of 25 m per pixel.

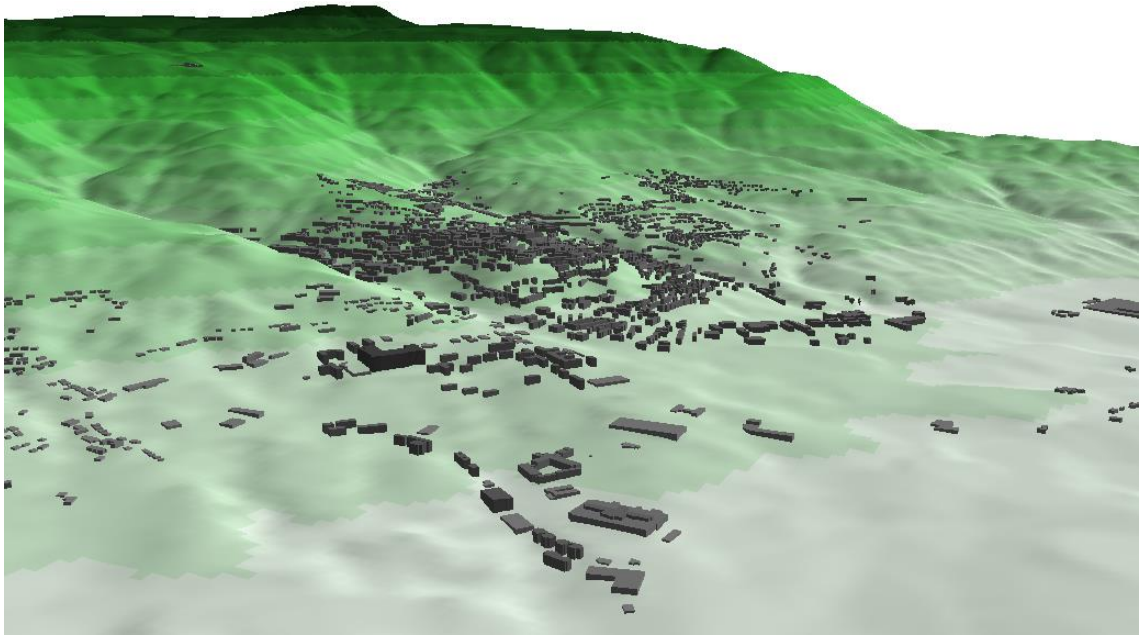

Figure 4.29 Pixel database for the city of Covilhã terrain and buildings.

In Figure 4.29, it can be observed that the city is located on a very hilly terrain at the bottom of the highest mountain in continental Portugal. Cellular planning in this type of geographical location is a challenging engineering problem.

The parameters considered for the BS, SS and RS are similar to the ones considered in the field trials from [106] with only slight changes (Table 4.7), namely the SS is considered to be at 2 m height, and the gain from 120º tri-sectored antenna from the BS is 15.3 dBi, instead of 17 dBi, while the BS/RS and SS noise figures are 3 and 5 dB, respectively.

Table 4.7 Parameters for the analysis of the system capacity.

	System Parameters
Operating frequency	3.5 GHz
Duplex mode	FDD/TDD or FDD
Channel bandwidth	3.5 MHz
BS height	20 m
SS height	2 m
SS antenna gain	9 dBi
BS/RS antenna gain	15 (OMNI), 15.3 (120º Sectored), 17 (240º Sectored)
BS/RS transmitter power	28 dBm
BS/RS noise figure	3 dB
SS noise figure	5 dB
Reuse pattern, *K*	3

The OFDM parameters considered in the simulations are the ones from Alvarion's μBS, shown in Table 4.8.

Table 4.8 OFDM parameters.

	OFDM Parameters
FFT size	256
Subcarrier Spacing [kHz]	15.625
Useful Symbol Time [μs]	64
Oversampling Rate	8/7
No. of Data Subcarriers (DL)	192
No. of Pilot Subcarriers (DL)	8
No. of Guard Subcarriers (DL)	56

The cellular planning exercises assume K = 3 and topologies formed by a central cell and six first tier interferers using frequency f_1, for two different configurations, as follows:

- Zoomed-out cells with no RSs, covering the same area as the cells with RSs, with $R_{z\text{-}out} = \sqrt{3}R'$ = 1732 m;
- Cells with RSs (shape from Figure 4.24.a), as shown in Figure 4.30, tri-sectored BSs, with R' = 1000 m.

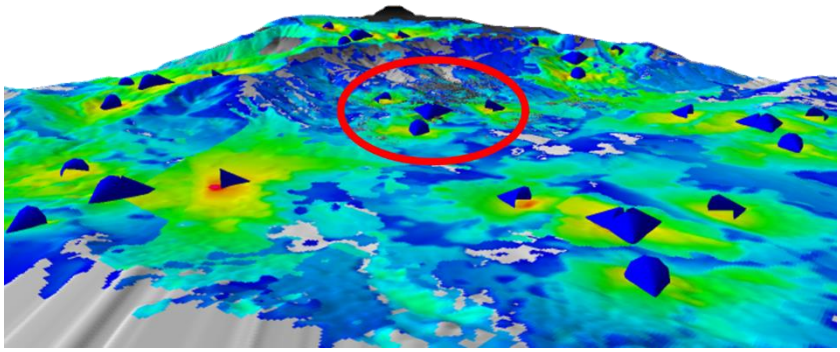

Figure 4.30 CNIR in the central cell (marked with the orange circle) comprising tri-sectored BSs and three RSs with RT.

Note that the cells using f_2 and f_3 are not considered in the simulations and the CNIR results are only adequate in the central cell, the only one that suffers interference from six co-cells.

By considering the co-channel interference and noise, one has been able to obtain results for the coverage and determine if there are some zones of the cell with no coverage guarantee, i.e., where CNIR < 3.3 dB. The area of the cell with no coverage and the equivalent supported throughput are shown in Table 4.9 and Table 4.10 for the RT propagation functionality and DP model, respectively.

While in the presence of RSs there is a reasonably adequate coverage, with "no RSs" there are coverage gaps, as the "illumination" is inadequate throughout the cell. For the

latter topology, in the tri-sectored case, although the non-covered area reaches 18.10 %, if RT coverage is considered, the supported throughput reaches 5.192 Mbps, a value lower than the theoretical 6.7 Mbps but higher than 5.05 Mbps obtained from Table 4.10 with the DP model instead of RT (besides, if adaptive frame format was possible, the supported throughput would be 15.58 Mbps, and not ~20Mbps).

Table 4.9 Summary of the cellular planning results considering RT coverage in the simulations.

	Area not covered		$(Rb\text{-}sup)_{equiv}$[Mbps]	
Type of cell	Omni.	Tri-sect.	Omni.	Tri-sect.
Zoomed-out cells, no RSs	41.68 %	18.10 %	-	5.192
Cells with RSs	4.35 %	4.25 %	2.67	8.616

Table 4.10 Summary of the planning results considering the DP model.

	Area not covered		$(Rb\text{-}sup)_{equiv}$[Mbps]	
Type of cell	Omni.	Tri-sect.	Omni.	Tri-sect.
Zoomed-out cells, no RSs	38.77 %	19.44 %	-	5.05
Cells with RSs	6.08 %	5.22 %	2.76	8.67

Figure 4.31 presents results for the cell/sector throughput in the central cell with tri-sectored antennas and the presence of RSs with RT. The reuse topology is the same as in Figure 4.30 (where six "first tier" interferers are considered). In configurations with RSs, the results for the supported throughput obtained from Winprop™ with RT are clearly better in the tri-sectored case (8.616 Mbps compared to 2.67 Mbps in the omnidirectional case) but slightly worse than the ones obtained with the DP model (8.67 and 2.76 Mbps, respectively).

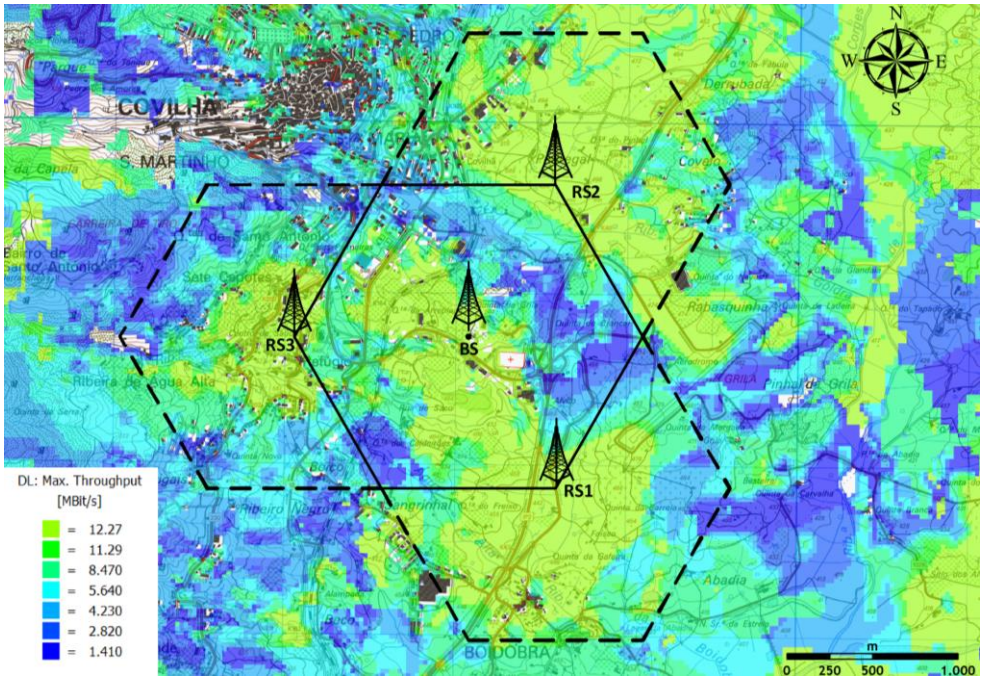

Figure 4.31 Spatial variation of the throughput with tri-sectored BS antenna and the presence of relays with RT.

4.5 Conclusions

In this chapter, an analytical approach was used to determine the trade-offs between the coverage distance and interference minimization whilst increasing system capacity. From the analysis, it is clear that both noise and interference present strong limitations to the performance of fixed WiMAX, mainly for higher MCS levels. With a reuse pattern $K = 7$, cell throughputs near the maximum are only achieved, in the UL, if sub-channelization is used together with sectorization. With the use of sub-channelization alone, although the noise power decreases, the improvement is not so clear.

For the shortest coverage distances, the use of sectorization alone in the UL allows for obtaining a substantial gain in the physical throughput. However, for larger coverage distances, in the absence of sub-channelization, the achievable gain is not comparable with the case where sub-channelization is used.

In general terms, the use of sectorization in fixed WiMAX enables to reduce the reuse pattern while considering sub-channelization allows for improvement on the coverage. The reduction of the reuse pattern directly corresponds to an increase in the system capacity but the improvement in the coverage range (through sub-channelization) can also allow for an improvement in UL system capacity, as adaptive MCS are used. The presence of relay stations (either fixed or mobile), with limited coverage, introduces new challenges into the design process, as interference can be mitigated in different ways whilst increasing coverage (e.g., by decreasing the transmitter power or by using advanced scheduling techniques).

The planning and optimization of fixed WiMAX networks with RSs in conjunction with cell zooming was addressed. The challenging case of a propagation measurement-based scenario in the hilly region of Covilhã, Portugal, has been chosen, whereby precise details of the measurement campaign have been outlined. The formulation for the CNIR with and without RSs has been addressed. Innovative DL and UL sub-frames have also been proposed. In this proposal for RSs, the FDD mode is considered and the frames need to guarantee resources for BS-to-MS communications but also for BS-to-RS and RS-to-MS communications. These requirements leads to a 1:5 asymmetry factor between the UL and DL in the omnidirectional BS case and to a 3:7 asymmetry factor in the case of tri-sectored BSs. The system capacity and the supported cell/sector physical throughput formulation were also presented.

From the cellular planning exercise in actual environments it has been shown that the coverage is adequate in the presence of RSs and the obtained results are similar to theoretical results for a full-coverage scenario. Through RT and the application of the DP model, it has been shown that without RSs the supported throughput is lower in practice, as coverage is not 100 % (even with tri-sectored BSs). If omnidirectional BS antennas are used without RSs, the proportion of the cell with no coverage reaches 41.68 % or 38.77 %, through RT and the application of the DP model, respectively.

Chapter 5

Cost/Revenue Trade-off and Energy Saving Through Relay Sleep Modes and Cell Zooming

5.1 Introduction

WiMAX deployment Optimization can be achieved by appropriately parameterising a merit function, taking costs and revenues into account. The Optimization of the cost/revenue trade-off provides a means of combining several contributing factors in cellular planning: determination of the reuse pattern, coverage distance, and the resulting supported physical throughput.

Given the current state of national frequency spectrum assignments throughout Europe, the Fixed WiMAX achievable frequency reuse pattern, *K*, determines the reduction in the initial fixed cost if the required spectrum bandwidth is reduced to values comparable to the ones for Wideband Code Division Multiple Access (WCDMA) systems. In turn, the supported throughput will determine the achievable revenue, which has interdependencies with the use (or not) of sub-channelization and/or sectorization. The optimization of the cost/revenue trade-off for different topologies is thus of fundamental importance, and can be achieved by varying system parameters and implied coverage and reuse distances.

A cost/revenue function has to be developed by taking into account the cost of building and maintaining the infrastructure, and the way the number of channels available in each cell affects operators' and service providers' revenues. Fixed costs for licensing and spectrum bandwidth auctions (often known as "beauty contests") should also be taken into account. The economic analysis is referred as a cost/revenue performance analysis, because the Optimization (i.e., minimization) of cost does not necessarily mean the optimization of net revenues. Although one considers a project duration of five years as a working hypothesis in radio and network planning, it is decided to analyse costs and revenues on an annual basis. Furthermore, this analysis is under the assumption of a null discount rate. By no means is it intended to perform a complete economic study, the aim is simply to present initial contributions that facilitate cellular planning Optimization. Appropriate refinements would be needed to perform a complete economic analysis based on discounted cash flows (e.g., to compute the net present value).

5.2 Models

The economics of cellular systems can be viewed from the points of view of the different entities: subscribers, network operators, service providers, the regulator, and equipment vendors [107], [108] and [109]. In this work, although it is possible that for mobile multimedia networks the operator and service providers can be different entities, they are do not distinguish in the context of this research. Thus on considers the operator/service provider's point of view, whose primary objective is to improve his business.

In the cellular planning process, the objective of the operator is to determine an optimal operating point that maximizes expected revenues. Examples of major decisions affecting this include the type of technology to be used, the size of the cell, and the number of radio resources in use in each cell. Therefore, it is important to identify the main components of the system's cost and revenues, in particular those that have a direct relationship to either the maximum cell coverage distance or the reuse pattern. Here one considers the cost per unit area of a 2D system incurred during the system lifetime. The system is considered to have a transmission structure formed by a set of frequency carriers or channels (or the corresponding WiMAX sub-channels), each supporting a TDD frame structure. Each Base Station (BS) comprises a number of transceivers equal to the number of carriers assigned to the BS (or to the BS sector), which is assumed to be one in this study. i.e., it is assumed as a simplification that one carrier will be sufficient per cell/sector.

System cost has two major parts: (i) capital costs (normal backhaul, cell site planning and installation), and (ii) operating expenses (operation, administration and maintenance) [110] and [111].

The capital cost is taken to consist of:

- A fixed part (e.g., licensing and spectrum auctions or fees);
- A part proportional to the number of BSs per kilometre or square kilometre (e.g., the installation costs of BSs including the cost of obtaining cell sites, the normal backhaul, and the cost of hardware and core equipment common to all);
- A part proportional to the total number of transceivers per kilometre or square kilometre (e.g., the cost of the transceivers).

It is assumed that the cost of the connection between BSs and the Switching Centre, i.e., the fixed part of the network (e.g., the cost of laying fibre), is not a fixed cost. Instead, one considers this to be proportional to the number of BSs, which can be true if, e.g., the mobile operator's service is contracted from a fixed network operator.

The operating cost during a system's lifetime is taken to contain:

- A part proportional to the number of BSs per kilometre or square kilometre;
- A part proportional to the number of transceivers per kilometre or square kilometre.

These costs will be incurred on an annual basis. A similar approach was followed in [112] for hierarchical WiMAX-WiFi networks. However, the approach from [113] is followed in this work. The cost per unit area is given by:

$$C_{ost} = C_{fi[€/km^2]} + C_b \cdot N_{hex/km^2} \tag{5.1}$$

where C_{fi} is the fixed term of the costs, and C_b is the cost per BS assuming that only one transceiver is used per cell/sector. The number of hexagonal coverage zones per unit area (for which the equivalent supported throughput is computed) is given by:

$$N_{hex/km^2} = \frac{2}{3 \cdot \sqrt{3} \cdot R^2} \tag{5.2}$$

and the cost per BS is given by [113]:

$$C_b = \frac{C_{BS} + C_{bh} + C_{Inst}}{N_{year}} + C_{M\&O} \tag{5.3}$$

where N_{year} is the project's lifetime (assumed here to be N_{year} = 5), C_{BS} is the cost of the BS, C_{bh} is the cost for the normal backhaul, C_{Inst} is the cost of the installation of the BS, and $C_{M\&O}$ is the cost of operation and maintenance (M&O).

The revenue in a hexagonal-shaped coverage zone per year, $(R_v)_{cov\_zone}$, can be obtained as a function of the supported throughput per BS or sector (in the omnidirectional and sectorial cases, respectively), $R_{b\text{-}sup[kbps]}$, and the revenue of a channel with a data rate $R_{b[kbps]}$, $R_{Rb[€/MByte]}$, by:

$$(R_v)_{cov\_zone} = \frac{N_{hex[km]^2} R_{(b-sup)_{equiv}} . T_{bh} . R_{R_b[€/min]}}{R_{b-ch[kbps]}} \tag{5.4}$$

where N_{hex} is the number of hexagonal areas T_{bh} is the equivalent duration of busy hours per day, and $R_{b\text{-}ch}$ is the bit rate of the basic "channel". In the tri-sectorial case, as one assumes that each sector has one different transceiver, there is a separate frequency channel available for it.

The revenue per unit area per year, $R_{v[€/km^2]}$, is obtained by multiplying the revenue per cell by the number of cells per unit area:

$$R_{v[€/km^2]} = N_{hex[km^2]} \cdot (R_v)_{cell} = N_{hex[km^2]} \cdot \frac{R_{b-sup[kbps]} \cdot T_{bh} \cdot R_{R_b[€/min]}}{R_{b-ch[kbps]}} \tag{5.5}$$

The (absolute) profit is given by:

$$P = R_v - C_{ost} \tag{5.6}$$

from which, the profit in percentage terms is given by:

$$P_{[\%]} = \frac{R_v - C_{ost}}{C_{ost}} \cdot 100 \tag{5.7}$$

5.3 Assumptions with no Relays

Following the approach from [113], it is hypothesised that project duration is of 5 years and there is a null discount rate, costs and revenues are taken on an annual basis. One considers six busy hours per day, 240 busy days per year [114], and a revenue/price of a 144 kbps "channel" per minute (approximately corresponding to the price of one MByte, as 144·60 = 8640 kb ≈ 1 MB), $R_{144[€/\text{MByte}]}$. The revenue per cell can be obtained as:

$$(R_v)_{\text{cell}\,[€]} = \frac{N_{sec} \cdot R_{b-\sup[\text{kbps}]} \cdot 60 \cdot 6 \cdot 240 \cdot R_{144[€/\text{min}]}}{144_{[\text{kbps}]}} \tag{5.8}$$

Diverse assumptions for the price of the 144 kbps channel (or MByte of information) are considered for each scenario. The hypotheses for the cost are shown in Table 5.1.

Table 5.1 Fixed WiMAX cost assumptions (extracted from [94]).

Costs		*Omnidirectional*	*Tri-sectored*
$C_{fi\ [€/\text{km}^2]}$	$K = 1$	15.71	47.14
	$K = 3$	47.14	141.43
	$K = 4$	62.86	188.57
	$K = 7$	110.00	330.00
$C_{BS\ [€]}$		9,000	15,000
$C_{Inst\ [€]}$		1,000	1,500
$C_{bh\ [€]}$		2,500	2,500
$C_{M\&O\ [€/\text{year}]}$		1,000	1,500

Assuming that the annual cost of a license is 50,000,000 € for 2x24.5 MHz bandwidth (UL & DL, K = 7), considering a total area of 91,391.5 km^2 as the area of Portugal, for example, the fixed cost per unit area is:

$$C_{fi\ [€/\text{km}^2]} = \frac{50{,}000{,}000}{91{,}391.5 \times 5} = 109.42 \approx 110\ €/\text{km}^2 \tag{5.9}$$

If one considers that only one carrier will be allocated to each cell (or sector), if K = 4 or K = 3 then the available bandwidth (and the respective cost) will be 4/7 or 3/7 of the value for K = 7, respectively.

Given that the total bandwidth (BW) is given by:

$$BW_{omni\ [MHz]} = N_{sec} \cdot K \cdot 3.5 \tag{5.10}$$

The necessary spectrum bandwidths can be obtained as in Table 5.2. Besides, Note that N_{sec} = 1 for omnidirectional cells and N_{sec} = 3 for sectorial cells.

Table 5.2 Required spectrum bandwidth for different cell configurations and reuse patterns (extracted from [94]).

K	*BW* [MHz]	
	Omnidirectional	Tri-sectored
1	3.5	10.5
3	10.5	31.5
4	14.0	42.0
7	24.5	73.5

5.4 Assumptions with Relays

If the topology with RSs from the previous chapter is considered, i.e., omnidirectional case with three carriers and the tri-sectored case with one carrier, the costs assumptions are:

i. Cost for BS and RSs

- $C_{BS\text{-}omni}$ = 14,400 €;
- $C_{RS\text{-}BS\text{-}omni}$ = 14,400/5=2,880 €;
- $C_{BS\text{-}trisect}$ = 15,000 €;
- $C_{RS\text{-}BS\text{-}\ trisect}$ = 1,800 €.

In this topology there are three hexagonal coverage areas, one for the BS plus two which correspond to the three RS areas (the three RS coverage zones exactly correspond to an area of two hexagons). The cost for the "equivalent BS" is an average between the BS and the RS for the three coverage areas, given by:

$$C_{BS-equivalent} = \frac{(C_{BS} + 3 \cdot C_{RS})}{3} \tag{5.11}$$

For omnidirectional BS, as one considers $C_{BS\text{-}omni}$ = 14,400 € and C_{RS} = 2,880 € then one obtains $C_{BS-equivalent}$ = 7,680 €. For the tri-sectored case, one considers C_{BS-tri} = 15,000 € and C_{RS} = 1,800 € (assuming the RS is cheaper because it is simpler), yielding $C_{BS\ -\ equivalent}$ = 6,800 €.

ii. Cost for backhaul

As only the central BS needs a fixed backhaul i.e., the central coverage area/hexagon, $C_{Bh\ -\ equivalent}$ is one third of the value for a normal BS for each hexagonal area:

$$C_{bh-equivalent} = \frac{1}{3} C_{bh} \tag{5.12}$$

iii. Installation Cost

The installation cost is the same for every BS and RS. As one needs to install one BS and three RSs, it is four times the installation cost of a BS, C_{inst}. Hence, one needs to multiply C_{inst} by 1/3 to obtain the installation cost for each coverage area, given by:

$$C_{inst-equivalent} = 4/3\, C_{inst} \tag{5.13}$$

iv. Maintenance and operation cost

It is assumed that the maintenance and operation costs for the BS are the same as in the previous case, i.e., without RSs, and the costs for the RS are half of these. Hence the equivalent (M&O) is given as:

$$C_{M\&O-equivalent} = \frac{\left(C_{M\&O} + 3/2\, C_{M\&O}\right)}{3} \tag{5.14}$$

These equations may be applied to the topology with RSs and omnidirectional BSs. In this case the following parameters were used, Table 5.3:

- $C_{BS\text{-}omni}$ = 14,400 € and C_{RS}=2,880 € (i.e., $C_{BS\text{-}equivalent}$ = 7,680 €);
- C_{inst} = 1,000 € (i.e., $C_{inst\text{-}equivalent}$ = 1,333.33 €);
- C_{bh} = 2,500 € (i.e., $C_{bh\text{-}equivalent}$ = 833.33 €);
- $C_{M\&O}$ = 1,000 € (i.e., $C_{M\&O\text{-}equivalent}$ = 833.33 €).

For the tri-sectored BS antennas the parameters are the following, Table 5.3 (note that the costs for the backhaul, and maintenance and operation are the same):

- $C_{BS\text{-}tri\text{-}sect}$ = 15,000 € and C_{RS}=1,800 € (i.e., $C_{BS\text{-}equivalent}$ = 6,800 €);
- C_{inst} = 1,500 € (i.e., $C_{inst\text{-}equivalent}$ = 2,000 €);
- C_{bh} = 2,500 € (i.e., $C_{bh\text{-}equivalent}$ = 833.33 €);
- $C_{M\&O}$ = 1,000 € (i.e., $C_{M\&O\text{-}equivalent}$ = 833.33 €).

According to the assumptions with RSs, the cost parameters from Table 5.3 were considered for K = 3 and K = 1. The value of the fixed cost is 'per carrier'. For different values of K, the fixed cost, C_{fi}, increases proportionally to K while the values for the other parameters keep being the same. For example, for K = 3, it becomes C_{fi} = (110×K/7)×3 = 141.43 €/km^2 in the omnidirectional case with three carriers (the number 3 represents the three carriers), and C_{fi} = (110×K/7)×3 = 141.43 €/km^2 in the tri-sectored case (in this case there is only one carrier and the number 3 is multiplied since this is the tri-sectored case).

Table 5.3 Costs with relays with different antennas and K = 3 and K = 1 (three carriers for the omnidirectional and one carrier for the tri-sectored).

Costs	*Omnidirectional*	*Tri-sectored*
	K = 3	K = 1
C_{fi} [€/km^2]	141.43	141.43
C_{BS} [€]	7,680.00	6,800.00
C_{Inst} [€]	1,333.33	2,000.00
C_{bh} [€]	833.33	833.33
$C_{M\&O}$ [€/year]	833.33	833.33

5.5 Cost/Revenue Trade-off in the Optimization of Fixed WiMAX Deployment with Relays

In seeking profit Optimization, revenues should be maximised with respect to costs. By using the previous assumptions, Table 5.1 and Table 5.3, and the results for the supported throughput, one obtained the curves for costs, revenues and profit in percentage. Although Table 5.3 considers omnidirectional BS antenna with three carriers, the omnidirectional case with only one carrier is firstly analyses, the profit for this case is later address. Omnidirectional BS with three carriers will only be considered in the next section. This means that one first considers a C_{fi} value equal to 47.14 in the case of omnidirectional BS antenna

The costs and revenues with relays (K = 3), in €/km^2, are depicted in Figure 5.1, for $R_{144[€/MByte]}$ = 0.0025 and 0.005. Note that the volume of information transferred during 60 s (1 min) at 144 kbps is 144·60/8 = 1080~1 MByte, hence, from now on the term €/$_{MByte}$ will be used as the unit for the price.

In order to optimize the broadband wireless access network, the profit per unit area is of fundamental importance. However, it is not sufficient to compute the absolute profit because, as is shown in Figure 5.1, a certain level of profit may correspond to different values of cost. For example, cost is higher for tri-sectored cells, therefore, revenue needs to be higher to obtain the same profit. This justifies the need to represent the profit in percentage, as defined by (5.7). The operator's/services provider's goal is to optimise this profit in percentage.

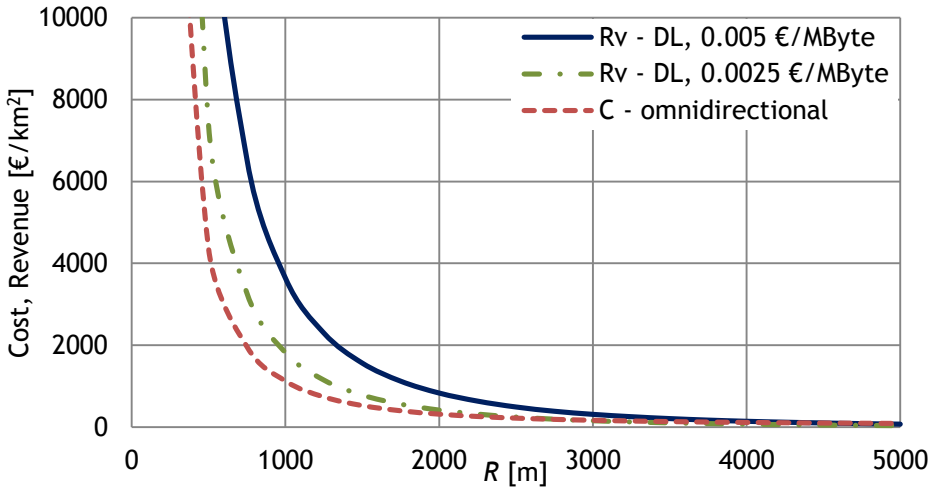

Figure 5.1 Cost and revenues with RSs (K = 3, omni. BS) for MByte $R_{144[€/MByte]}$ = 0.0025 and 0.005, in the DL.

Figure 5.2 presents the results for $R_{144[€/MByte]}$ = 0.0025 and 0.005 in the DL for K = 3. The case without relays ("omni. no RSs"184) is also presented, for comparison purposes. It is clear that the use of relays without sectorization in the BS leads to a lower profit. Only the

use of sectorization enables to achieve higher profit. In this case, values above 800 % only occur for coverage distances up to approximately 1200 m.

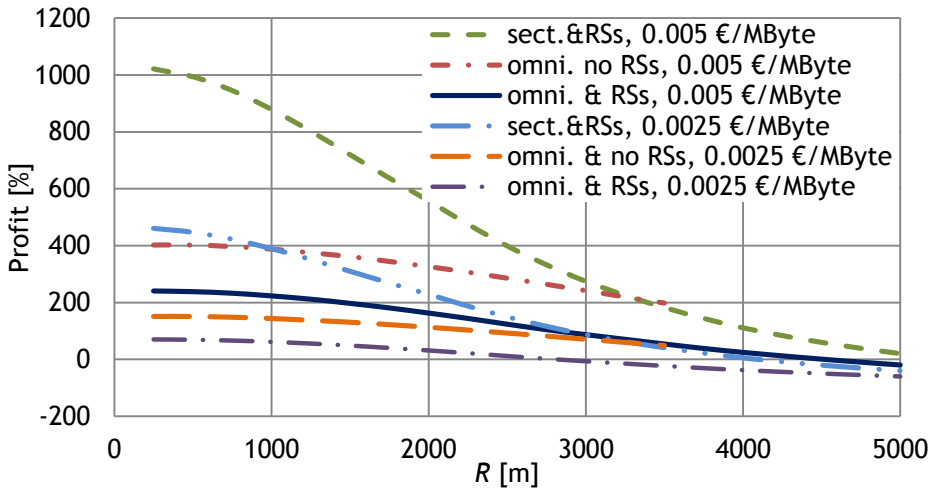

Figure 5.2 Profit in percentage for $R_{144[€/MB]}$ = 0.0025 and 0.005, in the DL and K = 3, without and with RSs (omnidirectional and trisectored BS antennas).

The analysis for costs and revenues in the UL with K = 3 has also been addressed by considering the cost presented in Table 5.3. In this case the profit is lower since the supported throughput in the UL is lower than in the DL. Figure 5.3 shows that, in the omnidirectional BS antennas (one carrier), there is no profit, i.e., revenues are always lower than costs. The profit in percentage is defined as in (5.7), and the prices per MByte of $R_{144[€/MByte]}$ = 0.0025 and 0.005 are considered. Results are shown with relays with trisectored (identified by "sect.& RSs") and omnidirectional (identified by "omni.& RSs") BS antennas.

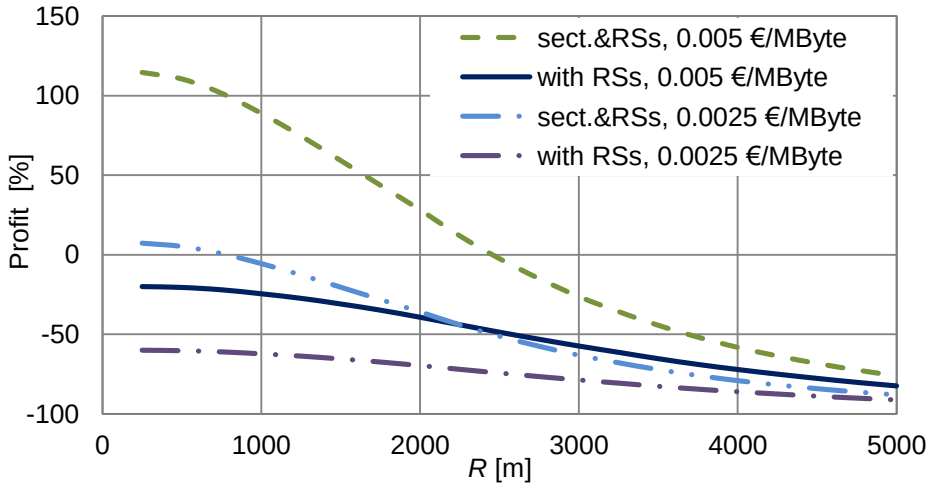

Figure 5.3 Profit in percentage for a price per MByte R_{144} = 0.0025 and 0.005, in the UL and K = 3, with RSs (omnidirectional and trisectored BS antennas for the latter).

In the UL, with relays only the use of trisectored BS antennas and $R_{144[€/MByte]}$ = 0.005 enables to achieve a positive profit in percentage. As verified for the DL, the maximum values also occur for coverage distances up to 700–1000 m. With $R_{144[€/MByte]}$ = 0.0025, a positive profit is achievable only up to R ~700 m. No subchannelization is considered in these curves. Results with no RSs for omnidirectional antennas are not included for K = 3, as the CNIR is very low and it was impossible to obtain results for the supported throughput.

5.6 Economic and Environmental Impact of Cell Zooming

The analysis of the impact of cell zooming assumes the values for the power of the BS and RS equipment from

Table 5.4 , which is partially extracted from [92]. The values for the power consumption of the BS were chosen based on the powers for the Alvarion BS equipment while the power consumption of the RS equipment refer to the powers of the micro-BS Alvarion equipment (the comparison is done because, as the RS, it can also be connected to two ODUs). Each BS sector has a different ODU, whose power consumption is 40 W each. It is assumed that the RSs will have an ODU for the communication with the RS and a second one for the communication with the SSs (40+40 = 80 W total).

Table 5.4 Power consumption parameters for the BSs and RSs (extracted from [92]).

Station	BSs		RS
	Tri-sectored	Omni.	
Power for the full chassis [W]	420		80
Number of sectors	3	1	-
Power for the outdoor unit(s) [W]	120	40	80
Total power of the BS/RS equipment alone [W]	540	460	160
Power consumption for the router/switch [W]	100		-
Power consumption for the ventilator [W]	40		20
Total power consumption for the stations [W]	680	600	180
Annual energy consumption [kWh]	6000	5250	1750

The power consumption for the fan of the cooler ventilation system is assumed to be 40 W for the BS equipment and 20 W for the RS equipment. Besides, it is presumed that the power consumption for the switch/router at the BS is 100 W (and there is no such switch/router at the RS shelter). As a consequence, the total power consumption values are the: P_{BS-tri} = 540+100+40 = 680 W, $P_{BS-omni}$ = 460+100+40 = 600 W and P_{RS} = 160+20 = 180 W, where P_{BS-tri}, $P_{BS-omni}$ and P_{RS} are the values for the trisectored BS, omnidirectional BS and the RS, respectively. From this analysis, one may conclude that, by itself, the use of RSs instead of full functionality BSs lead to circa 70 % reduction in the power consumption for their coverage zones.

These RSs can be switched-off in periods when the traffic exchange is low. In a scenario where RSs are zoomed in to zero during the night periods and weekends, by switching the RS equipment off, and the central BS coverage zone is zoomed out, leading to a

coverage distance of $R_{z-out} = \sqrt{3}R'$, the total power becomes now simply the power of the central BS (either 680 or 600 W, for tri-sectored and omnidirectional BSs, respectively). In the full functionality cell with RSs the total power is 680+3·180 = 1220 W for tri-sectored BS or 600+3·180 = 1140 W for omnidirectional BSs. This is approximately twice the power of the zoomed out cell. The 540 W power decrease corresponds to a given reduction in operation costs, proportional to the time the RSs remain switched-off.

During the whole year, the total energy waste in RSs is 24·365·540 = 4730.4 kW·h. If the price of the energy is 0.10 €/kW·h the electricity cost is 473.04 €/year. If the RSs are switched-off overnight (for eight hours each night during the working days) and during the whole weekend (48 hours) then the total period when the energy is saved is 5·8+2·24 = 88 hours (against 80 hours of full functionality cell operation), i.e., full operation lasts only for 80/168 = 47.6 % of the time. Therefore, by switching-off the RSs the economic annual expenditure resulting from the power reduction in each cell is 473.04×0.476 = 225.17 €/year per cell, corresponding to a reduction in the annual cost per cell of 247.17 €/year. The aforementioned reduction in the cost per cell corresponds to a reduction of the operation costs of the "equivalent BS" of 247.17/3 = 82.62 €/year (~10 % of $C_{M\&O}$).

If it is assume that the proposed DL sub-frame format cannot be changed to a more favourable one when the RSs are switched-off, the economic performance is the one presented in the first three curves from Figure 5.4. This is an example, for a revenue per MByte of 0.005 € [92], and does not consider the case of omnidirectional BS antennas in the absence of RSs. As the throughput is lower with no RSs (see results in Figure 5.4) the economic performance is lower compared to the cases with the presence of RSs. For $R_{z\text{-}out}$ = 1732 m, in the case of the zoomed out central BS coverage zone (with the RSs in the sleeping mode and its cooling system switched-off) and tri-sectored BS antenna ("sect.& no RSs, zoomed Out, 1 carrier/sect."), the profit in percentage terms [93] achieves 544.5 %.

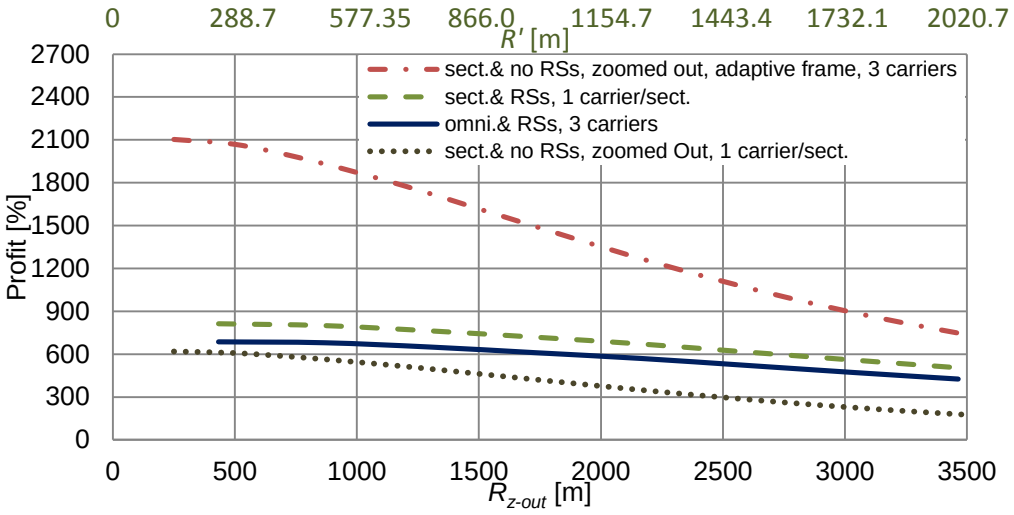

Figure 5.4 Comparison of the economic performance between omnidirectional (three carriers) and tri-sectored (one carrier/sector) BSs in the presence of RSs and with the central BS coverage zoomed out (while RSs coverage zoom in to zero) under the same total BW, in the DL and K = 3.

However, in the presence of RSs, for *R'* = 1000 m (corresponding to the same equivalent area), the profit is 610.2 and 718.8 %, for the omnidirectional (three carriers) and tri-sectored (one carrier/sector) cases, an increase of 12.1 and 32 %, respectively. As the coverage is adequate with RSs (more than 95.65 % of the cell is covered, if Ray tracing, RT, coverage is considered, as shown in Table 4.9), it is show that the use of RSs leads to an actual increase of the economic performance whilst clearly increasing the cell coverage.

By putting the RSs into sleep mode during the night and at weekends, with tri-sectored BS antennas, there is an increase of the area of the cell with no coverage to 18.10 %. This coverage is not adequate, but this situation still leads to a reasonable economic performance. The use of omnidirectional BS antennas is not a viable option, as the area with no coverage is almost 40 %.

If the frames could be adaptively adjusted when the RSs go into the sleep mode and the BS zooms out, the economic performance would reach, in theoretical terms, 1871.6 %. However, this is not entirely credible, as the non-covered area is 18.10 % and the throughput does not reach the theoretical 20 Mbps (from Figure 4.28), but only 15.58 Mbps (3×5.193).

5.7 Conclusions

Relays are usually considered cheaper equipment and by helping to improve coverage while mitigating interference, they may lead to lower costs. Hence it is worthwhile to analyse the impact of using them on costs and revenues. Moreover, this work has investigated the energy efficiency and economic implications of the use of power saving modes for RSs in conjunction with cell zooming in WiMAX deployments. Firstly the formulation for the economic model was introduced. The hypotheses and costs assumptions in the presence and absence of RSs were introduced. In this context, the costs with RSs and K = 3 for different antennas were computed. In the omnidirectional case, three carriers are assumed whereas in the tri-sectored only one carrier is considered.

Under a fixed total bandwidth, by comparing the topologies with omnidirectional and tri-sectored BS antennas, it is shown that with RSs and with coverage distances up to ~1300 m the achievable profit is only clearly higher with the use of tri-sectored BSs. Results also show that under the same fixed bandwidth and for the example where the coverage distance is set at R = ~500 m, it is preferable to consider K = 1 with three carriers per sector instead of K = 3 with one carrier per sector, whereby profit in this case is increased by more than 45 % from ~1000 % to ~1450 %. Moreover, if the price per MByte is increased from 0.0025 to 0.005 €/MByte, the achievable profit more than doubles under the aforementioned improved configuration.

The power consumption parameters for the BSs and RSs were addressed. The energy consumption reduction and the respective economic performance were computed under de assumption that the RSs can be switched-off in periods when the traffic exchange is low, in a

scenario where RSs are zoomed in to zero during the night periods and weekends, by switching the RS equipment off, and the central BS coverage zone is zoomed out.

Under the use of RS power saving modes in conjunction with cell zooming, assuming that the downlink sub-frame format cannot be changed to a more favourable one at times when the RSs are sleeping, the economic performance is better in the presence of RSs. The performance is reduced since without RSs the supported throughput decreases. However, it is important to highlight that, contrary to the omnidirectional case (where coverage is extremely weak with no RSs), in the tri-sectored case, if RSs go into sleep mode (thereby saving energy and money), although there is an increase of the area of the cell with no coverage from 4.25 % to 18.10 % (RT coverage), there is still a reasonable economic performance. The use of omnidirectional BS antennas, however, is not a viable option as the area with no coverage is approximately 40 %.

It was also shown that through the use of power saving by RSs at low traffic times, average energy savings for RSs (excluding BSs) of some 47.6 % can be achieved. On a system-level, this translates to a financial saving for the operator of 10 % in the summed operation and maintenance.

Chapter 6

Carrier Aggregation for Wireless Cellular Networks Capacity Enhancement

6.1 Introduction

To meet the increasing demand for wireless broadband services from fast-growing mobile users, aggregating frequency spectrum is one of the viable techniques to enhance data rates. The concept of spectrum aggregation is introduced by 3GPP in its LTE-Advanced (LTE-A), e.g. LTE R10, a candidate radio interface technology for IMT-Advanced systems standards. However, the introduction of spectrum aggregation or carrier aggregation (CA), as referred to in LTE R10, has required some changes from the baseline LTE R8, although each component carrier (CC) in LTE-A remains backward compatible with LTE R8, as described in [115].

Carrier aggregation is considered as a key enabler for LTE-A [116], which can meet or even exceed the IMT-Advanced requirement for large transmission bandwidth (40 MHz-100 MHz) and high peak data rate (500 Mbps in the uplink and 1 Gbps in the downlink) [117]. Each aggregated carrier is referred to as a Component Carrier (CC). The component carrier can have a bandwidth of 1.4, 3, 5, 10, 15 or 20 MHz and a maximum of five CCs can be aggregated and can also be of different bandwidths. Therefore, the maximum aggregated bandwidth is 100 MHz. In this context, user equipment (UE) may simultaneously receive or transmit data on one or multiple CCs, whereas in the 3GPP R8 specifications [118] each UE uses only one CC to communicate at one time. Moreover, since it is important to keep backward compatibility with R8 and R9 UEs, the aggregation is based on R8/R9 carriers and can be used for both FDD and TDD modes.

The easiest way to arrange aggregation would be to use contiguous component carriers within the same operating frequency band (as defined for LTE), the so called intra-band contiguous. However, in practice, such a large portion of continuous spectrum is rarely available. CA, where multiple CCs of smaller bandwidth are aggregated, is an attractive alternative to increase data rate. Additional advantages are offered by CA in terms of spectrum efficiency, deployment flexibility, backward compatibility, and more. By aggregating non-contiguous carriers, fragmented spectrum can be more efficiently utilized [119]. For non-contiguous allocation it could either be intra-band, i.e., the component carriers belong to the same operating frequency band, but have a gap, or gaps, in between, or it could be inter-band, in which case the CCs belong to different operating frequency bands [120]. In [121], [122] and [123] the authors addressed the problem of how to optimize the resource allocation process in a multi-carrier system, while maintaining low complexity. Both simple theoretical and simulation results were obtained, which show that with low number of users and low percentage of LTE-A users, the load balancing method of Round

Robin achieves better performance than the Mobile Hashing (MH) balancing. It was also found that using independent packet scheduling per CC suffers from poor coverage performance. In this context, the authors proposed a cross CC packet scheduler algorithm, which is a simple extension of the existing Proportional Fair scheduler. The cross CC algorithm is aware of the user throughput over all the aggregated CCs. As a result, it was shown that the cross CC algorithm maximizes the network utility even if users are provided with different number of CCs. This approach however only accounts for the cell throughput and disregards the QoS. Besides, full buffer traffic is addressed, which is not representative of nowadays and future cellular networks traffic. In [124], a scheduling strategy for CA using pre-organized Resource Blocks (RB) sets was presented. Besides, an analytical evaluation framework was performed to determine the expected number of RBs required by users, based on a mapping of Channel Quality Indicator (CQI) values to data rates per RB and the statistical behaviour of the CQI. RBs can be grouped into sets based on the predefined maximum number of RBs and spectrum availability. By scheduling these RB sets this scheme can help to reduce the scheduling delay. Nevertheless, this adds further scheduling complexity due to the RB pre-organization functionality.

In this context, this work addresses LTE-A CA and proposes an updated integrated Common Radio Resource Management (iCRRM), from [131], that performs CCs scheduling to satisfy user's Quality of Service (QoS) and experience (QoE) requirements while maximizing spectral efficiency. Two inter-band CA, Band 7 (2.6 GHz) and Band 20 (800 MHz) are considered. As stated above, large portion of continuous spectrum is rarely available and the aggregation of smaller bandwidth is an attractive solution to reduce spectrum underutilization. Besides, the Portuguese communication regulator, Anacom, auctioned in 2011 LTE's bands 7 and 20. During this event only 5 MHz ("lots") were made available for the considered CCs [125]. In this context, 5 MHz bandwidth CCs are considered for this research. Additionally, following the forecast from [1], video traffic is addressed under the premise that in 2013 it represented more than half (53 %) and will reach 69 % of all worldwide mobile data traffic by 2018. Additionally, a normalised transmitter power formulation is proposed. One the one hand, this formulation allows for computing the required eNB power to maintain a constant average cell SINR for different cell radii, hence to have comparable CA results for different cell radii. On the other hand, the formulation guarantees lower energy consumptions, e.g., small cell radii, require lower transmitter power than their counterpart with larger radii to achieve comparable SINR and coverage.

By considering extensive simulations results the iCRRM performance metrics, i.e., packet loss, delay, goodput (application level throughput), and user's expected QoE, are analysed and compared with a CRRM, which performs basic multi-band scheduling, and the summed capacity of two CCs LTE systems, i.e., without CA. Finally, a cost/revenue analysis shows the performance and economic gain achieved with all multi-band schedulers while comparing their performance with the one from the system without CA.

6.2 Definition of key terms for LTE-Advanced Carrier Aggregation

Before continuing the discussion on CA, it is important to first define some of the main key terms used by 3GPP [126] related to this matter:

Aggregated Channel Bandwidth: The radio frequency (RF) bandwidth in which a UE transmits and receives multiple contiguously aggregated carriers.

Aggregated Transmission Bandwidth Configuration (ATBC): The number of resource block allocated within the aggregated channel bandwidth.

Carrier aggregation: Aggregation of two or more component carriers in order to support wider transmission bandwidths.

Carrier aggregation band: A set of one or more operating bands across which multiple carriers are aggregated with a specific set of technical requirements.

Carrier aggregation bandwidth class: A class defined by the aggregated transmission bandwidth configuration and maximum number of component carriers supported by a UE. In R10 and R11, three classes are defined, A, B and C (Table 6.1), whereas classes D, E and F are at the time in the study phase.

Table 6.1 CA bandwidth classes (extracted from [126]).

CA bandwidth class	ATBC, N_{RB_agg} [RBs]	Number of CC's
A	$N_{RB\_agg} \leq 100$	1
B	$N_{RB\_agg} \leq 100$	2
C	$100 < N_{RB\_agg} \leq 200$	2
D	$200 < N_{RB\_agg} \leq 300$	Under study
E	$300 < N_{RB\_agg} \leq 400$	Under study
F	$400 < N_{RB\_agg} \leq 500$	Under study

N_{RB_agg} is the number of aggregated Resource Blocks (RBs) in which a UE can transmit (receive) simultaneously, i.e., N_{RB_agg} is the sum of the transmission bandwidth configurations (N_{RB}) of the CCs.

Carrier aggregation configuration: A combination of CA operating band(s) and CA bandwidth class(es) supported by a UE. The following three examples are provided to illustrate CA configuration, it is important to note that these cases might not correspond to real implementation and are just use for illustration purposes:

1) **CA_1C** indicates intra-band contiguous CA on Evolved Universal Terrestrial Radio Access (E-UTRA) operating band 1 and CA bandwidth class C;
2) **CA_1A_1A** indicates intra-band non-contiguous CA on band 1 with a one CC on each side of the intra-band gap;
3) **CA_1A-5B** indicates inter-band CA, on operating band 1 with bandwidth class A and operating band 5 with bandwidth class B.

In LTE-A R10 three CA configurations are defined [126], shown in Table 6.2, further configurations are or will be defined in future LTE-A releases.

Table 6.2 LTE-A R10 CA configurations (extracted from [126]).

Type of CA and duplex type	CA configuration	Maximum aggregated bandwidth (MHz)	Max number of CC
Intra-band contiguous FDD	CA_1C	40	2
Intra-band contiguous TDD	CA_40C	40	2
Inter-band FDD	CA_1A_5A	20	1 + 1

In R11 and R12 a large number of additional CA configurations are defined, but will not be presented in the framework of this theses. Moreover, it is already worthwhile to note that inter-band non-contiguous CA on Band 7 (2.6 GHz) and Band 20 (800 MHz), i.e., LTE_CA_B7_B20 considered in R11 [127], will be addressed in the following sections.

Channel edge: The lowest and highest frequency of the carrier, separated by the channel bandwidth.

Channel bandwidth: The RF bandwidth supporting a single E-UTRA RF carrier with the transmission bandwidth configured in the uplink or downlink of a cell. The channel bandwidth is measured in MHz, and is considered as a reference for transmitter and receiver RF requirements.

Contiguous carriers: A set of two or more carriers configured in a spectrum block where there are no RF requirements based on co-existence for un-coordinated operation within the spectrum block.

Inter-band carrier aggregation: Carrier aggregation of component carriers in different operating bands (carriers aggregated in each band can be contiguous or non-contiguous).

Intra-band contiguous carrier aggregation: Contiguous carriers aggregated in the same operating band.

Intra-band non-contiguous carrier aggregation: Non-contiguous carriers aggregated in the same operating band. Figure 6.1 depicts intra and inter-band CA allocation opportunities.

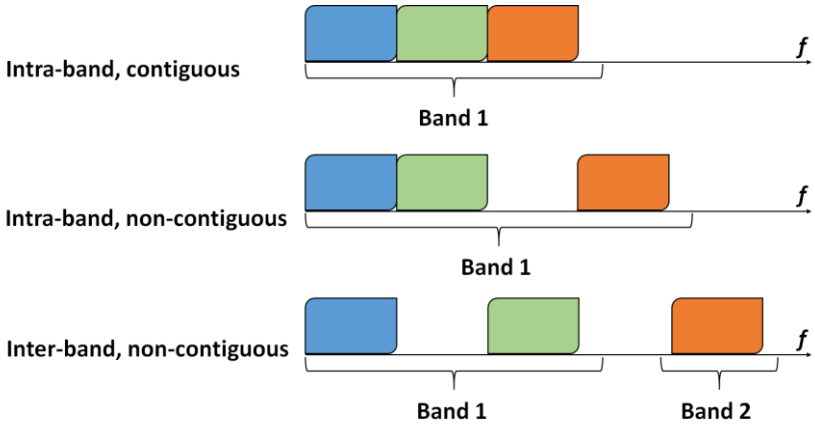

Figure 6.1 Carrier Aggregation, intra-band and inter-band aggregation alternatives (adapted from [120]).

Furthermore, when carriers are aggregated, each carrier is referred to as a CC and they can be classified into two categories:

Primary component carrier: This is the main carrier in any group. There will be a primary downlink carrier and an associated uplink primary component carrier.

Secondary component carrier: There may be one or more secondary component carriers.

3GPP does not define which carrier should be used as a primary component carrier. Different UE may use different carriers. The configuration of the primary component carrier is UE/terminal specific and depends of the loading on the various carriers and other relevant parameters [120].

6.3 3GPP Carrier Aggregation Deployment Scenarios

Carrier aggregation systems are usually deployed to improve data rates for users within overlapped areas of cells. 3GPP Technical Specification 3GPP TS 36.300 (Table J.1-1) [118] shows some of the potential deployment scenarios for CA with two component carriers at frequencies of F1 and F2, Figure 6.2. In R10, for the UL, the focus is laid on the support of intra-band carrier aggregations (e.g. scenario 1, as well as scenarios 2 and 3 when F1 and F2 are in the same band). For the DL in R10, all scenarios should be supported [118].

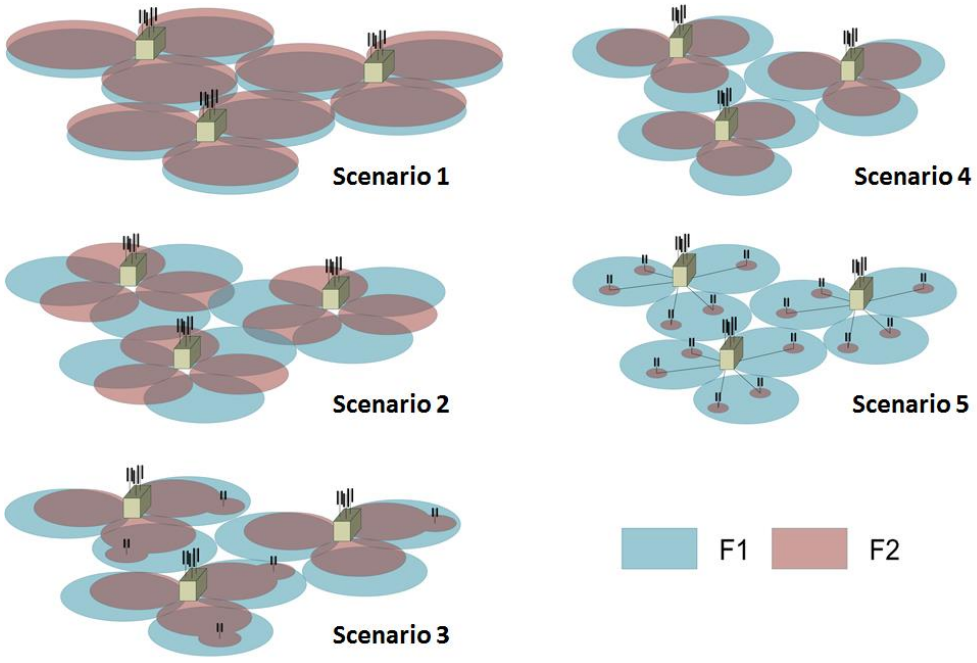

Figure 6.2 Carrier aggregation deployment scenarios (adapted from [118]).

Deployment scenario 1: Cells with carrier frequencies F1 and F2 are collocated and overlaid, providing nearly the same coverage. Both layers provide sufficient coverage and

mobility can be supported on both layers. The likely scenario is that F1 and F2 are of the same radio band.

Deployment scenario 2: Cells with carrier frequencies F1 and F2 are collocated and overlaid, but F2 has smaller coverage due to larger path loss. Only F1 provides sufficient coverage and F2 is used to improve throughput. Mobility is performed based on F1 coverage. The likely scenario is that F1 and F2 are of different radio bands.

Deployment scenario 3: Cells of carrier frequencies F1 and F2 are co-located but F2 antennas are directed to the cell boundaries of F1 so that cell edge throughput is increased. F1 provides sufficient coverage but F2 potentially has holes, e.g., due to larger path loss. Mobility is based on F1 coverage. Likely scenario is when F1 and F2 are of different bands. It is expected that F1 and F2 cells of the same Evolved Node B (eNB) can be aggregated where coverage overlaps.

Deployment scenario 4: Cells of carrier frequency F1 provide macro coverage and on F2 Remote Radio Heads (RRHs) are used to improve throughput at hot spots. Mobility is performed based on F1 coverage. The likely scenario is that F1 and F2 are on different radio bands, it is expected that F2 RRHs cells can be aggregated with the underlying F1 macro cells.

Deployment scenario 5: Similar to scenario 2, however, frequency selective repeaters are deployed so that coverage is extended for one of the carrier frequencies. In this case it is expected that the cells of carrier frequency F1 and F2 from the same eNB can be aggregated whenever their respective coverage areas are overlapped.

6.4 Common Radio Resource Management for Carrier Aggregation, Objective and System Model

The RRM framework for LTE-A retains many similarities with the one from LTE. With CA, however, it becomes possible to simultaneously schedule a user on multiple CCs, each of which may exhibit different radio channel characteristics. Supporting multi-CC operations introduces therefore some new challenging issues in RRM framework for LTE-A systems [128].

Figure 6.3 illustrates the RRM structure for a multi-component carrier LTE-A system. The eNB first performs admission control to decide which users to serve, and then employs layer-3 CC Selection to allocate the users on different CCs [121]. Once the users are assigned onto certain CC(s), the layer-2 Packet Scheduling (PS) is performed. In order to allow for backward compatibility so LTE and LTE-A users can co-exist, it has been decided to use independent layer-1 transmissions, which contain Link Adaptation (LA) and Hybrid Automatic Repeat Request (HARQ) etc., per CC, in line with the LTE assumptions mentioned in [115].

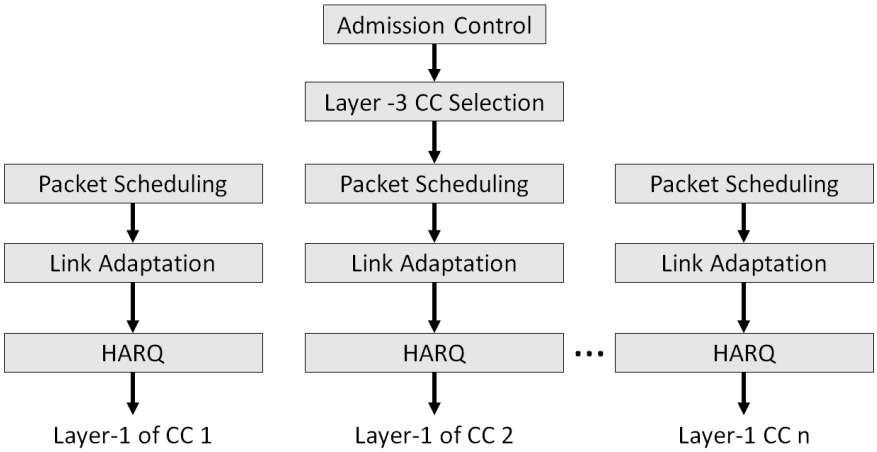

Figure 6.3 Structure of a multi-component carrier LTE-A system (extracted from [121]).

The use of independent link adaptation for each CC may help to optimize transmission according to radio conditions. Different levels of coverage can be provided by setting each CC with its own transmission power. This is especially the case of inter-band CA, since the radio channel characteristics such as propagation, path loss and building penetration loss, may vary according to the operating radio frequency bands, i.e., selecting different transmission parameters, such as modulation scheme, code rate, and transmit power per CC, it is expected to be useful to further improve user QoS.

In the context of research, one investigates a non-contiguous CA from an upper layer point of view and proposes an integrated CRRM (iCRRM) entity where CRRM and CA functionalities are performed together. First, by using an Integer Programming (IP) based algorithm, the inter-frequency handovers are achieved in an optimised way, performing the scheduling via the optimal solution of a General Multi-Band Scheduling (GMBS) problem. Additionally, due to the complexity and the impossibility of allocating UEs to more than one CC an Enhanced Multi-Band Scheduling (EMBS) is alternatively incorporated into the iCRRM entity. This EMBS performs the scheduling functionalities instead of the GMBS with significantly reduced complexity while facilitating to allocate UEs to multiple CCs.

The employed Resource Allocation (RA) algorithms allocate the user packets to the available radio resources in order to satisfy the user requirements, and to ensure efficient packet transport, e.g., minimise loss or maximize spectral efficiency. The RA is envisioned to have an inherent tuning flexibility to maximise the spectral efficiency of the system for any type of traffic QoS or QoE requirements. The RA adopted here maps packets of variable size into CCs for transmission over the Physical (PHY) layer depending on the channel quality.

The integration of spectrum and network resource management functionalities that leads to higher performance and system capacity gains is the novelty of the proposed iCRRM approach. The key to such integration is the pooling of resources together, the integration allows for mapping service requirements onto an available spectrum amount and translates the latter into network load. As stated above, the iCRRM uses inter-band aggregation to

achieve shorter delay and higher user throughput, by exploiting the channel diversity. These bands show independent Channel Quality Indicators (CQIs) over time and space, which becomes a source of diversity at the PHY layer, with an important chance to achieve higher spectrum efficiency. Information from the network about the system state (e.g., received signal strength, transmitted power, UEs velocity, etc.) are used in RRM and procedures such as load, admission and congestion control can successfully be combined with dynamic spectrum use.

In the context of CA in a LTE-A scenario, two frequency bands, i.e., two CCs, are available to the operator, band 7 and band 20, i.e., 2.6 GHz and 800 MHz. The addressed scenario resembles the 3GPP scenario 2. Although propagation loss is higher at 2.6 GHz, through transmitter power tuning, a constant average Signal to Interference plus Noise Ratio (SINR) is guaranteed in this study. Thus, comparable results between CCs are assured. The network is deployed with two collocated omnidirectional hexagonal coverage zones with radio frequency band 7 and 20, and the corresponding first tier of interferers have been considered. For future reference, it is worthwhile to note that a full Radio Access Network (RAN) infrastructure sharing configuration [129] is assumed, e.g., the mast, eNB and Radio Network Controllers (RNC) are shared by both CCs. The addressed scenario and infrastructure sharing configuration are shown in Figure 6.4.

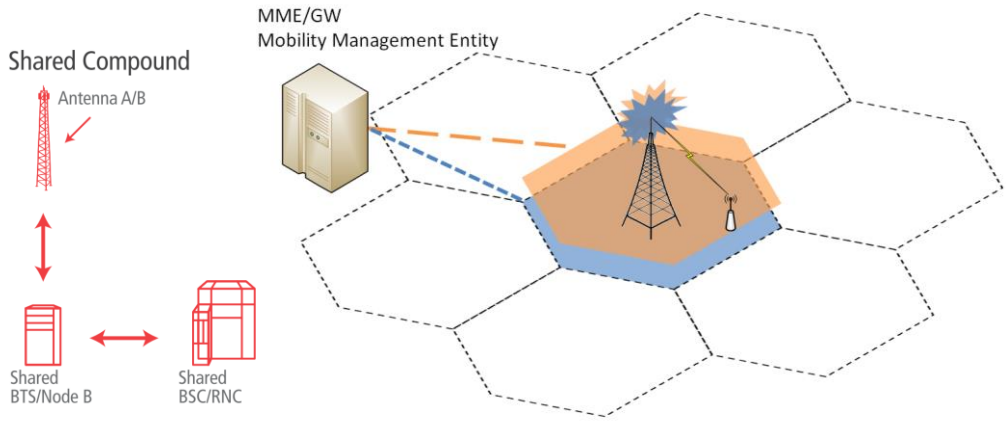

Figure 6.4 Inter band carrier aggregation infrastructure sharing configuration and deployment scenario.

The considered radio channel follows the ITU radio propagation COST-231 Hata model, for macro cell propagation scenarios in urban and suburban areas, outside the high rise core where the buildings are of nearly uniform height [130]. The channel loss between the UE and the eNB is modelled by using a shadowing loss with log-normal distribution and by considering fast fading with Jakes model. The COST-231 Hata path loss (*PL*) model is given by:

$$PL = 40(1 - 4 \times 10^{-3} \times D_{hb}) \log_{10}(R_{[km]}) - 18 \log_{10}(D_{hb}) + 21 \log_{10}(f) + 80 \text{ dB} \quad (6.1)$$

where R is the eNB - UE separation in kilometres, f is the carrier frequency and D_{hb} = 15 m is the base station antenna height, measured from the average rooftop level. The interference in the UE is calculated by considering the signal strength received from the first ring of neighbouring BSs and the thermal noise. The parameters and models assumed for both the 800 MHz and 2.6 GHz bands are shown in Table 6.3.

Table 6.3 Parameters and models used for 800 MHz and 2.6 GHz bands.

Carrier frequency	**800 MHz (band 7)**	**2.6 GHz (band 20)**
Bandwidth [MHz]	5	
Path loss model	$L_{800MHz} = 119.8 + 37.6\log_{10}(R_{km})$	$L_{2.6GHz} = 130.5 + 37.6\log_{10}(R_{km})$
Omni antenna gain [dBi]	14	

6.5 General Multi-Band Scheduling

The following General Multi-Band Scheduling (GMBS) is an adaptation to LTE of the work proposed in [131] where the authors implemented an iCRRM, able to schedule users between the 2 GHz and 5 GHz High-Speed Downlink Packet Access (HSDPA) frequency bands. CA offers an added dimension for user scheduling at the Transmission Time Interval (TTI) level and poses an optimization problem for improving network resource exploitation. The scheduling problem can be formulated as a General Assignment Problem (GAP) [132]. In this specific scenario, the user allocation problem is referred to as GMBS. The proposed Profit Function (PF) maximises the total throughput of the operator via a single objective problem.

In the context of this research, the GMBS problem is solved with Integer Programming (IP), using binary variables. The PF is defined considering the ratio between the rate available on the DL channel and the requested rate by the service flow, and is expressed as follows:

$$(\text{PF}) \sum_{b=1}^{m} \sum_{u=1}^{n} W_{b,u} \cdot x_{b,u} \tag{6.2}$$

where $x_{b,u}$ is the allocation variable, i.e., a Boolean variable that indicates if UE u is allocated on band b. The normalised metric $W_{b,u}$ is given by:

$$W_{b,u} = \frac{\left[1 - BER(CQI_{b,u})\right] \cdot R(CQI_{bu})}{S_{rate}} \tag{6.3}$$

where S_{rate} is the video service encoding bit rate, $BER\ (CQI_{b,u})$ is the average Bit Error Rate (BER) occurred in previous DL transmissions for user u on band b for the Modulation and Coding Scheme (MCS) supported, and $R(CQI_{b,u})$ is the DL throughput for user u on band b, also as a function of the supported MCS.

The constraints for GMBS vary depending on the ability of the UEs to simultaneously transmit and receive in multiple frequencies (multiple transceivers at the UEs), or just over a single band at the time. The LTE standard allows allocating multiple RBs for each UE and each UE may have multiple flows. However, in this work it is assumed that UEs only use a single video flow with S_{rate} = 128 kbps and that each UE will only transmit and receive in a single frequency band at a time. In this context the GMBS constraints are twofold:

1) **Allocation Constraint (ACt)**, each user can be allocated only to a single frequency band:

$$(\text{ACt}) \sum_{b=1}^{m} x_{b,u} \leq 1, x_{b,u} \in \{0,1\} \quad \forall u \in \{0,\ldots,n\} \tag{6.4}$$

2) **Bandwidth Constraint (BC)**, the total number of users on each band is upper bounded by the maximum normalised load that can be handled in the band, $L_b^{\max} \in \{0,1\}$, as follows:

$$(\text{BC}) \sum_{u=1}^{n} \frac{S_{rate} \cdot (1 + R_{Tx} \cdot BER(CQI_{b,u}))}{R(CQI_{b,u})} \cdot x_{b,u} \leq L_b^{\max} \quad \forall u \in \{0,\ldots,n\} \tag{6.5}$$

where the first term is the requested service throughput for user u, including bit loss, normalized with the maximum throughput that the network can offer to the user u on band b which is $R(CQI_{b,u})$. The bandwidth constraint accounts for the user traffic requirement, DL capacity and overhead caused by losses.

Upon the maximization of the PF, a Boolean multi-band allocation matrix is created, $X = [x_{b,u}]$. This matrix is used, in conjunction with available downlink packet schedulers, to allocate RBs to the network users. The allocation matrix returns 1 to allocate u to b or 0 for no allocation.

Finally, one of the LTE simulator implemented downlink packet schedulers computes metrics for the allocated CC/band RBs, and assigns them according to the highest metric value. Well-known downlink packet scheduling strategies, such as Proportional Fair, Modified Largest Weighted Delay First (M-LWDF), and Exponential Proportional Fair have also been implemented into LTE-Sim. The study of the aforementioned opportunistic packet scheduling algorithms is beyond the scope of this thesis. However, through extensive simulations it has been found that in the context of addressed video applications the M-LWDF scheduler outperforms the others, and will be used for the purpose of capacity analysis in this research. M-LWDF is an algorithm designed to support multiple real-time data users and supports multiple data users with different QoS requirements. Every Transmission Time Interval (TTI), the scheduler computes a metric, $w_{i,j}$, for the i-th flow in the j-th sub-channel. If the i-th flow is a real time flow, the metric is computed as follows [135]:

$$w_{i,j} = a_i D_{HOL,i} \times \frac{r_{i,j}}{\overline{R_i}} \tag{6.6}$$

where $D_{HOL,i}$ is the i-th flow head of line (HOL) packet delay, $r_{i,j}$ is the instantaneous available rate (of the i-th flow in the j-th sub-channel) and $\overline{R_i}$ is i-th flow average transmission rate, computed as follows [135]:

$$\overline{R_i}(k) = 0.8\overline{R_i}(k-1) + 0.2R_i(k) \tag{6.7}$$

where $R_i(k)$ is the throughput achieved by the i-th flow during the k-th TTI and $\overline{R_i}(k-1)$ is the throughput estimation in the previous TTI.

Given two flows with equal HOL, a_i weights the metric so that the user with the strongest requirements in terms of acceptable loss rate and deadline expiration will be preferred for allocation [137], and is given by [135]:

$$a_i = -\frac{\log(\delta_i)}{\tau_i} \tag{6.8}$$

where τ_i is packet delay threshold and δ_i is maximum probability that $D_{HOL,i}$ exceeds the delay threshold of the i-th flow, respectively.

Although it will not be the case in this research, it is worthwhile to mention that, for non-real time flows, the metric is computed as are the ones for the Proportional Fair scheduler, mentioned by [135]:

$$w_{i,j} = \frac{r_{i,j}}{\overline{R_i}} \tag{6.9}$$

Table 6.4 presents a sample of the allocation matrix with b = {20, 7}, u = {1, 64} and $L^{\max} = \left[L_{20}^{\max}, L_{7}^{\max}\right]$with the M-LWDF scheduler. It is shown that each user is only allocated to one band/CC, i.e., the metric value is 0 for the other one (band/CC). The remaining RBs (available RBs on the band available to the UE) will be allocated to UEs according to the highest value of the metric computed by the M-LWDF scheduler.

Further details on the implementation of the GMBS into LTE-Sim are provided in Appendix B.

Table 6.4 Example of the allocation matrix over two frequency bands.

	Band 20						Band 7				
	RB						RB				
u	0	1	…	23	24	…	25	26	48	…	49
1	0.06000	0.20766	…	0.13687	0.06000	…	0	0	0	…	0
2	2.38263	0.44553	…	1.72402	3.07999	…	0	0	0	…	0
3	1.73774	0	…	1.73774	1.73774	…	0	0	0	…	0
4	0	0	…	0	0	…	0.61114	0.97452	1.47004	…	0.37990
5	0	0	…	0	0	…	2.11113	2.69350	2.11113	…	2.11113
6	1.97797	0.94878	…	0.36987	0.94878	…	0	0	0	…	0
7	0	0	…	0	0	…	0.18153	0.21653	0.01150	…	0.18153
8	0	0	…	0	0	…	3.22437	2.13750	3.22437	…	2.13750
9	0	0	…	0	0	…	2.89859	2.09735	1.39038	…	3.74695
10	0.35329	1.55087	…	0.73651	0.95208	…	0	0	0	…	0

6.6 Enhanced Multi-Band Scheduling

One of the main issues of the above mentioned multi-band scheduler is the increased complexity of the optimization process, specifically when the number of UEs in the network growths. Besides, this scheduler does not consider the possibility of UEs to use more than one band at the same time, unlike 3GPP specifications for LTE-A, LTE R9 and above. Although, it is arguable that the PF could be modified to consider allocating UEs to multiple CCs, this would imply that an allocation variable $x_{b,u}$ should be computed for all RBs instead of (in this case) two CCs, e.g., considering two 5 MHz CCs (25 RBs ×2), the PF should compute 50 allocation variable per UE. Therefore, the computation complexity of resource scheduling (optimization) would become unacceptable. Besides, both of these downsides have already been identified in the literature, in [115]. Hence, in the context of this Ph.D. research an Enhanced Multi-Band Scheduling (EMBS) has been developed and proposed. On the one hand, IP optimization is no longer employed, instead a more traditional scheduling approach is used, i.e., a scheduling metric for each RB of each CC is computed. In return, the RBs allocation is performed according to the highest value obtained. On the other hand, this approach allows allocating UE in either or both bands simultaneously, e.g., according to the metric value.

The scheduling metric is computed has fallows:

$$w_{i,j,b} = D_{HOL,i} \times \frac{R\left(CQI_{i,j,b}\right)^2}{\overline{R_i} \times S_{rate}} \tag{6.10}$$

where $D_{HOL,i}$, $\overline{R_i}$ and S_{rate} stand for the same, as above (for the GMBS), and $R(CQI_{i,j,b})$ is the DL throughput of band b for the i-th flow in the j-th sub-channel of as a function of the

supported MCS. Hence, the channel diversity of both CCs is also accounted for during the scheduling (RBs allocation) process. In this case $D_{HOL,i}$ insures that video flows/UEs with the higher delay, i.e., the difference between the time in which the transmission was requested and the current simulation time, obtain a higher metric value. $R(CQI_{i,j,b})$ is squared to guarantee that RBs with higher CQIs achieve a higher metric value, and as a consequence higher throughputs should be obtained.

Additional information on the implementation of the EMBS into LTE-Sim are provided in Appendix B.

6.7 Basic Multi-Band Scheduling

Finally, for comparison purposes, another multi-band scheduler has been implemented in this CRRM context and considered for CA evaluation. This scheduler is rather simpler than the ones proposed above and implements basic CRRM functionalities. Its aim is to allocate UEs to a preselected frequency band, e.g., band 20 until $L_b^{\max}$ is reached. Beyond this capacity threshold, the remaining UEs are allocated to the second available frequency band, say band 7. Similarly to the previous case, UE can only be allocated to one band at the time. Given these considerations, the allocation variable $x_{b,u}$ is given by:

$$x_{bu} = \begin{cases} 1 & if \quad L_b \le L_b^{\max} \\ 0 & if \quad L_b > L_b^{\max} \end{cases} \tag{6.11}$$

Additional details on the implementation of the CRRM's basic multi-band scheduling into LTE-Sim are shown in Appendix B.

6.8 System Capacity

Following the formulation proposed in Chapter 4 the system capacity of both 800 MHz and 2.6 GHz systems is also performed. For simplicity the following analysis will only consider the supported throughput in the DL for k equal to 1, 3 and 7. In terms of assumptions, one considers the transmitter power, P_t = 13 dBW, the transmitter gain, G_t = 14 dBi, receiver gain, G_t = 0 dBi and the noise figure, NF = 8 dB. Table 6.5 shows an overview of the parameters for the analysis of the system capacity.

Table 6.5 Parameters for the analysis of the system capacity.

Parameter	Value
b_{rf}	5 MHz
f	2.6 GHz, 800 MHz
P_t	13 dBW
G_t	14 dBi (BS)
G_r	0 dBi
NF	8 dB

Additionally, to map the reference SINR into supported throughput one considered the values provided by [133], more specifically Tables 7.1.7.1-1 and 7.1.7.2.1-1. By extrapolating the gathered information it is possible to map the SINR into CQI, MCS index, Transport Block Size (ITBS) index and TBS. Furthermore, assuming TTI = 1 ms the throughput is obtained by multiplying the TBS by this value, and has a 5 MHz bandwidth is considered, i.e., 25 PRBs, column N_{PRB} = 25 in Table 7.1.7.2.1-1 is also assumed has shown in Table 6.6.

Table 6.6 Mapping of the SINR into throughput for a 5 MHz bandwidth.

SINR	CQI Index	MCS Index	Modulation Order	ITBS	TBS (25 PRBs)	Throughput [Mbps]
-4.63	1	0	2	0	680	0.68
-3.615	1	1	2	1	904	0.904
-2.6	2	2	2	2	1096	1.096
-1.36	2	3	2	3	1416	1.416
-0.12	3	4	2	4	1800	1.8
1.17	3	5	2	5	2216	2.216
2.46	4	6	2	6	2600	2.6
3.595	4	7	2	7	3112	3.112
4.73	5	8	2	8	3496	3.496
6.13	6	9	2	9	4008	4.008
7.53	6	10	4	9	4008	4.008
8.1	6	11	4	10	4392	4.392
8.67	7	12	4	11	4968	4.968
9.995	7	13	4	12	5736	5.736
11.32	8	14	4	13	6456	6.456
12.78	8	15	4	14	7224	7.224
14.24	9	16	4	15	7736	7.736
14.725	9	17	6	15	7736	7.736
15.21	10	18	6	16	7992	7.992
16.92	10	19	6	17	9144	9.144
18.63	11	20	6	18	9912	9.912
19.975	11	21	6	19	10680	10.68
21.32	12	22	6	20	11448	11.448
22.395	12	23	6	21	12576	12.576
23.47	13	24	6	22	13536	13.536
25.98	13	25	6	23	14112	14.112
28.49	14	26	6	24	15264	15.264
31.545	14	27	6	25	15840	15.84
34.6	15	28	6	26	18336	18.336
-	15	29	2	reserved	-	-
-	15	30	4	reserved	-	-
-	15	31	6	reserved	-	-

The main difference between the following analysis and the approach from Section 4.3.4 is the number of *J* coverage rings. Here, the number of coverage rings is equal to 27, i.e., equal to the number of ITBS, as each index corresponds to a different throughput value. The remaining formulation from Section 4.3.4 is kept the same. Figure 6.5 shows the values obtained for the 800 MHz band, whereas Figure 6.6 shows the results for the 2.6 GHz band.

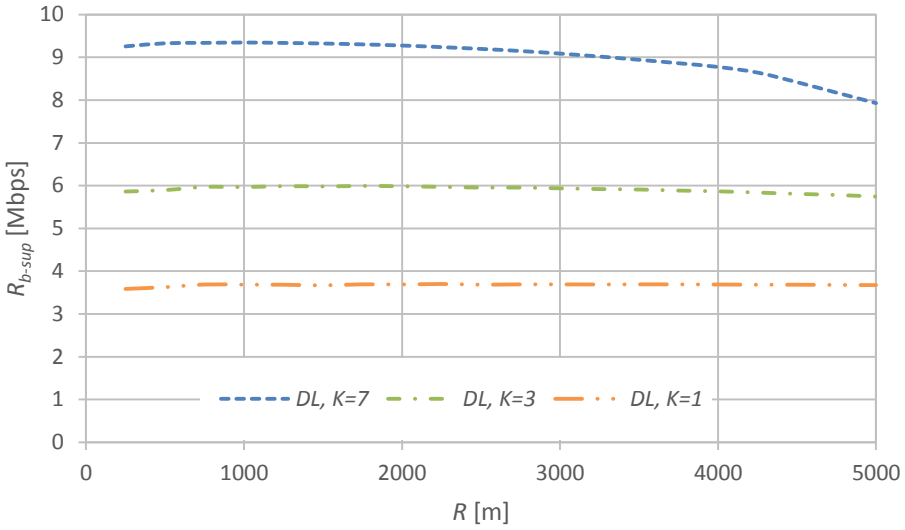

Figure 6.5 Comparison of the equivalent supported throughput between cells K = 1, 3 and 7 at 800 MHz.

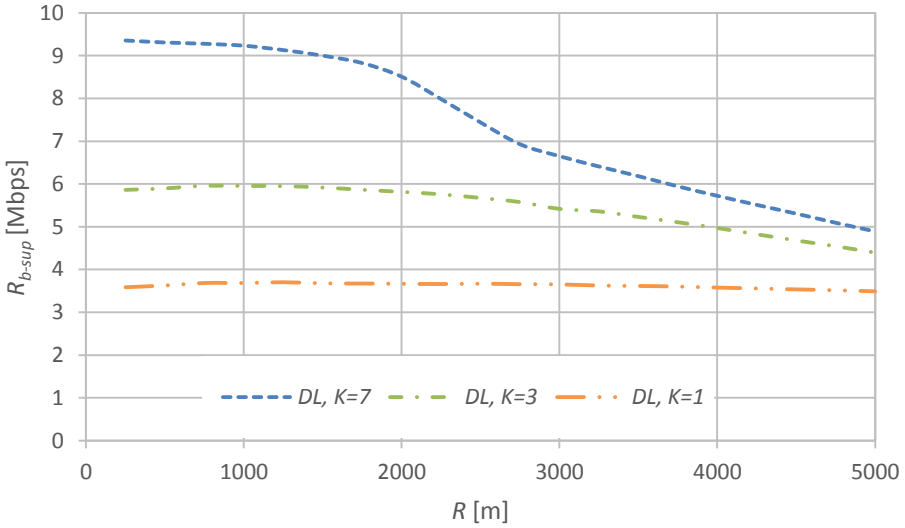

Figure 6.6 Comparison of the equivalent supported throughput between cells K = 1, 3 and 7 at 2.6 GHz.

Overall, it can be observed that the main difference between both bands is the decline of the supported throughput as a function of the distance. This decay is apparent it both cases, however, it is more noticeable at 2.6 GHz. This difference is expected since the path loss at 2.6 GHz is higher than the one at 800 MHz. Furthermore, although K = 7 presents the higher values of the supported throughput, it also the reuse pattern which presents the greater reduction as a function of the distance. On the opposite side of the previous remarks, K = 1 shows slit to none reduction of the supported throughput with the distance, but presents the lower values of the three addressed reuse patterns. Finally, K = 3 presents a mixture of the previous cases. On the one hand, the obtained values are slightly affected by

the distance at 800 MHz, whereas at 2.6 GHz the reduction is more apparent. On the other, the supported throughput values are in-between the ones obtained with K = 1 and 7.

Finally, it is also interesting to note that the maximum supported throughput, obtained at the lower addressed distance, R = 250 m, is approximately the same for both bands, i.e., 3.6, 5.9 and 9.3 Mbps, for K = 1, 3 and 7, respectively. In perspective, considering R = 2500 m and only K = 7 the achieved results are 9.2 and 7.4 Mbps in the DL for the 800 MHz and 2.6 GHz bands, respectively.

Additionally, the percentage of covered cell area by each MCS index/throughput value as a function of R can also be performed. In this case it is important to note that according to [133] although the MCS index 9 - 10, and 16 - 17 have different modulation order, 2 - 4 and 4 – 6, respectively, the corresponding ITBS are the same, e.g., MCS index 9 and 10 correspond to ITBS 9, hence the same throughput. This fact is of particular importance in the results below since each coverage ring/percentage of covered area is differentiated according to the supported throughput. Furthermore, this analysis will be dedicated only for K = 3 since these conditions are the focus of this research. Figure 6.7 show the percentage of area covered by each MCS index versus R for K = 3 at 800 MHz while Figure 6.8 shows the analogous case for the 2.6 GHz band. In both figures the right and left part represent the percentage of area, while the left hand part allows for better visualizing the variation between coverage areas, the right hand part of the figures presents a better global overview. On the right corner of the figure a caption presents the MCS index value(s) as well as the corresponding throughput.

From the analysis of both figures, the most noticeable feature is the ability to maintain higher MCS index with the 800 MHz band. More specifically, at 800 MHz MCS index 7 to 28 are supported, whereas, at 2.6 GHz, the lowest index is 4 and the highest is also 28. Another evident characteristic is the highest percentage of covered area, which is provided by the 9 – 10 MCS index, an average of 17.7 and 15.9 % for the 800 MHz and 2.6 GHz bands, respectively.

Additionally, it is also clear that at 2.6 GHz the support of higher MCS decreases as R increases and for $R \geq 3000$ m lower MCS, i.e., 4, 5 and 6, must be used to maintain the cell coverage. At 800 MHz this trend is less noticeable and it is possible to maintain MCS index 7 for the considered values of R. To conclude, at 800 MHz, it is possible to cover higher percentage of the cell with superior MCS indexes, whereas with at 2.6 GHz lower MCS must be employed and the percentage of area covered by the highest MCS is comparatively reduced.

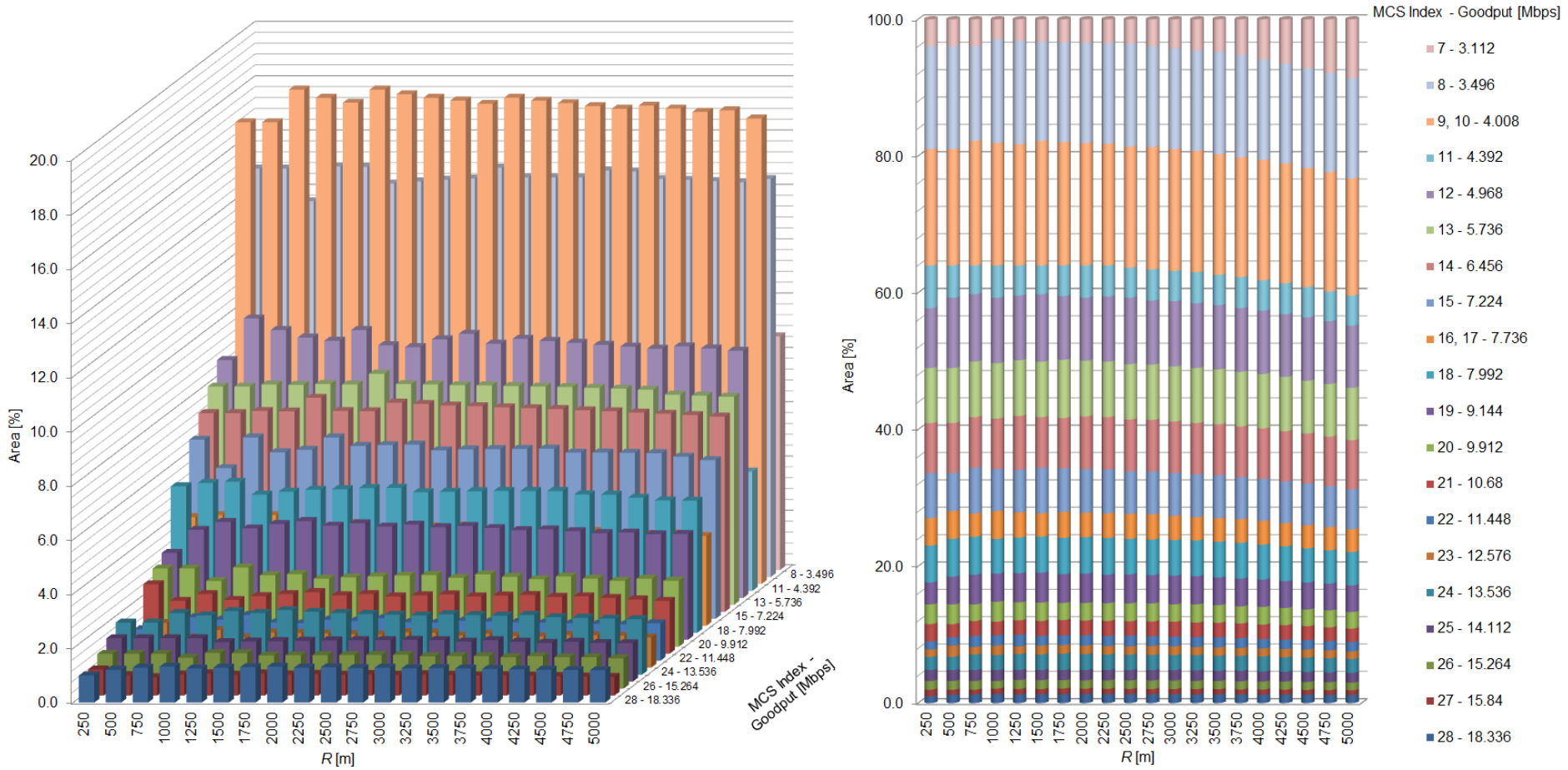

Figure 6.7 Area covered by each MCS index versus *R* for *K* = 3 at 800 MHz.

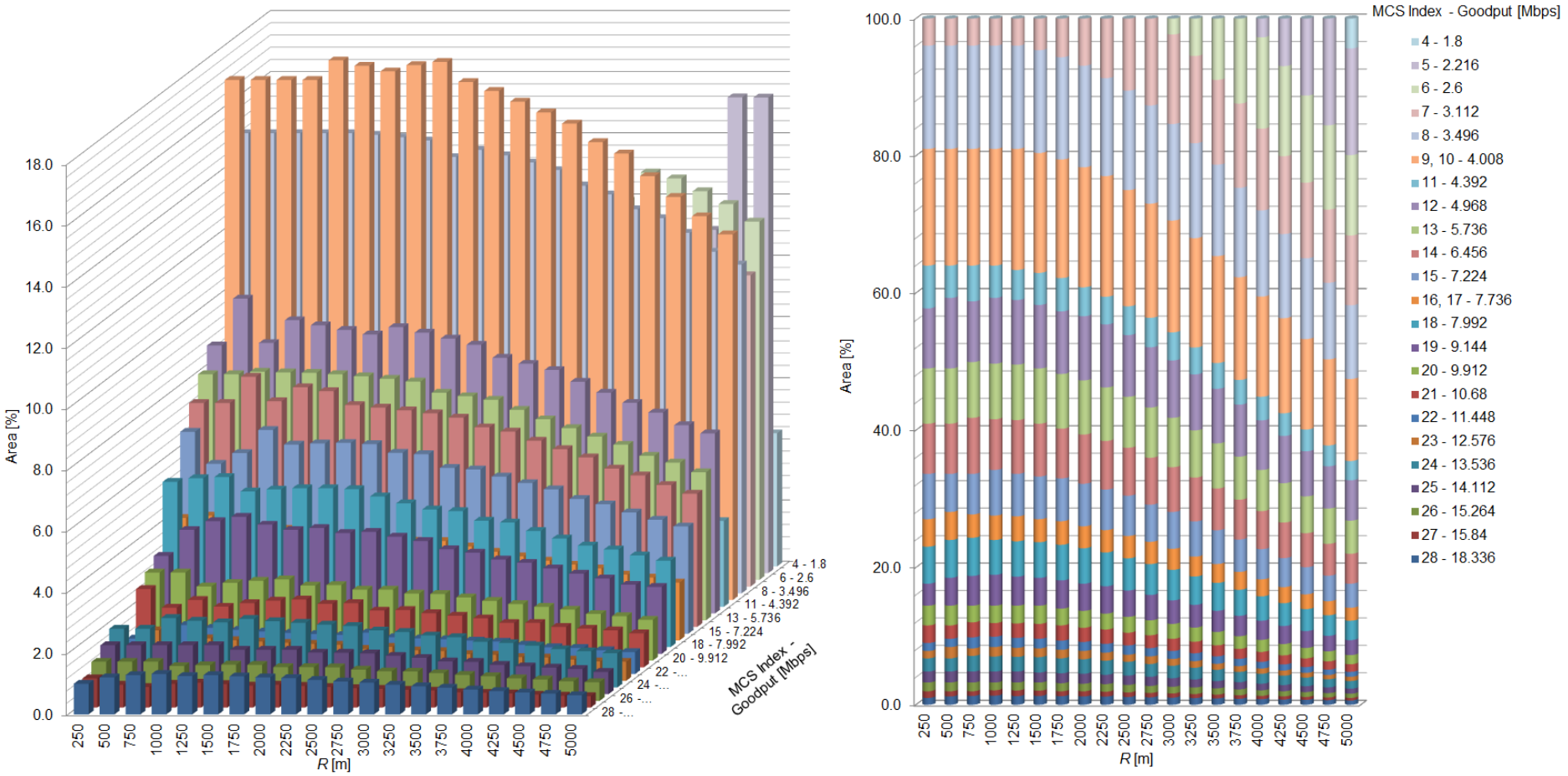

Figure 6.8 Area covered by each MCS index versus R for K = 3 at 2.6 GHz.

6.9 Average SINR Analysis with Reuse Pattern Equal to Three

In this work, the CA gain is evaluated for several inter-cell distances with frequency reuse pattern three. In order to have comparable results between results for different values for the coverage distance, CA needs to be analysed at constant average SINR. To obtain the average SINR, a method similar to the described in chapter 12 from [134] was applied. By tuning the BSs/eNBs transmitter power, the average SINR was kept constant. Moreover, this formulation allows for decreasing energy consumptions small cells are considered, i.e., small cells use lower transmitter power than larger ones to achieve the similar SINR.

6.9.1. SINR at a Given Position

According to [134], for a topology with a BS in a given position (y, 0) and for K = 3, the inter-cell BSs distance is $3R$, as shown in Figure 6.9.

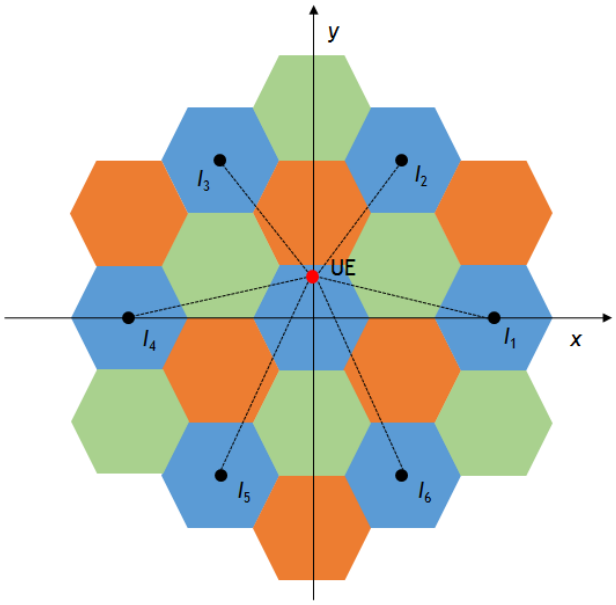

Figure 6.9 Topology considered for the inter and intra cell interference for an LTE network with K = 3.

Given a BS transmitter power, P_{Tx}, the BS SINR at position (x, y) is expressed by:

$$SINR(P_{Tx},x,y)=\frac{P_{ow}(P_{Tx},x,y)}{(1-a)P_{ow}(P_{Tx},x,y)+P_{nh}(P_{Tx},x,y)+P_{noise}} \quad (6.12)$$

where a is the orthogonality factor, for simplicity and according to [134] a is equal to 1, P_{ow} is the power received from the own cell, P_{nh} is the total interfering power coming from the neighbour cells, e.g., 6 cells in the hexagonal cell deployment model, and the thermal noise power, P_{noise}, depends on UE noise figure (typical of 7-9 dB for LTE). P_{noise} is expressed as:

$$P_{noise} = -174 + 10 \cdot \log_{10}(BW) + NF \tag{6.13}$$

where NF = 8 dB, and BW = 5 MHz. At 800 MHz, P_{ow} is expressed by:

$$P_{ow-800MHz}(P_{Tx}, x, y) = P_{Tx} G_{Tx} G_{rx} 10^{-\frac{1119.8 + 37.6 \log_{10}\sqrt{y^2 + x^2}}{10}} \tag{6.14}$$

Whereas at 2.6 GHz, P_{ow} is expressed by:

$$P_{ow-2.6GHz}(P_{Tx}, x, y) = P_{Tx} G_{Tx} G_{rx} 10^{-\frac{130.5 + 37.6 \log_{10}\sqrt{y^2 + x^2}}{10}} \tag{6.15}$$

where G_{Tx} and G_{Rx} are the transmitter and receiver gains respectively.

As stated above, $P_{nh}(P_{Tx}, x, y)$ is the interfering power received by a UE from the ring of six cells with a distance of $3R$ due to K = 3, shown in Figure 6.9, is given by:

$$P_{nh}(P_{Tx}, x, y) = \sum_{i=1}^{6} I_i(P_{Tx}, x, y) \text{ with, } I_1 = I_4,\ I_2 = I_3,\ I_5 = I_6 \tag{6.16}$$

where $I_i(P_{Tx}, x, y) = P_{Tx} G_{Tx} G_{rx} 10^{-\frac{PL(x,y)^i}{10}}$ and i represents the cell from which the interference comes from. The PL at 800 MHz that corresponds to the interference from cell i, also defined in [131], is given by:

$$\begin{aligned} PL(x,y)^{1,4} &= 119.8 + 37.6 \cdot \log_{10}\sqrt{\left(\frac{3R}{2}\right)^2 - \left(\frac{3\sqrt{3}R}{2} - y\right)^2} \\ PL(x,y)^{2,3} &= 119.8 + 37.6 \cdot \log_{10}\sqrt{\left(\frac{3R}{2}\right)^2 + \left(\frac{3\sqrt{3}R}{2} + y\right)^2} \\ PL(x,y)^{5,6} &= 119.8 + 37.6 \cdot \log_{10}\sqrt{3R^2 + y^2} \end{aligned} \tag{6.17}$$

In turn, at 2.6 GHz the PL is given as follows:

$$\begin{aligned} PL(x,y)^{1,4} &= 130.5 + 37.6 \cdot \log_{10}\sqrt{\left(\frac{3R}{2}\right)^2 - \left(\frac{3\sqrt{3}R}{2} - y\right)^2} \\ PL(x,y)^{2,3} &= 130.5 + 37.6 \cdot \log_{10}\sqrt{\left(\frac{3R}{2}\right)^2 + \left(\frac{3\sqrt{3}R}{2} + y\right)^2} \\ PL(x,y)^{5,6} &= 130.5 + 37.6 \cdot \log_{10}\log_{10}\sqrt{3R^2 + y^2} \end{aligned} \tag{6.18}$$

The geometry symmetries have been considered and I_i is the i-th cell interference.

6.9.1. Average Cell SINR

The average SINR within a cell is the SINR measured by a UE with uniform probability density function for its deployment over the cell area. It depends on the cell radius, R, and on the eNB transmitter power, P_{Tx}, as follows:

$$\overline{SINR}(P_{Tx},x,y)=\frac{\bar{P}_{ow}(P_{Tx},x,y)}{(1-a)\bar{P}_{ow}(R,P_{Tx})+\bar{P}_{nh}(R,P_{Tx})+P_{noise}} \tag{6.19}$$

For simplicity, by considering that a is equal to 1 (6.19) can be re-written as:

$$\overline{SINR}(P_{Tx},x,y)=\frac{\bar{P}_{ow}(P_{Tx},x,y)}{\bar{P}_{nh}(R,P_{Tx})+P_{noise}} \tag{6.20}$$

where $\bar{P}_{nh}(R,P_{Tx})$ is the average interference power from the six neighbouring cells. The average interference generated by a neighbour cell can be calculated by integrating each fraction of the interfering power over the area of the affected cell. Figure 6.10 shows one affected cell in the origin of the coordinates and one interfering cell, at (x_0, y_0).

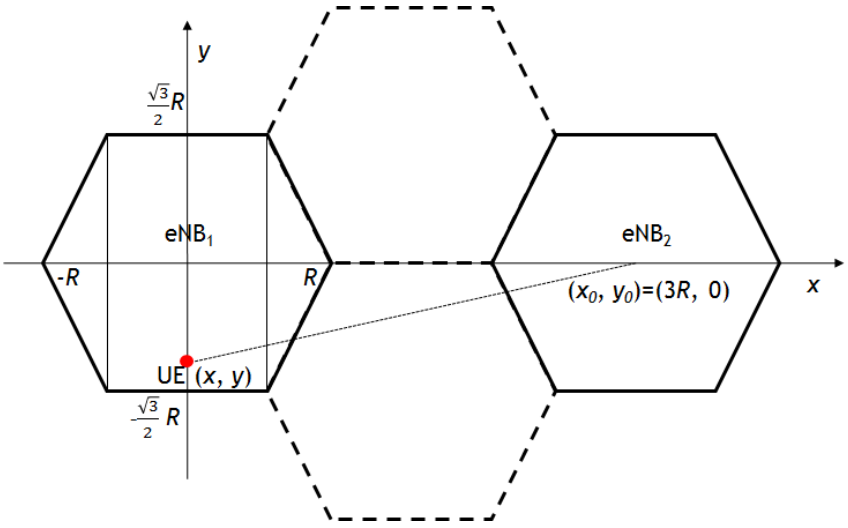

Figure 6.10 Geometry for the interference received from neighbouring cells.

By integrating over the hexagonal cell area, the average level of received power from a neighbour cell $\bar{I}$ may be calculated as follows:

$$\bar{I}(R,P_{Tx})=\int_y\int_x f_I(P_{Tx},x,y)dxdy=\int_y\int_x \frac{P_{Tx}G_{Tx}G_{Rx}}{A_{cell}}PL(x,y)dxdy= \tag{6.21}$$

where A_{cell} is the total affected cell area given by $3\sqrt{3}/2\ R^2$. $\bar{P}_{nh}(R,P_{Tx}) = 6\bar{I}(R,P_{Tx})$ as the surrounding interfering neighbours are all at the same distance, $3R$. Additional details on the calculation of the average interference can be found in [131].

$\bar{P}_{ow}(P_{Tx},x,y)$is the average signal power within a cell and it is constant for the same frequency model no matter what value of k is use. $\bar{P}_{ow}(P_{Tx},x,y)$ may be obtained following a similar approach to the one for $\bar{P}_{nh}(R,P_{Tx})$, with a different integrand function, f_p, which, due to the geometry of the problem, has a simpler expression. The integrand function for the 800 MHz frequency band is given by:

$$fP_{ow-800MHz}(P_{Tx},x,y) = \frac{P_{Tx}G_{Tx}G_{rx}}{A_{ow}} 10^{-\frac{119.2+37.6\log_{10}\sqrt{y^2+x^2}}{10}} \tag{6.22}$$

The integrand function for 2.6 GHz is the following one:

$$fP_{ow\ 2.6GHz}(P_{Tx},x,y) = \frac{P_{Tx}G_{Tx}G_{rx}}{A_{ow}} 10^{-\frac{130.5+37.6\log_{10}\sqrt{y^2+x^2}}{10}} \tag{6.23}$$

where A_{ow} is the total integration area equal to $3\sqrt{3}/2\ R^2 - 4F_r^2$, Fr is the Fraunhofer distance and its value is different for each frequency band/CC. The results for the average SINR for P_{Tx} = 13 dBW are shown in Figure 6.11. It can be observed that the average SINR rapidly decreases for cell radii longer than 300 m. The average SINR at 2.6 GHz decreases faster than the one at 800 MHz, as it suffers higher effect from the PL. A detailed calculation of the average SINR is reported in the Appendix A.

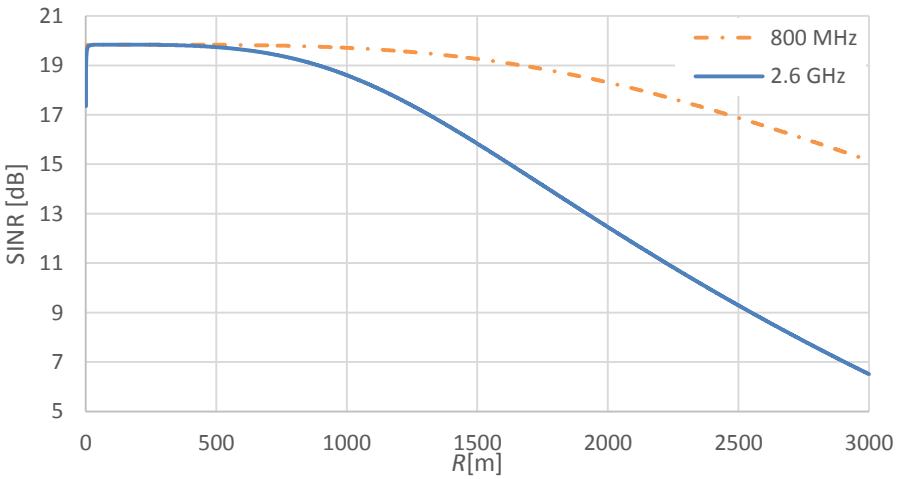

Figure 6.11 Average SINR [dB] as a function of the cell radius, in meters.

6.10 Transmitter Power Normalization Procedure

The aim of the average cell SINR analysis is to compute a set of transmitting powers P_{Tx} in order to have a constant average SINR for all cell radii. From equations (6.19) and (6.20), and assuming constant antenna gains, it can be concluded that the average cell SINR for a given cell radius, R_0, only depends on P_{Tx}.

To compute the P_{Tx} values that should be used at 800 MHz and 2.6 GHz, the first step is to compute the average SINR horizontal asymptotes, for each frequency band. Secondly, as the obtained horizontal asymptotes correspond to very high values for P_{Tx}, the normalized P_{Tx} required in both bands is computed within a 10 % variation, V, of the horizontal asymptotes. Finally, $P_{Tx,R}$ is found for $R \in \{300; 3000\}$ m such that:

$$\overline{SINR}(R, P_{TX}) = \overline{SINR} - V\% \tag{6.24}$$

where V is equal to 10 %. Table 6.7 presents some of the obtained normalized values for P_{Tx}.

Table 6.7 Values for the normalized transmitter power $P_{Tx[dBw]}$ for the 800 MHz and 2.6 GHz bands.

V [%]	Freq. Band (MHz)	Radius[m]						
		300	600	900	1200	1500	1800	2100
10	800	-12.160	-0.842	5.779	10.477	14.121	17.098	19.615
	2600	-1.931	9.387	16.007	20.705	24.349	27.326	29.843

Figure 6.12 presents a graphical representation of the normalized P_{Tx} for V = 10 % and both frequency bands. To maintain a similar average cell SINR in both bands, it is clear that the required normalized P_{Tx} at 2.6 GHz value must be higher than at 800 MHz to compensate for the higher PL.

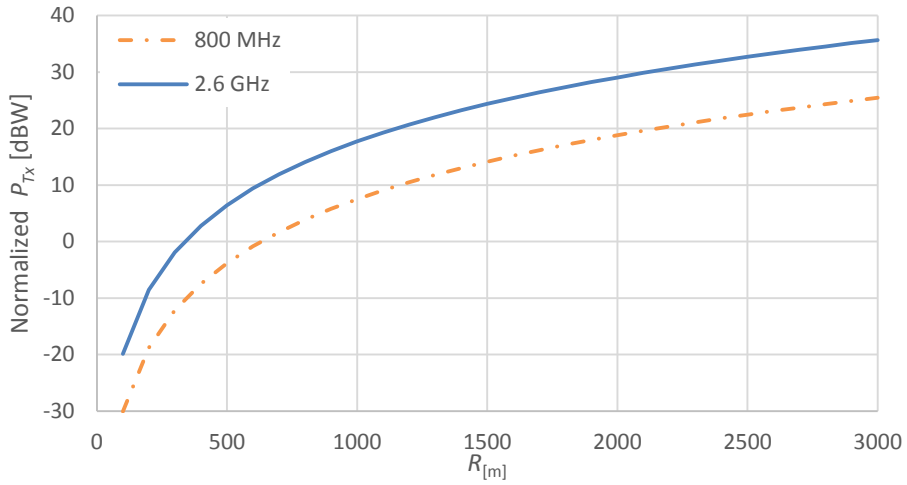

Figure 6.12 Normalized transmitter power in [dBW], as a function of the cell radius in [m] for V = 10 %.

6.11 Cell Capacity Analysis

The analysis of cell capacity has been performed considering the obtained values for the normalized transmitter power. The SINR, CQI, MCS and supported throughput are considered for both carriers (800 MHz and 2.6 GHz). The following results have been obtained through averaging the results from 100 simulations performed with LTE-Sim (with 80 active UEs per simulation), i.e., the above parameters were recorded at each (x, y) coordinate and each one corresponds to the position and the considered parameters observed by 80 simulated UEs. To perform a 3D graphical representation and due to the extremely high number of coordinates/points necessary to plot this charts/mesh, only results for a 300 m cell radius are shown in Figures 6.13 to 6.16. The distance d varies between 0 and R = 300 m

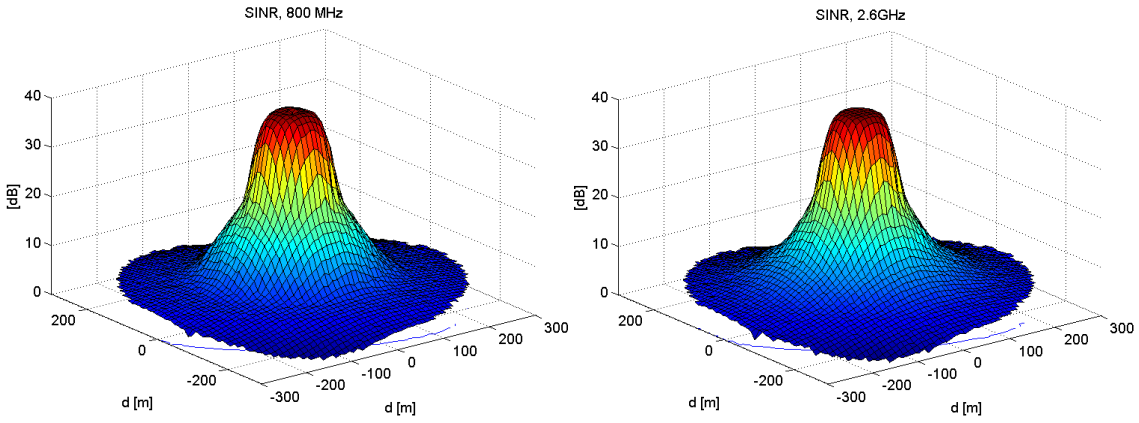

Figure 6.13 3D representation of the cell SINR for both carriers.

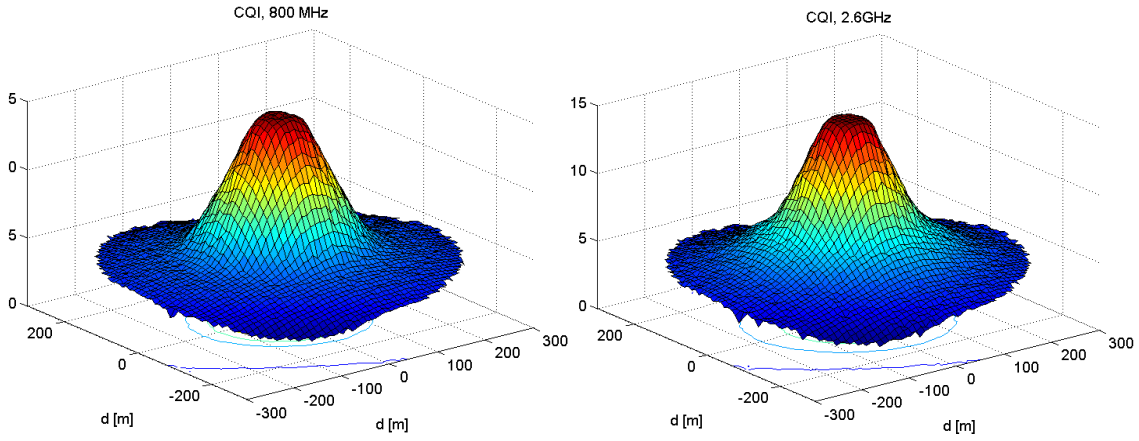

Figure 6.14 3D representation of the cell CQI for both carriers.

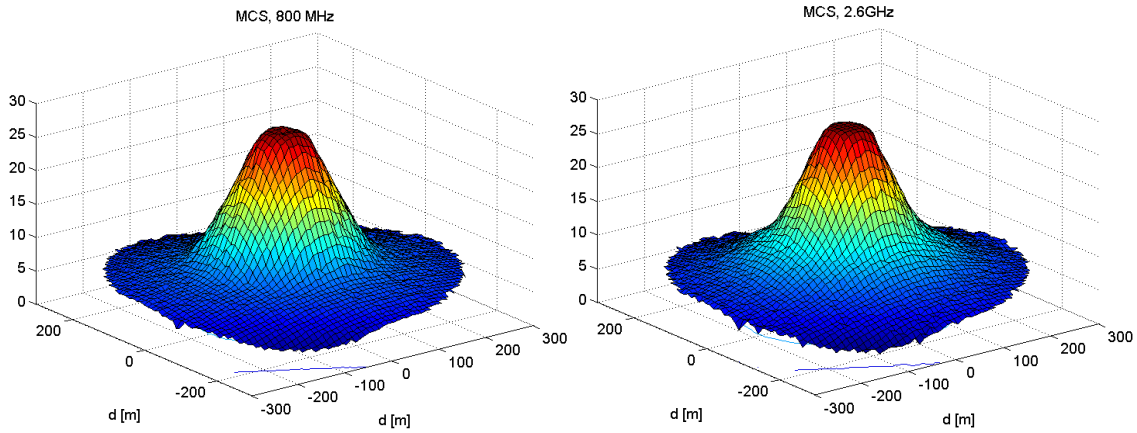

Figure 6.15 3D representation of cell MCS for both carriers.

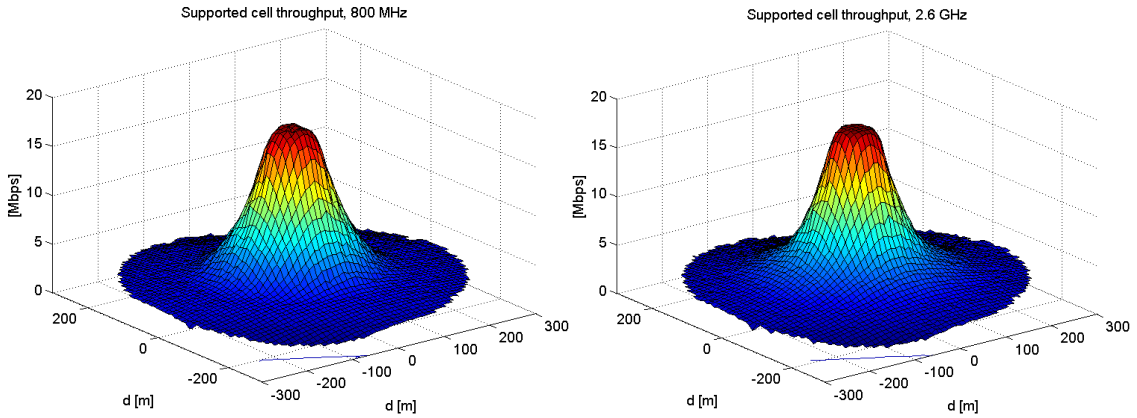

Figure 6.16 3D representation of the supported cell throughput for both carriers.

Overall, it can be observed that a consequence of considering the transmitter power normalization process is that the results obtained for both frequency carriers are comparable, i.e., globally the maximum and minimum results are similar. The difference between both bands is the shape like cone radius. The top of the cones radius is approximately the same, as one descends through the cone, i.e., going in the descending direction of the values for the simulated results (SINR, CQI, MCS, etc.), the cone radius increases. However, it increases somewhat more in the 800 MHz case. In other words, as the distance from the cell centre increases so does the radius of the cone and this occurrence is more apparent at 800 MHz. This means that the values from the simulations at 800 MHz are slightly higher than the ones at 2.6 GHz as the distance from the cell centre increases.

In terms of SINR, Figure 6.13, the obtained values vary from 1 to 4 dB at the cell edge, and reaches approximately 40 dB at the centre. This variation at the cell edge is expected, has seen in Chapter 4, section 4.2 as the distance, $D \pm R$, between the UE and the interfering cells fluctuates, so does the SINR, e.g., the worst case position.

The highest CQI is obtained at the cell centre, i.e., 15, and its value diminishes to 3 – 4 at the cell edge, Figure 6.14. As anticipated, the MCS, shown in Figure 6.15, behaves in the

same way, i.e., values range between 28 at the cell centre and 4 to 6 at the edge. Finally, the achievable supported throughput reaches approximately 18.3 Mbps at the centre and oscillates between approximately 2 and 4 Mbps at cell edge, depending on the considered position near the boundary.

Figure 6.17 shows the difference of the SINR and supported cell throughput parameters between the 800 MHz and 2.6 GHz band The difference is explained by the fact that apparently the LTE system at 800 MHz is slightly more dependent on the coverage (and less on the interference) that the system at 2.6 GHz.

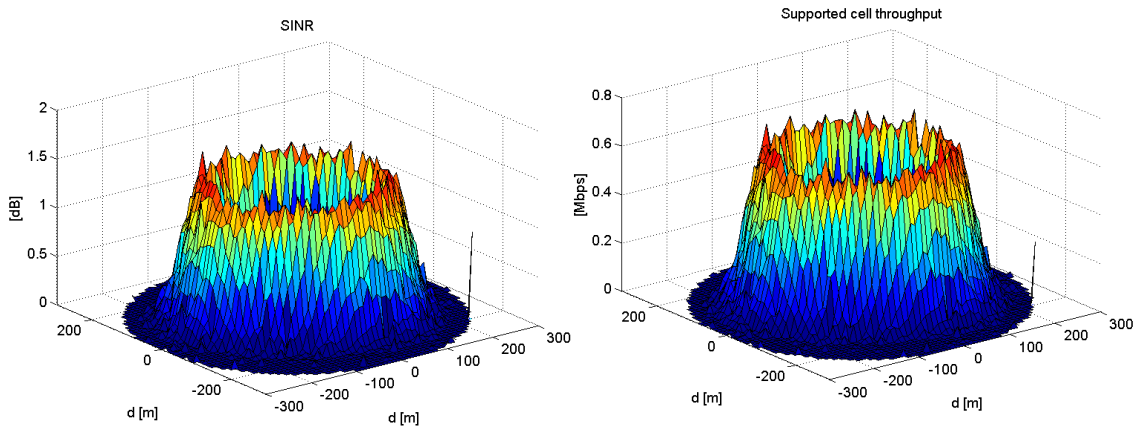

Figure 6.17 Difference between the 800 MHz and 2.6 GHz SINR and supported cell throughput.

In terms of cell capacity analysis, in the context of CA, it is still possible to compute the aggregated cell achievable throughput, shown in Figure 6.18. These values are obtained by adding the 800 MHz and 2.6 GHz bands supported throughput. Simply, the aggregated cell achievable throughput ranges from approximately 37 Mbps at the cell centre to 4 -8 Mbps near the cell edge.

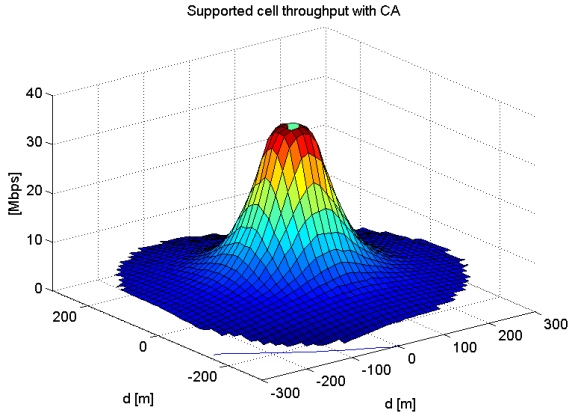

Figure 6.18 3D representation of the supported cell throughput with CA.

6.12 Simulation Environment

To study the performance of the proposed iCRRM, several LTE system level simulations have been performed within a LTE-A scenario. The comparison parameters include the average cell supported goodput, delay, Packet Loss Ratio (PLR) and spectral efficiency. The LTE simulator chosen to perform this evaluation is LTE-Sim [135], developed at the University of Bari. LTE-Sim is an event-driven simulator, written in C++, using the object-oriented paradigm. Several traffic generators at the application layer have been implemented and the management of data radio bearer is supported. In particular, the video traffic addressed in this research is a trace-based application which sends packets based on realistic video trace files. To study the performance of the proposed iCRRM the inter-band CA scenario shown in Figure 6.4 is considered. UEs are constantly moving at 3 kmph using LTE-Sim random direction mobility model, each UEs only use one H.264 128 kbps video bit rate flow, and maximum delay of 1 ms is considered. LTE-Sim [135] provides a support for radio resource allocation in a time – frequency domain and, in this configuration, the duration of one LTE radio frame is 10 ms. One frame is divided into 10 sub-frames of 1 ms each, and each sub-frame is divided into two slots of 0.5 ms each. Each slot contains either six or seven OFDM symbols, depending on the Cyclic Prefix (CP) length [137]. The normal CP is used in urban cells and high data rate applications while the extended CP is used in special cases like multi-cell broadcast and in very large cells (e.g., rural areas, low data rate applications).

Furthermore, LTE radio resources are allocated in units of RBs or Physical RBs (PRBs). Each PRB contains 12 subcarriers and one slot. If the normal CP is used, a PRB will contain 12 subcarriers over 7 symbols. If the extended CP is used, the PRB contains only six symbols. In the context of CA, normal CP frames is assumed, each carrier band has a 5 MHz bandwidth and thus a total of 25 +25 = 50 PRBs are available for scheduling. An overview of the simulation parameters are presented in Table 6.8.

Table 6.8 Simulation parameters.

Simulation parameters	
Reuse pattern	3
Simulation duration	46 s
Flow duration	40 s
Frame structure	FDD
Bandwidth	5 MHz per CC
Slot duration	0.5 ms
Scheduling time (TTI)	1 ms
Number of RBs	25 RB per CC
Max delay	0.1 s
Video bitrate	128 kbps
UE mobility	random direction, 3 kmph

6.13 Simulation Results

The evaluation of the proposed iCRRM entity involved performing several simulation scenarios:

1) Two LTE system operating separately at 800 MHz and 2.6 GHz, i.e., without CA;
2) One LTE-A scenario with both frequency bands managed with basic CRRM functionalities (basic multi-band scheduling);
3) One LTE-A scenario with both frequency bands managed with the proposed iCRRM entity:
    a. One set performed with GMBS;
    b. One set performed with EMBS.

Each scenario was simulated twenty times, these results were averaged and the confidence intervals were determined. The average cell Packet Loss Ratio (PLR) and delay analyses are performed by averaging the results from 1) while comparing them with the ones from 2) and 3). In terms of the analyses from average cell supported goodput, the system capacity obtained in 1) is summed and compared with the results from 2) and 3). Additionally, it is worthwhile to note that the following results obtained without CA were compared and are well within the range of ones obtained in packet scheduling algorithms studies performed in [135], [137] and [137].

6.13.1. Packet Loss Ratio

Figure 6.19 shows the average cell PLR as a function of the number of UEs for a cell with *R* = 1000 m. As expected, both CRRM and iCRRM outperform the scenario without CA.

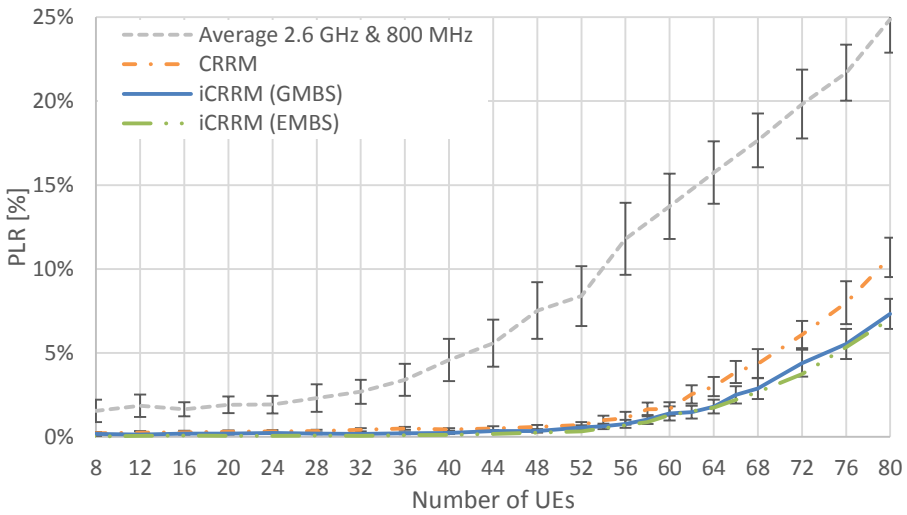

Figure 6.19 Average cell PLR as function of the number of UEs for *R* = 1000 m.

However, according to the ITU-T G.1010 [49] and 3GPP TS 22.105 [50] recommendations, presented in Chapter 2 (Table 2.1), the PLR should not exceed 1 %. In this context, the 1 % PLR threshold is only exceeded above approximately 58 UEs with iCRRM general (GMBS) and enhanced (EMBS) multi-band scheduling (1.03 % and 0.88 %, respectively), whereas CRRM only supports up to 54 UEs (0.99 %). Without CA, the minimum obtained PLR is approximately 2 %. Besides, it is also verified that overall the iCRRM EMBS enables to obtained lower PLR values than the ones with the GMBS. Figure 6.20 shows again the obtained results, the average PLR without CA ("Average 2.6 GHz & 800 MHz") is not shown, since the minimum obtained value is superior to 2 %, which is the maximum shown PLR.

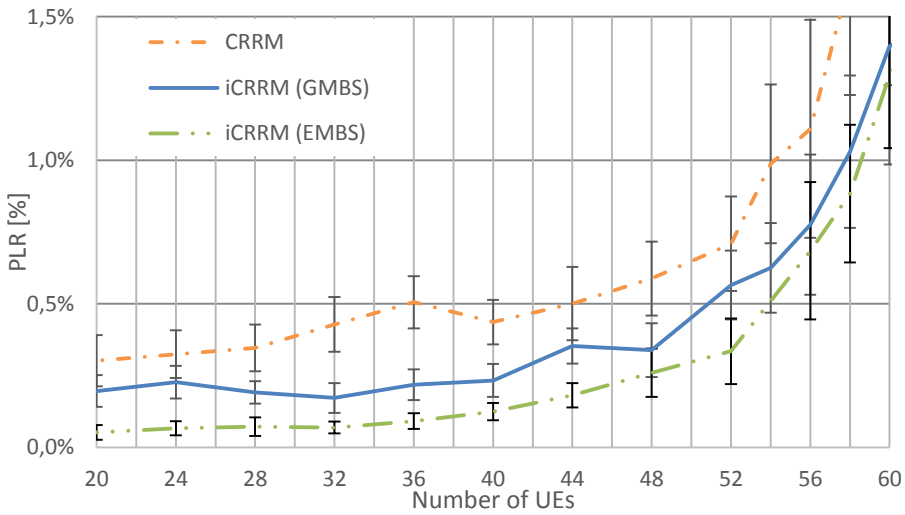

Figure 6.20 Average cell PLR as function of the number of UEs.

6.13.2. Delay

The average cell delay for *R* = 100m is shown in Figure 6.21. As in the previous case, both CRRM and iCRRM present better results than without CA, i.e., lower delay. Moreover, iCRRM EMBS outperforms the GMBS again. Similarly to the PLR, ITU-T G.1010 [49] and 3GPP TS 22.105 [50] also define delay performance targets, i.e., 150 ms preferred and 400 ms limit delay. For the considered number of UE none of these targets is exceeded. Nonetheless, when the previous 1 % performance target is exceed, i.e., 54 and 58 UEs, with CRRM and iCRRM, respectively, the achieved delay is approximately 11.22, 11.44 and 7.68 ms with CRRM, GMBS and EMBS scheduling, respectively. Without CA the average cell delay is always superior to the ones from the above cases.

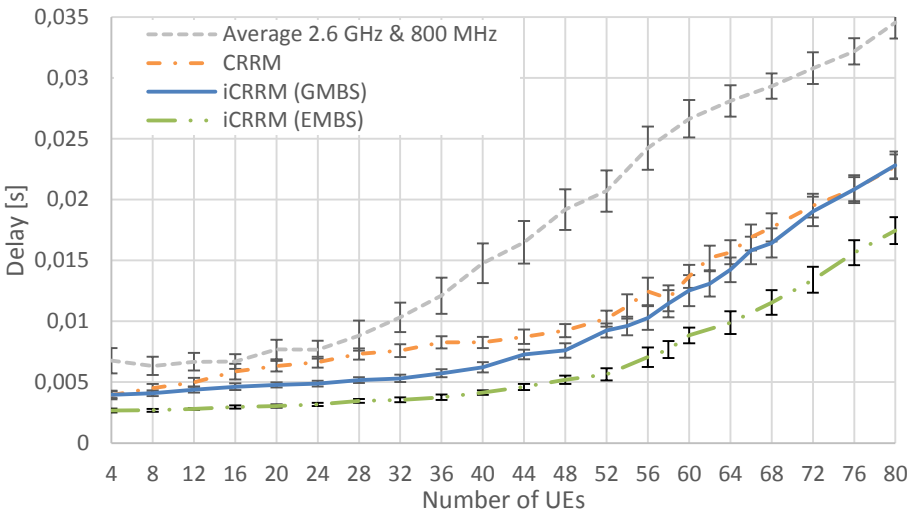

Figure 6.21 Average cell delay as function of the number of UEs for *R* = 1000 m.

6.13.3. Quality of Experience

In the context of CA and the proposed iCRRM entity, besides assessing the network service level parameters the Quality of Experience (QoE) can also be evaluated by employing the model for the mapping between QoS and QoE proposed in Chapter 3. Considering equation (3.22) as well as the previous PLR and delay simulation results, Figure 6.22 shows the predicted QoE as a function of the number of active UEs in a cell with *R* = 1000 m.

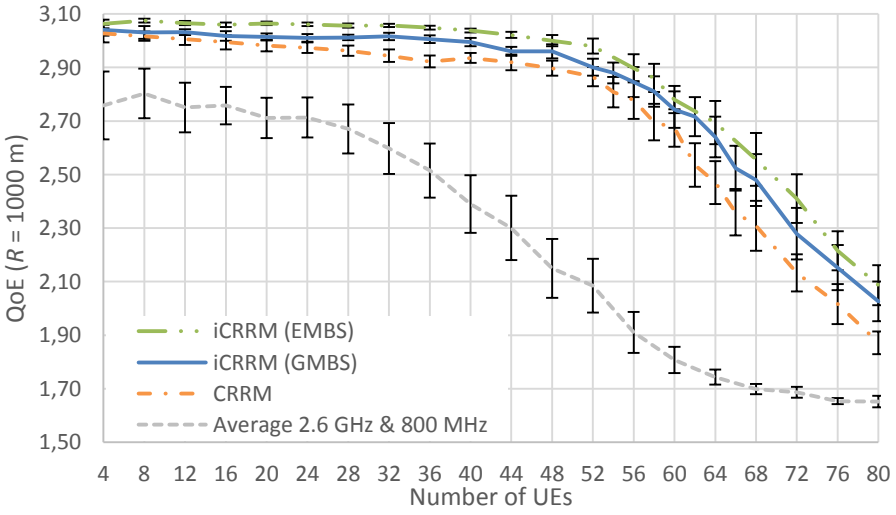

Figure 6.22 QoE as a function of the number of active UEs in the cell for *R* = 1000 m.

From Figure 6.22, it is clear that employing CA improves the average cell QoE. Without CA an average QoE of 2.7 is obtain below 28 UEs, beyond this values the quality substantially decreases and reaches its lower value with the maximum considered UEs. With

CA, as expected by the obtained PLR and delay the EMBS provides the better results followed by the GMBS and the CRRM. Moreover, it is interesting to note that, as expected by ITU-T G.1010 [49] and 3GPP TS 22.105 [50], the higher decline of the estimated QoE value occurs approximately with the same number of UEs from which the 1 % PLR is exceeded, i.e., 54 and 58 UEs with CRRM and iCRRM, respectively.

6.13.4. Goodput

The supported average goodput is shown in Figure 6.23 considering *R* = 1000 m. In this case, the performance gap between iCRRM, CRRM and no CA is less apparent. With the exception of the case without CA all the remaining scenarios can support the cell traffic requirement up to approximately 52, 56 and 58 UEs with CRRM, iCRRM GMBS and iCRRM EMBS, respectively. However, it is clear that as the number of UEs within the cell increases so thus the iCRRM performance gain, in comparison with both CRRM and no CA results. In the context of the iCRRM it has also been shown that above 58 UEs the goodput obtained with the EMBS is higher than the one obtained with the GMBS.

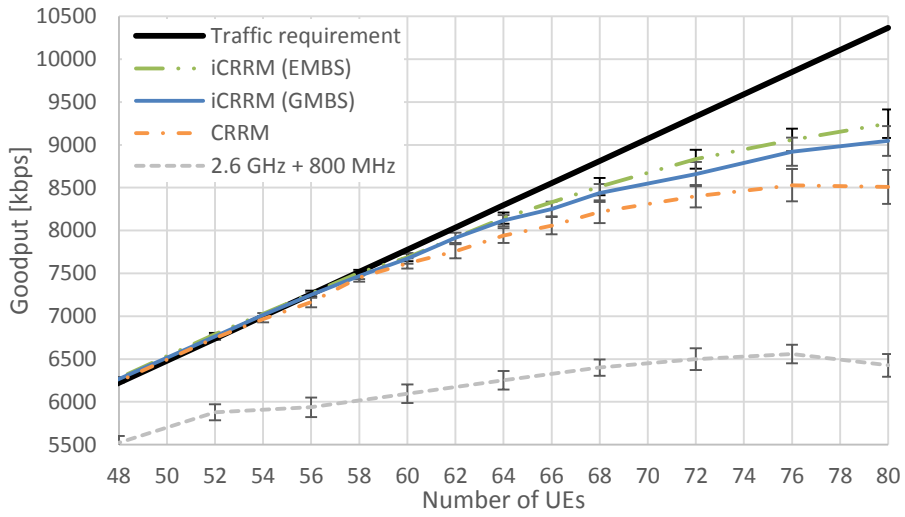

Figure 6.23 Average cell supported goodput as function of the number of UEs for *R* = 1000 m.

Additionally, it is also important to consider the supported goodput within ITU-T G.1010 [49] and 3GPP TS 22.105 [50] performance target. In this context, considering the number of UE supported within the 0.1 % PLR margin, i.e., 58 and 54 UEs with iCRRM and CRRM, respectively, the supported goodput improvement between both RRM is evident, as shown in Figure 6.24. With iCRRM an average of 7500 and 7400 kbps are supported, with the EMBS and GMBS, respectively, whereas only 6900 kbps are supported with CRRM. The case without CA is not considered since the lowest obtained PLR is approximately 2 %.

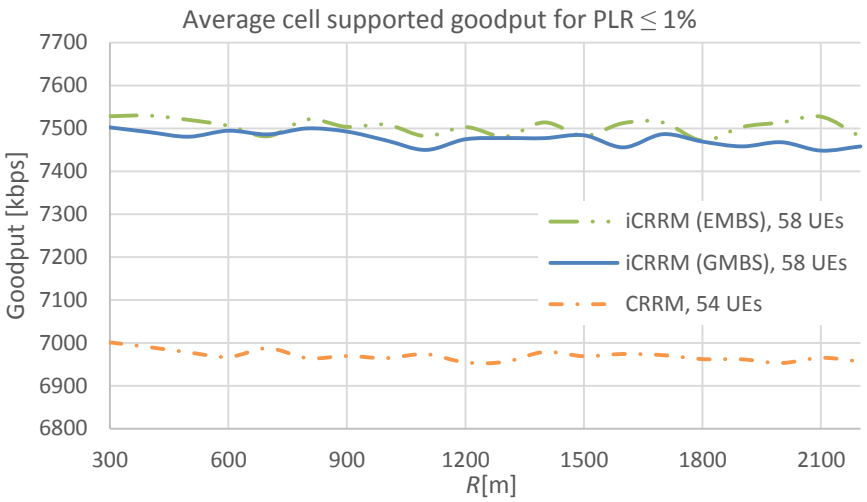

Figure 6.24 Average supported cell goodput with PLR ≤ 1 % as a function of cell radii.

Similarly to the above ITU-T and 3GPP target performance considerations and bearing in mind the ITU-T ACR scale [70] whose lower QoE value is 1 and highest is 5, a value equal to 2.5 is henceforward considered as a threshold below which the QoE is not acceptable. In this context, and considering the results from Figure 6.22, without CA, the average cell QoE is no longer considered sufficient above 36 UEs. With CA, the 2.5 threshold is no longer achieved above 64, 68 and approximately 70 UEs, with CRRM, iCRRM GMBS and iCRRM EMBS, respectively. Finally, the number of UEs supported by the cell below this QoE threshold can also be reflected in terms of average supported cell goodput, as shown in Figure 6.25. Given these considerations, the average supported goodput is approximately 8800, 8450, 7950 and 3500 kbps with iCRRM EMBS, iCRRM GMBS, CRRM and without CA, respectively.

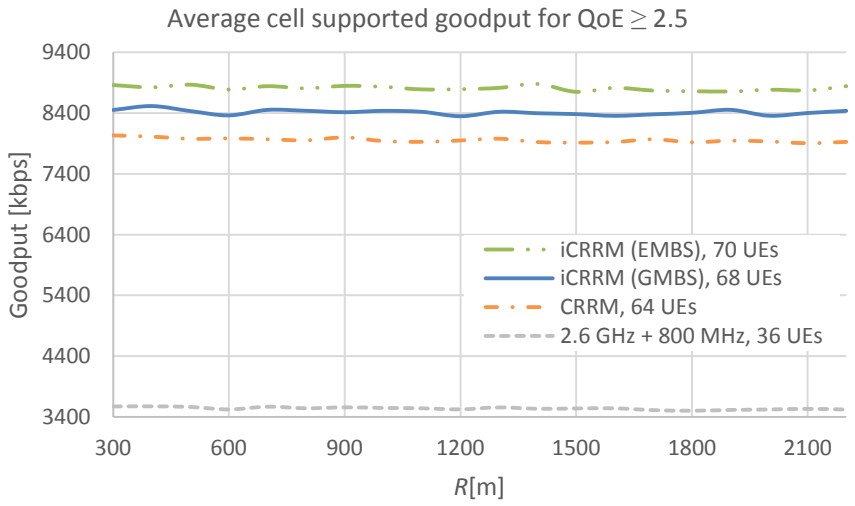

Figure 6.25 Average supported cell goodput for QoE ≥ 2.5 as a function of cell radii.

6.13.5. Spatial Distribution and Allocation of Radio Resources with iCRRM

The analysis of the spatial allocation of radio resources within the cell has also been performed, i.e., the geographic position in which CCs were allocated by each scheduler. This study allows identifying the behaviour of both GMBS and EMBS and, for instance, to determine if the CCs are optimally used, e.g., cell edge users are allocated with the CC with lower losses/attenuation. In the first case, i.e., iCRRM's GMBS, since UEs can only be allocated to one CC at a time, the following results show the spatial percentage of allocated UEs to each CC, regardless of the allocated RBs. In the second case, i.e., iCRRM's EMBS, given that UEs can be allocated to both CCs the obtained results show the percentage of allocated RBs belonging to each CC.

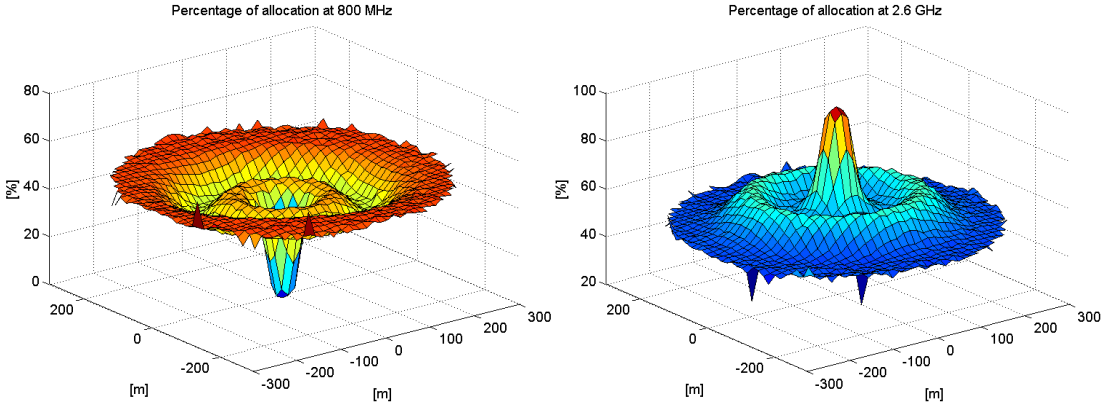

Figure 6.26 3D representation of the geographic allocation of CCs for the GMBS.

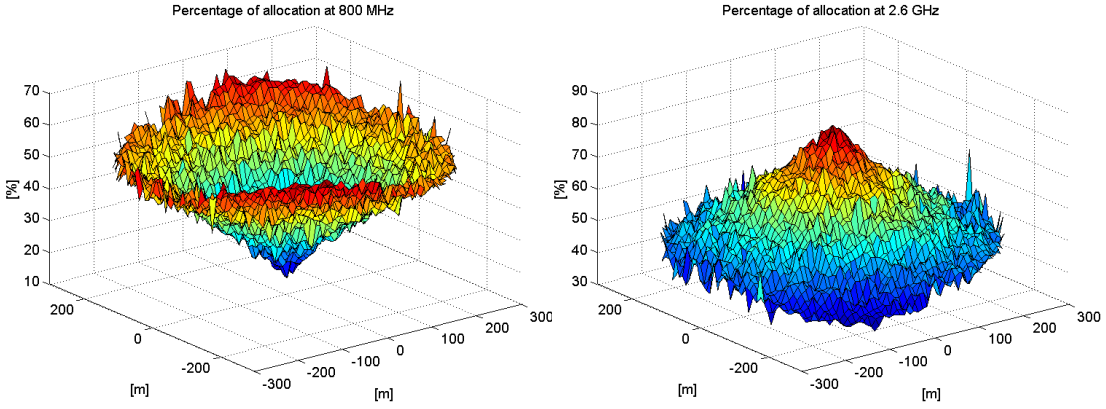

Figure 6.27 3D representation of the geographic allocation of CCs for the EMBS.

As in section 6.11, the results represent the average of 100 simulations with 80 active UEs, Figure 6.26 shown the allocation for the GMBS whereas Figure 6.27 shows EMBS's. On the one hand, it is clear that both schedulers have a similar behaviour, i.e., in both cases UEs in the cell centre are mostly allocated at 2.6 GHz, then this percentage decreases as the

distance from the cell centre increases (UEs move away from the cell centre) and, at the cell edge, UEs allocation on the 800 MHz CC is preferred. On the other hand, the way this trend of UEs allocation is performed in a very different way by both schedulers. When employing the GMBS, at the cell centre almost 95 % of UEs are allocated at 2.6 GHz, at 50 m from the centre this value/allocation is diminished to 50 %. At mid cell range, i.e., 150 m from the centre, the allocation at 2.6 GHz reaches approximately 65 %. Finally at the cell edge the observed allocation at 2.6 GHz ranges from 40 to 50 %, Figure 6.26. With EMBS at the cell centre an average of 80 % of UEs are allocated on the 2.6 GHz carrier (the remaining 20 % are allocated at 800 MHz), every 100 m (distance from the cell centre to its edge) the allocation percentage diminishes approximately 20 % and reaches approximately 30 to 40 % at the cell edge (depending on the edge), Figure 6.27.

6.13.6. Spatial Distribution of the Supported Goodput with iCRRM

The analysis of the supported goodput through the cell has also been performed considering the previously mentioned 100 simulations and R = 300 m. In this context, Figure 6.28 and Figure 6.29 show the obtained goodput with GMBS and EMBS, respectively.

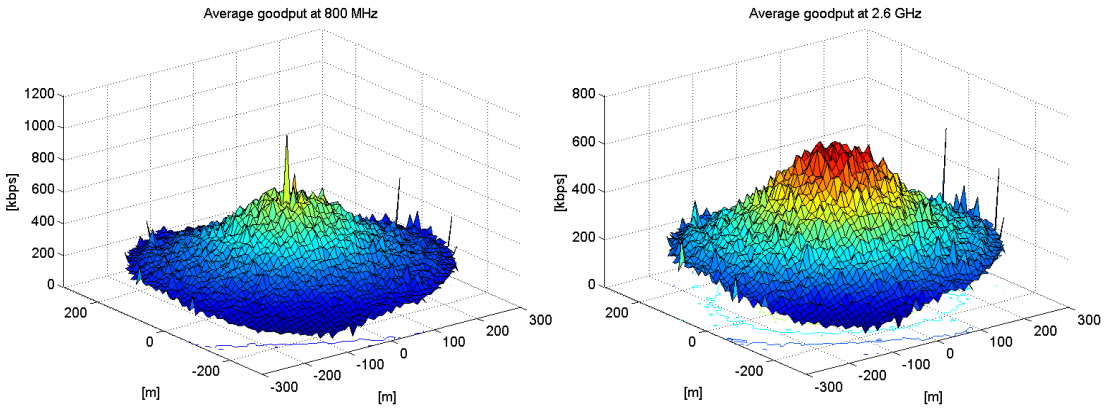

Figure 6.28 3D representation of the geographic allocation of CCs for the GMBS.

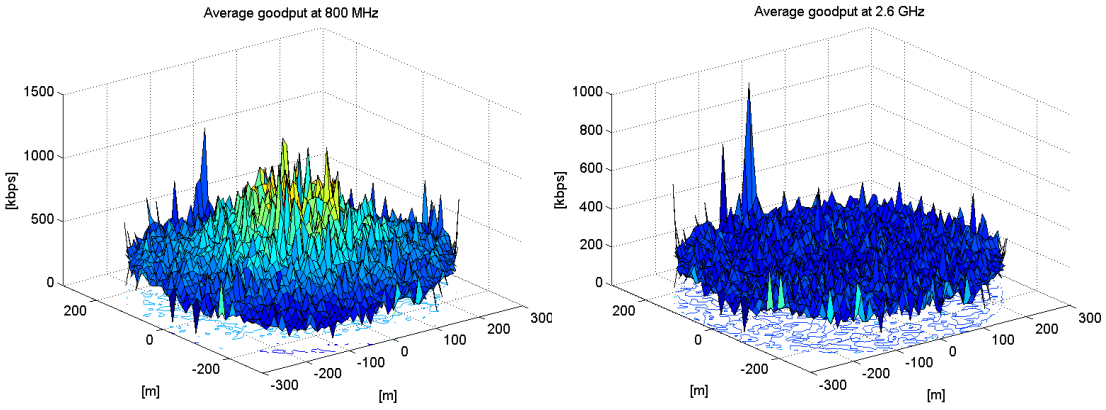

Figure 6.29 3D representation of the geographic allocation of CCs for the EMBS.

From the obtained results it has been found that throughout the cell the goodput is on average higher with the 800 MHz CC. Considering GMBS, as shown in Figure 6.28, at the cell edge, the goodput ranges from 130 (lower left edge) to 230 kbps (lower right edge), at 800 MHz, whereas, at 2.6 GHz this value is, on average, 20 to 50 kbps lower on the same position. At the cell centre results with the GMBS are approximately the same for both CCs, i.e., 650 kbps. The goodput decreases as the distance from the centre increases and this reduction is more noticeable on the 2.6 GHz CC.

With the EMBS, the difference between CCs at the cell edge is more striking, as shown in Figure 6.29. On some locations, the goodput at 800 MHz is 100 to 150 kbps higher than the one at 2.6 GHz. Overall, the results with EMBS are higher than the ones with GMBS and values between 200 are 400 kbps are obtained. The difference between the values of the supported goodput at cell edge are not so noticeable with this scheduler, it can be seen the 3D plot is more jagged and no clear tendency may be established. At the cell centre, the performance gap between both CCs is even higher. At 800 MHz the goodput reaches values between 600 and 900 kbps, however, values as high as 1 Mbps are also obtained. With the 2.6 GHz CC, values of 100 to 200 kbps are obtained. Finally, it has also been observed that the goodput at 800 MHz clearly decreases as the distance from the centre increases, whereas at 2.6 GHz the average supported goodput is maintained throughout the cell.

It can be also observed that these figures present some anomalies, i.e., usually at the cell edge some goodput peaks are shown. In the previous section these anomalies were barely noticeable, whereas in the present analysis they cannot be ignored. It must be noted that the simulations results are averaged according to their position in the cell, in other words, all the goodput values obtained at a given position are summed and divided by the number of occurrences. Each simulation has a different seed, parameters such as the UEs initial position and direction of movement are random. Besides, during these simulations the 80 UEs are not continuously active, as a matter of fact, during the first TTIs typically only a couple of UES are actually transmitting. Furthermore, the following results only show the spatial distribution of the goodput, and not its temporal distribution. Hence, one believes that these anomalies can be explained if one assumes that, at any given point in time only few UEs were active in the cell, which means that the MBSs would allocate most of the available resources to them, i.e., allowing higher goodput values for these UEs, at that location and moment in time. At these locations only a few (if any) more results were obtained, meaning that the peak goodput obtained at that position (at a time with few active UEs) may not have been averaged with goodput values when more UEs were active and lower goodput per UE were obtained. This means that the following analysis is interesting but yet imperfect to characterize how the available goodput is spatially allocated. As both schedulers operate on a TTI bases, a more accurate evaluation should be performed every millisecond, which would be impracticable considering the 46 s simulated time, i.e., 46000 3D plots should be analysed to achieve a flawless analyses.

6.14 Cost/Revenue Analysis

Following the approach and formulation presented in Chapter 5, the cost/revenue analysis in the context of CA may also be performed. Once again one considers a LTE system deployed in Portugal. The BS/eNB cost C_{BS} is assumes to be the value referenced in [139], i.e., 10.000 €, for both CCs. The cost of one BS/eNB site, C_{BSsite} = 7,000 € (since both BS/eNB share the same location only the cost of one C_{BSsite} should be accounted for). The BS installation cost, C_{Inst} = 22,500 €, is obtained by assuming 2,500 € for the radio installation plus 20,000 € for the infrastructure cost, e.g., site acquisition, site design and site construction. The backhaul cost is considered to be C_{bh} = 5,000 €. Finally the operation and maintenance costs which include first-line maintenance, rental costs and preventive and corrective infra maintenance, are $C_{M\&O}$ = 1,500 € per year of operation. The period of time assumed here is once again N_{year} = 5, and by replacing these assumptions in (5.3), one obtains C_b = 9,000 € per BS/eNB.

Bearing in mind Anacom's auction results it is known that each 2 × 5 MHz of bandwidth was sold for 45,000,000 € and 3,000,000 € for the 800 MHz and 2.6 GHz CCs, respectively. Considering k = 3, the total license cost for the 800 MHz and 2.6 GHz are 3 × 45,000,000 € = 135,000,000 € and 3 × 3,000,000 € = 9,000,000 €, respectively. Assuming these values and considering a total area of Portugal, the fixed cost per unit area is:

$$C_{fi800MHZ\ [€/km^2]} = \frac{135{,}000{,}000}{91{,}391.5 \times 5} \approx 295\ €/km^2 \tag{6.25}$$

$$C_{fi2.6GHZ\ [€/km^2]} = \frac{9{,}000{,}000}{91{,}391.5 \times 5} \approx 19.70\ €/km^2 \tag{6.26}$$

A summary of the assumptions for the costs is presented in Table 6.9.

Table 6.9 Costs assumptions.

Costs	Value
$C_{fi800MHz\ [€/km^2]}$	295.00
$C_{fi2.6GHz\ [€/km^2]}$	19.70
$C_{BS\ [€]}$	33,000.00
$C_{Inst\ [€]}$	22,500.00
$C_{bh\ [€]}$	5,000.00
$C_{M\&O\ [€]}$	1,500.00

Although nowadays the trend is to consider flat rate/fee for data and multimedia traffic revenues, in this work, one still considers the price per megabyte, MByte, of information, $R_{144[€/MByte]}$. In this context, two price per megabyte are considered, $R_{144[€/MByte]}$ = 0.005 and $R_{144[€/MByte]}$ = 0.01. Moreover, even though N_{year} = 5 the costs and revenues are computed on an annual basis and a null discount rate is considered. Assuming the above costs and channel price, the simulated average supported goodput results, $R_{b\text{-}sup[kbps]}$, with 80 UEs (no CA), and assuming an equivalent duration of busy hours per day, T_{bh}, equal to 6 busy hours per day, 240 busy days per year, one computes the total cost, *C total*, and the total

revenue per unit area per year, *Rv total* ($R_{v[€/km^2]}$), from equations (5.3) and (5.5), respectively. Figure 6.30 shows that *C total* and *Rv total* decrease as the as the cell radius increases, the revenues are higher than the total cost and higher revenues are obtained with higher MByte prices.

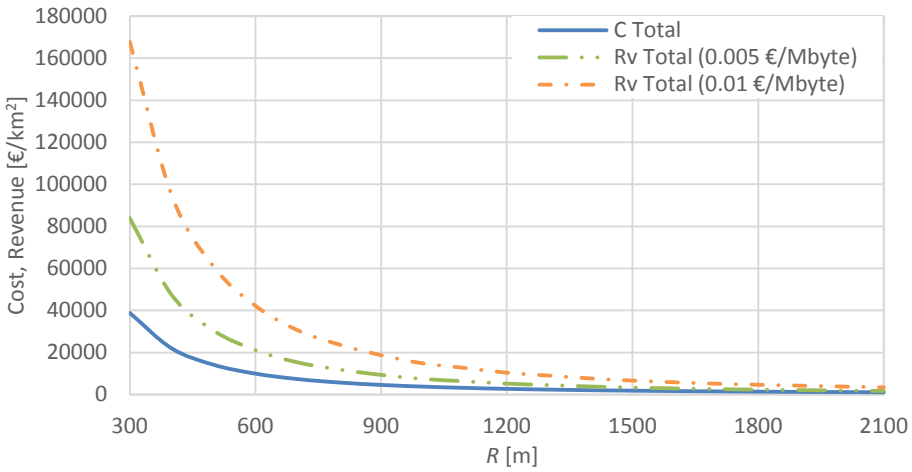

Figure 6.30 Total cost and revenue for different cell radii, for $R_{144[€/MByte]}$ = 0.005 and $R_{144[€/MByte]}$ = 0.10.

The analysis of the percentage of profit obtained by using equation (5.7) by considering two values of the simulated results of $R_{b\text{-}sup[kbps]}$ for the $R_{v[€/km^2]}$ computation. Initially, one considers the average supported goodput for PLR ≤ 1 %, this also means that as the scenario without CA thus not support this performance threshold it will not be considered. Secondly, the $R_{b\text{-}sup[kbps]}$ reached with QoE ≥ 2.5 is addressed. Figure 6.31 and Figure 6.32 show the percentage of profit with $R_{144[€/MByte]}$ = 0.005 for PLR ≤ 1 % and QoE ≥ 2.5, respectively, whereas Figure 6.33 and Figure 6.34 show the percentage of profit with $R_{144[€/MByte]}$ = 0.01 under the same goodput constraints.

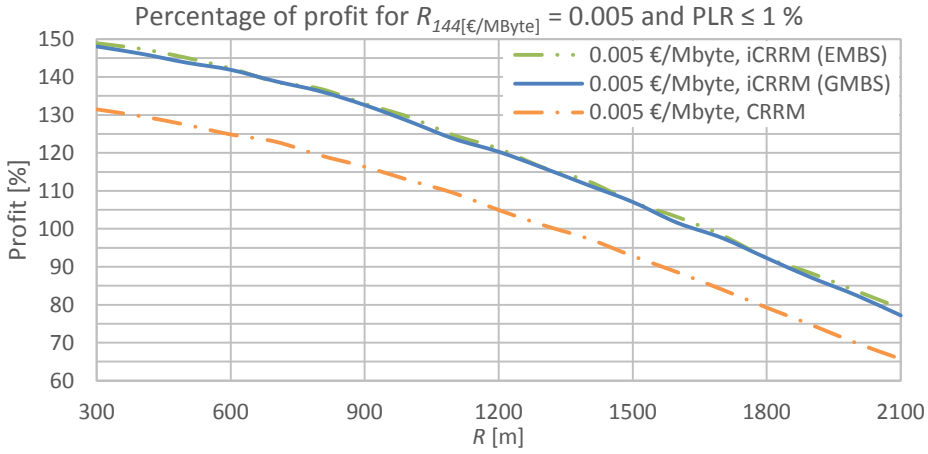

Figure 6.31 Profit in percentage as a function of the cell radius and PLR ≤ 1 %, $R_{144[€/MByte]}$ = 0.005.

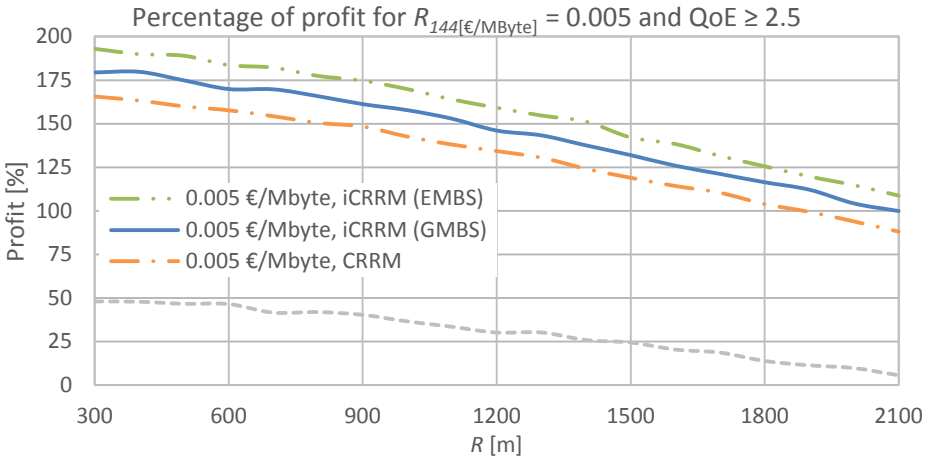

Figure 6.32 Profit in percentage as a function of the cell radius and QoE ≥ 2.5, $R_{144[€/MByte]}$ = 0.005.

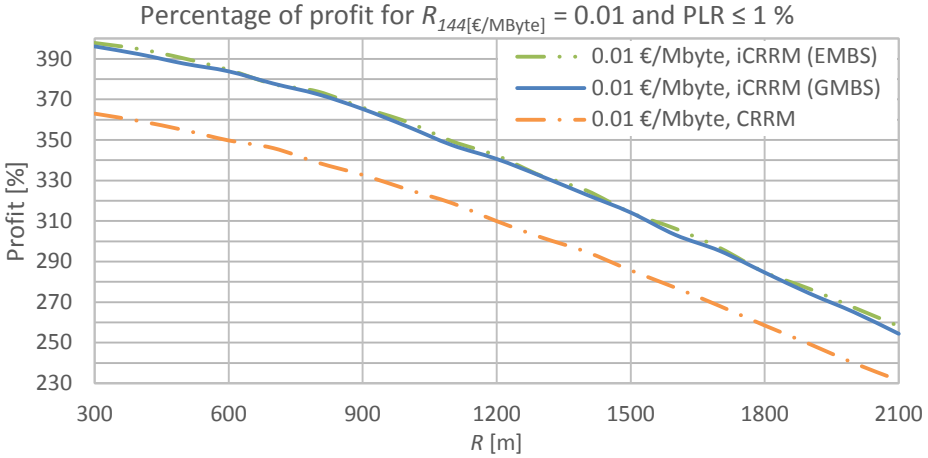

Figure 6.33 Profit in percentage as a function of the cell radius and PLR ≤ 1 %, $R_{144[€/MByte]}$ = 0.01.

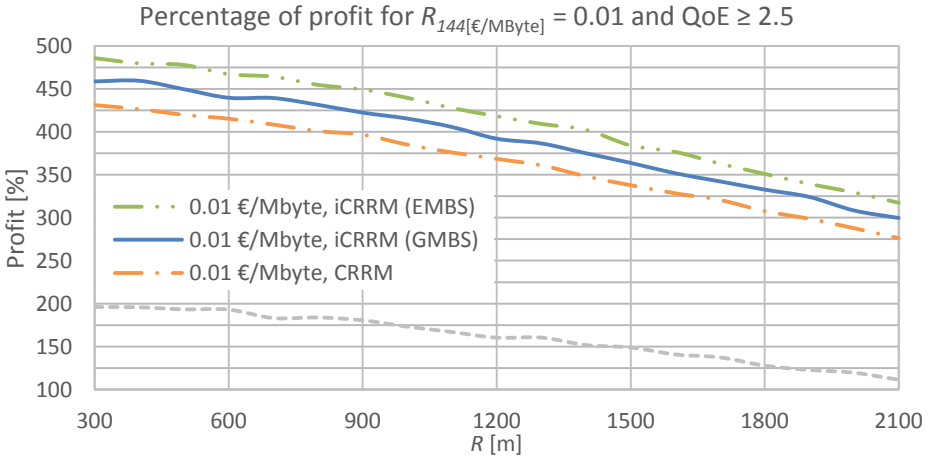

Figure 6.34 Profit in percentage as a function of the cell radius and QoE ≥ 2.5, $R_{144[€/MByte]}$ = 0.01.

Overall, it is evident that the profit increases as the price per MByte increases and that it also diminishes as a function of the cell radius, i.e., as the cell radius increases profits are lower. Considering PLR ≤ 1 % as the scenario without CA thus not supported this performance threshold the CRRM presents the lower results, whereas iCRRM's EMBS and GMBS reach comparable profits as their respective goodputs are also similar. Under the QoE ≥ 2.5 goodput constraint, as expected given their supported goodputs, i.e., higher number of supported UEs, iCRRM EMBS presents the higher profits, followed by iCRRM GMBS and CRRM, the case without CA obtains by far the lower results.

Besides the obvious profit gains with higher MByte price it is interesting to note that although the scenario without CA may reach the QoE ≥ 2.5 constraint it has been shown that under the addressed simulations and cost assumptions, with $R_{144[€/MByte]}$ = 0.005, a profit of 0 % is obtained for R = 2100 m. Employing iCRRM's EMBS and considering R = 1000 m profits of 130 and 360 % are obtained for PLR ≤ 1 % with $R_{144[€/MByte]}$ equal to 0.005 and 0.01, respectively. For the QoE ≥ 2.5 limitation the profit reaches 170 and 440 % for the same MByte price. With iCRRM's GMBS and the same cell radius, profits of 129 and 357 % are achieved for PLR ≤ 1 % and 158 and 416 % for QoE ≥ 2.5 considering $R_{144[€/MByte]}$ equal to 0.005 and 0.01, respectively. Using the basic CRRM with R = 1000 m profits of 113 and 326 % and 143 and 385 % are obtained for PLR ≤ 1 % and QoE ≥ 2.5 with MByte prices of 0.005 and 0.01 €/MByte, respectively. Finally, without CA profits of 37 and 173 % are achieved for QoE ≥ 2.5 and $R_{144[€/MByte]}$ = 0.005 and $R_{144[€/MByte]}$ = 0.01, respectively.

6.15 Conclusions

This work proposes an adaptation and update of the application of the integrated CRRM entity proposed in [131] for HSDPA, to an LTE-A scenario. The iCRRM entity implements inter-band Carrier Aggregation (CA) by performing scheduling between two Component Carriers (CCs), i.e., band 7 (2.6 GHz) and band 20 (800 MHz), with the aim of increasing user's quality of service requirements and improve spectral usage. Besides, iCRRM may operate with one of two multi-band schedulers, the general multi-band schedulers (GMBS) operates in parallel with a classic downlink packet schedulers, i.e., iCRRM assigns users to one CC and the scheduling of Resource Blocks (RBs) of each CC (to the allocated users) is performed by a downlink packet scheduler, the enhanced multi-band schedulers (EMBS) operates on its own and allocates RBs from both CCs. Moreover, with the GMBS UEs can only be allocated to one CC at a time whereas with EMBS UEs can be allocated to both CCs. Additionally, considering available bandwidths auctioned by the Portuguese communication regulator, Anacom, in 2011, CA research was addressed considering 5 MHz bandwidth CCs. Furthermore, bearing in mind CISCO's mobile traffic forecast, e.g., video traffic embodied 53 % of all traffic in 2013 and will reach 69 % by 2018, one addressed this work considering that each users generates one video traffic flow. In simulation terms, each flow is characterize as one trace based H.264 128 kbps video bit rate flow. Additionally, through extensive simulations, it has been

found that the Modified Largest Weighted Delay First (M-LWDF) scheduler provided the best results for this type of traffic and hence was selected to operate in conjunction with iCRRM's GMBS.

The analyses of the iCRRM performance for several cell radii with comparable conditions has been considered. To reduce energy consumption, the average cell interference-plus-noise ratio (SINR) must be kept constant by reducing the transmitter power for low cell radii. In this context, a formulation was proposed to compute the transmitter power needed to cover cells of different sizes whilst maintaining the average cell SINR approximately constant, and near the maximum, considering frequency reuse pattern three.

A 3D cell capacity analysis has been performed considering the SINR, CQI, MCS and supported goodput for both carriers. The spatial behaviour of the above parameter has shown that similar values (maximum and minimum) are obtained for the 800 MHz and 2.6 GHz. The main difference lays on the spatial distributions of resources. Overall, as the distance from the cell centre increases the 800 MHz band allows reaching higher values than the 2.6 GHz. Moreover, it has been found that at the cell centre, or close to it, goodput values of approximately 18.3 Mbps may be achieved, due to the interference geometry this value decreases to 2 to 4 Mbps depending on the cell considered edge. Employing CA allows to support goodput values of 37 and 8 Mbps at the cell centre and edge, respectively.

Extensive simulations were performed with LTE-Sim and the performance analysis was performed addressing ITU-T G.1010 [49] and 3GPP TS 22.105 [50] performance targets and the corresponding supported goodputs. Simulations results have shown that the 1 % Packet Loss Ratio (PLR) margin is only exceeded above 58 and 54 UEs with iCRRM and CRRM, respectively. Without CA the minimum obtained PLR is approximately 2 %. In this condition, the average supported cell goodput is approximately 7500 and 7400 kbps with iCRRM's EMBS and GMBS, respectively, and 6900 kbps with CRRM. The ITU-T G.1010 [49] and 3GPP TS 22.105 [50] 150 ms preferred average cell delay performance target has not been reached in the performed simulations.

Considering the unified model for the mapping of Quality of Service (QoS) parameters into Quality of Experience from Chapter 3, the perceived impact of CA has been estimated. It has been found that a minimum QoE value of 2.5 can only be supported up to 64, 68 and approximately 70 UEs with CRRM, GMBS and EMBS, respectively, whereas without CA only 36 UEs can be supported. Moreover, the average cell goodput equivalent to the number of UEs supported within this QoE threshold is approximately 8800, 8450, 7950 and 3500 kbps with iCRRM EMBS, iCRRM GMBS, CRRM and without CA, respectively.

Besides, a spatial distribution analysis of resources has been performed. One hundred simulations results have been averaged on a cell location/coordinates bases. On the one hand, it was shown that both iCRRM multi-band schedulers primarily allocate UEs to the 2.6 GHz CC at or near the cell centre, whereas, at cell edge, the 800 MHz CC is favoured. On the other hand, the allocation with both schedulers show a different behaviour in terms of average goodput. With GMBS, both CCs show higher goodput values at cell centre which

decrease as the distance from the cell boundary narrows. Overall, the 800 MHz CC presents higher values than the 2.6 GHz CC. Considering EMBS, at 800 MHz, the spatial goodput distribution resembles GMBS's, but with higher values. Meanwhile the goodput at 2.6 GHz is globally constant throughout the cell.

The cost/revenue analysis was performed using the formulation from Chapter 5 and considering two values for the supported goodput, i.e., number of supported UEs, under the PLR ≤ 1 % and QoE ≥ 2.5 performance targets. In addition, two MByte price have been considered, $R_{144[€/MByte]}$ equal to 0.005 and 0.01. It has been found that without CA the profit cannot be evaluated under PLR ≤ 1 % since this constraint is not satisfied and that for QoE ≥ 2.5 null profits were obtained for R = 2100 m. Besides, for PLR ≤ 1 % iCRRM's EMBS and GMBS, the values of the profit in percentage are the highest and yet similar, since the number of supported UEs is alike. For R = 1000 m and PLR ≤ 1 %, profits of 130 and 360 %, 129 and 357 %, and 113 and 326 % were obtained for iCRRM EMBS, iCRRM GMBS and CRRM, for $R_{144[€/MByte]}$ equal to 0.005 and 0.01, respectively. Considering the QoE ≥ 2.5 performance target, the use of EMBS corresponds to the higher values of the profit. Given its higher number of supported UEs, the GMBS comes in second place as the most profitable technique whereas CRRM is ranked in third. Using the R = 1000 m reference for QoE ≥ 2.5, profits equal to 170 and 440 %, 158 and 416 % and, 143 and 385 % are obtained for the EMBS, GMBS and CRRM, with $R_{144[€/MByte]}$ equal to 0.005 and 0.01, respectively.

Chapter 7

Conclusions and Future Research Direction

7.1 Conclusions

The last few years have shown an increasing adoption of mobile services and applications. In 2014 it is expected that mobile-connected devices will exceed the world's population whereas 2013's global mobile traffic will be 11 fold by 2018 [1]. These numbers clearly show a growth of not only the traffic, but also of the number of terminals connected to wireless cellular networks. In this context, the research addressed in this thesis aims at contributing to the evolution and optimization of wireless network planning.

On the one hand, a combination of architectures, i.e., cellular topologies in the presence/absence of Relay Stations (RSs) are envisioned. Mobile multi-hop relay technology extends the service area of mobile networks and also improves the transmission quality. Such proliferation of architectures should allow for an enhancement of coverage and system capacity. On the other hand, both the Worldwide Interoperability for Microwave Access (WiMAX) and Long Term Evolution (LTE) radio access technologies are addressed. LTE networks have been globally implemented by cellular operators and functionalities introduced in LTE-Advanced (LTE-A) such as Carrier Aggregation (CA) are expected optimize the management of poorly utilized portions of the spectrum, e.g., small portion of the spectrum, but also allowing for drastically increase throughput. However, not only coverage and throughput are the goal of a proper cellular planning, service lever parameters such as loss, delay and user quality of experience also need to be characterized and addressed. Besides, from an operator point of view, economic aspects must also be taken into account during the cellular planning process to guarantee lower cost and optimize revenues and the overall profits.

From the research performed in the framework of the Ubiquimesh project, Chapter 2 describes deployment scenarios and application characterization proposed for wireless mesh networks in a multiple concatenated network environment. The main recommendations from regulators/standardization bodies, e.g., ITU, 3GPP and WiMAX, were considered, as well as, key elements proposed by a major European project, EU-MESH. Instead of developing new and distinct sets of deployment scenarios it is rather assumed that, for a better cooperation with the national and international scientific community, one should rather assume the above recommendations and assumptions. In this context, eight scenarios form EU-MESH are considered. These scenarios are the following:

- the mobile business user scenario which involves access to services and applications by business users that are continuously on the move;

- the nomadic business scenario considers people moving from place to place, that require information exchange and communication services available for business purposes when they stop moving;
- the gaming user scenario addresses users playing online games with the need for a broadband connection with adequate throughput, low latency and jitter;
- the fixed home user-leisure activity scenario considers the typical needs of the Internet occasional user at home with low usage levels;
- the fixed home user-entertainment activity scenario addresses mesh networks supporting increased activities related to entertainment, mainly music, television over IP and video;
- the tourist/attraction visitor scenario delivers services and free public access based on the location information and the user personal profile;
- the video surveillance/home monitoring scenario considers the deployment of surveillance, monitoring equipment based on a new mesh network environment;
- the mobile commerce scenario refers to a set of applications offered to mobile users that allow them to buy goods and services using their handheld devices through wireless network access.

A detailed description of the key parameters that most impact users, i.e., delay, delay variation and information loss has been provided and considered for performance considerations of audio, video data and background applications. It has been found that audio applications are classified into three types: conversational voice, voice messaging and streaming audio. Conversational voice requirements are heavily influenced by one-way delay. Voice messaging requirements for information loss are essentially the same as for conversational voice, except a higher tolerance for delay, since there is no direct conversation involved. Streaming audio should provide the lowest packet loss for audio applications, nevertheless, as with voice messaging, there is no conversational element involved and delay requirements can be higher. Video applications are classified as videophone and one-way video. Videophone implies a full-duplex system and the same delay requirements as for conversational voice. Some degree of packet loss is acceptable depending on the specific video coder and amount of error protection used. The main distinguishing feature of one-way video is the absence of conversational elements, meaning that the delay requirement will not be so stringent, and can follow the one from streaming audio. The requirements for data transfer applications are to guarantee a minimal loss of information. Delay variation is not generally noticeable to users. Nevertheless, data applications are distinguished according to the delay which can be tolerated by the end-user. The last category is background applications. The only requirement for this type of applications is that information should be delivered to the user essentially error free. However, there is still a delay constraint, since data is effectively useless if it is received too late for any practical purpose.

The performance targets for audio, video and data applications extracted from the ITU-T G.1010 recommendation, 3GPP TS 22.105 and EU-MESH were addresses in Chapter 2. Moreover, specific and more detailed characterization of voice and video application, defined by the WiMAX Forum Application Working Group were considered. For these applications the throughput requirements are addressed according to the compression technology. Additionally, five classes of applications from a user perspective were defined and characterized, i.e., interactive gaming, VoIP and video conferencing, streaming media, basic Internet applications and file transfer/media download. This classification for applications allows for estimating the importance of audio/video compression techniques. Audio encoding schemes and video compression play a major role in throughput requirements. Furthermore, information on video data rates requirements is provided according to the display size of user's terminals. Finally, Chapter 2 is concluded by a proposal for the requirements for services and applications. With the gathered information, an analysis and update of applications requirements from ITU, 3GPP, EU-MESH and WiMAX Forum was addressed. The video and voice DL/UL were thoroughly updated according to compression and encoding techniques. Bearing in mind that next generation wireless networks should provide superior data rates, the targeted throughput, DL and UL speeds, were chosen whenever possible by considering the highest value addressed by ITU, 3GPP and EU-MESH. It was found that the most complex application characterizations are the ones involving voice and video communication, given that data rate requirements depend on the used encoding scheme. The remaining application characterization follows the recommendations from one or more information provided by the above regulators or projects. The overall final proposal is a mix of recommendations and optimal key parameters values provided by the considered entities and European project.

A proposal for the mapping between Quality of Service (QoS) onto Quality of Experience (QoE) has also been created within Ubiquimesh and is addressed in Chapter 3. It is expected that future wireless networks are bound to provide various multimedia services. In this context, the QoE performance metric is introduced to describe the satisfaction of subscribers/users. As so, QoE evaluation in nowadays competitive market is becoming critical for operators to guarantee their clients satisfaction. Therefore, to enable operators to assess the overall network performance, a strategy to instantly measure QoE must be defined. Chapter 2 addressed many of the network QoS parameters that affect the way users perceive their experience, however QoE is very subjective in nature and the most accurate approach to evaluate the QoE is the subjective quality assessment, since there is no better indicator of personal quality then the one given by a human being. This assessment is essentially a subjective measurement of the network performance at the service level, from the user's point of view. Four main types of applications have been addressed, i.e., gaming, web-browsing, video and audio. The process to obtain the mapping between QoS and QoE, for each type of application, involves the identification of the relationship between QoS performance and its effects onto QoE. As such, Mean Opinion Score (MOS) experiments have been

considered for gaming and video applications, whereas the sub-models for web-browsing and audio applications consider ITU-T recommendations since no MOS results were available. MOS were mathematically fit to find the best equation to characterize the QoE according to the available QoS parameters. The regression analysis and fittings validation were performed by computing the mean square error, and the coefficients of determination and correlation. These terms provide a measure of how well the model fits to experimental MOS measurements. It was shown that the values for the coefficient of determination between the obtained model and the available data (either experimental or the values from ITU-T recommendations) are higher than R^2 = 0.9387, 0.9842 and 0.8379 for gaming, audio and video, respectively. The computed mean square error is approximately zero in all cases.

Within the scope of the work performed in the context of the PLANOPTI and Opportunistic-CR projects, Chapter 4 presented an analytical approach to determine the trade-offs between the coverage distance and interference minimization whilst increasing system capacity in the presence and absence of relay nodes and dynamic sleep modes. It has been shown that the performance of fixed WiMAX is strongly limited by both noise and interference. For instance, with a reuse pattern K = 7, higher MCS levels, i.e., cell throughputs near the maximum, are only achieved in the UL if sub-channelization is used together with sectorization. With the use of sub-channelization alone the improvement is not so significant, even with lower noise power. Moreover, it has been found that the use of sectorization alone for shortest coverage distances allows for obtaining a substantial gain in the physical throughput in the UL. Nonetheless, for larger coverage distances, in the absence of sub-channelization, the achievable gain is not comparable with the case where sub-channelization is used. Overall, the use of sectorization enables to reduce the reuse pattern whereas considering sub-channelization allows for improvement on the coverage. On the one hand, the reuse pattern reduction translates into an increased system capacity. On the other, sub-channelization coverage expansion allows for UL system capacity improvement, as adaptive MCS are used.

The planning and optimization of fixed WiMAX networks in the presence of RSs in conjunction with cell zooming has been addressed considering the real and challenging propagation scenario of the hilly region at Covilhã. In this context, detailed measurement campaigns were performed. Moreover, innovative RSs DL and UL sub-frames have also been proposed that insure resources for the Base Station-to-Mobile Station (BS-to-MS), BS-to-RS and RS-to-MS communications, and consider the FDD mode. As so, these sub-frames present a 1:5 asymmetry factor between the UL and DL in the omnidirectional BS case and to a 3:7 asymmetry factor in the case of tri-sectored BSs. Besides, the system capacity and the supported cell/sector physical throughput formulation in the scope of the proposed sub-frames were also addressed. With these considerations, the cellular planning of the hilly area of Covilhã was performed and revealed and adequate coverage in the presence of RSs. Furthermore, the obtained results shown to be similar to theoretical ones for a full-coverage scenario. The cellular planning through Ray Tracing (RT) and Dominant Path (DP) model

shown that without RSs the supported throughput is lower in practice, as coverage is not 100 % (even with tri-sectored BSs). If omnidirectional BS antennas are used without RSs, the proportion of the cell with no coverage reaches 41.68 % or 38.77 %, through RT and the application of the DP model, respectively.

Still within the scope of the work addressed in the framework of PLANOPTI and Opportunistic-CR projects and considering the results obtained in Chapter 4, Chapter 5 investigated the energy efficiency and economic implications in WiMAX deployments with the use of power saving modes for RSs in conjunction with cell zooming. At first, the formulation for the economic model was introduced, followed by the costs hypotheses and assumptions in the presence and absence of RSs. Considering K = 3 with RSs one considers three carriers in the omnidirectional configurations whereas only one carrier is assumed in the tri-sectored case. By addressing omnidirectional and tri-sectored BS antennas topologies, it was shown that with RSs and with coverage distances up to ~1300m the achievable profit is only clearly higher with the use of tri-sectored BSs. Furthermore, it was found that for a coverage distance of R = ~500 m, it is preferable to consider K = 1 with three carriers per sector instead of K = 3 with one carrier per sector, whereby the profit is increased by more than 45 % from ~1000 % to ~1450 %. Moreover, if the price per MByte is increased from 0.0025 to 0.005 €/MByte, the achievable profit more than doubles under the aforementioned improved configuration.

Assuming that the RSs can be switched-off or zoomed out to zero in periods when the traffic exchange is low, such as nights and weekends periods, and that the central BS coverage zone is zoomed out, energy consumption may be reduced whereas economic performance may be improved. Assuming that the DL sub-frame format cannot be changed to a more favourable one at times when the RSs are sleeping, the economic performance is better in the presence of RSs. Thus, in the absence of RSs, the economic performance is reduced since the supported throughput decreases. However, it is worthwhile to highlight that, contrary to the omnidirectional case (where coverage is extremely weak with no RSs), in the tri-sectored case, if RSs go into sleep mode (thereby saving energy and costs), although there is an increase of the area of the cell with no coverage from 4.25 % to 18.10 % (RT coverage), there is still a reasonable economic performance. However, the use of omnidirectional BS antennas, is not a viable option as the area with no coverage is approximately 40 %. Finally, it was also shown that through the use of power saving through RSs sleeping, average energy savings for the RSs (excluding BSs) near 47.6 % can be achieved. On a system-level, this translates to a financial saving for the operator of 10 % in the summed operation and maintenance.

The work presented in Chapter 6 was performed in the framework of the CREaTION project. This research addressed capacity enhancement of LTE networks with CA. An integrated Common Radio Resource Management (iCRRM) entity is proposed that implements inter-band CA by scheduling resources between two Component Carriers (CCs). Considering the Portuguese communication regulator 2011's auction, the 800 MHz and 2.6 GHz CCs with 5

MHz bandwidths have been assumed. Moreover, video traffic is addressed given CISCO mobile traffic forecast, i.e., video applications accounted for more than half of all worldwide traffic in 2013 and is expected to reach 69 % by 2018. Firstly, to analyse the iCRRM performance with several cell radii with comparable conditions, and to reduce energy consumption for cells with low radius, a formulation was proposed to compute the transmitter power needed to maintain a constant average cell SINR. Considering these results a 3D cell capacity analysis was performed showing that the cell present very similar values for the SINR, CQI, MCS and achievable throughput for both bands. The main difference lays on the spatial distributions of resources, as the distance from the cell centre increases the 800 MHz band allows reaching higher values, i.e., SINR, CQI, MCS and achievable throughput, than with the 2.6 GHz band. Moreover, it has been found that at the cell centre, goodput values of approximately 18.3 Mbps may be supported with both bands, at the cell edge this value decreases to 2 to 4 Mbps depending on the considered cell edge, whereas with CA these values are approximately two fold.

The proposed iCRRM entity has been implemented with two different Multi-Band Schedulers (MBS). The first, the General MBS (GMBS) is an adaptation and update from an originally proposed MBS for the 2 GHz and 5 GHz High-Speed Downlink Packet Access (HSDPA) frequency bands. The disadvantages of this scheduler include an increased complexity of the optimization process, specifically with numerous UEs in the network and this MBS does not consider the possibility of UEs using more than one CC at the same time. The second, the Enhanced MBS (EMBS) has been proposed. In this case, the scheduling process was simplified and UEs may be allocated to both CCs at the same time. Finally, for comparison purposes, a simplified CRRM entity has been implemented to perform basic MBS, i.e., UEs are allocated to one of the CCs until its capacity is reached and the remaining UEs, if any, are allocated to the second CC. Extensive simulations were performed with LTE-Sim and the performance analysis was performed considering ITU-T G.1010 and 3GPP TS 22.105 performance targets and the corresponding values for the supported goodput. Simulation results have shown that the 1 % Packet Loss Ratio (PLR) margin is only exceeded above 58 and 54 UEs with iCRRM and CRRM, respectively, whereas without CA the minimum obtained PLR is approximately 2 %. The corresponding supported average cell goodput for these numbers of UEs is approximately 7500, 7400 and 6900 kbps with iCRRM's EMBS and GMBS, and CRRM, respectively. The ITU-T and 3GPP 150 ms preferred average cell delay performance target has not been reached in context of the performed simulations. Considering the unified model for the mapping of QoS parameters onto QoE from Chapter 3, the perceived impact of CA has been estimated. Bearing in mind ITU-T ACR scale and assuming that a QoE value of 2.5 is a threshold below which the QoE is not acceptable, it has been found that this performance margin can only be supported up to approximately 70, 68, 64 and 36 UEs, with EMBS, iCRRM GMBS, CRRM and without CA, respectively. In this instance, the equivalent supported average cell goodput is approximately 8800, 8450, 7950 and 3500 kbps with EMBS, iCRRM GMBS, CRRM and without CA, respectively. Additionally, a spatial distribution analysis of resources has been performed.

One hundred simulations results have been averaged on a cell position/coordinates bases. It has been shown that both iCRRM multi-band schedulers primarily allocate UEs to the 2.6 GHz CC at or near the cell centre, whereas at the cell edge the 800 MHz CC is preferred. Moreover, both schedulers allocation show a different behaviour in terms of average goodput. With both multi-band schedulers the 800 MHz CC constantly shows higher goodput values than the 2.6 GHz CC. With the EMBS, at 800 MHz the spatial goodput distributions resembles GMBS's, but with higher values. However the achieved goodput at 2.6 GHz is globally constant throughout the cell. With the GMBS both CCs show higher goodput values at cell centre which decrease as the distance from the cell borders narrows. Besides, as stated above, the 800 MHz CC goodput is overall higher than the one with the 2.6 GHz CC.

The cost/revenue analysis has been performed using the formulation from Chapter 5 and considering two values for supported goodput, i.e., the number of supported UEs, under the PLR ≤ 1 % and QoE ≥ 2.5 performance targets. In addition, two MByte prices have been considered, $R_{144[€/MByte]}$ equal to 0.005 and 0.01. It was shown that without CA the profit cannot be evaluated under PLR ≤ 1 %, since this constraint is not satisfied and that for QoE ≥ 2.5 the lowest profit values were obtained. Besides, for PLR ≤ 1 % iCRRM's EMBS and GMBS percentage of profits are the highest and comparable since the number of supported UEs is practically identical. Assuming R = 1000 m and the PLR ≤ 1 % restriction values of the profit in percentage of 130 and 360 %, 129 and 357 %, and 113 and 356 % are obtained for EMBS, GMBS and CRRM, for $R_{144[€/MByte]}$ equal to 0.005 and 0.01, respectively. Considering the QoE ≥ 2.5 performance target, the EMBS shows the higher profits given its higher number of supported UEs, followed by the GMBS and CRRM. Assuming once more R = 1000 m, profits equal to 170 and 440 %, 158 and 416 %, 143 and 385 %, and 37 and 173 % were obtained for EMBS, GMBS, CRRM and without CA, for $R_{144[€/MByte]}$ equal to 0.005 and 0.01, respectively.

In the context of the work addressed in Chapter 6, it is also worthwhile to note that in time, the implementation of CA will certainly be a reality in Europe. In some Asian countries, such as South Korea, network operators and equipment manufacturers have already release 4G LTE-A technology. Smartphones and other consumer products are commercially available. These equipments can reach maximum speeds of 225 Mbps by communicating over two radio channels (10MHz and 20 MHz).

The research from this thesis has proposed enhancement methods such as the implementation of cell zooming and RSs with dynamic sleep modes and CA for heterogeneous networks coverage and capacity enhancements. Overall, innovative contributions on the following main issues have been given:

- A detailed and updated service and applications characterization was presented considering the performance targets for the key parameters that most affect users;
- A model for the mapping between the QoS and QoE was proposed for multimedia applications. This model allows operators and service providers to assess user's perceptual quality in real time;

- The planning and optimization of fixed WiMAX networks with RSs in conjunction with cell zooming was addressed. An analytical approach was proposed to determine the trade-offs between the coverage distance and interference minimization whilst increasing system capacity in the presence and absence of relay nodes and dynamic sleep modes. Innovative DL and UL sub-frames were also proposed in the context of, which are needed to guarantee resources for BS-to-MS communications but also for BS-to-RS and RS-to-MS communications;
- An implicit formulation to obtain the supported throughput as a function of the CNIR in DL and UL was proposed. This is done by weighting the physical throughput in each concentric coverage ring by the size of the ring;
- A formulation for the optimization of the cost/revenue trade-off, from the point of view of network operators and service providers, was developed by taking into account the cost of building and maintaining the infrastructure, and the way the number of channels available in each cell affects operators' and service providers' revenues;
- This part of the work also investigated the energy efficiency and economic implications of the use of power saving modes for RSs in conjunction with cell zooming in WiMAX deployments in the region of Covilhã. Assuming that the RSs can be switched-off or zoomed out to zero in periods when the traffic exchange is low, such as nights and weekends periods, and that the central BS coverage zone is zoomed out, it was shown that energy consumption may be reduced whereas economic performance may be improved;
- An iCRRM entity was proposed that implements inter-band CA by performing scheduling between two CCs. Extensive simulations were performed and results shown a clear improvement of QoS, QoE and economic aspects with CA;
- The analyses of the iCRRM performance for several cell radii with comparable conditions was considered. To reduce energy consumption, the average cell SINR must be kept constant by reducing the transmitter power for low cell radii. In this context, a formulation was proposed to compute the transmitter power needed to cover cells of different sizes whilst maintaining the average cell SINR approximately constant.

7.2 Suggestions for Future Research

One of the main new functionalities introduced in LTE-A is CA, which has been addressed in the framework of this thesis. However, other enhancements are being studied to provide substantial improvements to LTE and allow it to meet or exceed IMT-Advanced requirement. Examples of some physical layer enhancement techniques being studied include relays, small cells (femtocells, picocells, microcells, and metrocells) and advanced multi-antenna techniques. A multitier network where small cells are overlaid on macrocells is generally referred to as a heterogeneous network (HetNet) [138]. In HetNets, small cells

serve as offloading spots in the radio access network to relocate users and their associated traffic from congested macrocells. Small cells provide a fast, flexible, energy/cost-efficient, and customer-need-oriented solution for cellular service providers, enhance their QoS and increase the overall system capacity [138].

However, the presence of neighbouring macrocells, users, relays and the co-existence of multiple small cells create high inference scenarios. There are certain threshold levels for the signal-to-noise-plus-interference ratio at the receiver and BS below which the service cannot be granted. Thus, interference mitigation, advanced signal processing and resources management must be considered for an adequate network planning. Hence, the advent of self-organizing networks (SON) should be also addressed. The main advantages of SONs are self-configuration in which the seamless introduction of new nodes when needed will provide service provisioning and compensate cell outage, and self-healing where mobility load balancing, handover optimization and energy saving management should be provided through self-optimization [140].

The optimization of the cost/revenue trade-off, from the point of view of network operators and service providers, has been analysed by considering fixed prices per Mbyte. However, the flat rate pricing model is being employed worldwide. This model refers to a pricing structure in which the customer is charged a single fixed fee for a service, regardless of usage. Given these considerations, upcoming work will also address the economic impact of CA with this business model.

Additionally, one believes that, with additional Mean Opinion Score (MOS) measurements, the model for the mapping between quality of service and experience can be updated and enhanced. QoE is so subjective in nature that the more experimental MOS results are made available, the more accurate would be the computed trend; hence a more precise estimation of QoE would be inferred. The considered experimental MOS results have been obtained from different networks and conditions (trials), it is also thought that the model can also benefit from obtained MOS in a more controlled environment, i.e., MOS experiments performed in the same networks (conditions) for all multimedia applications. Moreover, as application have greatly evolved along the last few years it is thought that new MOS should be performed to better portray today's users experience. For instance, although one of the most delay sensitive type of online gaming was considered for this model, it should be expected that current generation games, created with innovative programming techniques, allowing for a higher tolerance to network latency, as well as a variety in game design, scene complexity, game pace, and so on, are not best represented by the MOS available in the context of this thesis.

Appendix A

Calculation of the Average SINR

In this appendix, detailed calculations of the average SINR are presented for various cell radii, in a cellular network with reuse pattern equal to three. First, the average interference from a neighbour cell is addressed. Then, the average signal power in the central cell is calculated in order to derive the SINR as function of the cell radius and transmit power.

The average interference, $\bar{I}$, from one neighbour cell is obtained, referring to the coordinate system in Figure 6.10, as follows:

$$\bar{I}(R,P_{Tx}) = \int_y \int_x f_I(P_{Tx},x,y)dxdy = \int_y \int_x \frac{P_{Tx}G_{Tx}G_{Rx}}{A_{cell}} PL(x,y)dxdy = \tag{A.1}$$

where A_{cell} is the total affected cell area given by $3\sqrt{3}/2\, R^2$. The PL follows the models specified in Table 6.3, the distance being determined by $d = \sqrt{(y-y_0)^2+(x-x_0)^2}$, P_{Tx} = 13 dBW, G_{Tx} = 14 dBi and G_{Rx} = 0 dBi. Figure 6.10shows the division of the central hexagonal cell into three sub-regions. Assuming x_0 = 3R, y_0 = 0, [134] one may calculate the average interference as:

$$\bar{I}(R,P_{Tx}) = \sum_{r=1}^{3} \int_{\Gamma_x^r} \int_{\Gamma_y^r} f_{nh}(P_{Tx},x,y)dxdy \tag{A.2}$$

where the integration regions are as follows:

$$\Gamma_x^r = \left\{\left[-R,-\frac{R}{2}\right],\left[-\frac{R}{2},\frac{R}{2}\right],\left[\frac{R}{2},R\right]\right\} \tag{A.3}$$

$$\Gamma_y^r = \left\{\left[-\sqrt{3}x-\sqrt{3}R,\sqrt{3}x+\sqrt{3}R\right],\left[-\frac{\sqrt{3}}{2}R,\frac{\sqrt{3}}{2}R\right],\left[\sqrt{3}x-\sqrt{3}R,-\sqrt{3}x+\sqrt{3}R\right]\right\} \tag{A.4}$$

For the 800 MHz CC, $fP_{nh-800MHz}(P_{Tx},x,y)$ is given by:

$$fP_{nh-800MHz}(P_{Tx},x,y) = \frac{P_{Tx}G_{Tx}G_{rx}}{A_{cell}} 10^{-\frac{119.8+37.6\log_{10}\sqrt{y^2+x^2}}{10}} \tag{A.5}$$

$$fP_{nh-800MHz}(P_{Tx},x,y)=\frac{P_{Tx}G_{Tx}G_{rx}}{A_{cell}}10^{-\frac{119.2+37.6\log_{10}\sqrt{y^2+x^2}}{10}} \quad (A.6)$$

For the 2.6 GHz CC, $fP_{nh-2.6GHz}(P_{Tx},x,y)$ is given by:

$$fP_{nh-2.6GHz}(P_{Tx},x,y)=\frac{P_{Tx}G_{Tx}G_{rx}}{A_{cell}}10^{-\frac{130.5+37.6\log_{10}\sqrt{y^2+x^2}}{10}} \quad (A.7)$$

As R is positive (A.2) is solvable. Then:

$$\int_{\Gamma^r_{x,y}} f_{nh-800MHz}(P_{Tx},x,y)dxdy = P_{Tx}G_{Tx}G_{rx}\cdot 10^{-\frac{\sum_{r=1}^{3}\int_{\Gamma^r_{x,y}}119.8+37.6\log_{10}\sqrt{y^2+x^2}dydx}{10\cdot A_{cell}}} \quad (A.8)$$

$$\int_{\Gamma^r_{x,y}} f_{nh-2.6GHz}(P_{Tx},x,y)dxdy = P_{Tx}G_{Tx}G_{rx}\cdot 10^{-\frac{\sum_{r=1}^{3}\int_{\Gamma^r_{x,y}}130.5+37.6\log_{10}\sqrt{y^2+x^2}dydx}{10\cdot A_{cell}}} \quad (A.9)$$

By determining the exponent in (A.6) and (A.7), one obtains (A.10) and (A.11), respectively:

$$\sum_{r=1}^{3}\int_{\Gamma^r_{x,y}}\frac{119.8+37.6\log_{10}\sqrt{y^2+x^2}dydx}{10\cdot A_{cell}} = ((\frac{1}{4}R^2(18\sqrt{3}-4\pi+2arc\cot\left[\frac{5}{\sqrt{3}}\right]-2arc\cot\left[\frac{7}{\sqrt{3}}\right]+$$
$$76arc\cot\left[\frac{19}{\sqrt{3}}\right]-24arc\cot\left[2\sqrt{3}\right]+48artTan\left[\frac{2}{\sqrt{3}}\right]+144\arctan\left[\frac{5}{\sqrt{3}}\right]-144\arctan\left[\frac{7}{\sqrt{3}}\right]+ \quad (A.10)$$
$$64\sqrt{3}\log[2]-15\sqrt{3}log[13]-\sqrt{3}log[5488]-2\sqrt{3}\log[16807]+2\sqrt{3}\log[62748517]+10\sqrt{3}log[R]+$$
$$2\sqrt{3}\log[64R])\times\left(\frac{18.6}{\log[10]}\right))+(A_{cell}(119.8-(37.6\times 3)))$$

$$\sum_{r=1}^{3}\int_{\Gamma^r_{x,y}}\frac{130.5+37.6\log_{10}\sqrt{y^2+x^2}dydx}{10\cdot A_{cell}} = ((\frac{1}{4}R^2(18\sqrt{3}-4\pi+2arc\cot\left[\frac{5}{\sqrt{3}}\right]-2arc\cot\left[\frac{7}{\sqrt{3}}\right]+$$
$$76arc\cot\left[\frac{19}{\sqrt{3}}\right]-24arc\cot\left[2\sqrt{3}\right]+48\arctan\left[\frac{2}{\sqrt{3}}\right]+144\arctan\left[\frac{5}{\sqrt{3}}\right]-144\arctan\left[\frac{7}{\sqrt{3}}\right]+ \quad (A.11)$$
$$64\sqrt{3}\log[2]-15\sqrt{3}\log[13]-\sqrt{3}\log[5488]-2\sqrt{3}\log[16807]+2\sqrt{3}\log[62748517]+10\sqrt{3}\log[R]+$$
$$2\sqrt{3}\log[64R])\times\left(\frac{18.6}{\log[10]}\right))+(A_{cell}(130.5-(37.6\times 3)))$$

$\overline{P}_{ow}(P_{Tx},x,y)$ is the average signal power within a cell and it is constant for the same frequency model no matter what value of k is use. It may be obtained following a similar

approach to the one for $\overline{P}_{nh}(R, P_{Tx})$, with a different integrand function, fP_{ow}, this function for the 800 CC frequency band is given by:

$$fP_{ow-800MHz}(P_{Tx}, x, y) = \frac{P_{Tx} G_{Tx} G_{rx}}{A_{ow}} 10^{-\frac{119.8+37.6\log_{10}\sqrt{y^2+x^2}}{10}} \quad \text{(A.12)}$$

The integrand function for 2.6 GHz is the following one:

$$fP_{ow\ 2.6GHz}(P_{Tx}, x, y) = \frac{P_{Tx} G_{Tx} G_{rx}}{A_{ow}} 10^{-\frac{130.5+37.6\log_{10}\sqrt{y^2+x^2}}{10}} \quad \text{(A.13)}$$

where A_{ow} is the total integration area equal to $3\sqrt{3}/2\ R^2 - 4F_r^2$, Fr is the Fraunhofer distance and its value is different for each frequency band/CC.

The average power is calculated as follows:

$$\overline{P_{ow}}(R, P_{Tx}) = \sum_{r=1}^{6} \int_{\Gamma_x^r} \int_{\Gamma_y^r} fP(P_{Tx}, x, y) dy dx \quad \text{(A.14)}$$

where

$$\Gamma_x^r = \left\{ \left[-R, -\frac{R}{2}\right], \left[-\frac{R}{2} - Fr\right], [-Fr, Fr][-Fr, Fr], \left[Fr, \frac{R}{2}\right], \left[\frac{R}{2}, R\right] \right\} \quad \text{(A.15)}$$

and

$$\Gamma_y^r = \left\{ \begin{array}{l} \left[-\sqrt{3}x - \sqrt{3}R, \sqrt{3}x + \sqrt{3}R\right], \left[-\frac{\sqrt{3}}{2}R, \frac{\sqrt{3}}{2}R\right], \left[-\frac{\sqrt{3}}{2}R, -Fr\right], \left[Fr, \frac{\sqrt{3}}{2}R\right], \\ \left[-\frac{\sqrt{3}}{2}R, -\frac{\sqrt{3}}{2}R\right], \left[\sqrt{3}x - \sqrt{3}R, -\sqrt{3}x + \sqrt{3}R\right] \end{array} \right\} \quad \text{(A.16)}$$

Equation (A.14) is unsolvable if the integration region includes (x, y) = (0, 0) (where the BS is located). An approximation of the Fraunhofer distance, Fr, is therefore adopted, for an antenna radiator equal to 72 cm. If $R > Fr$ the integral is solvable. With a square approximation of the Fraunhofer region centered in (0, 0).

By determining the exponent in (A.13) and (A.13), one obtains (A.17) and (A.18), respectively:

$$\begin{aligned} &\sum_{r=1}^{6} \int_{\Gamma_{x,y}^r} \frac{119.8 + 37.6\log_{10}\sqrt{y^2+x^2}\, dy dx}{10 \cdot A_{ow}} = ((12Fr^2 - \frac{9\sqrt{3}R^2}{2} + \frac{3\pi R^2}{2} - 4Fr^2 arc\cot\left[\frac{2Fr}{\sqrt{3}R}\right] - \\ &4Fr^2 \arctan\left[\frac{2Fr}{\sqrt{3}R}\right] - -2Fr^2\log[4] - 8Fr^2\log\left[Fr^2\right] + 3\sqrt{3}R^2\log[R]) \times (\frac{18.6}{\log[10]})) \\ &+ (A_{cell}(119.8 - (37.6 \times 3))) \end{aligned} \quad \text{(A.17)}$$

$$\sum_{r=1}^{6}\int_{\Gamma_{x,y}^{r}}\frac{130.5+37.6\log_{10}\sqrt{y^2+x^2}\,dydx}{10\cdot A_{ow}}=((12Fr^2-\frac{9\sqrt{3}R^2}{2}+\frac{3\pi R^2}{2}-4Fr^2 arc\cot\left[\frac{2Fr}{\sqrt{3}R}\right]- \quad (A.18)$$

$$4Fr^2\arctan\left[\frac{2Fr}{\sqrt{3}R}\right]--2Fr^2\log[4]-8Fr^2\log\left[Fr^2\right]+3\sqrt{3}R^2\log[R])\times(\frac{18.6}{\log[10]}))$$

$$+(A_{cell}(130.5-(37.6\times 3)))$$

The average power can now be obtained for the whole hexagon, except in the square with the side length equal to the Fraunhofer distance and the average SINR in (6.12) can be finally calculated.

Finally, Figure A.1 shows the variation of the average received power and interference with the cell radius for α = 1 and P_{Tx}= 13 dBW.

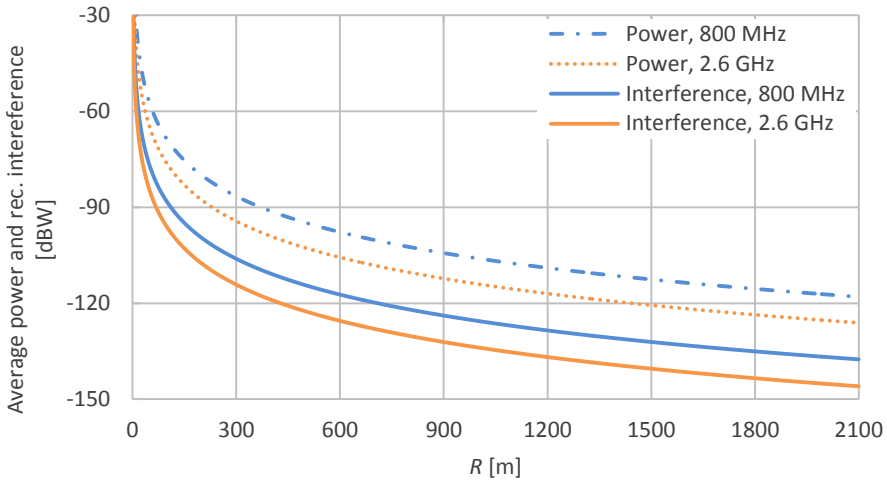

Figure A.1 Average power and interference (dBW) within a cell as a function of the inter-cell distance (m), P_{Tx}= 13 dBW.

Appendix B

Implementation of Carrier Aggregation into LTE-Sim

This appendix addresses the implementation of carrier aggregation into LTE-Sim. The source code for the General Multi-Band Scheduling (GMBS), Enhanced Multi-Band Scheduling (EMBS) and the basic Common Radio Resource Management (CRRM) basic scheduling will be presented in detail. Moreover, it is worthwhile to note that the following C++ instructions are run at each TTI.

General Multi-Band Scheduling

The GMBS maximises the total throughput of the operator via the Profit Function (PF) shown in equation (6.2). The GMBS problem is solved with Integer Programming (IP), using the GLPK (GNU Linear Programming Kit) which embodies the main implementation challenge. For simplicity, the M-LWDF scheduler is not shown here. The source code is given below with detail comments:

```
std::vector<int>
DownlinkPacketScheduler::Compute_G_M_BAND_SchedulerMetric_iCRRM (void)
{
      int RBs = GetMacEntity ()->GetDevice ()->GetPhy ()-
>GetBandwidthManager ()->GetNofRBs (); // retrieves the total number
of resource blocks
      int problem_size = GetFlowsToSchedule()->size(); // auxiliary
variable, later used to define the number of rows (bounds, i.e.,
Lbmax) and columns (structural variables, i.e., xb,u )
      int serv_rate=128000; //defines the video bit rate
      glp_prob *lp;
      int ia[(problem_size*2)*(problem_size+1+1)+1]; // GLPK pre-
allocates memory for problem resolution
      int ja[(problem_size*2)*(problem_size+1+1)+1]; // GLPK pre-
allocates memory for problem resolution
      double ar[(problem_size*2)*(problem_size+1+1)+1], z; // GLPK
pre-allocates memory for problem resolution
      lp = glp_create_prob(); //creates a problem IP object
      FlowsToSchedule* flows = GetFlowsToSchedule ();
      glp_set_prob_name(lp, "GMBS"); // assigns a symbolic name,
"GMBS", to the problem object
      glp_set_obj_dir(lp, GLP_MAX); // optimization direction flag set
to maximization
      glp_add_rows(lp, (problem_size+1+1)); // adds bounds
      for (int i=1; i<=problem_size; i++) // bounds of variables
(rows)
      {
            glp_set_row_bnds(lp, i, GLP_UP, 0, 1); // one user can only
use one band, i.e., xb,u ≤ 1 (Allocation Constraint), equation (6.4)
      }
```

```
      glp_set_row_bnds(lp, (problem_size + 1), GLP_UP, 0.0, 18336); //
Lbmax, max load in band 1 (Bandwidth Constraint for 5 MHz = 18336)
      glp_set_row_bnds(lp, (problem_size + 2), GLP_UP, 0.0, 18336); //
Lbmax, max load in band 2 (Bandwidth Constraint for 5 MHz = 18336)
      glp_add_cols (lp, problem_size*2); //adds columns
      for (int i = 1; i <=(problem_size*2); i++) // sets the columns
objective coefficient
      {
            if (i <= problem_size)
            {
                  double effective_sinrband1 = GetEesmEffectiveSinr
(flows->at ((i-1))->GetBearer ()->GetDestination ()->GetPhy () -
>GetSINRBand1()); // retrieves the SINR of user i on band 1
                  if (effective_sinrband1 > 40) effective_sinrband1 =
40;
                  int cqiband1  = flows->at ((i-1))->GetBearer ()-
>GetDestination ()->GetProtocolStack()->GetMacEntity ()->GetAmcModule
()->GetCQIFromSinr (effective_sinrband1); // retrieves the CQI of user
i on band 1
                  int MCSband1_ = flows->at ((i-1))->GetBearer ()-
>GetDestination ()->GetProtocolStack()->GetMacEntity ()->GetAmcModule
()->GetMCSFromCQI (cqiband1); // retrieves the MCS of user i on band 1
                  int TBSband1_ = flows->at ((i-1))->GetBearer ()-
>GetDestination ()->GetProtocolStack()->GetMacEntity ()->GetAmcModule
()->GetTBSizeFromMCS (MCSband1_, RBs); // retrieves the TBS
(achievable goodput) of user i on band 1
                  double blerband1 = GetBLER_TU (effective_sinrband1,
MCSband1_); // retrieves the BLER of user i on band 1
                  double Wbu2_6 = ((1-blerband1)*TBSband1_)/serv_rate;
// computes Wb,u of user i on band 1
                  glp_set_obj_coef(lp, i, Wbu2_6); // sets columns with
"i" objective coefficient (band1 - 2.6GHz)
                  glp_set_col_kind(lp, i, GLP_BV); // x1,i (xb,u)is
Boolean variable, equation (6.4)
            }
            else
            {
                  double effective_sinrband2 = GetEesmEffectiveSinr
(flows->at ((i-1-problem_size))->GetBearer ()->GetDestination ()-
>GetPhy () ->GetSINRBand2()); // retrieves the SINR of user i on band
2
                  if (effective_sinrband2 > 40) effective_sinrband2 =
40;
                  int cqiband2  = flows->at ((i-1-problem_size))-
>GetBearer ()->GetDestination ()->GetProtocolStack()->GetMacEntity ()-
>GetAmcModule ()->GetCQIFromSinr (effective_sinrband2); // retrieves
the CQI of user i on band 2
                  int MCSband2_ = flows->at ((i-1-problem_size))-
>GetBearer ()->GetDestination ()->GetProtocolStack()->GetMacEntity ()-
>GetAmcModule ()->GetMCSFromCQI (cqiband2); // retrieves the CQI of
user i on band 2
                  int TBSband2_ = flows->at ((i-1-problem_size))-
>GetBearer ()->GetDestination ()->GetProtocolStack()->GetMacEntity ()-
>GetAmcModule ()->GetTBSizeFromMCS (MCSband2_, RBs); // retrieves the
TBS (achievable goodput) of user i on band 2
                  double blerband2 = GetBLER_TU (effective_sinrband2,
MCSband2_); // retrieves the BLER of user i on band 2
                  double Wbu800 = ((1-blerband2)*TBSband2_)/serv_rate;
// computes Wb,u of user i on band 2, equation (6.3)
```

```
                  glp_set_obj_coef(lp, i, Wbu800); //sets columns "i"
with objective coefficient (band2 - 800MHz)
                  glp_set_col_kind(lp,i, GLP_BV); // x2,i (xb,u)is
Boolean variable, equation (6.4)
            }
      }
      // definition of constraints
      int locus=1;
      for (int i = 1; i <= (problem_size+1+1); i++)
      {
            for (int j = 1; j <= (problem_size*2); j++)
            {
                  if (i<=problem_size)
                  {
                        if (i==j || j==problem_size+i)
                        {
                              ia[locus]=i;
                              ja[locus]=j;
                              ar[locus]=1;
                        }
                        else
                        {
                              ia[locus]=i;
                              ja[locus]=j;
                              ar[locus]=0;
                        }
                  }
                  else if (i==problem_size+1)
                  {
                        if (j<=problem_size)
                        {
                              double effective_sinrband1 =
GetEesmEffectiveSinr (flows->at ((i-1))->GetBearer ()->GetDestination
()->GetPhy () ->GetSINRBand1()); // retrieves the SINR of user i on
band 1
                              if (effective_sinrband1 > 40)
effective_sinrband1 = 40;
                              int cqiband1  = flows->at ((i-1))-
>GetBearer ()->GetDestination ()->GetProtocolStack()->GetMacEntity ()-
>GetAmcModule ()->GetCQIFromSinr (effective_sinrband1); // retrieves
the CQI of user i on band 1
                              int MCSband1_ = flows->at ((i-1))-
>GetBearer ()->GetDestination ()->GetProtocolStack()->GetMacEntity ()-
>GetAmcModule ()->GetMCSFromCQI (cqiband1); // retrieves the MCS of
user i on band 1
                              int TBSband1_ = flows->at ((i-1))-
>GetBearer ()->GetDestination ()->GetProtocolStack()->GetMacEntity ()-
>GetAmcModule ()->GetTBSizeFromMCS (MCSband1_, RBs); // retrieves the
TBS (achievable goodput) of user i on band 1
                              double blerband1 = GetBLER_TU
(effective_sinrband1, MCSband1_); // retrieves the BLER of user i on
band 1
                              ia[locus]=i;
                              ja[locus]=j;
                              ar[locus]=
(serv_rate*(1+blerband1))/TBSband1_; // computes W1,i (Wb,u)for user
i, equation (6.3)
                        }
                        else
                        {
```

```
                              ia[locus]=i;
                              ja[locus]=j;
                              ar[locus]=0;
                        }
                  }
                  else if (i==problem_size+2)
                  {
                        if (j<=problem_size)
                        {
                              ia[locus]=i;
                              ja[locus]=j;
                              ar[locus]=0;
                        }
                        else
                        {
                              double effective_sinrband2 =
GetEesmEffectiveSinr (flows->at ((i-1-problem_size))->GetBearer ()-
>GetDestination ()->GetPhy () ->GetSINRBand2()); // retrieves the SINR
of user i on band 2
                              if (effective_sinrband2 > 40)
effective_sinrband2 = 40;
                              int cqiband2  = flows->at ((i-1-
problem_size))->GetBearer ()->GetDestination ()->GetProtocolStack()-
>GetMacEntity ()->GetAmcModule ()->GetCQIFromSinr
(effective_sinrband2); // retrieves the CQI of user i on band 2
                              int MCSband2_ = flows->at ((i-1-
problem_size))->GetBearer ()->GetDestination ()->GetProtocolStack()-
>GetMacEntity ()->GetAmcModule ()->GetMCSFromCQI (cqiband2); //
retrieves the CQI of user i on band 2
                              int TBSband2_ = flows->at ((i-1-
problem_size))->GetBearer ()->GetDestination ()->GetProtocolStack()-
>GetMacEntity ()->GetAmcModule ()->GetTBSizeFromMCS (MCSband2_, RBs);
// retrieves the TBS (achievable goodput) of user i on band 2
                              double blerband2 = GetBLER_TU
(effective_sinrband2, MCSband2_); // retrieves the BLER of user i on
band 2
                              ia[locus]=i;
                              ja[locus]=j;
                              ar[locus]=
(serv_rate*(1+blerband1))/TBSband1_; // computes W2,i (Wb,u)for user
i, equation (6.3)
                        }
                  }
                  locus++;
            }
      }
      locus--;
      glp_term_out (GLP_OFF); // disables terminal output (glpk
message on screen)
      glp_load_matrix(lp, locus, ia, ja, ar); // loads information
into the problem object
      glp_simplex(lp, NULL); // calls simplex method to solve the IP
problem
      z = glp_get_obj_val(lp); // obtains a computed value of the
objective function
      std::vector<int> myvector (problem_size*2);
      for (unsigned i=0; i<myvector.size();
                  {
                  myvector.at (i)= glp_get_col_prim(lp, i+1); // stores
every xb,u onto myvector
```

```
                  }
                  CA_schedule_table=myvector;   ); // loads each user's
xb,u onto scheduling table
      glp_delete_prob(lp); // deletes problem
      return SA_schedule_table; // returns scheduling table, i.e.,
each user's xb,u
}
```

Enhanced Multi-band scheduling

The EMBS has been proposed in the context of this thesis to overcome the GMBS complexity and inability to allocate users on more than one CC a time. A scheduling metric, equation (6.10), for each RB of each CC is computed and the RBs allocation is performed according to the highest value obtained. As in the previous case, the C++ code is given below with detail comments:

```
double
EMBS_PacketScheduler::ComputeSchedulingMetric (RadioBearer *bearer,
double spectralEfficiency, int subChannel)
{
      double metric; // declares metric variable
      if ((bearer->GetApplication ()->GetApplicationType () ==
Application::APPLICATION_TYPE_INFINITE_BUFFER) // if the type of
traffic is infinite buffer
                  ||
                  (bearer->GetApplication ()->GetApplicationType () ==
Application::APPLICATION_TYPE_CBR)) // or if the type of traffic is
constant bit rate
      {
            metric = (spectralEfficiency * 180000.)
                                    /
                                    bearer-
>GetAverageTransmissionRate(); // the metric is computed as by the
proportional fair scheduling
      }
      else
      {
            AMCModule *amc = GetMacEntity ()->GetAmcModule ();
            int cqi  = amc->GetCQIFromEfficiency (spectralEfficiency);
// returns CQI of the addressed user on band b
            double sinr = GetMacEntity ()->GetAmcModule ()-
>GetSinrFromCQI (cqi); // returns SINR of the user on addressed sub-
channel on band b
            int MCS = amc->GetMCSFromCQI (cqi); // returns MCS of the
user on addressed sub-channel on band
            int TBS = amc->GetTBSizeFromMCS (MCS, 1); // returns
transport block size of the user on addressed sub-channel on band
            QoSForM_LWDF *qos = (QoSForM_LWDF*) bearer-
>GetQoSParameters ();

            double HOL = bearer->GetHeadOfLinePacketDelay (); //
returns the user's HOL
            metric = ((TBS/0.001)*(TBS/0.001)*HOL)
                              /
                              ((bearer->GetAverageTransmissionRate
())*serv_rate); // computes the metric as given in equation (6.10)
```

```
            return metric;
      }
}
```

Common Radio Resource Management - Simple Multi-Band Scheduling

Finally, the simple scheduling implements only basic CRRM functionalities and is employed for comparison purposes. In this case, users are allocated on one of the bands until its capacity is reached, the remaining, if any, are allocated on the second band.

```
std::vector<int>
DownlinkPacketScheduler::Compute_SchedulerMetric_CRMM (void)
{
      int RBs = GetMacEntity ()->GetDevice ()->GetPhy ()-
>GetBandwidthManager ()->GetNofRBs (); // retrieves the total number
of resource blocks (band 1 + band 2)
      double TotalDataToTransmit = 0; // initiates total data to
transmit variable
      FlowsToSchedule* flows = GetFlowsToSchedule ();
      for (int i = 0; i < flows->size (); i++) // for all active users
      {
            double effective_sinrband1 = GetEesmEffectiveSinr (flows-
>at ((i-1))->GetBearer ()->GetDestination ()->GetPhy () -
>GetSINRBand1()); // retrieves the SINR of user i on band 1
            if (effective_sinrband1 > 40) effective_sinrband1 = 40;
            int cqiband1  = flows->at ((i-1))->GetBearer ()-
>GetDestination ()->GetProtocolStack()->GetMacEntity ()->GetAmcModule
()->GetCQIFromSinr (effective_sinrband1); // retrieves the CQI of user
i on band 1
            int MCSband1_ = flows->at ((i-1))->GetBearer ()-
>GetDestination ()->GetProtocolStack()->GetMacEntity ()->GetAmcModule
()->GetMCSFromCQI (cqiband1); // retrieves the MCS of user i on band 1
            int TBSband1_ = flows->at ((i-1))->GetBearer ()-
>GetDestination ()->GetProtocolStack()->GetMacEntity ()->GetAmcModule
()->GetTBSizeFromMCS (MCSband1_, RBs); // retrieves the TBS (number of
bits that can be transmitted for the considered TTI) of user i on band
1
            TotalDataToTransmit = TotalDataToTransmit + TBSband1_; //
updates the total number of bits to be transmitted on band 1
            if (TotalDataToTransmit < 18336) //if data to transmit in
band 1 <= max load band 1
            {
                  myvector.at (i) = 1; // allows user i allocation on
band 1 (x1,i = 1), equation (6.10)
                  myvector.at (i+flows->size ()) = 0; // denies user i
allocation on band 2 (x2,i = 0), equation (6.10)
            }
            else
            {
                  myvector.at (i) = 0; // denies user i allocation on
band 1 (x1,i = 0), equation (6.10)
                  myvector.at (i+flows->size ()) = 1; // allows user i
allocation on band 2 (x2,i = 1), equation (6.10)
            }
      }
```

```
      SA_schedule_table=myvector; // loads each user's xb,u, onto
scheduling table
      return SA_schedule_table; // returns scheduling table, i.e.,
each user's xb,u,
}
```

References

[1] Cisco Visual Networking Index: Global Mobile Data Traffic Forecast Update, 2013-2018, white paper, Feb. 2014.

[2] Junaid Shaikh, Markus Fiedler, Denis Collange, "Quality of Experience from user and network perspectives", *Annals of Telecommunications, Quality of Experience 1 - Metrics and performance evaluation*, vol. 65, no. 1-2, pp. 47–57, 2010 (available online DOI 10.1007/s12243-009-0142-x).

[3] B. Lane, "Cognitive Radio Technologies in the Commercial Arena", in *Proc. of FCC Workshop on Cognitive Radio Technologies*, Washington, DC, USA, May 2003.

[4] L. M. Correia, D. Zeller, O. Blume, D. Ferling, Y. Jading, I. Gódor, G. Auer, L. Van Der Perre, "Challenges and enabling technologies for energy aware mobile radio networks", *IEEE Communications Magazine*, vol. 48, no. 11, pp. 66-72, Nov. 2010 (available online DOI 10.1109/MCOM.2010.5621969).

[5] Zhisheng Niu, Yiqun Wu, Jie Gong, Zexi Yang, "Cell zooming for cost-efficient green cellular networks", *IEEE Communications Magazine*, vol. 48, no. 11, pp. 74–79, Nov. 2010 (available online DOI 10.1109/MCOM.2010.5621970).

[6] D. Niyato, E. Hossain, Dong In Kim Zhu Han, "Relay-centric radio resource management and network planning in IEEE 802.16j mobile multihop relay networks", *IEEE Transactions on Wireless Communications*, vol. 8, no. 12, pp. 6115-6125, Dec. 2009 (available online DOI 10.1109/TWC.2009.12.090640).

[7] H. Koumaras, F. Liberal, L. Sun, "Quality of experience issues in multimedia provision", *Telecommunication Systems*, vol. 49, no. 1, pp. 1-3, Jan. 2012 (available online DOI 10.1007/s11235-010-9349-4).

[8] Hyun Jong Kim, Dong Hyeon Lee, Jong Min Lee, Kyoung Hee Lee, Won Lyu, Seong Gon Choi, "The QoE Evaluation Method through the QoS-QoE Correlation Model", in *Proc. of Conference on Networked Computing and Advanced Information Management - NCM '08*, Sept., 2008 (available online DOI 10.1109/NCM.2008.202).

[9] M. Fiedler, T. Hossfeld, Phuoc Tran-Gia, "A generic quantitative relationship between quality of experience and quality of service", *IEEE Network*, vol. 24, no. 2, pp. 36-41, Mar.-Apr. 2010 (available online DOI 10.1109/MNET.2010.5430142).

[10] P. Brooks, B. Hestnes, "User measures of quality of experience: why being objective and quantitative is important", *IEEE Network*, vol. 24, no. 2, pp. 8-13, Mar.-Apr. 2010 (available online DOI 10.1109/MNET.2010.5430138).

[11] COST 2100. EU COST Action 2100: Pervasive Mobile Ambient Wireless Communications. Available: http://www.cost2100.org (accessed on Oct. 2013).

[12] COST IC1004. EU COST Action IC1004: Cooperative Radio Communications for Green Smart Environments. Available: http://www.ic1004.org/ (accessed on Oct. 2013).

[13] COST IC0905 TERRA. EU COST Action IC0905 TERRA: Techno-Economic Regulatory Framework for Radio Spectrum Access for Cognitive Radio/Software Defined Radio. Available: http://www.cost-terra.org (accessed on Oct. 2013).

[14] Cross-Layer Optimization in Multiple Mesh Ubiquitous Networks (Ubiquimesh). Available: http://ubiquimesh.av.it.pt (accessed on Oct. 2013).

[15] Opportunistic Aggregation of Spectrum and Cognitive Radios: Consequences on Public Policies (Opportunistic-CR). Available: http://www.e-projects.ubi.pt/opportunistic-cr (accessed on Oct. 2013).

[16] Planning and Optimization for the Coexistence of Mobile and Wireless Networks Towards Long Term Evolution (PLANOPTI). Available: http://www.e-projects.ubi.pt/planopti (accessed on Oct. 2013).

[17] Cognitive Radio Transceiver Design for Energy Efficient Data Transmission (CREaTION). Available: http://www.av.it.pt/creation (accessed on Oct. 2013).

[18] Ajay R. Mishra, *Advanced Cellular Network Planning and Optimization: 2G/2.5G/3G... Evolution to 4G*, England, John Wiley & Sons Ltd., 2006 (ISBN-13: 978-0470014714).

[19] Daniel Robalo, Fernando J. Velez, Orlando Cabral, Marilia Curado, Susana Sargento, *Deployment Scenarios and Characterization Parameters for Concatenated Multiple Mesh Networks Applications*, Covilhã, Portugal, Instituto de Telecomunicações, Jan. 2012.

[20] Daniel Robalo, Fernando J. Velez, "A Model for Mapping between the Quality of Service and Experience for Wireless Multimedia Applications", in *Proc. of IEEE 79th Vehicular Technology Conference*, Seoul, Korea, May 2014.

[21] Daniel Robalo, Fernando J. Velez, "Characterization of Parameters for Wireless Networks Services and Applications*", 3rd Meeting of the Management Committee of COST TERRA- Techno-Economic Regulatory Framework for Radio Spectrum Access for Cognitive Radio Software Defined Radio, WG1*, Brussels, Belgium, June 2011.

[22] Daniel Robalo, Fernando J. Velez, "Wireless Networks Services and Applications Parameters Characterization and Model for the mapping between the Quality of Service and Experience for multimedia applications", *8th Meeting of the Management Committee of COST IC 1004 - Cooperative Radio Communications for Green Smart Environments*, TD(13)08069, Ghent, Belgium, Sep. 2013.

[23] Daniel Robalo, Fernando J. Velez, *Report on a unified model for the mapping between the Quality of Service and Experience in multimedia applications*, Covilhã, Portugal, Instituto de Telecomunicações, Jan. 2012.

[24] Daniel Robalo, Fernando J. Velez, "Model for the Correlation between Quality of Service and Experience in Cognitive Radio Networks", (invited paper) in *Proc. of International Symp. on Applied Sciences in Biomedical and Communication Technologies – ISABEL-CogART*, Barcelona, Spain, Oct. 2011.

[25] Fernando J. Velez, Pedro Sebastião, Rui Costa, Daniel Robalo, Cláudio Comissário, António Rodrigues, Hamid Aghvami, "Radio and Network Planning", Chapter 8 in the book *WiMAX Networks: Techno-Economic Vision and Challenges*, edited by Ramjee Prasad and Fernando J. Velez, Springer, 2010 (ISBN: 978-90-481-8751-5).

[26] Fernando J. Velez, M. Kashif Nazir, Hamid Aghvami, Oliver Holland, Daniel Robalo, "System capacity", Chapter 9 in the book *WiMAX Networks: Techno-Economic Vision and Challenges*, edited by Ramjee Prasad and Fernando J. Velez, Springer, 2010 (ISBN: 978-90-481-8751-5).

[27] Fernando J. Velez, M. Kashif Nazir, Ramjee Prasad, Hamid Aghvami, Oliver Holland, Daniel Robalo, "Business Models and Cost/revenue Optimization", Chapter 10 in the book WiMAX Networks: *Techno-Economic Vision and Challenges*, edited by Ramjee Prasad and Fernando J. Velez, Springer, 2010 (ISBN: 978-90-481-8751-5).

[28] Pedro Sebastião, Fernando J. Velez, Rui Costa, Daniel Robalo, António Rodrigues, "Planning and Deployment of WiMAX Networks", *WIRE - Wireless Personal Communications*, vol. 55, no. 3, pp. 305-323, Nov. 2010.

[29] Pedro Sebastião, Fernando J. Velez, Rui Costa, Daniel Robalo, Cláudio Comissário, António Rodrigues, "Planning and Deployment of WiMAX and Wi-Fi Networks for Health Sciences Education", *Telektronikk*, vol. 105, no. 2, pp. 173-185, 2009.

[30] Fernando J. Velez, M. Kashif Nazir, Hamid Aghvami, Oliver Holland, Daniel Robalo, "Cost/Revenue Trade-off in the Optimization of Fixed WiMAX Deployment with Relays", *IEEE Transaction on Vehicular Technology*, vol. 60, no. 1, pp. 298-312, Jan. 2011.

[31] Marina Barbiroli, Claudia Carciofi, Vitorio Esposti, Franco Fuschini, Paolo Grazioso, Doriana Guiducci, Daniel Robalo, Fernando J. Velez, "Characterization of WiMAX Propagation in Microcellular and Picocellular Environments", in *Proc of European Conf. on Antennas & Propagation - EUCAP*, Barcelona, Spain, Apr. 2010.

[32] Frederico Varela, Pedro Sebastião, Américo Correia, Francisco Cercas, Fernando J. Velez, Daniel Robalo, "Unified Propagation Model for Wi-Fi, UMTS and WiMAX Planning in Mixed Scenarios", in *Proc. of PIMRC 2010 21st Annual IEEE International Symposium on Personal, Indoor and Mobile Radio Communications,* Istanbul, Turkey, Sept., 2010.

[33] Frederico Varela, Pedro Sebastião, Américo Correia, Francisco Cercas, Fernando J. Velez, Daniel Robalo, "Validation of the Unified Propagation Model for Wi-Fi, UMTS and WiMAX Planning", in *Proc. of PIMRC 2010 21st Annual IEEE International Symposium on Personal, Indoor and Mobile Radio Communications,* Istanbul, Turkey, Sept., 2010.

[34] Daniel Robalo, João Oliveira, Fernando J. Velez, Valeria Petrini, Marina Barbiroli, Claudia Carciofi, Paolo Grazioso, Franco Fuschini, "Experimental characterisation of WiMAX propagation in different environments", in *Proc. of EUROCON and Conftele' 2011- International Conference on Computer as a Roll*, Lisbon, Portugal, Apr. 2011.

[35] Fernando J. Velez, João Oliveira, Daniel Robalo, Oliver Holland, Hamid Aghvami, "Energy Saving in the Optimization of the Planning of Fixed WiMAX with Relays in Hilly Terrains: Impact of Sleep Modes and Cell zooming", (invited paper) in *Proc. of ISWCS 2012 - The Ninth International Symposium on Wireless Communication Systems (invited Session on Green Wireless Communications)*, Paris, France, Aug. 2012.

[36] Fernando J. Velez, João Oliveira, Daniel Robalo, Oliver Holland, Hamid Aghvami, "Cost/Revenue Optimization of WiMAX Networks with Relay Power Saving Modes: Measurement-Based Scenario in a Hilly Region", in *Proc. of Globecom 2012 - Global Communications Conference Exhibition & Industry Forum*, Anaheim, CA, USA, Dec. 2012.

[37] Marina Barbiroli, Claudia Carciofi, Vitorio Esposti, Franco Fuschini, Paolo Grazioso, Doriana Guiducci Guiducci, Daniel Robalo, Fernando J. Velez, "Characterization of WiMAX Propagation in Microcellular and Picocellular Environments", *11th Meeting of the Management Committee of COST2100 - Pervasive Mobile & Ambient Wireless Communications*, TD(10)11007, Denmark, Aalborg, June 2010.

[38] Daniel Robalo, Valeria Petrini, João Oliveira, Fernando J. Velez, Marina Barbiroli, Claudia Carciofi, Paolo Grazioso, Franco Fuschini, "Experimental characterisation of WiMAX propagation in different environments", *12th Meeting of the Management Committee of COST2100 - Pervasive Mobile & Ambient Wireless Communications*, TD(10)12030, Bologna, Italy, Nov. 2010.

[39] Fernando J. Velez, João Oliveira, Daniel Robalo, Oliver Holland, Hamid Aghvami, "Energy Saving in the Optimization of the Planning of Fixed WiMAX with Relays in Hilly Terrains: Impact of Sleep Modes and Cell Zooming", *5th Meeting of the Management Committee of COST IC 1004 - Cooperative Radio Communications for Green Smart Environments*, TD(12)05025, Bristol, UK, Sep. 2012.

[40] Daniel Robalo, João Oliveira Fernando J. Velez, Oliver Holland, Hamid Aghvami, "Dynamic Configuration and Optimization of WiMAX Networks with Relay Power Savings Modes: Measurement-Based Scenario in a Hilly Region", submitted to *Wireless Personal Communnications*, Feb. 2014.

[41] Jessica Acevedo, Daniel Robalo, Fernando J. Velez, "Transmitted Power Formulation for the Implementation of Spectrum Aggregation in LTE-A over 800 MHz and 2 GHz Frequency Bands", in *Proc. of WPMC 2013 - International Symposium on Wireless Personal Multimedia Communications*, Atlantic City, New Jersey, USA, June 2013.

[42] Jessica Acevedo, Daniel Robalo, Fernando J. Velez, "Transmitted Power Formulation for the Implementation of Spectrum Aggregation in LTE-Advanced over 800 MHz and 2 GHz Frequency Bands", *6th Meeting of the Management Committee of COST TERRA Techno-Economic Regulatory Framework for Radio Spectrum Access for Cognitive Radio Software Defined Radio, WG2*, Brussels, Belgium, Nov. 2012.

[43] Jessica Acevedo Flores, Daniel Robalo, Fernando J. Velez, "Transmitted Power Formulation for the Implementation of Spectrum Aggregation4in LTE-A over 800 MHz and 2 GHz Frequency Bands", *9th Meeting of the Management Committee of COST IC 1004 - Cooperative Radio Communications for Green Smart Environments*, TD(13)09079, Ferrara, Italy, Feb. 2014.

[44] Jessica Acevedo Flores, Fernando J. Velez, Orlando Cabral, Daniel Robalo, Oliver Holland, Hamid Aghvami, Filippo Meucci, Albena Mihovska, Neeli Rashmi Prasad, Ramjee Prasad, "Cost/Revenue Performance in an IMT-Advanced Scenario with Spectrum Aggregation Over Non-Contiguous Frequency Bands", in *Proc. of International Conference on Telecommunications 2014 (ICT 2014)*, Lisboa, Portugal, May 2014.

[45] Jessica Acevedo, Daniel Robalo, Fernando J. Velez, "Cost/Revenue Performance of LTE Employing Spectrum Aggregation with Multi-Band User Allocation over Two Frequency Bands", 8th *Meeting of the Management Committee of COST TERRA- Techno-Economic Regulatory Framework for Radio Spectrum Access for Cognitive Radio Software Defined Radio, WG2*, Biel, Switzerland, Nov. 2013.

[46] Jessica Acevedo, Fernando J. Velez, Orlando Cabral, Daniel Robalo, Oliver Holland, Hamid Aghvami, Filippo Meucci, Albena Mihovska, Neeli R. Prasad, Ramjee Prasad, "Cost/Revenue Performance in an IMT-Advanced Scenario with Spectrum Aggregation Over Non-Contiguous Frequency Bands", *9th Meeting of the Management Committee of COST IC 1004 - Cooperative Radio Communications for Green Smart Environments*, TD(13)09080, Ferrara, Italy, Feb. 2014.

[47] Jessica Acevedo, Daniel Robalo, Fernando J. Velez, "Transmitted Power Formulation for the Optimization of Spectrum Aggregation in LTE-A over 800 MHz and 2 GHz Frequency Bands", accepted for publication with minor revisions *in Special Issue of the Wireless Personal Communications Journal*, July 2014.

[48] Daniel Robalo, Fernando J. Velez, "Enhanced Multi-Band Scheduling for Carrier Aggregation in LTE-Advanced Scenarios", submitted to *Special Issue on Technical advances in the design and deployment of future heterogeneous networks of EURASIP Journal on Wireless Communications and Networking*, Aug. 2014

[49] ITU-T, *End-user multimedia QoS categories*, Recommendation of the ITU-T, Recommendation G.1010, International Telecommunication Union, Geneva, Switzerland, 2001.

[50] 3GPP, *TS 22.105 (2013-12) Services and service capabilities (Release 9)*, 3GPP Technical Specification Group Services and System Aspects, Services and service capabilities, V11.1.0, 2013.

[51] EU-MESH: Enhanced, Ubiquitous, and Dependable Broadband Access using MESH Networks, Public Deliverables, "D2.1 Usage Scenarios and Application Requirements", Apr. 2008. http://www.eu-mesh.eu/files/public_deliverables/ICT-215320-EU-MESH-D2.1_v1.4-final.pdf (accessed on Oct. 2013).

[52] ITU-T, *Framework Recommendation for multimedia services*, Recommendation of the ITU-T, Recommendation F.700, International Telecommunication Union, Geneva, Switzerland, 2000.

[53] ITU-T, *Control of talker echo*, Recommendation of the ITU-T, Recommendation G.131, International Telecommunication Union, Geneva, Switzerland, 1996.

[54] ITU-T, *One-way transmission time*, Recommendation of the ITU-T, Recommendation G.114, International Telecommunication Union, Geneva, Switzerland, 2000.

[55] WiMAX Forum: WiMAX System Evaluation Methodology. Version 2.1, July 2008.

[56] Bong Ho Kim *et al.*, Application Performance guideline, WiMAX Forum AWG meeting, Orlando, FL, Feb. 2009.

[57] Bong-Ho Kim, Jungnam Yun, Yerang Hur, Chakchai So-In, Raj Jain, Abdel-Karim Al Tamimi, "Capacity Estimation and TCP Performance Enhancement over Mobile WiMAX Networks", *IEEE Communications Magazine*, vol. 47, no. 6, pp. 132-141, June 2009.

[58] WiMAX Forum AWG, "WiMAX Application Usage Profile", Apr. 2006.

[59] F. H. P. Fitzek, M. Reisslein, "MPEG-4 and H.263 Video Traces for Network Performance Evaluation", *IEEE Network*, vol. 15, no. 6, pp. 40-54, 2001.

[60] Bong H. Kim, and Y Hur", Application Traffic Model for WiMAX Simulation", POSDATA, Ltd., Apr. 2007.

[61] J. A. Hassan, S. K. Das, M. Hassan, C. Bisdikian, D. Soldani, "Improving quality of experience for network services [Guest Editorial]", *IEEE Network*, vol. 24, no. 2, pp. 4-6, Mar.-Apr. 2010 (available online DOI 10.1109/MNET.2010.5430137).

[62] H. Koumaras, F. Liberal, L. Sun, "Quality of experience issues in multimedia provision", *Telecommunication Systems*, vol. 49, no. 1, pp. 1-3, 2012 (available online DOI 10.1007/s11235-010-9349-4).

[63] P. Brooks, B. Hestnes, "User measures of quality of experience: why being objective and quantitative is important", *IEEE Network*, vol. 24, no. 2, pp.8-13, Mar.-Apr. 2010 (available online DOI 10.1109/MNET.2010.5430138).

[64] K. Chen, P. Huang, C. Lei, "How sensitive are online gamers to network quality?", *Communications of the ACM-Entertainment networking*, vol. 49, no. 11, pp. 34–38, Nov. 2006 (available online DOI 10.1145/1167838.1167859).

[65] Michael Jarschel, Daniel Schlosser, Sven Scheuring, Tobias Hobfeld. "Gaming in the clouds: QoE and the users' perspective", *Mathematical and Computer Modelling*, Dec. 2011 (available online DOI 10.1016/j.mcm.2011.12.014).

[66] Yu-Chun Chang, Kuan-Ta Chen, Chen-Chi Wu, Chien-Ju Ho, Chin-Laung Lei, "Online game QoE evaluation using paired comparisons", in *Proc. of IEEE International Workshop Technical Committee on Communications Quality and Reliability (CQR)*, Vancouver, Canada, June 2010 (available online DOI 10.1109/CQR.2010.5619923).

[67] Lothar Pantel, Lars C. Wolf, “On the impact of delay on real-time multiplayer games”, in *Proc. of the 12th international workshop on Network and operating systems support for digital audio and video* (NOSSDAV '02), New York, NY, USA, 2002 (available online DOI 10.1145/507670.507674).

[68] M. Claypool, K. Claypool, “On latency and player actions in online games”, *Communications of the ACM-Entertainment networking*, vol. 49, no. 11, pp. 40-45, Nov. 2006 (available online DOI 10.1145/1167838.1167860).

[69] A. F. Wattimena, R. E. Kooij, J. M. Van Vugt, O. K. Ahmed, “Predicting the perceived quality of a First Person Shooter: the Quake IV G-model”, in *Proc. of NetGames 2006*, Singapore, Oct. 2006, (available online DOI 10.1145/1230040.1230052).

[70] ITU-T, *Methods for Subjective Determination of Transmission Quality*, Recommendation of the ITU-T, Recommendation P.800, International Telecommunication Union, Geneva, Switzerland, 1996.

[71] DSL Forum, Technical Report TR-126: Triple-play Services Quality of Experience (QoE) Requirements, Dec. 2006.

[72] R. Schatz, T. Hossfeld, P. Casas, “Passive YouTube QoE Monitoring for ISPs”, in *Proc. of Sixth International Conference on Innovative Mobile and Internet Services in Ubiquitous Computing (IMIS)*, Palermo, Italy, July 2012 (available online DOI 10.1109/IMIS.2012.12).

[73] R. K. P. Mok, E. W. W. Chan, R. K. C. Chang, “Measuring the quality of experience of HTTP video streaming”, in *Proc. of Symposium on Integrated Network Management*, Dublin City, Ireland, May 2011 (available online DOI 10.1109/INM.2011.5990550).

[74] K. D. Singh, Y. Hadjadj-Aoul, G. Rubino, “Quality of experience estimation for adaptive HTTP/TCP video streaming using H.264/AVC”, in *Proc. of Consumer Communications and Networking Conference (CCNC),* Las Vegas, Nevada, USA, Jan. 2012 (available online DOI 10.1109/CCNC.2012.6181070).

[75] G. Gardikis, G. Xilouris, E. Pallis, A. Kourtis, “Joint assessment of Network and Perceived-QoS in video delivery networks”, *Telecommunication Systems*, vol. 49, no. 1, pp. 75-84, Jan. 2012 (available online DOI 10.1007/s11235-010-9349-4).

[76] J. Shin, J. G. Kim, J. Kim, Jay Kuo, “Dynamic QoS mapping control for streaming video in relative service differentiation networks”, *European Transactions on Telecommunications*, vol. 12, no. 3, May–Jun, 2001.

[77] M. Venkataraman, M. Chatterjee, “Inferring video QoE in real time”, *IEEE Network*, vol. 25, no. 1, pp. 4-13, Jan. - Feb. 2011.

[78] S. Egger, T. Hossfeld, R. Schatz, M. Fiedler, “Waiting times in quality of experience for web based services”, in *Proc. of Fourth International Workshop on Quality of Multimedia Experience (QoMEX)*, Yarra Valley, Australia, July 2012 (available online DOI 10.1109/QoMEX.2012.6263888).

[79] D. Rossi, M. Mellia, C. Casetti, “User patience and the Web: a hands-on investigation”, in *Proc. of Global Telecommunications Conference, GLOBECOM '03*, San Francisco, CA, USA, Dec. 2003 (available online DOI 10.1109/GLOCOM.2003.1259011).

[80] S. Khirman, P. Henriksen, “Relationship between Quality-of-Service and Quality-of-Experience for Public Internet Service”, in *Proc. of Passive and Active Measurement (PAM2002)*, Fort Collins, Colorado, USA, Mar. 2002.

[81] R. Schatz, S. Egger, A. Platzer, “Poor, Good Enough or Even Better? Bridging the Gap between Acceptability and QoE of Mobile Broadband Data Services”, in *Proc. of IEEE International Conference on Communications (ICC),* Kyoto, Japan, June 2011 (available online DOI 10.1109/icc.2011.5963220).

[82] Junaid Shaikh, Markus Fiedler, Denis Collange, “Quality of Experience from user and network perspectives”, *Annals of Telecommunications*, vol. 65, no. 1-2, pp. 47-57, Feb. 2010 (available online DOI 10.1007/s12243-009-0142-x).

[83] ITU-T, *Estimating end-to-end performance in IP networks for data applications*, Recommendation of the ITU-T, Recommendation G.1030, International Telecommunication Union, Geneva, Switzerland, 2005.

[84] Beerends, Van Der Gaast, Ahmed, Web browse quality modelling, White contribution COM 12-C 3 to ITU-T Study Group 12, 2004.

[85] Van Der Gaast, Beerends, Ahmed, Meeuwissen, “Quantification and prediction of end-user perceived web-browsing quality”, *TIJDSCHRIFT- NERG (*Kluwer Academic*)*, vol. 73, no. 1, pp. 21-29, 2008.

[86] Maxim Graubner, Parag S. Mogre, Ralf Steinmetz, and Thorsten Lorenzen, “A new QoE model and evaluation method for broadcast audio contribution over IP”, in *Proc. of the 20th international workshop on Network and operating systems support for digital audio and video* (NOSSDAV '10), New York, NY, USA, June 2010 (available online DOI 10.1145/1806565.1806581).

[87] Lingfen Sun, E. C. Ifeachor, “Voice quality prediction models and their application in VoIP networks”, *IEEE Transactions on Multimedia,* vol. 8, no. 4, pp. 809-820, Aug. 2006 (available online DOI 10.1109/TMM.2006.876279).

[88] ITU-T, *The E-model: a computational model for use in transmission planning*, Recommendation of the ITU-T, Recommendation G.107, International Telecommunication Union, Geneva, Switzerland, 2009.

[89] R. G. Cole, J. Rosenbluth, "Voice over IP Performance Monitoring", *SIGCOMM Computer Communications Review*, vol. 31, no. 2, pp. 9-24, Apr. 2001 (available online DOI 10.1145/505666).

[90] Lingfen Sun, *Speech Quality Prediction for Voice Over Internet Protocol Networks*, Ph.D. thesis, University of Plymouth, Plymouth, United Kingdom, Jan. 2004.

[91] ITU-T, *Objective measuring apparatus, Appendix 1: Test signals*, ITU-T Recommendation P.50, International Telecommunication Union, Geneva, Switzerland, 1998.

[92] Fernando J. Velez, Maria del Camino Noguera, Oliver Holland, Hamid Aghvami, "Fixed WiMAX Profit Maximisation with Energy Saving through Relay Sleep Modes and Cell Zooming", Journal of Green Engineering (Special Issue from WPMC 2010), vol. 1, no. 4, July 2011, pp. 355-381.

[93] Fernando J. Velez, M. Kashif Nazir, Hamid Aghvami, Oliver Holland, Daniel Robalo, "Cost/Revenue Trade-off in the Optimization of Fixed WiMAX Deployment with Relays", *IEEE Transactions on Vehicular Technology*, vol. 60, no. 1, Jan. 2011, pp. 298-312.

[94] Ramjee Prasad, Fernando J. Velez, *WiMAX Networks: Techno-economic Vision and Challenges,* The Netherlands, Springer, 2010 (ISBN 978-90-481-8752-2).

[95] Fernando. J. Velez, Luís. M. Correia, J. M. Brázio, "Frequency reuse and system capacity in Mobile Broadband Systems: Comparison between the 40 and 60 GHz Bands", *Wireless Personal Communications,* vol. 19, no. 1, Aug. 2001.

[96] Fernando J. Velez, Vitor Carvalho, Dany Santos, Rui P. Marcos, Rui Costa, Pedro Sebastião, António Rodrigues, "Aspects of Cellular Planning for Emergency and Safety Services in Mobile WiMax Networks", in *Proc. of ISWPC' 2006 - 1st International Symposium on Wireless Pervasive Computing 2006*, Phuket, Thailand, Jan. 2006.

[97] Pedro Sebastião, Fernando J. Velez, Rui Costa, Daniel Robalo, António Rodrigues, "Planning and Deployment of WiMAX Networks", *WIRE - Wireless Personal Communications*, Aug. 2009 (available online DOI 10.1007/s11277-009-9803-3).

[98] M. Kashif Nazir, *Modelling and Simulation of Efficient Broadband Wireless Access Architectures (WiMAX) with Multi-hop Relays*, MSC thesis, Department of Electronic Engineering, King's College London, London, UK, 2009.

[99] Daniel Robalo, João Oliveira, Fernando. J. Velez, Valeria Petrini, Marina Barbiroli, Claudia Carciofi, Paulo Grazioso, Franco Fuschini, "Experimental propagation characterisation for WiMAX at 3.5 GHz in different environments", in *Proc. of URSI Seminar of the Portuguese Committee*, Lisbon, Portugal, Nov. 2011.

[100] Rodhe&Schwarz, 2010, Sept. 21 [Online]. Available: http://www2.rohde-schwarz.com/en/products/test_and_measurement/spectrum_analysis/FSH4_8-|-Brochures_and_Data_Sheets-|-19-|-4912.html.

[101] V. Erceg, K. V. S. Hari, M. S. Smith, D. S. Baum, K. P. Sheikh, C. Tappenden, J. M. Costa, C. Bushue, A. Sarajedini R. Schwartz, D. Branlund, T. Kaitz, D. Trinkwon, "Channel Models for Fixed Wireless Applications", tech. rep. IEEE 802.16.3c-01/29r4 IEEE 802.16 Broadband Wireless Access Working Group, 2001.

[102] Christian Hoymann, Karsten Klagges, Marc Schinnenburg, "Multi-hop Communication in Relay Enhanced IEEE 802.16 networks", in *Proc. of PIMRC 2006- 17th IEEE International Symposium on Personal, Indoor and Mobile Radio Communications*, Helsinki, Finland, Sep. 2006.

[103] IEEE Std P802.16j-2009. "Air Interface for Broadband Wireless Access Systems, Amendment 1: Multiple Relay Specification", The Institute of Electrical and Electronics Engineers, New York, NY, USA, June 2009.

[104] Jeffrey G. Andrews, Arunabha Ghosh, Rias Muhamed, *Fundamentals of WiMAX - Understanding Broadband Wireless Networking*, Prentice Hall, Upper Saddle River, NJ, USA, 2007 (ISBN 978-0132907804).

[105] Christian Hoymann, Stephan Goebbels, "Dimensioning Cellular WiMAX Part I: Singlehop Networks", in *Proc. of EW'2007 - European Wireless 2007*, Paris, France, Apr. 2007.

[106] Fernando J. Velez, João Oliveira, Daniel Robalo, Oliver Holland, Hamid Aghvami, "Cost/Revenue Optimization of WiMAX Networks with Relay Power Saving Modes: Measurement-Based Scenario in a Hilly Region", in *Proc. of IEEE Globecom 2012: Second International Workshop on Rural Communications - RuralComm 2012*, Anaheim, United States, Dec. 2012.

[107] B. Gavish, S. Sridhar, "Economic aspects of configuring cellular networks", *Wireless Networks*, vol. 1, no. 1, pp. 115–128, Feb. 1995.

[108] Fernando J. Velez, Luís M. Correia, "Optimization of mobile broadband multi-service systems based in economics aspects", *Wireless Networks*, vol. 9, no. 5, Sep. 2003, pp. 525-533.

[109] Klas Johansson, Anders Furuskär, Peter Karlsson, Jens Zander, "Relation Between Cost Structure and Base Station Characteristics in Cellular Systems", in *Proc. of PIMRC' 2004 - 15th IEEE International Symposium on Personal, indoor and Mobile Radio Communications*, Barcelona, Spain, Sep. 2004.

[110] D. Reed, "The Cost Structure of Personal Communications", *IEEE Communications Magazine*, vol. 31, no. 4, pp. 102-108, Apr. 1993.

[111] J. Sarnecki *et al.*, "Microcell Design Principles", *IEEE Communications Magazine*, vol. 31, no. 4, pp. 76-82, Apr. 1993.

[112] M. Ibrahim, K. Khawam, A. E. Samhat, S. Tohme, "Analytical framework for dimensioning hierarchical WiMax-WiFi networks", *Computer Networks*, vol. 53, no. 3, 2009, pp. 299-309.

[113] Fernando J. Velez, Hamid Aghvami, Oliver Holland, "Basic Limits for Fixed WiMAX Optimization Based in Economic Aspects", *IET Communications – Special Issue on WiMAX Integrated Communications* , vol. 4, no. 9, June 2010, pp. 1116-1129 (available online DOI 10.1049/iet-com.2009.0190).

[114] Fernando J. Velez, Luís M. Correia, "Cost/Revenue Optimization in Multi-service Mobile Broadband Systems", in *Proc. of PIMRC' 2002-13th IEEE International Symposium on Personal, Indoor and Mobile Radio Communications*, Lisbon, Portugal, Sep. 2002.

[115] H. Lee, S. Vahid, K. Moessner, "A Survey of Radio Resource Management for Spectrum Aggregation in LTE-Advanced", *IEEE Communications Surveys & Tutorials*, no. 99, pp.1-16, Second Quarter, 2014 (available online DOI 10.1109/SURV.2013.101813.00275).

[116] 3GPP TS 21.101, *Technical specifications and technical reports for a UTRAN-based 3GPP system (Release 10)*, 3GPP Technical Specification Group Services and System Aspects, V10.2.0, Mar. 2012.

[117] Xingqin Lin, J. G. Andrews, A. Ghosh, "Modeling, Analysis and Design for Carrier Aggregation in Heterogeneous Cellular Networks", *IEEE Transactions on Communications,* vol. 61, no. 9, Sept., 2013, pp. 4002 -4015 (available online DOI 10.1109/TCOMM.2013.071813.120880).

[118] 3GPP, TS 36.300, "Evolved Universal Terrestrial Radio Access (E-UTRA) and Evolved Universal Terrestrial Radio Access Network (E-UTRAN), (Release 10)", TSG RAN, V11.8.0.

[119] Liu Fei, Zheng Kan, Xiang Wei, Zhao Hui, "Design and Performance Analysis of An Energy-Efficient Uplink Carrier Aggregation Scheme", *IEEE Journal on Selected Areas in Communications,* vol. 32, no. 2, Feb. 2014, pp.197-207 (available online DOI 10.1109/JSAC.2014.141202).

[120] http://www.3gpp.org/technologies/keywords-acronyms/101-carrier-aggregation-explained (accessed on February 2014).

[121] Yuanye Wang, K. I. Pedersen, P. E. Mogensen, T. B. Sorensen, "Resource allocation considerations for multi-carrier LTE-Advanced systems operating in backward compatible mode", in *Proc. of 2009 IEEE 20th International Symposium on Personal, Indoor and Mobile Radio Communications*, Sept., 2009 (available online DOI 10.1109/PIMRC.2009.5450150).

[122] Yuanye Wang, K. I Pedersen, T. B. Sorensen, P. E. Mogensen, "Carrier load balancing and packet scheduling for multi-carrier systems", *IEEE Transactions on Wireless Communications*, vol. 9, no. 5, pp. 1780-1789, May 2010 (available online DOI 10.1109/TWC.2010.05.091310).

[123] Yuanye Wang, K. I Pedersen, T. B. Sorensen, P. E. Mogensen, "Utility Maximization in LTE-Advanced Systems with Carrier Aggregation", in *Proc. of IEEE 73rd Vehicular Technology Conference (VTC Spring),* May 2011(available online DOI 10.1109/VETECS.2011.5956494).

[124] Galaviz et al.: A resource block organization strategy for scheduling in carrier aggregated systems. *EURASIP Journal on Wireless Communications and Networking* 2012.

[125] Auction regulation for the allocation of rights of use of frequencies in the 450 MHz, 800 MHz, 900 MHz, 1800 MHz, 2.1 GHz and 2.6 GHz bands, Anacom, Oct. 2011.

[126] 3GPP, TR 36.807 (2012-07), *User Equipment (UE) radio transmission and reception (Release 10)*, 3GPP Technical Specification Group Radio Access Network, V10.0.0, 2012.

[127] 3GPP, TR 36.850 (2013-07), *Inter-band carrier aggregation(Release 11)*, 3GPP Technical Specification Group Radio Access Network, V11.1.0, 2013.

[128] H. Wang, C. Rosa, K. Pedersen, "Uplink component carrier selection for lte-advanced systems with carrier aggregation", in *Proc. of 2011 IEEE Int. Conf. Commun. (ICC)*, June 2011.

[129] GSMA report on Mobile Infrastructure Sharing, GSMA, Sep. 2012 (available online: www.gsma.com/ publicpolicy/ wp-content/ uploads/ 2012/ 09/ Mobile-Infrastructure-sharing.pdf).

[130] 3GPP TR 25.942 v10.1.0, *Radio Frequency (RF) system scenarios. (Release 10)*. The 3rd. Generation Partnership Project. Technical Specification Group Radio Access Network, June 2012.

[131] O. Cabral, F. Meucci, A. Mihovska, Fernando. J. Velez, N. R. Prasad, "Integrated Common Radio Resource Management with Spectrum Aggregation over Non-Contiguous Frequency Bands", *Wireless Personal Communications*, vol. 59, no. 3, pp. 499-523, Aug. 2011.

[132] J. K. Karlof, Integer Programming: Theory and Practice, 1st ed. CRC, 2005 (ISBN-10: 0849319145).

[133] 3GPP TS 36.213 v12.2.0, *Physical Layer Procedures (Release 12)*. The 3rd. Generation Partnership Project. Technical Specification Group Radio Access Network, June 2014.

[134] K. C. Chen, J. Roberto, B. de Marca, *Mobile WiMAX 1st Edition*, John Wiley & Sons Ltd., West Sussex, UK, 2008 (ISBN 978-0470519417).

[135] H. Holma, A. Toskala Ed., *WCDMA for UMTS -HSPA evolution and LTE 4th Edition*, John Wiley & Sons Ltd., West Sussex, UK, 2007 (ISBN: 978-0-470-51252-4).

[136] G. Piro, L. A. Grieco, G. Boggia, F. Capozzi, P. Camarda, "Simulating LTE Cellular Systems: an Open Source Framework", *IEEE Trans. on Vehicular Technology*, vol. 60, no. 2, pp.1-16, Feb. 2011.

[137] Tara Ali-Yahiya, *Understanding LTE and its Performance*, Springer, The Netherlands, 2011 (ISBN 978-1-4419-6456-4).

[138] F. Capozzi, G. Piro, L. A. Grieco, G. Boggia, P. Camarda, "Downlink Packet Scheduling in LTE Cellular Networks: Key Design Issues and a Survey", *IEEE Communications Surveys & Tutorials*, vol. 15, no. 2, pp. 678-700, 2013, (available online DOI 10.1109/SURV.2012.060912.00100).

[139] H. ElSawy, E. Hossain, Dong In Kim, "HetNets with cognitive small cells: user offloading and distributed channel access techniques", *IEEE Communications Magazine*, vol. 51, no. 6, June 2013 (available online DOI 10.1109/MCOM.2013.6525592).

[140] A. A. W. Ahmed, J. Markendahl, C. Cavdar, "Interplay between cost, capacity and power consumption in heterogeneous mobile networks", in *Proc. of 21st International Conference on Telecommunications (ICT)*, pp. 98-102, May 2014 (available online DOI: 10.1109/ICT.2014.6845088).

[141] J. Hoydis, M. Kobayashi, M. Debbah, “Green Small-Cell Networks”, *IEEE Vehicular Technology Magazine*, vol. 6, no.1, pp. 37-43, Mar. 2011(available online DOI 10.1109/MVT.2010.939904).